

Expression of biopharmaceuticals in *Ustilago maydis*

Inaugural-Dissertation

Zur Erlangung des Doktorgrades
der Mathematisch-Naturwissenschaftlichen Fakultät
der Heinrich-Heine-Universität Düsseldorf

vorgelegt von

Marius Terfrüchte
aus Essen

Düsseldorf, November 2016

aus dem Institut für Mikrobiologie
der Heinrich-Heine-Universität Düsseldorf

Gedruckt mit der Genehmigung der
Mathematisch-Naturwissenschaftlichen Fakultät der
Heinrich-Heine-Universität Düsseldorf

Referent: Prof. Dr. Michael Feldbrügge

Korreferent: Prof. Dr. Karl-Erich Jaeger

Tag der mündlichen Prüfung: 12.01.2017

Eidesstattliche Erklärung

Ich versichere an Eides Statt, dass die Dissertation von mir selbstständig und ohne unzulässige fremde Hilfe unter Beachtung der „Grundsätze zur Sicherung guter wissenschaftlicher Praxis an der Heinrich-Heine-Universität Düsseldorf“ erstellt worden ist. Die Dissertation wurde in ihrer jetzigen oder ähnlichen Form noch bei keiner anderen Hochschule eingereicht. Ich habe zuvor keine erfolglosen Promotionsversuche unternommen.

Ort, Datum

Marius Terfrüchte

Die Untersuchungen zur vorliegenden Arbeit wurden von August 2013 bis August 2016 in Düsseldorf an der Heinrich-Heine-Universität im Institut für Mikrobiologie unter der Betreuung von Herrn Prof. Dr. Michael Feldbrügge durchgeführt.

Teile dieser Arbeit wurden zur Veröffentlichung im Applied Environmental Microbiology Journal eingereicht (**Terfrüchte M., Wewetzer S., Schlepütz T., Feldbrügge M., Büchs J. and Schipper K.**, Optimizing cultivation conditions for unconventional secretion of heterologous proteins in *Ustilago maydis*.)

Summary

To satisfy the rapidly increasing biopharmaceutical market, a broad variety of microbial protein expression systems is requested by the industry. High demands are made on safety, variability, feasibility and production yields. One alternative system is based on unconventional secretion in *Ustilago maydis* and enables secretory expression of large unglycosylated proteins of pro- and eukaryotic origin. To prove the potential of the system in the production of pharmaceutically relevant proteins, various antibody fragments were expressed. Severe yield losses due to the high proteolytic potential of the fungus were tackled by deletion of secreted proteases and the application of strong promoters could increase the expression rate. Nevertheless, yield and stability of unconventionally secreted proteins were not satisfying. Hence, the optimization of the expression system on multiple levels was subject of this study. To determine an optimal expression construct design, a set of nanobody variants against the fluorescence reporter protein Gfp was used. The investigations yielded constructs for optimized stability and purification. Expression of nanobodies in fusion with the horseradish peroxidase demonstrated functionalization and simplified detection, but led to interferences with nanobody activity in the supernatant. Expression and unconventional secretion of a nanobody antitoxin directed against Botulinum neurotoxin A could furthermore prove the flexibility and applicability of the expression constructs. Moreover, the potential malaria antigen PfRh5 was successfully secreted by this pathway. Yet application of the different optimization steps did not allow efficient purification of the potential vaccine candidate, indicating that each target needs carefully designed individual construct modifications.

A very important factor for the establishment of an expression platform is to consider the cultivation parameters and cell physiology. These parameters strongly influence the effectivity of the expressing organism and play a crucial role in product yield and stability. RAMOS cultivations for online monitoring of the organisms condition during cultivation in combination with detailed offline analyses of crucial parameters revealed a link between culture broth acidification and proteolytic degradation of the product. The use of protease deficient expression strains combined with tight pH control and optimized nutrient availability thus led to a substantial increase of product yield. Quantifications revealed a maximum yield of at least 420 µg/L unconventionally secreted protein, representing a 14-fold increase compared to previous studies.

Overall, considerable improvements in product yield, product stability, downstream processing and applicability could be achieved and critical factors that need further improvement could be identified. Hence insights obtained in this study essentially contribute to the steady advancement of the *U. maydis* expression system towards an industrially used expression platform for biopharmaceuticals.

Zusammenfassung

Um den rasch wachsenden Markt für biopharmazeutische Produkte zu bedienen, wird eine Vielzahl mikrobieller Expressionssysteme benötigt. An diese werden besonders hohe Ansprüche in den Bereichen Sicherheit, Variabilität, Ausbeute und Wirtschaftlichkeit gestellt. Ein alternatives System basiert auf unkonventioneller Sekretion in *Ustilago maydis* und ermöglicht die sekretorische Expression großer, unglykosylierter Proteine sowohl eu- als auch prokaryotischen Ursprungs. Um die Anwendung des Systems für die Expression pharmazeutisch relevanter Proteine zu untersuchen, wurden bereits verschiedene Antikörperfragmente produziert. Zur Verringerung von Verlusten aufgrund des hohen proteolytischen Potentials des Pilzes wurden sekretierte Proteasen deletiert. Weiterhin konnte durch den Einsatz starker Promotoren das generelle Expressionslevel gesteigert werden. Trotz aller Erfolge und Verbesserungen waren Ausbeute und Stabilität der unkonventionell sekretierten Produkte unbefriedigend. Aus diesem Grund wurde in dieser Untersuchung der Fokus auf die weitere Optimierung des Expressionssystems gelegt.

Zur Identifizierung geeigneter Expressionskonstrukte wurde eine Reihe unterschiedlicher Nanobody Varianten gegen das Fluoreszenzprotein Gfp hergestellt. Hierbei konnten Konstrukte zur verbesserten Produktstabilität und -aufreinigung etabliert werden. Die Expression eines Nanobody-HRP Fusionsproteins vereinfachte die Detektion und zeigte weiterhin ein Beispiel für die Funktionalisierung von Nanobodies. Unglücklicherweise führte dies jedoch zu verminderter extrazellulärer Nanobody Aktivität. Die Expression und unkonventionelle Sekretion eines Nanobody-basierten Antitoxins gegen Botulinum Neurotoxin A konnte zudem die Flexibilität und Anwendbarkeit der Expressionskonstrukte untermauern. Darüber hinaus wurde das potentielle Malaria Antigen PfRH5 erfolgreich sekretiert. Trotz diverser Optimierungsversuche waren Aufreinigung und Ausbeute des potentiellen Impfstoffs jedoch nicht erfolgreich, was darauf hindeutet, dass jedes Zielprotein individuelle Modifikationen des Expressionskonstrukts erfordert.

Ein weiterer wichtiger Faktor bei der Etablierung eines Expressionssystems ist die Optimierung der Kultivierungsbedingungen, da physiologischer Zustand und Fitness des Organismus eine zentrale Rolle für die Produktausbeute und -stabilität spielen. Die Verwendung des RAMOS Kultivierungssystems in Verbindung mit Offline-Analysen essentieller Parameter konnte hierbei einen Zusammenhang zwischen Ansäuerung des Mediums und Proteolyse des Produkts aufzeigen. Die Verwendung Protease-defizienter Stämme in Kombination mit stabilisiertem pH und optimierter Nährstoffverfügbarkeit führte daher zu einer signifikant erhöhten Ausbeute. Durch Quantifizierungen konnte eine maximale Ausbeute von mindestens 420 µg/L unkonventionell sekretiertem Protein ermittelt werden. Dies entspricht einer vierzehnfachen Steigerung im Vergleich zu vorherigen Studien.

In dieser Arbeit konnten somit erhebliche Verbesserungen im Bereich Produktausbeute, -stabilität, Aufreinigung und Anwendung erreicht werden. Ferner konnten Faktoren identifiziert werden, welche zusätzliche Untersuchungen und Optimierung erfordern. Die Ergebnisse dieser Studie tragen daher substantiell zur Weiterentwicklung des *U. maydis* Expressionssystems hin zu einer industriell genutzten Expressionsplattform für Biopharmazeutika bei.

List of Abbreviations

°C	Degree centigrade	<i>in planta</i>	Inside a living plant
μL	Microliter	<i>in silico</i>	By using computational simulation
aa	Amino acid	<i>in vitro</i>	Independent of a living organism
Acb	Acyl-CoA binding protein	<i>in vivo</i>	In a living organism
Acyl-CoA	Acyl coenzyme A	<i>ip</i>	Iron-sulphur protein
AM	Ammonium minimal	IPTG	Isopropyl-β-D-1-thiogalactopyranoside
Amp ^R	Ampicillin resistance	Kan ^R	Kanamycin resistance
AOX	Alternative oxidase	kb	Kilobases
BoNTA	Botulinum toxin A	kDa	Kilodalton
bp	Base pair	L	Liter
BSA	Bovine serum albumin	M	Molar
Cam ^R	Chloramphenicol resistance	mg	Milligram
CAZymes	Carbohydrate-active enzymes	min	Minute
CBB	Coomassie brilliant blue	mL	Milliliter
CBP	Calmodulin binding peptide	MOPS	3-(<i>N</i> -morpholino)propanesulfonic acid
cbx	Carboxin	mRNA	Messenger RNA
C _H , C _L	Constant heavy-, constant light chain	mRNP	Messenger ribonucleoparticle
CM	Complete medium	NB	Nanobody
C-terminal	Carboxyterminal	Ni ²⁺ -NTA	Nickel-nitrilotriacetic acid
DIG	Digoxigenin	N-terminal	Aminoterminal
DNA	Deoxyribonucleic acid	OD	Optical density
dNTP	Deoxynucleoside triphosphate	ORF	Open reading frame
ELISA	Enzyme linked immunosorbent assay	OTR	Oxygen transfer rate
et al.	And others	phleo	Phleomycin
Fab	Fragment antigen binding	RAMOS	Respiration Activity MOnitoring System
Fc	Fragment crystallizable	RFU	Relative fluorescence unit
Fig.	Figure	RNA	Ribonucleic acid
FLP	Flippase recombinase	rpm	Rounds per minute
Frc	Fructose	RT	Room temperature
g	Gram	s	Second
gDNA	Genomic DNA	scFv	Single-chain variable fragment
Gent ^R	Gentamycin resistance	Strep	Streptavidin
Gfp	Green fluorescent protein	supsp.	subspecies
Glc	Glucose	Tab.	Table
Gus	β-glucuronidase	TAP	Tandem affinity purification
h	Hour	TCA	Trichloric acid
H ₂ O _{bid.}	Distilled water	U	Unit
HA	Hemagglutinin	UTR	Untranslated region
HCl	Hydrochloric acid	UV	Ultraviolet light
His	Histidine	v/v	Volume per volume
HEPES	4-(2-Hydroxyethyl)piperazine-1-ethanesulfonic acid	V _H , V _L	Variable heavy-, variable light chain
hpi	Hours post inoculation	V _{HH}	Heavy chain antibody variable domain
HRP	Horseradish peroxidase	w/v	Weight per volume
hyg	Hygromycin	WT	Wildtype
Hz	Hertz	x g	x fold gravitational force
Ig	Immunoglobulin	α	Anti
IMAC	Immobilized metal ion affinity chromatography	Δ	Deletion

Table of Contents

SUMMARY	I
ZUSAMMENFASSUNG	II
LIST OF ABBREVIATIONS	IV
1 INTRODUCTION.....	1
1.1 Protein expression systems.....	1
1.2 Classical and unconventional protein secretion.....	3
1.2.1 Diversity in secretion mechanisms	3
1.2.2 Exploiting unconventional secretion for export of heterologous proteins	6
1.3 <i>U. maydis</i> – From basic research to applied science	8
1.4 Transforming <i>U. maydis</i> into a protein expression platform	11
1.4.1 Strain engineering.....	11
1.4.2 Process engineering.....	14
1.5 Biopharmaceuticals as export targets for unconventional protein secretion	15
1.5.1 Vaccines	16
1.5.2 Antibodies	17
1.6 Aim of the thesis.....	19
2 RESULTS	20
2.1 Optimizing the expression, purification and biochemical characterization of α Gfp nanobodies in <i>U. maydis</i>	20
2.1.1 Studies on the effects of proteases	20
2.1.2 Studies on the effects of construct design.....	22
2.1.3 Nanobody functionalization via HRP fusion	27
2.2 Expression, unconventional secretion and biochemical characterization of an α BoNTA nanobody	29
2.3 Application of unconventional secretion for expression of the potential malaria antigen PfRH5	31
2.3.1 Expression and purification of UmRH5	32
2.3.2 Biochemical characterization of UmRH5.....	35
2.4 Optimization of cultivation conditions for heterologous protein expression in <i>U. maydis</i>	36
2.4.1 Online monitoring of standard <i>U. maydis</i> cultivations using RAMOS	36

2.4.2	Determination of optimal buffer conditions for Gus-Cts1 expression in <i>U. maydis</i>	39
2.4.3	Combining protease deficient <i>U. maydis</i> strains with optimized buffering	40
2.4.4	Studying the effects of carbon and nitrogen concentration on growth and unconventional secretion	43
2.4.5	Studying unconventional secretion in minimal media.....	46
2.5	Application and upscaling of optimized cultivation conditions	47
2.5.1	Expression, unconventional secretion and biochemical analysis of α BoNTA from buffered cultivation	47
2.5.2	Upscaling unconventional secretion of Gus-Cts1 and α Gfp-NB-Cts1 in batch fermentations	48
3	DISCUSSION.....	51
3.1	Towards improved nanobody expression in <i>U. maydis</i>	51
3.2	Expression of a potential malaria antigen in <i>U. maydis</i>	57
3.3	Increasing the yield by cultivation optimization	60
3.4	Outlook and future perspectives	65
4	MATERIAL AND METHODS	68
4.1	Materials	68
4.1.1	Chemicals, enzymes, kits	68
4.1.2	Solutions and media	70
4.1.3	Oligonucleotides	71
4.1.4	Plasmids	74
4.1.5	Strains.....	84
4.2	Methods	88
4.2.1	Molecular biology methods.....	88
4.2.2	Microbiological methods	91
4.2.3	Protein biochemical methods	94
4.2.4	Computer programs and bioinformatics	105
5	REFERENCES	106
6	APPENDIX.....	123
	AUTHOR CONTRIBUTIONS	124
	ACKNOWLEDGEMENTS	125

1 Introduction

1.1 Protein expression systems

The biotechnological industry is constantly gaining market shares compared to the classical industry. In numbers, around 170 billion dollars were spent on biopharmaceuticals in 2013, reaching an estimated value of 220 billion dollars by 2017 (<https://www.statista.com/topics/1634/biotechnology-industry/> and (Berlec and Štrukelj, 2013)). The vast majority of biotechnological products is produced in microbial systems, highlighting the importance of microbial expression systems in industry (Berlec and Štrukelj, 2013). Compared to the classical way of isolating proteins from natural resources, biotechnological approaches reveal outstanding properties with higher yields, low production costs, safety and flexibility. Especially for the detergent, food and feed industry, biotechnologically produced products are essential. Enzymes facilitate washing processes, enable automation of food production processes or increase the shelf life of convenient food (Bhat, 2000; Ghorai et al., 2009; Kirk et al., 2002). With the upcoming of personalized medicine, gene therapies and tissue modeling, the importance of proteinaceous medicals in pharmaceutical industry is also increasing substantially (Berlec and Štrukelj, 2013; Ecker et al., 2015). To cover the whole range of potentially relevant proteins, a broad arsenal of different expression hosts is needed (Adrio and Demain, 2010; Demain and Vaishnav, 2009; van Dijk and Hecker, 2013). Depending on the requirements and application of the product, it is important to choose the right expression host. Especially the expression of proteinaceous medicals for pharmaceutical industry is placing high demands on the specificities of the host organism (Gellissen, 2000; Schmidt, 2004; Spadiut et al., 2014).

A vast amount of proteins is still expressed in the gram-negative bacterium *Escherichia coli* to date (Berlec and Štrukelj, 2013; Huang et al., 2012; Terpe, 2006). This is mainly due to the fact that it is one of the best studied microorganisms, established in almost all laboratories worldwide and it has been used as an expression host for decades. It is easy to handle in large scale cultivations, grows very fast on comparably cheap media and a lot of effort has been put into the development of strains to obliterate the drawbacks of this organism (Blount, 2015; Terpe, 2006). These include strains that are free of endotoxins like pyrogenic lipopolysaccharides, strains with an increased ability to promote disulfide bridge formation and strains that are able to perform *N*-glycosylation on heterologous proteins (Huang et al., 2012; Mamat et al., 2015; Messens and Collet, 2006; Valderrama-Rincon et al., 2012). Other prokaryotes that are widely used in the field of protein expression are *Bacillus* or *Pseudomonas* species, mainly due to their ability to efficiently secrete proteins into the medium (Degering et al., 2010; Terpe, 2006; van Dijk and Hecker, 2013). However, as a lot of bacteria produce

virulence factors or toxins, they are mostly not the first choice for the expression of pharmaceutically relevant products.

The pharmaceutical industry is focusing mainly on eukaryotic expression systems which are often capable of essential posttranslational modifications and in many cases safe to handle. These platforms are very diverse and include yeasts and other fungi, insects, mammalian cell culture, cell free systems, and genetically modified animals and plants (Adrio and Demain, 2010; Berlec and Štrukelj, 2013; Demain and Vaishnav, 2009). To date most approved biopharmaceuticals are produced in mammalian cell lines as they are capable of human-like posttranslational modifications. This is crucial for proper action of several therapeutic proteins such as interferons or erythropoietin, and to avoid immune reactions (Berlec and Štrukelj, 2013; Gerngross, 2004; Wurm, 2004). In large scale applications Chinese hamster ovary cell lines (CHO) and other rodent derived cell lines are mainly used (Berlec and Štrukelj, 2013). Genetically modified animals secrete proteins into their blood, milk or urine from where the product can be gathered. Those systems share the problem that generation of cell lines is very cost and time consuming and the use of transgenic plants or animals is socially still not widely accepted (Maksimenko et al., 2013; Thomas et al., 2011). In contrast, fungal expression systems can be established and manipulated a lot faster and easier. They are generally efficiently genetically amenable, safe to handle and share a lot of beneficial characteristics with bacterial organisms (Feldbrügge et al., 2013; Gerngross, 2004; Punt et al., 2002). Besides filamentous fungi like *Trichoderma reesei* or *Aspergillus* species, yeasts are of great interest for heterologous protein production (Berlec and Štrukelj, 2013; Ward, 2012). They have comparably high space-time-yields and can be cultivated in large scale bioprocesses. They have the ability to perform common posttranslational modifications and often have highly efficient inherent secretion machineries. The latter is very important with regard to downstream processing, being the most cost intensive factor especially in pharmaceutical industry (Berlec and Štrukelj, 2013; Mattanovich et al., 2012). Commonly exploited yeast systems are *Saccharomyces cerevisiae*, *Kluyveromyces lactis* and *Pichia pastoris* (Berlec and Štrukelj, 2013). As research and strain development for *S. cerevisiae* has been conducted for more than a century it is to date the first choice in biopharmaceutical protein expression. It is furthermore classified as GRAS (generally regarded as safe) organism, capable of posttranslational modification, and able to secrete proteins in relevant amounts. Around 15 % of the approved pharmaceuticals are produced in *S. cerevisiae* (Berlec and Štrukelj, 2013). With 1 % share of the approved biopharmaceutical production, *P. pastoris* is used less frequently although it displays some key advantages. The secretion machinery that is based on an extremely strong methanol inducible alternative oxidase promoter (AOX1) can be used to secrete grams per liter on a very affordable carbon source (Ahmad et al., 2014).

Nevertheless, methanol is absolutely undesired in pharmaceutical products and therefore this system is mostly not preferred.

The major drawback of protein expression and secretion with fungal organisms is their extremely high proteolytic potential (de Souza et al., 2015; Mattanovich et al., 2004; Ward, 2012). Especially in filamentous fungi this can cause severe product loss. Another problem is posttranslational modification. Albeit it can be necessary to have glycosylation on an active protein, the consequences of wrong glycosylation patterns can be disastrous. This is especially a problem in human medicine as severe immunogenic reactions can occur upon treatment with proteins harboring foreign glycosylation patterns (Gerngross, 2004). Thus the demand for specialized systems for the expression of proteins with a wide variety of requirements is tremendously high. In order to provide cost efficient downstream processing, systems in which proteins are secreted are generally preferred.

1.2 Classical and unconventional protein secretion

Secretion in general describes the translocation of a molecule or protein from the intracellular space throughout a membrane or cell wall into the environment (Economou et al., 2006; McCotter et al., 2016; Rabouille et al., 2012). It constitutes a key property for the survival of microorganisms and is involved in diverse processes like nutrition, reproduction or infection.

1.2.1 Diversity in secretion mechanisms

Organisms in all three kingdoms of life have developed secretion machineries with a wide variety of function and shape.

In prokaryotic organisms secretion is mainly used for cargo to either be transported to the periplasmic space, to be inserted into the cell envelope or to be injected into another organism. As prokaryotic organisms do not have cell organelles, translocation of the cargo is mediated directly across the plasma membrane via pore-transporter complexes. The two basic export mechanisms are the Sec- and the Tat- machinery (twin-arginine motif), enabling export of unfolded and completely folded proteins, respectively. The Sec translocon is homologous to the secretory pore in eukaryotes and secretion is mediated by an N-terminal signal sequence while the Tat pathway is Sec independent and secretion is determined by two arginine residues (Natale et al., 2008). In order to span the distance and barriers of gram-negative bacterial cell envelopes or the thick peptidoglycan layer of gram-positive bacteria, multiple additional secretion strategies have evolved in procaryotes, involving sophisticated needle-shaped nanomachines and transporters (Costa et al., 2015; Economou et al., 2006).

In eukaryotic organisms most secreted proteins are equipped with an N-terminal signal sequence. Such a canonical signal peptide, consisting of 6 to 12 amino acids, is the key for the protein to be guided through the so called conventional secretion pathway (Fewell and

Brodsky, 2009; Nickel and Rabouille, 2008; Walter et al., 1982). After translation of the signal peptide by a cytosolic ribosome this sequence is recognized by a multi protein complex termed signal recognition particle (SRP) and translation is stopped. The SRP guides the bound ribosome-mRNA complex to the endoplasmic reticulum (ER), where the signal peptide is transferred to the translocon. Here the signal peptide is cleaved off and the membrane bound ribosome continues translation of the polypeptide chain into the ER lumen (Walter and Lingappa, 1986; Walter et al., 1982). After cotranslational translocation into the ER various chaperones and oxidoreductases located in the ER assist in the correct folding and the formation of disulfide bridges. Despite the cotranslational entry of proteins into the ER, several proteins have been found to enter the ER in a fully folded state (Johnson et al., 2013). This posttranslational transport is mediated by chaperones guiding the protein to the ER residing import machinery (Ellgaard et al., 2016; Fewell and Brodsky, 2009). The calnexin-calreticulin system and other chaperones like the immunoglobulin binding protein (BiP) are highly abundant in the ER and in charge of quality control. If a protein is terminally misfolded it is finally retro-translocated into the cytoplasm and subsequently degraded in the proteasome by a mechanism referred to as 'endoplasmic reticulum associated degradation' (ERAD) (Kleizen and Braakman, 2004; Walter et al., 1982). If unfolded or misfolded proteins accumulate in the ER, the unfolded protein response (UPR) is initiated. It involves the upregulation of chaperone synthesis, degradation of misfolded proteins and translation inhibition (Heimel, 2014; Vembar and Brodsky, 2008). Besides folding the ER is the organelle where posttranslational modifications are performed. The most important one is *N*-glycosylation. Initially an oligosaccharide core consisting of two N-acetylglucosamine, nine mannose- and three glucose residues is added to the peptide. This core structure is highly conserved throughout most eukaryotic organisms. The core is then individually modified by each organism during the following secretion process (Fernández-Álvarez et al., 2010; Schwarz and Aebi, 2011). Proteins that pass the quality control are then guided to the *cis* Golgi in COPII coated vesicles (coat protein complex). Retrograde transport from *cis* Golgi to *trans* ER is mediated by COPI coated vesicles enabling the direct recycling of ER components. At the Golgi apparatus, the vesicle incorporated proteins are recognized by so called tethering complexes and Golgi specific SNARE proteins (soluble N-ethylmaleimide-sensitive-factor attachment protein receptor), leading to the fusion of the vesicle and the Golgi membrane. In the Golgi further posttranslational modifications, such as O-glycosylation take place. The main task of the Golgi apparatus is then correct sorting and distribution of the proteins. The proteins are again incorporated into destination specific vSNARE coated vesicles that guide them to their tSNARE coated destination membrane. Final destinations include organelles, the plasma membrane or secretion into the cell exterior (Fig. 1.1; Lee et al., 2004; Rabouille et al., 2012).

It is well established that the vast majority of secreted proteins in eukaryotic organisms is passing through the above described conventional secretion pathway. Nevertheless, several proteins lacking an N-terminal signal peptide have also been found to be secreted (Nickel, 2005). Most of these so-called unconventionally secreted proteins are related to cell survival, immune surveillance and tissue organization. Typically unconventional secretion has been found to be induced by stress conditions (Rabouille et al., 2012). This could also be an explanation for the requirement of alternative secretion systems as stress responses might need to be very rapid and independent from the capious quality control machinery in the ER (Kleizen and Braakman, 2004). Another explanation for alternative secretion pathways is that several proteins must not be glycosylated to exhibit correct function and the oxidative environment in the ER could hinder proper folding. Secreted proteins that bind sugar moieties such as lectins, can simply not pass the ER, as they would get stuck by binding ER residing sugars (Nickel, 2003; Nickel, 2007). To date, four major types of unconventional secretion, separated into vesicle and non-vesicle based mechanisms, have been discovered (Fig. 1.1; Nickel and Rabouille, 2008; Rabouille et al., 2012). Type I is based on the self-sustained protein translocation across plasma membranes, triggered by binding of lipids. A very well studied example is the fibroblast growth factor 2 (FGF2) which, after being fully folded, binds to $\text{PtdIns}(4,5)\text{P}_2$ (phosphatidylinositol(4,5)-bisphosphate) and after subsequent

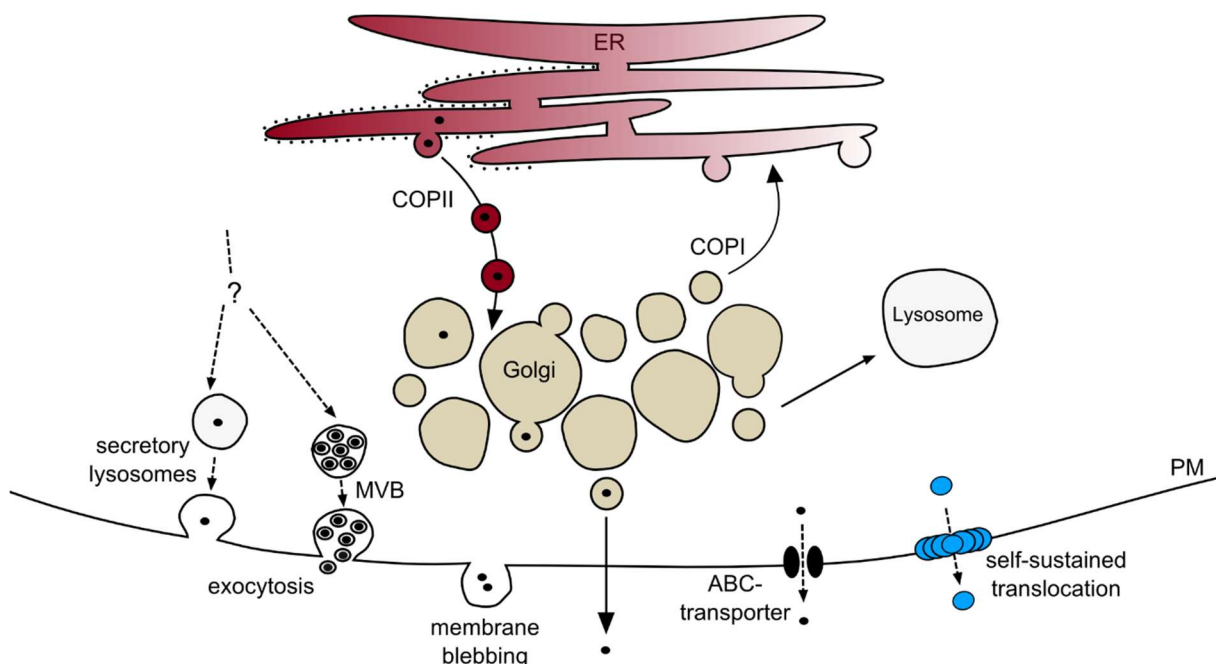


Fig. 1.1: Schematic representation of conventional and unconventional protein secretion in eukaryotes

Schematic representation of conventional and unconventional secretion mechanisms. Conventional secretion is initiated by co-translational translocation of the protein into the ER. The proteins are then transported to the Golgi apparatus in COPII coated vesicles and subsequently secreted via membrane fusion events. Alternatively proteins can be directed to other intracellular compartments like the lysosome, or can be integrated into the membrane. Unconventional secretion mechanisms are bypassing the ER and are divided into vesicular and non-vesicular mechanisms. Vesicular mechanisms include exocytosis via secretory lysosomes or multivesicular bodies as well as 'membrane-blebbing' or microvesicle shedding events. Non-vesicular mechanisms include the active export via ABC transporters or self-sustained translocation by pore formation. The model is adapted from Nickel and Rabouille, 2008; Rabouille et al., 2012 and Steringer et al., 2014.

phosphorylation forms hexameric structures. These hexameric rings are then opening and stabilizing a lipid pore in the membrane enabling translocation of FGF2 monomers. These bind to heparan sulfates on the outer leaflet of the membrane. (La Venuta et al., 2015; Rabouille et al., 2012; Steringer et al., 2014). Another prominent example for Type I unconventional secretion is the HIV-Tat protein (HIV-1 trans-activator of transcription) that is essential for viral gene expression during HIV infection (Zeitler et al., 2015). The second non-vesicular mechanism (type II) is based on membrane localized ABC transporters, transporting lipidized peptides across the membrane. The pheromone α -factor of *S. cerevisiae* is an example, being secreted unconventionally via the Ste6p ABC transporter (Michaelis, 1993; Rabouille et al., 2012). Type III unconventional secretion describes export that is driven by autophagosome-like vesicles. It has been proposed that those processes might involve a broad set of vesicle types including secretory lysosomes, microvesicles and multivesicular bodies (MVB). Well-studied cases for type III unconventional secretion are the inflammatory related protein interleukin 1 β (IL 1 β) and the acyl-CoA binding protein Acb1 from *S. cerevisiae* (Rabouille et al., 2012; Rubartelli et al., 1990). In the case of Acb1 autophagosome-like vesicles form at CUPS (compartment for unconventional protein secretion) and subsequently fuse with endosomes, resulting in MVBs (Curwin et al., 2016; Rabouille et al., 2012). Protein secretion that is resistant to brefeldin A treatment is defined as type IV unconventional secretion. Brefeldin A blocks the ER to Golgi transport, indicating that type IV secreted proteins are bypassing the Golgi. The mechanism is poorly understood but numerous examples have been found, including adhesion molecules like the integrin α PS1 from *D. melanogaster* or transmembrane proteins like CFTR (cystic fibrosis conductance regulator) (Gee et al., 2011; Rabouille et al., 2012; Schotman et al., 2008).

In many cases the underlying mechanisms still remain to be further investigated but a lot of examples already show that unconventionally secreted proteins might contribute more to the overall secretome than assumed so far.

1.2.2 Exploiting unconventional secretion for export of heterologous proteins

The application of unconventional secretion pathways for biotechnological purposes is a novel idea of great potential and interest. The lack of *N*-glycosylation occurring during ER passage for example is very beneficial for the expression of pharmaceutical proteins as host-unlike glycosylation patterns can cause severe immunogenic reactions (Walsh and Jefferis, 2006). Furthermore clogging of the conventional ER to Golgi pathway is a problem when it comes to an accumulation of proteins in the ER due to overexpression and subsequent secretion, especially with regard to very large proteins (Heimel, 2014; Mattanovich et al., 2004).

Recently, unconventional secretion has indeed been exploited for the first time for protein production in the smut fungus *Ustilago maydis*. Beforehand, unconventional secretion in this fungus had been demonstrated for the chitinase Cts1. The enzyme had been identified during basic research on long distance mRNA transport in a differential proteomic approach (Koepke et al., 2011). In this study it was shown that wild type filaments showed extracellular chitinase activity while in strains lacking a central protein for mRNA transport in fungal hyphae, Rrm4, this activity was strongly reduced (Koepke et al., 2011). As no classical N-terminal secretion signal could be found for Cts1 the idea of unconventional secretion arose. A Gus reporter system was used to verify that it is indeed unconventionally secreted. In addition, it could be shown that export also works in yeast like cells where it is independent of RNA transport (Fig. 1.2, Stock et al., 2012). In a recent study Cts1 export could furthermore be linked to cell separation. This is in line with its biological function in chitin degradation which it fulfills in concert with a second, conventionally secreted chitinase, Cts2 (Langner et al., 2015).

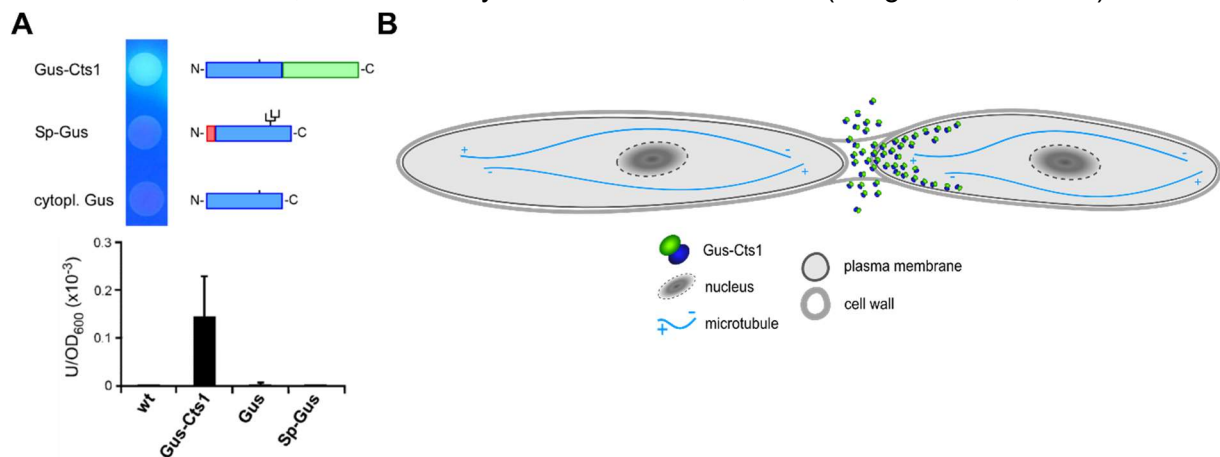


Fig. 1.2: Cts1-mediated unconventional protein secretion

A. β -Glucuronidase (Gus) reporter system to assay unconventional secretion. Gus plate (upper panel) and liquid assay (lower panel) results for different Gus reporter *U. maydis* strains. Gus-Cts1 fusion proteins show extracellular activity, determined through hydrolysis of the chemifluorescent substrate X-Gluc, indicating unconventional protein secretion. Signal-peptide fused Gus (Sp-Gus) does not show any extracellular activity, due to conventional secretion, N-glycosylation and subsequent inactivation. Wildtype (wt) and cytoplasmically expressed Gus (cell lysis control) do not show any activity. Figure modified from Stock, 2013; Stock et al., 2012. **B.** Schematic model of unconventional Gus-Cts1 fusion protein secretion in late stage of cell separation. Fusion protein is directed in a gradient manner from the daughter cell into the fragmentation zone. Single components are explained in the legend below the scheme.

In contrast to most secretory systems that are limited in the size of the secreted cargos proteins up to at least 173 kDa could be secreted using the Cts1 mediated pathway (Stock et al., 2012). To exploit the feature of unconventional secretion on heterologous protein expression in *U. maydis*, initial studies concentrated on the expression of Cts1 guided export of bacterial enzymes, different antibody formats and cofactor dependent enzymes. Using these proof of principles, scFv-Cts1 fusion protein directed against the c-myc epitope could successfully be secreted (Sarkari et al., 2014). The functional secretion of cofactor dependent peroxidases showed that cofactor integration as well as disulfide bridge formation is possible, using the Cts1-mediated pathway (Reindl, 2016). However, pitfalls so far were the overall low yields and

poor stability of the secreted constructs which could be mainly related to intrinsic proteases. Hence, optimization steps at different levels are needed to be conducted to further improve the system.

1.3 *U. maydis* – From basic research to applied science

The phytopathogenic fungus *U. maydis* is the causative agent of corn smut disease. It belongs to the family of *Ustilaginales* which are also termed smut fungi and share the characteristic to infect crop plants. *U. maydis* is a biotrophic pathogen with a very narrow host range infecting only maize (*Zea mays*) and its ancestor Teosinte (*Zea mays* subsp. *parviglumis*). Infection of maize plants results in the formation of galls in all aerial plant organs especially in the flowering tissue and the maize cobs. These galls are filled with heavily melanized teliospores being the final result of plant colonization. After maturation the galls burst and are thus name giving as this leads to a burned like appearance of infected maize plants (lat.: *ustilare* = burned) (Banuett, 1992; Christensen, 1963). Interestingly, heavily infected maize cobs are consumed as a delicacy in Central America mainly boiled and canned as ‘cuitlacoche’ or ‘corn smut’ (Fig. 1.3; Banuett, 1992; Feldbrügge et al., 2013; Vollmeister et al., 2012). *U. maydis* has a biphasic life cycle, undergoing a dimorphic switch from a haploid yeast like to a diploid hyphal state. The yeast like or sporidial state resembles the vegetative growth stage of the fungus in which it proliferates by budding. After recognition of a compatible mating partner, regulated by a biallelic mating type system, cells form conjugation hyphae, fuse and form a dicaryotic hypha. Hyphal, unipolar filamentous growth is a prerequisite for infection and enables the penetration of the plant tissue using appressoria-like structures. *In planta* the fungal mycelium proliferates primarily along the vascular bundles, fragmentizes and the fragments undergo meiosis, leading to the formation of teliospores. Haploid cells can again germinate from teliospores closing the

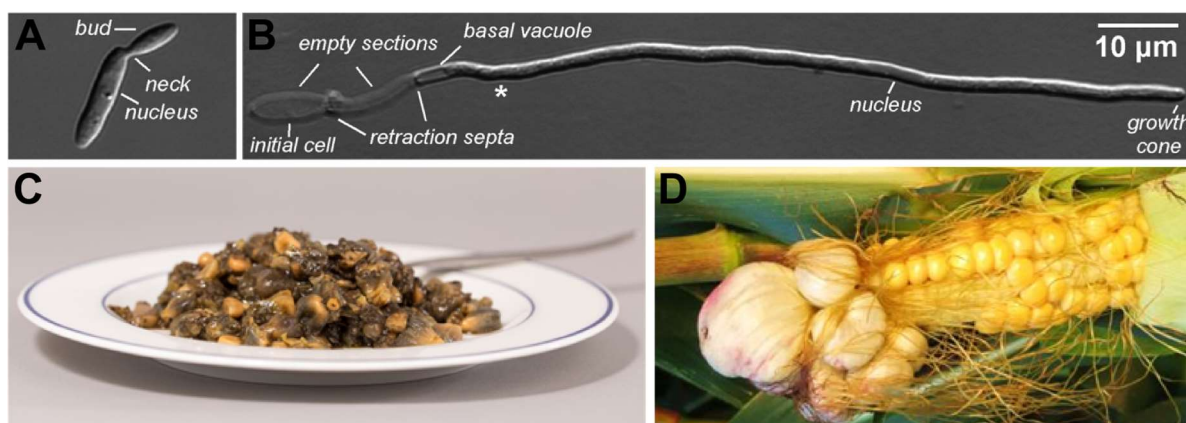


Fig. 1.3: The corn pathogen *U. maydis*

Microscopic differential interference contrast picture of a *U. maydis* yeast like growing haploid sporidium (A) and a haploid *U. maydis* AB33 filament (B). Pictures are modified from (Vollmeister et al., 2012a). C. Cooked and ready to eat corn smut galls. In this form infected corn cobs are sold as the delicacy “Cuitlacoche”. Picture by J. Köhler (HHU Düsseldorf). D. Corn cob infected by *U. maydis* with teliospore filled galls.

life cycle of *U. maydis* (Banuett and Herskowitz, 1989; Brefort et al., 2009; Feldbrügge et al., 2004; Vollmeister et al., 2012b).

The fact that *U. maydis* can be cultivated as haploid sporidia in submerged culture (Fig. 1.3 A) and on agar plates led to an early interest in studying the fungus as a eukaryotic model organism (Christensen, 1963; Holliday, 1974). A lot of basic research has been performed with *U. maydis* over the last century. Pioneering studies on DNA repair mechanisms and homologous recombination have been conducted in the 1960s and 1970s. Robin Holliday was first to describe the 'Holliday-Structure' and in later studies discovered key components of the DNA-repair machinery like the Rec1 exonuclease (Holliday, 1964; Holliday, 1974). Nowadays, plant-pathogen interaction is a major focus in *U. maydis* research (Brefort et al., 2009; Dean et al., 2012; Djamei and Kahmann, 2012; Matei and Doeblemann, 2016). Furthermore, the unipolar growth mode has set a focus on studying molecular mechanisms of microtubule dynamics and long distance transport in eukaryotic cells (Göhre et al., 2012; Pohlmann et al., 2015; Wedlich-Söldner et al., 2002; Zander et al., 2016). The extensive investigations resulted in a large molecular toolbox applicable for *U. maydis*. Since 2006 the genome sequence of *U. maydis* is freely available and manually annotated with high quality (Kämper et al., 2006). The *U. maydis* homologous recombination system is highly efficient and allows stable genetic manipulations such as reporter-gene fusions, genomic integration or deletion (Brachmann, 2001; Brachmann et al., 2004; Spellig et al., 1996). The advantage of using homologous recombination is the stability of resulting strains. In the stable strains there is no need to keep selection pressure with the presence of antibiotics in the media, which might be harmful and difficult to clear off in downstream applications. Thus, industry always prefers antibiotic-free cultivation (Kavšček et al., 2015). Besides gene deletions, defined loci can be used for stable integrations. The most frequently used is the *ip^S*-locus (Brachmann, 2001; Brachmann et al., 2004; Loubradou et al., 2001). The locus encodes the iron-sulphur protein subunit of succinate dehydrogenase and a single amino acid exchange can be attributed to the sensitivity of the fungus towards the systemic fungicide carboxin. A mutated version of this allele (*ip^R*) where the amino acid exchange is withdrawn from the encoded protein conveys resistance towards carboxin. By using constructs for genomic integration where parts of the *ip^R*-allele are used as flanking regions for homologous recombination, selection for integration can be performed on carboxin containing media. After verification of the integration by analytic methods no further use of antibiotics is required to keep the construct in the genome (Broomfield and Hargreaves, 1992; Stock et al., 2012). Furthermore, a set of fluorescence markers, antibiotic resistance markers and constitutive as well as inducible promoters has been established (Brachmann et al., 2004; Feldbrügge et al., 2013; Loubradou et al., 2001; Zarnack et al., 2006). Sophisticated cloning systems and strategies based on plasmid libraries containing the above mentioned elements have been developed and adjusted to state of the art cloning methodology. This

enables an efficient generation of mutants (Brachmann et al., 2004; Terfrüchte et al., 2014). Very important in the history of *U. maydis* research was the development of strains that are solopathogenic and thus do not need to mate prior to infection (Bölker et al., 1995; Djamei et al., 2011; Kämper, 2004). The same holds true for the laboratory strain AB33 harboring the responsible genes for filamentous growth under control of an inducible promoter (Fig. 1.3 B; Brachmann, 2001). These strains enable fast infection studies and give the possibility to study filamentous growth related phenomena in haploid strains using liquid cultures, independent of the plant. Endosomal transport of mRNA cargo throughout the filament has thereby been identified as a crucial factor in determining and maintaining the axis of polarity in filaments (Becht et al., 2005; Becht et al., 2006; Göhre et al., 2012; Pohlmann et al., 2015).

Recently the research interests expanded towards biotechnological applications (Feldbrügge et al., 2013; Klement et al., 2012; Sarkari et al., 2014; Stock et al., 2012). Prerequisites for successful use in biotechnological industry are mainly a short generation time, easy cultivation and robustness. Axenic *U. maydis* cultures have a doubling time of around two hours and strong agitation in combination with baffles does not harm the cells fitness. Due to its chitin containing cell wall, *U. maydis* is also very tolerant towards high osmotic stress conditions and thus enabling the use of high salt, sugar or buffer concentrations. *U. maydis* produces a variety of high value metabolites and enzymes such as itaconic acid, malate, lipases or glycolipids that are of industrial interest (Bölker et al., 2008; Buerth et al., 2014; Geiser et al., 2016a; Hewald et al., 2005). The *U. maydis* lipase Uml2 for example has been identified as a homolog of the widely used *C. antarctica* CalB but displays an additional phospholipid hydrolysis activity. This makes it an interesting biocatalyst for biotechnological processes (Buerth et al., 2014). The ability to express mannosylerythritol lipids and ustilagic acid that exhibit for example biosurfactant and antimicrobial activity is also a subject to investigations (Hewald et al., 2005; Hewald et al., 2006; Teichmann et al., 2007). It was shown recently that it is possible to uncouple the pathways from nitrogen-limitation enabling the constitutive production of these high value compounds (Rodríguez Estévez, 2016). Successful cultivation on alternative carbon sources and a broad hydrolytic enzyme arsenal provide *U. maydis* with the potential for use in future industrial valorization approaches from organic waste streams (Geiser et al., 2016b). Finally, the fungus possesses both the conventional and the Cts1-mediated unconventional secretion machinery that provides the export of proteins of interest into the culture medium and enables an efficient downstream processing (Djamei et al., 2011; Feldbrügge et al., 2013; Steinberg and Schuster, 2011; Stock et al., 2012). As the molecular understanding and the technical prerequisites are given the way is paved to develop *U. maydis* from a model organism to a versatile industrial protein and metabolite production platform. In this thesis, the secretory production of proteins using unconventional secretion and the optimization of this process in *U. maydis* are in the focus.

1.4 Transforming *U. maydis* into a protein expression platform

In nature microorganisms of course did not evolve to express vast amounts of non-essential proteins. Establishing an organism as an expression platform for heterologous proteins thus requires the optimization of multiple parameters on the genetic and process based level. Intense genetic modifications were performed for example on *E. coli* or *S. cerevisiae* in order to transform them into efficient and flexible expression hosts (Huang et al., 2012; Kavšček et al., 2015). Similar strategies do now need to be applied to *U. maydis* in order to increase yields and stability of protein produced via unconventional secretion.

1.4.1 Strain engineering

One of the big advantages of using eukaryotic organisms, especially fungi, over prokaryotic organisms is the ability of some to inherently secrete huge amounts of proteins into the supernatant (Berlec and Štrukelj, 2013). This facilitates the downstream processing a lot. Unfortunately, the vast amount of secreted proteins by fungi are hydrolytic enzymes as they are used to explore nutritional resources in their natural environment (Puxbaum et al., 2015; Ward, 2012). Among these are a lot of proteolytic enzymes being counterproductive with regard to the secretion of proteins into the supernatant. As long as the expressed product of interest is of host origin it is not directly prone to degradation. This changes when heterologous proteins are expressed that are not essential to the host (Ward, 2012). To tackle this, expensive protease inhibitors can be used in cultivation media that can result in a reduced growth and fitness. Especially for the production of proteins used for medical purposes this is not desired as these substances would have to be cleared off from the product (Bonnerjea, 2004). Another strategy is the elimination of proteases to reduce degradation. As fungi often have multiple proteases it is a complex task to tackle this problem. In *S. pombe* the deletion of multiple proteases led to an increased stability of heterologous proteins in the supernatant (Idiris et al., 2006). Similar approaches have been conducted in *U. maydis*. In one approach, the pre-pro-protease convertase Kex2 had been deleted resulting in a drastically reduced proteolytic potential. Unfortunately the deletion also resulted in a severe cell separation defect which reduces cell growth (Sarkari et al., 2014). Another disadvantage of this approach is the fact that Kex2 itself activates multiple other proteases that cannot be clearly predicted and therefore deletion of *kex2* is a rather rough approach (Brenner and Fuller, 1992; Sarkari et al., 2014). The second deletion strategy for proteases in *U. maydis* was the result of a secretome analysis showing that at least 26 proteases are secreted by the fungus (Sarkari, 2014). Using a FLP-FRT based recombination system, a total of five proteases also known to be harmful from other systems could sequentially be deleted in one single strain (Khrunyk et al., 2010; Sarkari et al., 2014; Terfrüchte et al., 2014). The resulting strain showed a radically reduced proteolytic potential without any detrimental effects for the cells (Sarkari et al., 2014).

To achieve high protein yields, a very important factor is the regulation of the transcription machinery as higher amounts of transcripts in most cases lead to higher amounts of translated protein. A very straight forward approach to regulate the transcription rate is to choose a suitable promoter (Ward, 2012). For some proteins it can even be beneficial to use inducible promoters as the generation of biomass requires a lot of energy that is thus not available for protein expression during growth phases (Berlec and Štrukelj, 2013). Inducible promoters are also beneficial for the production of toxic or antimicrobial substances as these often inhibit growth. It should also be considered that the promoter should not be too strong as this might be harmful to the cells. Especially when it comes to secretion, clogging of the ER to Golgi pathway can become a problem (Heimel, 2014; Mattanovich et al., 2004). In *U. maydis* a promoter screen with a variety of heterologous and homologous constitutively active promoters had been conducted and two very promising promoters have been selected for use in the expression system (Reindl, 2013) - on the one hand the medium strong P_{otef} promoter and on the other hand the very strong P_{oma} promoter (Hartmann et al., 1999; Sarkari et al., 2014; Spellig et al., 1996; Stock et al., 2012). As increased amounts of transcripts have to be efficiently processed, it is the corollary to optimize the tRNA availability for an efficient translation. In several *E. coli* strains, plasmids with rarely used codons have been introduced to support translation efficiency (Novy et al., 2001). If conventional secretion is used to export the product, it can also be of importance to screen for a suitable signal peptide as not all lead to the same secretion efficiency (Degering et al., 2010). Another approach is the adjustment of the translated products coding sequence to the codon usage of the expression host. For most expression systems it has become a standard technique to codon optimize the sequence of interest prior to cloning (Puigbò et al., 2007). Studies showed that for example AT rich regions can lead to premature polyadenylation and thus translation termination (Zarnack et al., 2006). A very accurate dissection of the codon usage led to the development of a dicodon usage table that can be applied to optimize the coding sequences of heterologous proteins for expression in *U. maydis* (Zarnack et al., 2006).

Despite the coding sequence of the protein of interest, it is also crucial to pay attention to the design of the expression construct. In *E. coli* it is often advantageous to fuse solubility tags to heterologous proteins or use co-expressed chaperones to increase solubility of the recombinant protein (Costa et al., 2014).

Depending on the further fate of the protein, it is also often necessary to purify the protein from the cytosol or from supernatants (Graslund, 2008). This requires purification tags on the one hand but can also be facilitated via size exclusion chromatography or antibody-based 'trap' systems (Graslund, 2008; Rothbauer et al., 2007; Schmidt et al., 1996; Terpe, 2003). If fusion proteins are expressed where only one part is of interest, the introduction of protease cleavage sites is advisable. A broad set of proteases that specifically hydrolyze peptides at a defined

recognition site is already available (Waugh, 2011). The most frequently used is the Tobacco etch virus derived TEV protease but proteases with other reaction conditions and specificities like the Human rhinovirus 3C protease (HRV 3C) or the SUMO protease from *S. cerevisiae* are gaining more and more interest (Waugh, 2011). Taking all of this information into account, the two standard integrative expression vectors pRabX1 and pRabX2 were designed for use in *U. maydis* (Fig. 1.4). pRabX1 consists of the gene of interest fused 5' to an SHH detection and purification linker (One-STrEP®-tag, a 3xHA-tag and a 10xHistag), followed by *cts1* encoding the secretion carrier (Stock, 2013). The construct is under the control of the constitutive P_{otef} promoter and terminated by the T_{nos} terminator on the 3'-end. For stable integration into the *U. maydis* genome, an ip^R allele is present on the vector (Brachmann, 2001; Spellig et al., 1996; Stock et al., 2012). To increase the variability of the vector, unique endonuclease recognition sites were integrated upstream and downstream of each element (Stock, 2013). The second expression construct pRabX2 consists of a 5' P_{oma} promoter, followed by a 10xHis-tag, the gene of interest, a TEV-protease cleavage site, a 3xHA-tag for detection, the Cts1 carrier and the T_{nos} terminator. This construct (Fig. 1.4 D) now enables not only secretion and purification of the respective fusion protein but also gives the opportunity to cleave off the protein of interest, getting rid of the Cts1 carrier molecule (Sarkari, 2014; Terfrüchte, 2013). Albeit these vectors are highly flexible and could already be used to express a proof of principle target portfolio in *U. maydis* (Reindl, 2013; Reindl, 2016; Sarkari et al.,

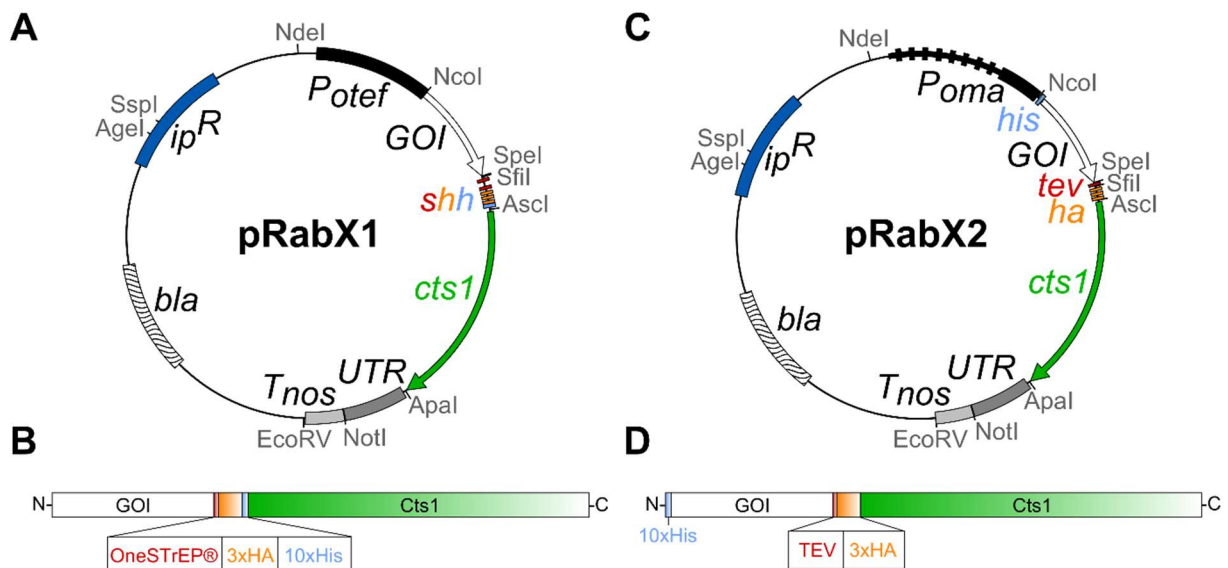


Fig. 1.4: Schematic representation of the expression plasmids pRabX1 and pRabX2

A. pRabX1 contains the expression cassette for a gene of interest (GOI) under the control of the P_{otef} promoter (black). The GOI can be inserted via *NcoI*/*SpeI* restriction and is expressed in fusion with a SHH linker (One-STrEP® = red, 3xHA = orange, 10xHis = light blue) and the Cts1 protein (green). The *ubi1* 3' UTR (dark grey) links the expression cassette to the T_{nos} terminator (light grey). For homologous recombination in *U. maydis*, the plasmid carries an ip^R allele (blue) and for selection in *E. coli*, the ampicillin resistance mediating β -lactamase (*bla* = wavy) is encoded. **B.** Schematic representation of the pRabX1 corresponding protein. **C.** pRabX2 is built up on the same vector backbone as pRabX1. The expression cassette has been exchanged by restriction with *NdeI*/*Apal* and encodes for a 10xHis-tag (light blue), followed by the GOI, a TEV-protease cleavage site (red), a 3xHA-tag (orange) and Cts1 (green). Expression is controlled by the P_{oma} promoter (black). **D.** Schematic representation of the pRabX2 corresponding protein.

2014; Stock et al., 2012), optimization on the construct level turned out to be always highly depending on the protein and the expression host. Thus it needs to be adjusted from case to case and on the respective designated application.

1.4.2 Process engineering

Despite the optimization of the organism and the product itself, having a close look on the process related parameters is crucial to maximize the efficiency of the expression system. Typically organisms used for expression were previously studied in basic research and a set of cultivation media and techniques is already available. Anyway, as these are usually not focusing on expression they need to be adjusted. This includes nutrition, predominantly carbon- and nitrogen sources, pH conditions and if necessary inducer compounds (Stöckmann et al., 2014).

The most difficult part in defining a suitable expression medium is to minimize costs and maximize product formation. Here the trend is leading towards the use of organic waste streams from agriculture as they usually exhibit huge unused nutritional value. As previously mentioned, fungi are often naturally feeding on plant material and are thus often able to use those organic materials (Geiser et al., 2016b; Klement et al., 2012). In parallel to the growth medium, it is important to adjust the cultivation conditions. Growth and behavior of cells in small laboratory scale formats such as glass tubes or shaking flasks can drastically change when transferred into large-scale cultivations (Anderlei et al., 2004; Wewetzer et al., 2015). Especially agitation and stirring conditions need to be considered. As it is desired to obtain high cell densities, stirring can become problematic as inefficient mixing leads to inefficient distribution of oxygen (Knoll et al., 2005). A simple technique to support the stirring procedure is the installation of turbulence inducing baffles into the bioreactor or shaking flask. By using pressurized bioreactors, the viscosity of high density cultures can be reduced and thereby efficient oxygen transfer into the medium can be maintained for higher cell densities (Knoll et al., 2005). Most organisms have temperature optima above room temperature (defined as 22°C). Thus, it is necessary to have temperature control during cultivation. As this requires a lot of energy, it represents a major cost factor (Knoll et al., 2005). A very important aspect in process optimization is the so called 'space-time yield', meaning that the overall goal is to use the minimal volume over a minimal period of time, resulting in the maximal amount of product (Klement et al., 2012; Puxbaum et al., 2015). To tackle this problem, the use of microorganisms with comparatively small size and short doubling times is desired. Additionally a wide range of cultivation systems has been developed to maximize the output (Akgün et al., 2004; Knoll et al., 2005; Wewetzer et al., 2015). If for example the product is only produced in a certain growth phase, continuous cultivations are preferred to keep the cells in the production state as long as possible. To do so, mainly fed-batch processes are being developed, using for example the constant addition of fresh medium (Akgün et al., 2004; De Gooijer et al., 1996; Rodolfi et al.,

2003). These can also have the advantage that in case of secreted product, the product can be continuously purified from the cultivation broth and medium can be recycled into the process (Weilhammer and Blass, 1994). This technique is also used for immobilized-cell cultivations where cells are fixed on surfaces, medium is constantly passing the cells and taking the product with it (Najafpour et al., 2004). A lot of investigations have to be conducted to define the optimal conditions for the above mentioned parameters. This development phase highly contributes to the overall production costs. To minimize the time frame for establishment of the expression process, high throughput tools have been developed. These allow to get deep insights into the cells condition during cultivation with varied parameters (Anderlei and Büchs, 2001; Anderlei et al., 2004; Wewetzer et al., 2015). A general indicator for metabolic activity and thus productivity of a cell is the OTR (oxygen transfer rate). This defines the overall amount of consumed oxygen and is thereby a projection of the cells respiration. For aerobe microorganisms, most processes linked to protein expression are oxidative and thus contribute to the OTR increase (Baez and Shiloach, 2014; Klement et al., 2012; Knoll et al., 2005). To monitor the OTR, sophisticated online monitoring systems have been established and successfully applied to optimize processes (Anderlei et al., 2004; Kensy et al., 2009). Besides online monitoring of the respiration, the formation of undesired byproducts as well as consumption of nutrients and its influence on the overall process has to be monitored. Mathematical prediction and the automation of such monitoring processes using high throughput methods and robotic systems is simplifying the work and speeding up the development of biotechnologically derived products (Knoll et al., 2005). The establishment and optimization of a biotechnological production process in general is very complex and still needs to be carefully planned for each and every new product and adapted to the respective organism.

Until now protein expression approaches in *U. maydis* have been performed using processes and cultivation conditions designed for basic research. It can be anticipated, however, that the requirements may be very different for efficient protein production. Hence, this gap needs to be filled using the described methods to establish a competitive expression platform.

1.5 Biopharmaceuticals as export targets for unconventional protein secretion

The pharmaceutical industry has traditionally used chemical compounds and natural molecules either isolated from natural resources like plants, fungi or animals, or from chemical synthesis. As it comes to availability, yield and effectiveness, the isolation of molecules from natural resources rapidly reaches its limits. To increase flexibility and yield, the production of proteinaceous pharmaceuticals in microorganisms turned out to be substantial. In 1922 the first proteinaceous biopharmaceutical, insulin, was produced by Banting and Best. As the

isolation of the molecule from pancreatic tissue was very expensive and often caused adverse effects, there was still need for further development. After successful solution of the protein structure, insulin was produced by chemical synthesis in 1963, albeit with very poor yields (Tattersall, 1995). Only with the mass production of human insulin in bacteria, insulin prices could drastically be decreased and it became widely available in the 1980s (Carter, 2011; Keen et al., 1980). This was possible as in the late 1970s genetic engineering was introduced (Jackson et al., 1972). From that time on, a lot of research has been conducted on the development of biopharmaceuticals. As proteins are very complex molecules and synthesis can be very challenging, the use of microorganisms that inherently possess the machinery for protein production is again preferred (Berlec and Štrukelj, 2013; Skelly, 2010). To date more than 200 biopharmaceuticals have been approved and most of them are produced in microorganisms (Berlec and Štrukelj, 2013). With gained knowledge in molecular biology the interest in gene therapy, personalized medicine and targeted medication is growing rapidly. The big advantage of pharmaceuticals on the basis of proteins is the extremely high efficiency and accuracy that proteins find their targets with. For example the fusion of chemotherapeutics to proteins that specifically bind tumor cells and thereby enable the specific treatment of cancerous cells, decreases adverse effects and destruction of healthy tissue (Carter, 2011). Other used proteinaceous biopharmaceuticals are vaccines and especially antibodies or antibody formats (Berlec and Štrukelj, 2013).

1.5.1 Vaccines

Vaccines are a strong driving factor of the biopharmaceutical industry. In 1796, the first proteinaceous vaccine was produced against cowpox. This event was name giving to all biological preparations that provide active acquired immunity to a certain disease (WHO) as the cowpox causative pathogen is termed *Variolae vaccinae* (Sánchez-Sampedro et al., 2015). Vaccines can be weakened or dead pathogens, isolated antibodies from host animals or antigens that are specific to the causative pathogen. By administrating the vaccine to the patient, the inherent immune system can produce antibodies against the antigen and subsequently build up resistance against the caused disease (Nabel, 2013). Vaccines are very potent to be used in large-area applications, as they often convey a long lasting immunity. Thus, it belongs to the preferred treatments for infectious diseases and diseases transferred by insects with epidemic potential. One of the most prominent examples here is the Malaria tropica, a febrile disease triggered by the protozoan *Plasmodium falciparum*. Around 3.2 billion people live in areas that are at risk of Malaria and 214 million cases were counted in 2015 (WHO fact sheet, 2016). Although medication, such as artemisinin, is available, previously used medications led to rapid resistance of the pathogen making it necessary to always find new therapeutics. Severe side-effects of anti-malaria drugs also resemble a huge drawback. A very promising candidate as a malaria antigen that could potentially be used for

vaccination, is the *P. falciparum* protein PfPRH5 (*Plasmodium falciparum* reticulocyte binding protein homologue 5) (Douglas et al., 2011; Rodriguez et al., 2008). It has been found to be essential for a very crucial step in the invasion of red blood cells by the pathogen and is thus ideally suited as an antigen (Reddy et al., 2015). It has been shown in primate studies that recombinant PfPRH5 can trigger the formation of antibodies, being able to inhibit red blood cell invasion and thereby proliferation of the pathogen (Bustamante et al., 2013; Ewer et al., 2015; Hjerrild et al., 2016). As the recombinant production of such an antigen can be conducted in large scales in microorganisms, it shows the great potential of a biopharmaceutical that could be used to treat half of the world's population. Nevertheless, PfPRH5 is a great example for a hard to express protein as it has highly specific needs. *N*-glycosylation of the 63 kDa protein should be avoided but disulfide bridge formation is needed (Bustamante et al., 2013; Crosnier et al., 2013; Wright et al., 2014). So far it could only be successfully produced in mammalian cell culture, insect cells and cell free expression systems that are all very expensive and time consuming (Berlec and Štrukelj, 2013; Bustamante et al., 2013; Hjerrild et al., 2016; Ord et al., 2012). Albeit expression in *E. coli* leads to formation of inclusion bodies, it can be renatured to an active state (Sony Reddy et al., 2014). However, all these systems are not well suited for large scale production and other expression systems need to be tested. Unconventional secretion seems to be especially suited because it combines the properties of a eukaryotic host with the ability to avoid *N*-glycosylation.

1.5.2 Antibodies

Antibodies are immunoglobulin molecules (Ig) with a very high target affinity and specificity. Most of the currently approved biopharmaceuticals belong to the group of monoclonal antibodies and thereby contribute a big portion to the general biopharmaceutical turnover (Berlec and Štrukelj, 2013; Joosten et al., 2003; Spadiut et al., 2014). Complete IgG antibodies consist of two identical light- (L) and heavy-chains (H) that convey a bivalent mode of action and enable the antibody to bind to the respective epitopes (Narciso et al., 2012). The β -barrel shaped H- and L chains are linked with disulfide bridges. Each chain can be divided into variable (V_H and V_L) and constant parts (C_{H1-H3} and C_L), whereas the variable chains exhibit antigen binding function. The non-antigen binding part (Fc fragment) is thus not essential for most therapeutic applications. V_H and V_L chains consist of conserved framework regions and hypervariable CDR regions (complementary determining regions) while the latter defines the antigen specificity (Fig. 1.5 A; Joosten et al., 2003).

As whole antibodies are often larger than 160 kDa, a lot of effort has been put in the development of smaller, functional antibody fragments. Fab fragments (fragment antigen binding) consist of V_H and C_{H1} connected via disulfide bonds to C_L and V_L . They are still capable of antigen binding and can either be produced recombinant or by digestion of whole antibodies. Heterodimers consisting of the V_H and V_L chain are called Fv fragments (fragment

variable). They are around 30 kDa large, still exhibit antigen binding capability but tend to dissociate and are thus instable. Combinations of the fragments are also available (Fig. 1.5 A; Joosten et al., 2003; Narciso et al., 2012). The smallest epitope binding antibody fragment has been identified in an alternative form of antibodies produced by members of the *Camelidae* family and cartilaginous fish (Hamers-Casterman et al., 1993; Streltsov and Nuttall, 2005). Those antibodies are lacking the light chains and are thus termed heavy-chain IgG (Fig. 1.5 B). Of those the variable V_{HH} domain alone is still binding the respective antigen with a high affinity. The small size of around 15 kDa makes the V_{HH} domain, also called nanobody (NB) highly interesting for therapeutic applications (Joosten et al., 2003; Muyldermans et al., 1994).

The classical production of antibodies is performed by injection of the respective antigen into a production host (mouse, rat, horse or other mammals) and subsequent isolation of the generated antibodies from the blood serum of the host (Leenaars and Hendriksen, 2005). This has several disadvantages with regard to medical applications and profitability (Liu, 2014; Spadiut et al., 2014). The timeframe for the generation of immunity against the antigen by the host can take from days to weeks and caretaking of those animals is very expensive. Moreover, antibodies from other animals are often recognized as foreign and immunogenic reactions can be observed (De Groot and Scott, 2007; Spadiut et al., 2014). Thus, the heterologous expression of antibodies and antibody fragments in microorganisms is a prerequisite for mass production of uniform molecules (Berlec and Štrukelj, 2013; Spadiut et al., 2014). Special attention is paid to NB as these display a lot of beneficial characteristics for therapeutic

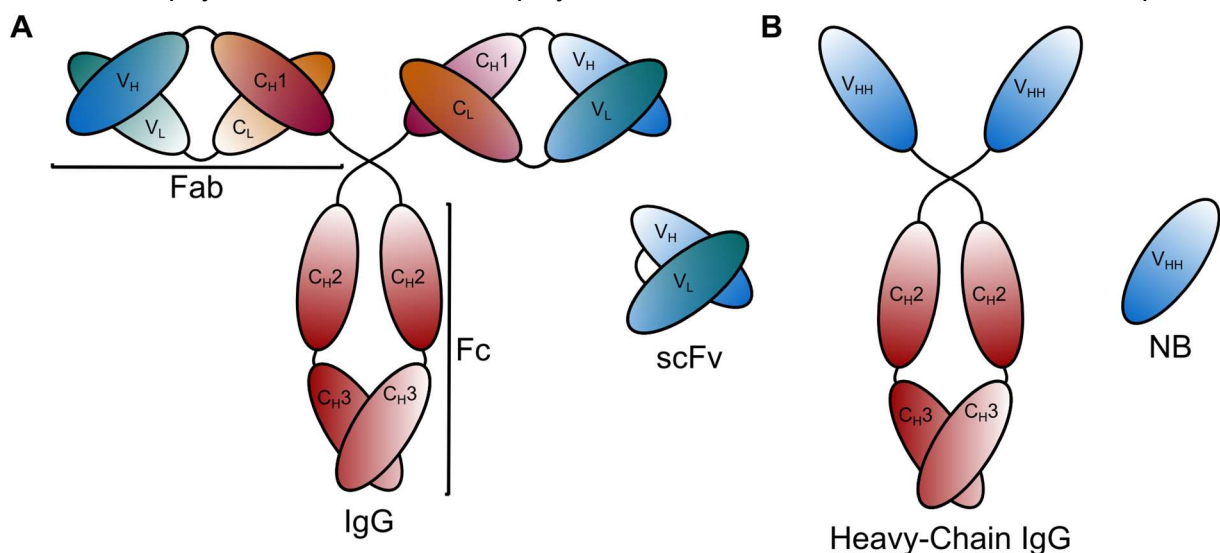


Fig. 1.5: Schematic representation of IgG antibodies and antibody fragments

A. Complete IgG antibody consisting of two identical heavy chain (H) and light chain (L) components. Heavy chains are built up of three constant domains (C_{H1} , C_{H2} , C_{H3}) and one variable domain (V_H), whereas the light chain consists of one constant (C_L) and one variable (V_L) domain. The antigen binding site is formed by the V_H and V_L domain. Hydrolysis of the antibody leads to two Fab fragments (fragment antigen binding) and one Fc moiety (fragment crystallisable). Peptide linked V_H and V_L fragments, yield an scFv fragment (single-chain variable fragment). **B.** Complete camelid type heavy-chain IgG antibody consisting of two identical heavy chains. Each chain is built up of one variable (V_{HH}) and two constant domains (C_{H2} , C_{H3}). The antigen binding site is given by the V_{HH} fragment. Isolated V_{HH} fragments are also termed nanobodies (NB), displaying high antigen binding potential and specificity. The figure is modified from Joosten et al., 2003.

treatment (Harmsen and De Haard, 2007). NB are very small and can even cross the blood-brain barrier making them very interesting for neuronal applications. The comparably high stability but low retention time can also be beneficial as it is often desired to have the therapeutic molecule cleared off the body as fast as possible. On the other hand, NB can be easily modified to increase retention in the patient making them widely applicable. Besides, NB are also frequently used in research and diagnostics as they can be used for immune-detection or purification methods where they serve as nanotraps (De Meyer et al., 2014; Harmsen and De Haard, 2007; Joosten et al., 2003; Rothbauer et al., 2007). Several methods have been established to generate NB libraries against target epitopes, enabling a fast generation of *de novo* synthesized NB. The most frequently used one is the phage display method but also the isolation of libraries from immunized animals is very common (Fridy et al., 2014; Harmsen and De Haard, 2007).

1.6 Aim of the thesis

The biotechnological potential of *U. maydis* has been analyzed in previous studies and a basic setup for expression of heterologous proteins via unconventional Cts1 secretion could be established (Feldbrügge et al., 2013; Sarkari et al., 2014; Stock et al., 2012). Despite an already considerable variety of successfully expressed targets, the overall yield of secreted protein was still low and not competitive (Reindl, 2016; Sarkari et al., 2014; Stock et al., 2012). To further advance the system on the way to an industrially relevant production organism, this project focuses on the optimization of the system on two different levels.

On the one hand the construct design for efficient expression and downstream processing should be addressed. This aim should be conducted on new biopharmaceutical targets that should be expressed and unconventionally secreted to expand the portfolio. For this purpose NB directed against the reporter protein Gfp (green fluorescent protein) and NB directed against Botulinum neurotoxin A (BoNTA) as well as the potential malaria antigen PfRH5 have been selected. After successful expression, secretion and purification, biochemical analyses and quantifications should be conducted.

On the other hand, the general optimization of the cultivation process is topic of this thesis. Hitherto, all work on protein expression in *U. maydis* has been done under standard laboratory conditions that might not be optimal for the expression of heterologous proteins. Thus, the composition of media, the cultivation conditions and upscaling possibilities of so far used processes should be analyzed and adjusted. To this end, the established Gus-Cts1 reporter system for unconventional secretion was used for sophisticated monitoring approaches using RAMOS technology (Anderlei et al., 2004; Stock et al., 2012; Stock et al., 2016).

In the end, the combination of molecular biology and process engineering optimization steps should result in an overall improved expression system.

2 Results

2.1 Optimizing the expression, purification and biochemical characterization of α Gfp nanobodies in *U. maydis*

In the past years several milestones in the development of *U. maydis* towards an expression platform for heterologous proteins have been achieved. In order to further optimize the expression system, the effects of proteases and construct design on purification and stability, using strains harboring modified pRabX2 expression constructs were investigated. To this end nanobodies directed against the green fluorescence protein (Gfp) from the jellyfish *Aequorea victoria* were used as expression target (Rothbauer et al., 2007). Two α Gfp-NB-Cts1 expression strains (AB33 α Gfp-NB-Cts1 and AB33kex2 Δ α Gfp-NB-Cts1) were already available from previous studies but not characterized in detail (Sarkari, 2014). These contained the coding sequence for the α Gfp-NB in a dicodon optimized version (Sarkari, 2014; Zarnack et al., 2006).

2.1.1 Studies on the effects of proteases

To analyze the influence of proteolytic degradation on heterologous α Gfp-NB-Cts1, *ip* insertion plasmid pRabX2- α Gfp-NB-Cts1 (pRabX2 P_{oma} His- α Gfp-NB-TH-Cts1, pUMa2240) was additionally integrated into the protease deletion strain AB33P5 Δ . Correct transformants were verified by Southern blot analysis and single insertion strains were used for further analysis. To compare expression levels, stability and secretion of α Gfp-NB-Cts1 in the three different strain backgrounds, Western blot analyses of whole cell extracts and precipitated supernatant samples were performed (Fig. 2.1 A). The full length protein (filled arrowheads) was expressed and secreted by all three strains, migrating slightly higher than the calculated 76 kDa. This phenomenon is in line with previous reports in which α -HA antibodies were used for detection (Stock et al., 2012). For cell extracts, it could be observed that full length α Gfp-NB-Cts1 was expressed in equal amounts, indicating no influence of the protease deletions on intracellularly residing protein (Fig. 2.1 A, left panel). By contrast, the amounts of full length α Gfp-NB-Cts1 differed for supernatant samples (Fig. 2.1, right panel, filled arrowheads). Albeit the amount of α Gfp-NB-Cts1 in AB33kex2 Δ α Gfp-NB-Cts1 supernatant was substantially higher compared to AB33 α Gfp-NB-Cts1 and AB33P5 Δ α Gfp-NB-Cts1 (filled arrowheads), the intensity of the observed degradation band (open arrowhead) was drastically decreased in AB33P5 Δ α Gfp-NB-Cts1. However, intensity of the degradation band varied in the experiments and could thus not clearly be accounted to a specific effect caused by the quintuple deletion strain (Fig. 2.1 A, B). In the next step α Gfp-NB-Cts1 protein was used in modified Western blot assays and ELISA to investigate the binding to its antigen Gfp. First, IMAC purified α Gfp-NB-Cts1 from AB33kex2 Δ α Gfp-NB-Cts1 cell extracts (Fig. 2.1 D, purification not shown) and supernatants

(Fig. 2.1 C, F) was used as primary antibody for the detection of immobilized triple Gfp in a Western blot analysis. To this end, 10 μ g of whole cell extracts of a *U. maydis* wildtype and a 3xGfp expressing strain were subjected to SDS-PAGE. The separated proteins were

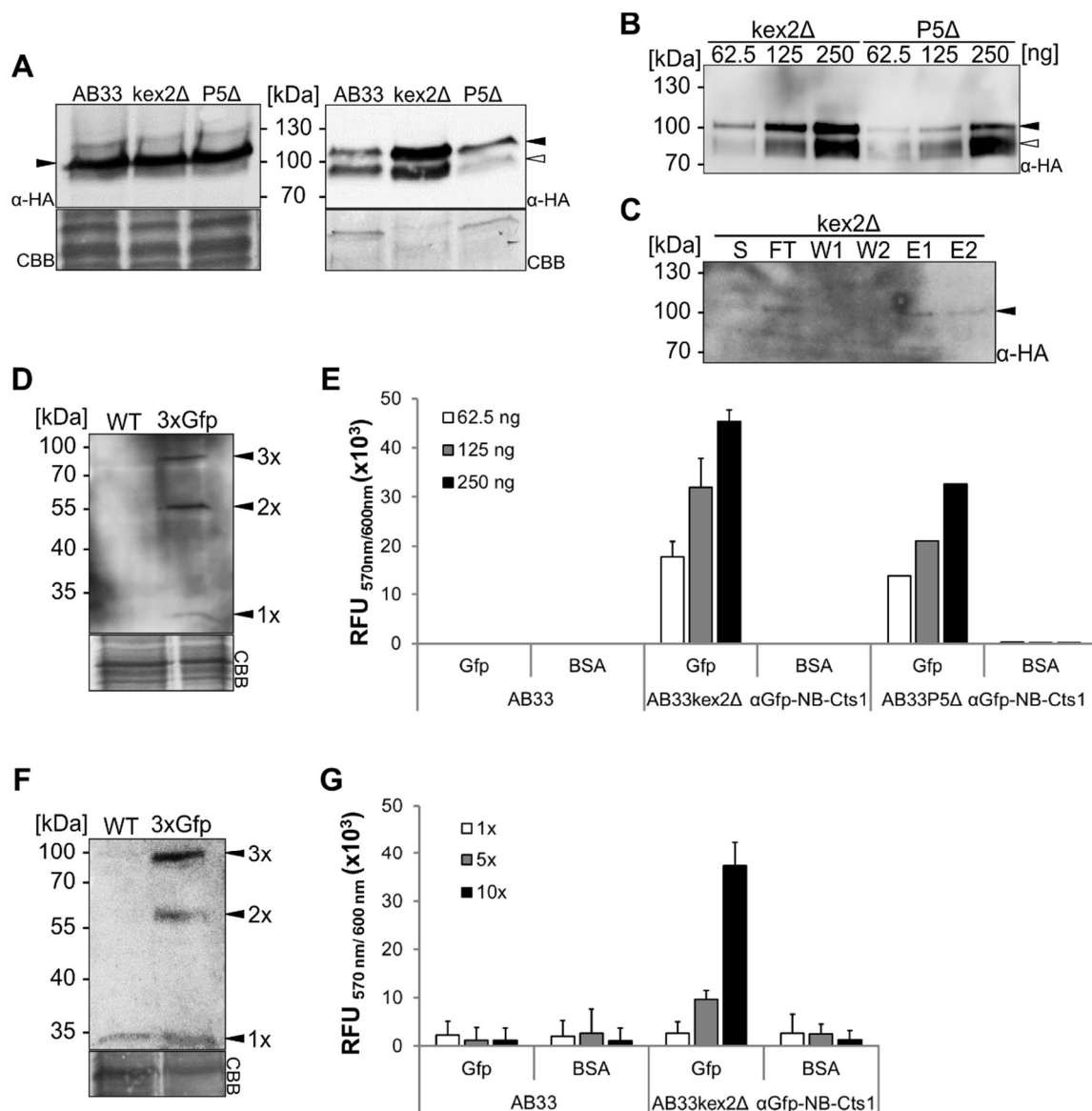


Fig. 2.1: Expression, purification and characterization of camelid V_{HH} derived α Gfp-NB proteins

A. Western blot analysis of whole cell extracts (left panel) and precipitated supernatants (right panel) of α Gfp-NB-Cts1 expressing *U. maydis* strains (AB33 α Gfp-NB-Cts1, AB33kex2 Δ α Gfp-NB-Cts1 and AB33P5 Δ α Gfp-NB-Cts1). 10 μ g of whole cell extracts or 1 mL of precipitated supernatants were subjected to SDS-PAGE and Western blot analysis. Fusion proteins were detected via the HA-tag and the membrane was stained with Coomassie brilliant blue after detection (CBB). **B.** Western blot analysis of α Gfp-NB-Cts1 in different amounts of whole cell extracts, expressed by AB33kex2 Δ α Gfp-NB-Cts1 and AB33P5 Δ α Gfp-NB-Cts1. Heterologous protein was detected using α -HA primary antibodies. Identical protein amounts were also used in ELISA (s. Fig. 2.1 E). **C.** Western blot analysis of IMAC purified α Gfp-NB-Cts1 from supernatant of strain AB33kex2 Δ α Gfp-NB-Cts1. 14 μ L of the supernatant (S), flow through (FT), wash fraction 1 and 2 (W1, W2) and elution fraction 1 and 2 (E1, E2) were analyzed. Detection was performed using α -HA primary antibodies. Enrichment of α Gfp-NB-Cts1 can be observed in E1 and E2, thus these fractions were used for ELISA (s. Fig. 2.1 G). **D.** Western blot to analyze the binding potential of α Gfp-NB-Cts1 to immobilized 3xGfp. 10 μ g of whole cell extracts of a 3xGfp expressing *U. maydis* strain (3xGfp) and the respective wild-type strain (WT; SG200) were subjected to SDS-PAGE and Western blot analysis. α Gfp-NB-Cts1 was IMAC purified from AB33kex2 Δ α Gfp-NB-Cts1 cell extracts as described in C., the elution fractions were pooled and used as primary antibody. **E.** Varying amounts of AB33, AB33kex2 Δ α Gfp-NB-Cts1 and AB33P5 Δ α Gfp-NB-Cts1 whole cell extracts (also see Fig. 2.1 B), were analyzed by ELISA against Gfp as antigen and BSA as antigen control. AB33 and AB33kex2 Δ α Gfp-NB-Cts1 cell extracts were analyzed in biological triplicates, whereas AB33P5 Δ α Gfp-NB-Cts1 samples have been analyzed in a single experiment. **F.** Western blot to analyze the binding potential

of α Gfp-NB-Cts1 to immobilized 3xGfp. The assay was performed as described in D., yet IMAC purified α Gfp-NB-Cts1 from AB33kex2 Δ α Gfp-NB-Cts1 supernatant was used (also see Fig. 2.1 C). **G.** Elution fractions from IMAC purifications of AB33 and AB33kex2 Δ α Gfp-NB-Cts1 supernatant (also see Fig. 2.1 C) were analyzed in different concentrations (10x, 5x, 1x) by ELISA against Gfp and BSA as antigen control. ELISA was performed in triplicates.

transferred to a PVDF membrane and incubated with purified α Gfp-NB-Cts1. Detection was performed using an α -HA antibody directed against the 3xHA-tag of α Gfp-NB-Cts1 and subsequently a secondary α -Mouse-HRP antibody. In both cases three bands with different sizes were detected. A 81 kDa band, corresponding to the 3xGfp and two bands of its degradation products, 2xGfp (54 kDa) and 1xGfp (27 kDa). Besides a faint signal at 27 kDa in the antigen control (Fig. 2.1 F), no unspecific signals could be detected. Similar results but with lower intensity bands could be obtained for α Gfp-NB-Cts1 from AB33P5 Δ α Gfp-NB-Cts1 (data not shown). The results confirm that the produced NB show specific antigen binding activity, detecting 3xGfp and its two defined degradation products. Next, the volumetric antigen-binding activity of *U. maydis* α Gfp-NB-Cts1 present in cell extracts and culture supernatants was analyzed quantitatively using ELISA. To this end, absorbing microtiter plates were coated with recombinant Gfp (purified from *E. coli*) or BSA (commercial) as antigen control. Either defined amounts of whole cell extracts (Fig. 2.1 B, E) or IMAC purified α Gfp-NB-Cts1 from supernatants (Fig. 2.1 C, G) of AB33, AB33kex2 Δ α Gfp-NB-Cts1 and AB33P5 Δ α Gfp-NB-Cts1 were applied. After incubation with α -HA antibodies and α -Mouse-HRP antibodies, activity was determined using a chemifluorescent horseradish peroxidase (HRP) substrate. In all cases specific, concentration-dependent binding of α Gfp-NB-Cts1 to Gfp could be detected with only very low background activity in antigen control (BSA) and negative control (AB33). The overall measured activity was slightly higher in AB33kex2 Δ α Gfp-NB-Cts1, reflecting the previous results (Fig. 2.1 A and B). Obviously secretion of α Gfp-NB-Cts1 is more efficient in AB33kex2 Δ α Gfp-NB-Cts1 but protein stability seems to be higher in AB33P5 Δ α Gfp-NB-Cts1 supernatants. The results confirm that active nanobodies can be produced by unconventional secretion in *U. maydis* and clearly demonstrate the potential of the modified construct design in pRabX2 in combination with protease deletion strains.

2.1.2 Studies on the effects of construct design

The pRabX2 expression construct insertion system turned out to be stable and functional in *U. maydis*. However, in order to further simplify and accelerate the applications of α Gfp-NB produced in *U. maydis*, two alternative approaches were tested: Optimizing the construct design first for streamlined detection, and second for proteolytic removal of the Cts1 carrier. The expression construct was equipped with a Protein A-tag to allow quick and simple detection. On the one hand, this was combined with an N-terminal OneSTrEP®-tag (OneSTrEP®- α Gfp-NB-Protein A-TEV-CBP-Cts1*-HA), and on the other hand with an N-terminal OneSTrEP®-tag and a C-terminal 10xHis-tag (OneSTrEP®- α Gfp-NB-Protein A-TEV-Cts1*-His-HA) for purification and detection (Fig. 2.2). The Protein A epitope is derived from

the *Staphylococcus aureus* protein A and bound by the immunoglobulin domain of various species (Hjelm et al., 1972; Richman et al., 1982). Thus, detection and purification can be conducted in a single step using IgG antibodies (Hjelm et al., 1972). As usually species specific secondary antibodies are covalently conjugated to detection elements like HRP, these are sufficient for detection of Protein A epitopes. A primary antibody incubation step is thus not needed. The Protein A-tag used in this study consists of two protein A epitope copies that were dicodon optimized for *U. maydis* (Beier, 2015; Zarnack et al., 2006). The construct design thus should not only allow for a simplified detection protocol, but also enable a modified tandem affinity purification strategy (Rigaut et al., 1999) by exploiting the C-terminal OneStrEP®-tag, the C-terminal 10xHis-tag and the protease cleavage site.

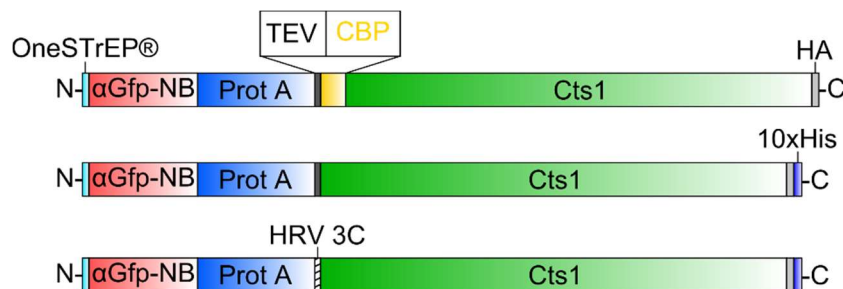


Fig. 2.2: Schematic representation of αGfp-NB-Protein A fusion proteins

In the basic fusion protein, the αGfp-NB (red) is C-terminally fused to a OneStrEP®-tag (light blue) and followed by the Protein A epitope (dark blue). The individual fusion proteins then differ in their composition. Depicted elements are the TEV protease cleavage site (dark grey), the HRV 3C protease cleavage site (dashed), the calmodulin binding peptide (yellow), the 1xHA-tag (light grey) and a 10xHis-tag (purple). All proteins are in fusion with Cts1 (green).

For many applications, especially in pharmaceutical and medical industry, therapeutic proteins need to be produced in very high purities and without foreign protein moieties (Bonnerjea, 2004). As the Cts1-mediated expression system requires expression of the target as a translational fusion with Cts1, application of specific proteases is needed to separate the two proteins after production. Hence, to allow removal of the Cts1 carrier an efficient proteolytic separation from the heterologous target needed to be established. Previous constructs carried a Tobacco etch virus protease (TEV) cleavage site. Now, a similar construct expressing a Human rhinovirus 3C protease (HRV 3C) cleavage site (OneStrEP®-αGfp-NB-Protein A-HRV 3C-Cts1-His) was generated (Fig. 2.2). This enabled the comparison of the two most often commercially used proteases for purification. As TEV- and HRV 3C protease have different properties in terms of temperature optimum, on-column cleavage and compatibility with different substances, they show varying efficiency depending on each protein and process (Dian et al., 2002; Terpe, 2003).

For all constructs used to compare the various detection and purification strategies, strain generation was conducted using integrative plasmids that target the *ip* locus (Brachmann, 2001; Broomfield and Hargreaves, 1992). Strains were verified by Southern blot analysis and single insertion strains were used for following investigations. Expression and secretion of the

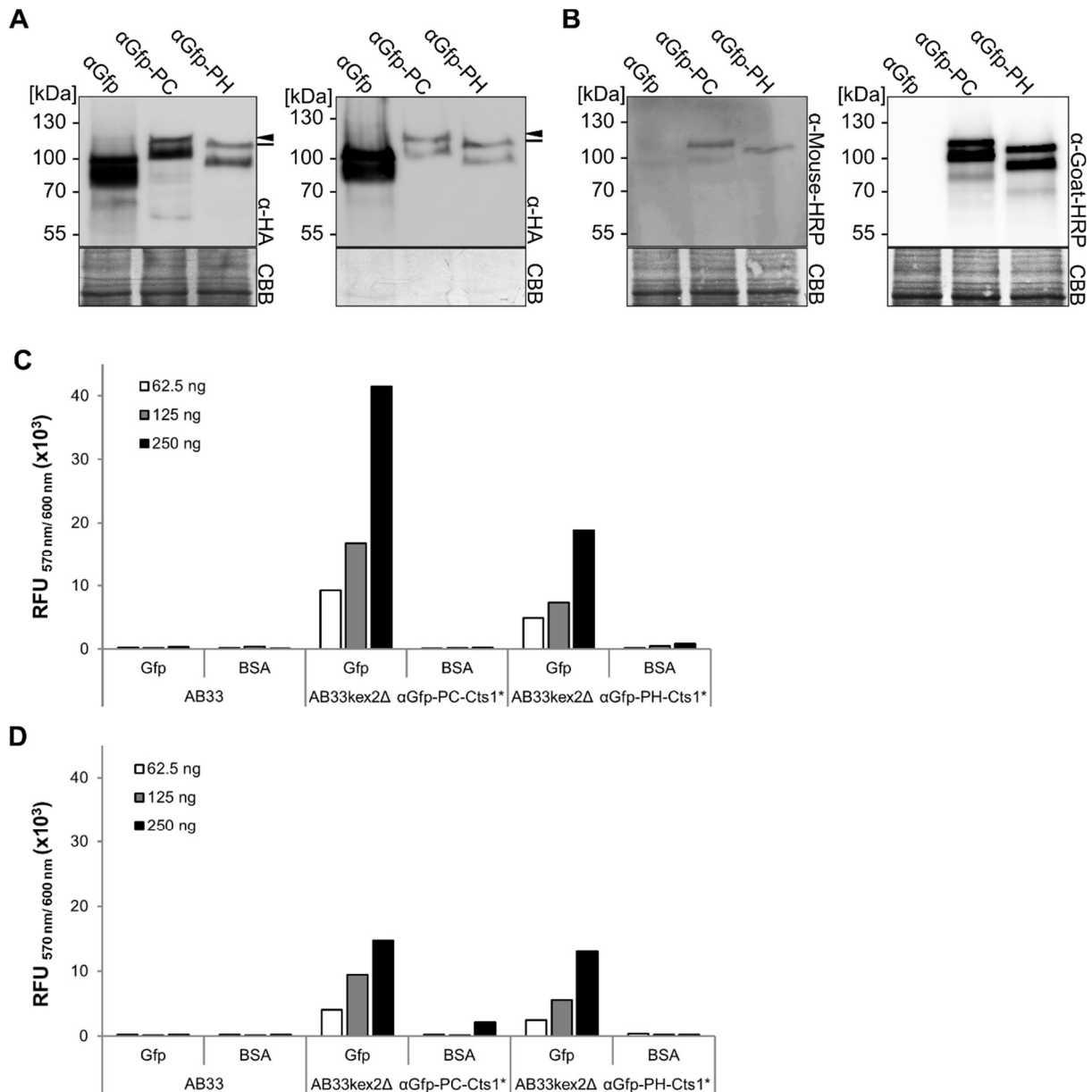


Fig. 2.3: Expression and characterization of camelid V_{HH} derived αGfp-NB-Protein A fusion proteins

A. Western blot analysis of whole cell extracts (left panel) and precipitated supernatants (right panel) of αGfp-NB-Protein A-Cts1* (αGfp-PC), αGfp-NB-Protein A-Cts1*-His (αGfp-PH) and αGfp-NB-Cts1 (αGfp) expressing *U. maydis* strains (AB33kex2Δ αGfp-NB-Protein A-Cts1*, AB33kex2Δ αGfp-NB-Protein A-Cts1*-His and AB33kex2Δ αGfp-NB-Cts1). 10 μg of whole cell extracts or 1 mL of precipitated supernatant were subjected to SDS-PAGE and Western blot analysis. Heterologous protein was detected via the HA-tag. Membranes were stained with Coomassie brilliant blue after detection (CBB). **B.** Western blot analysis of whole cell extracts, using only α-Mouse-HRP (left panel) or α-Goat-HRP (right panel) conjugates for detection. The Protein A containing full length proteins could be detected in both cases. Membranes were stained with Coomassie brilliant blue after detection (CBB). **C.** Varying amounts of whole cell extracts of AB33, AB33kex2Δ αGfp-NB-Protein A-Cts1* (AB33kex2Δ αGfp-PC-Cts1*) and AB33kex2Δ αGfp-NB-Protein A-Cts1*-His (AB33kex2Δ αGfp-PH-Cts1*) were analyzed by ELISA against Gfp as antigen and BSA as antigen control. ELISA was performed by using primary antibodies directed against the internal HA-tag, followed by secondary α-Mouse-HRP conjugates. **D.** Varying amounts of whole cell extracts of AB33, AB33kex2Δ αGfp-NB-Protein A-Cts1* and AB33kex2Δ αGfp-NB-Protein A-Cts1*-His were analyzed by ELISA against Gfp as antigen and BSA as antigen control. ELISA was performed by only using α-Goat-HRP conjugates, directed against the Protein A epitope.

proteins αGfp-NB-Prot A-TEV-CBP-Cts1*-HA, αGfp-NB-Prot A-TEV-Cts1*-HA-His and αGfp-NB-Prot A-HRV 3C-Cts1-HA-His in the AB33kex2Δ background could be confirmed by Western blot analysis using primary antibodies directed against the HA-tag (Fig. 2.2; Fig.

2.3 A). As a control, the previously described AB33kex2Δ strain expressing αGfp-NB-Cts1 (αGfp) in its initial setup was included. All full length proteins (αGfp-NB-Prot A-Cts1*-His (αGfp-PH) = 90 kDa (black line); αGfp-NB-Prot A-Cts1* (αGfp-PC) = 91.5 kDa (filled arrowhead); αGfp-NB-Cts1 = 76 kDa) could be detected. As described earlier (Sarkari et al., 2014; Stock et al., 2012), all proteins migrate higher as their calculated molecular weight and the previously described major degradation band is present in all samples, migrating slightly below the full length protein. However, the expression levels of strains expressing αGfp-PC and αGfp-PH fusions were in general lower than αGfp and secretion seemed to be impaired, suggesting that the fusion to Protein A may be disturbing (Fig. 2.3 A). To analyze direct detection via the Protein A-tag, cell extracts were directly treated with secondary α-Mouse-HRP or α-Goat-HRP conjugates (Fig. 2.3 B). Importantly, both strategies were successful, indicating that in principle the two Protein A copies enclosed in the fusion protein are functional. Detection with α-Goat-HRP resulted in more specific and intense signals and background detection of αGfp could not be observed, suggesting that these antibodies should be preferred for detection. Next, activity of the nanobodies was investigated using ELISA with Gfp purified from *E. coli* as antigen (also see 2.1.1). Defined amounts of whole cell extracts were applied and detection was either performed using primary antibodies directed against the HA-tag, followed by a secondary α-Mouse-HRP conjugate (Fig. 2.3 C), or by only using a α-Goat-HRP conjugate directed against the Protein A-tag (Fig. 2.3 D). In both assays volumetric activity could be confirmed and almost no background signal in the antigen control (BSA) or the wildtype strain (AB33) could be detected. The overall activity of αGfp-PC was higher compared to αGfp-PH using the α-HA based ELISA (Fig. 2.3 C) reflecting the slightly higher intensity of the αGfp-PC band in α-HA detected Western blots (Fig. 2.3 A, left panel). Using only the secondary α-Goat-HRP based ELISA (Fig. 2.3 D), the activity of both constructs was similar though lower compared to the α-HA based method. As signal intensity increases by the stacking of multiple antibodies, this result was expected and again confirms the functionality of the Protein A epitopes. To verify the functionality of the N-terminal OneSTrEP®- and the C-terminal 10xHis-tag, purification of αGfp-PC and αGfp-PH from cell extracts was performed (Fig. 2.4 B and C). Strep-Tactin® as well as IMAC purification resulted in an enrichment of the full length protein in the elution fractions suggesting that the introduced tags are functional.

To finally compare the hydrolysis efficiency of TEV and HRV 3C on the expressed fusion proteins, whole cell extracts of AB33kex2Δ αGfp-NB-Prot A-TEV-Cts1*-HA-His and AB33kex2Δ αGfp-NB-Prot A-HRV 3C-Cts1-HA-His were prepared in the respective protease reaction buffer. After incubation of the cell extracts with 1 U of either TEV or HRV 3C, the samples were analyzed by Western blotting (Fig. 2.4 A). In the untreated cell extract fraction (CE) full length protein (90 kDa, filled arrowheads) could be observed, whereas almost no αGfp containing cleavage product (30 kDa, open arrowheads) was detectable. This confirms the

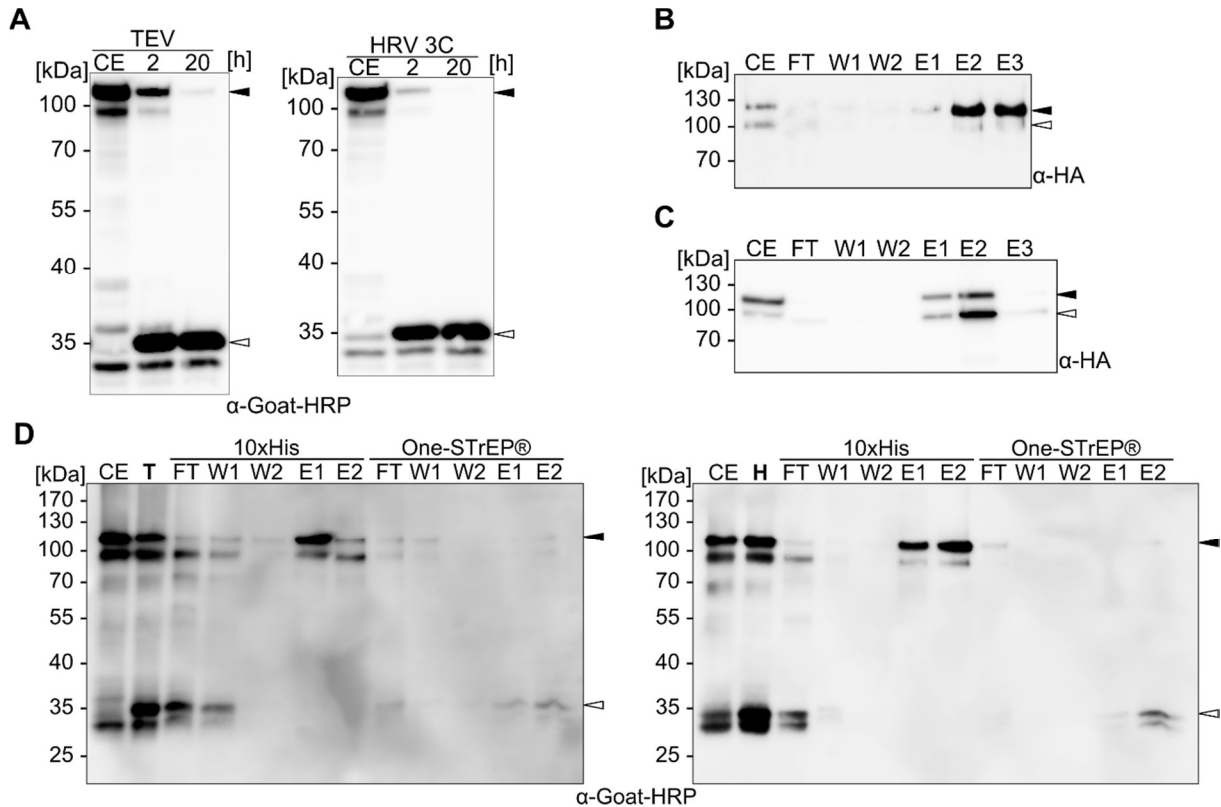


Fig. 2.4: Purification of V_{HH} derived α Gfp-NB-Prot A fusion proteins

A. Western blot analysis to compare the hydrolytic potential of Tobacco etch virus protease (TEV) and Human rhinovirus 3C protease (HRV 3C). Whole cell extracts of AB33kex2 Δ α Gfp-NB-Prot A-TEV-Cts1*-HA-His (left panel) and AB33kex2 Δ α Gfp-NB-Prot A-HRV3C-Cts1*-HA-His (right panel) were prepared in TEV- or HRV 3C-lysis buffer. Proteolysis was performed using 1 U of the respective protease and samples were taken after 2 h and 20 h incubation on 4°C. The samples were then subjected to SDS-PAGE and Western blot analysis. For detection α -Goat-HRP conjugates directed against the Protein A epitope were used. **B.** Western blot analysis of Strep-Tactin® purified α Gfp-NB-Prot A-TEV-Cts1* from whole cell extracts of AB33kex2 Δ α Gfp-NB-Prot A-TEV-Cts1*. 14 μ L of the cell extract (CE), flow through (FT), wash fraction 1 and 2 (W1, W2) and elution fraction 1, 2 and 3 (E1, E2, E3) were analyzed. Detection was performed using α -HA primary antibodies. The full length protein was migrating slightly higher, than the calculated 91.5 kDa (filled arrowhead). A major degradation band (open arrowhead) can be observed, migrating slightly below the full length protein. Enrichment of α Gfp-NB-Cts1 can be observed in E2 and E3. **C.** Western blot analysis of IMAC purified α Gfp-NB-Protein A-TEV-Cts1*-HA-His from whole cell extracts of AB33kex2 Δ α Gfp-NB-Prot A-TEV-Cts1*-HA-His. 14 μ L of the cell extract (CE), flow through (FT), wash fraction 1 and 2 (W1, W2) and elution fraction 1, 2 and 3 (E1, E2, E3) were analyzed. Detection was performed using α -HA primary antibodies and the full length protein was migrating slightly higher, than the calculated 90 kDa (filled arrowhead). A major degradation band can be observed (open arrowhead), migrating slightly below the full length protein. Enrichment of α Gfp-NB-Protein A-TEV-Cts1*-HA-His can be observed in E1 and E2. **D.** Western blot to compare the efficacy of TEV- (left panel) and HRV 3C- protease (right panel) based tandem affinity purifications. Native cell extracts of AB33kex2 Δ α Gfp-NB-Prot A-TEV-Cts1*-HA-His (left panel) and AB33kex2 Δ α Gfp-NB-Prot A-HRV3C-Cts1*-HA-His (right panel) were prepared and subjected to IMAC purification, using the C-terminal 10xHis-tag. Prior to that, the extracts were incubated with TEV- (bolt T) or HRV 3C protease (bolt H). The α Gfp-NB-Protein A containing flow through was then subjected to Strep-Tactin® purification, resulting in pure α Gfp-NB-Protein A in the elution fractions.

initial stability of the fusion protein. After 2 h of incubation about one third of the TEV-treated fusion protein was still intact (Fig. 2.4 A, left panel), whilst hardly any full length protein of the HRV 3C-treated sample was detectable (Fig. 2.4 A, right panel). The α Gfp containing cleavage product could be detected in increasing amounts with increasing incubation time. After 20 h of incubation, proteolytic hydrolysis of the fusion protein was completed by both proteases as only the α Gfp containing small fragment was present (Fig. 2.4 A). The samples were also analyzed using antibodies directed against the HA-tag to also visualize the Cts1 containing

cleavage product (data not shown). This assay confirmed that both tested proteases hydrolyzed the fusion protein over the incubation time though HRV 3C showed slightly higher activity and faster turnover.

To further purify the hydrolysate and clear off the Cts1 containing part, the two approaches were combined (Fig. 2.4 D). Whole cell extracts of AB33kex2Δ αGfp-NB-Protein A-TEV-Cts1*-HA-His and AB33kex2Δ αGfp-NB-Protein A-HRV 3C-Cts1-HA-His were prepared in the respective protease reaction buffer and incubated with 1 U of TEV or HRV 3C (Fig. 2.4 D, left panel, bold T (TEV hydrolysis); right panel, bold H (HRV 3C hydrolysis)). By subjecting the hydrolysate to IMAC purification using the C-terminal 10xHis-tag, the undesired Cts1 containing part and intact full length protein was retained at the Ni²⁺-NTA resin. The αGfp containing fragment (open arrowheads) however was eluted in the flow through. Last, it was tested if further purification of this fraction via a Strep-Tactin® resin is possible. The αGfp containing fragment was bound to the resin via the N-terminal OneSTrEP®-tag and could be eluted after washing. It is obvious that the hydrolysis in both cases was highly inefficient, probably due to insufficient amounts of protease. Nevertheless, the αGfp-NB fragment could be eluted in both cases (Fig. 2.4 D, open arrowheads; 30 kDa) with only very low contamination of full length protein (Fig. 2.4 D, filled arrowheads; 90 kDa). Increasing the amount of protease and thereby increasing the ratio of hydrolyzed to full length protein in the beginning would be needed to increase the amount of product in the end. The two-step purification would then allow to obtain very pure protein in which the carrier has been removed.

In summary, these experiments show that all constructs are expressed and the corresponding proteins can be purified. Hence, in principle an optimized, simplified downstream processing was obtained. Nevertheless, as secretion efficiency was drastically reduced due to the addition of the Protein A epitopes compared to previously tested constructs, experiments had to be primarily conducted with cell extracts and the procedure could not be tested for purification of the secreted proteins. In future experiments, the protein A epitopes should be avoided in the fusion protein to allow an efficient purification also from culture supernatants.

2.1.3 Nanobody functionalization via HRP fusion

In a parallel approach the possibility of functionalization of the produced nanobodies using the HRP from *Armoracia rusticana* was tested (Spadiut and Herwig, 2014). HRP catalyzes the hydrolysis of a variety of chemiluminescent and chemifluorescent substrates in the presence of hydrogen peroxide (Spadiut and Herwig, 2013). The enzyme had been functionally expressed in *U. maydis* before (Reindl, 2016). By now fusing the HRP to the αGfp-NB-Cts1, a fully functional antibody format for the detection of Gfp should be generated, enabling a direct readout. To this end, the strain AB33P5Δ His-HRP-αGfp-NB-TEV-HA-Cts1 was generated using the *ip* integration method (Brachmann, 2001; Broomfield and Hargreaves, 1992). Expression and secretion of full length HRP-αGfp-NB-Cts1 (HRP-αGfp = 110 kDa) was verified

by Western blot experiments, using antibodies directed against the internal HA-tag (Fig. 2.5 A). As controls, α Gfp-NB-Protein A-TEV-HA-Cts1-His (α Gfp-PH = 90 kDa) and α Gfp-NB-Cts1 (α Gfp = 76 kDa) were used. In cell extracts, full length bands of the controls and the HRP- α Gfp full length protein (Fig. 2.5 A, left panel, filled arrowhead) could be detected in similar

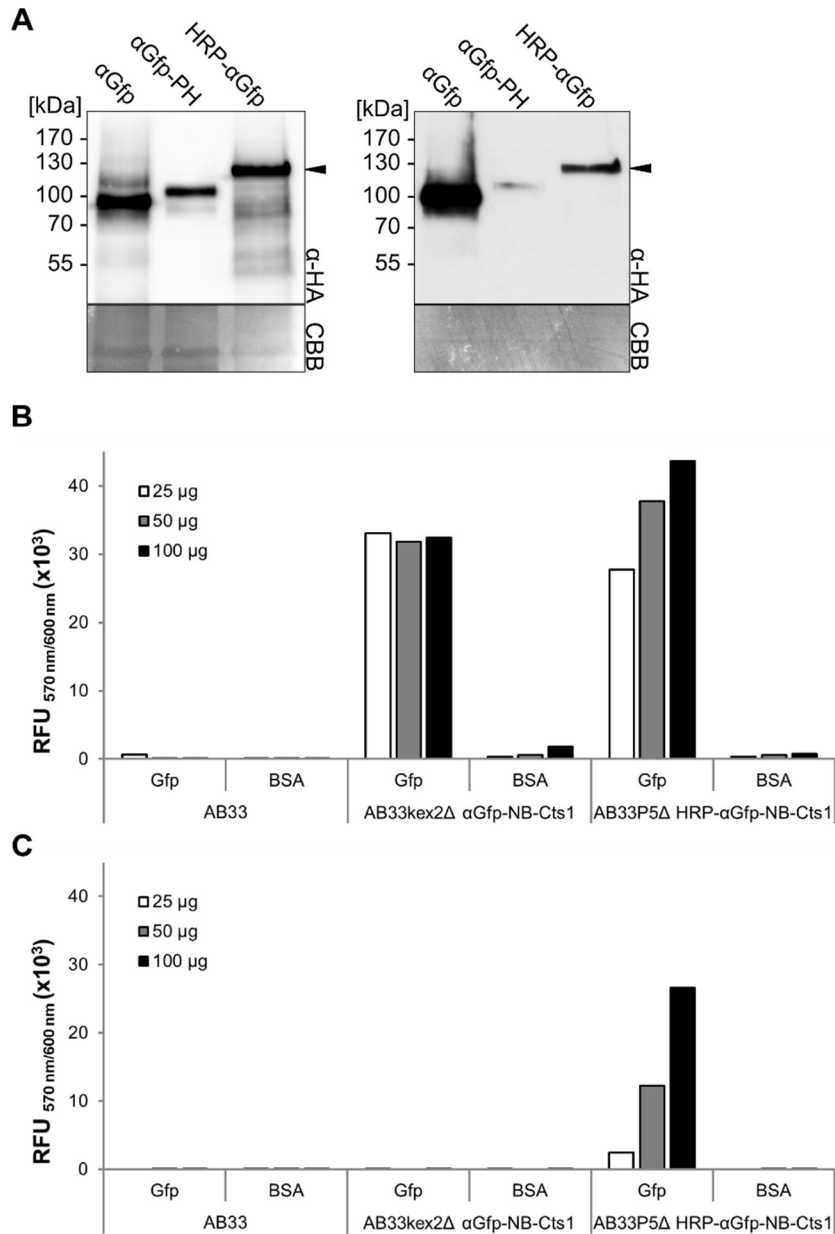


Fig. 2.5: Expression and characterization of camelid V_{HH} derived HRP- α Gfp-NB fusion proteins

A. Western blot analysis of whole cell extracts (left panel) and precipitated supernatants (right panel) of α Gfp-NB-Cts1 (α Gfp), α Gfp-NB-Protein A-Cts1-His (α Gfp-PH) and HRP- α Gfp-NB-Cts1 (HRP- α Gfp) expressing *U. maydis* strains (AB33kex2 Δ α Gfp-NB-Cts1, AB33kex2 Δ α Gfp-NB-Protein A-Cts1-His and AB33P5 Δ HRP- α Gfp-NB-Cts1). 10 μ g of whole cell extracts (left panel) or 1 mL of precipitated supernatant (right panel) were subjected to SDS-PAGE and Western blot analysis. Heterologous protein was detected using α -HA primary antibodies, followed by secondary α -Mouse-HRP conjugates and the membrane was stained with Coomassie brilliant blue after detection (CBB). **B.** Varying amounts of whole cell extracts of AB33, AB33kex2 Δ α Gfp-NB-Cts1 and AB33P5 Δ HRP- α Gfp-NB-Cts1 were analyzed by ELISA against Gfp as antigen and BSA as antigen control. ELISA was performed by using primary antibodies directed against the internal 3xHA-tag, followed by secondary α -Mouse-HRP conjugates. **C.** Varying amounts of whole cell extracts of AB33, AB33kex2 Δ α Gfp-NB-Cts1 and AB33P5 Δ HRP- α Gfp-NB-Cts1 were analyzed by ELISA against Gfp as antigen and BSA as antigen control. ELISA was performed by using only chemifluorescent HRP substrate, without prior antibody detection.

intensities. In precipitated supernatants (Fig. 2.5 A, right panel) secreted HRP- α Gfp full length protein could be detected (filled arrowhead). By contrast, the secretion of HRP- α Gfp-Cts1 was reduced whereas the previously described low secretion rate of α Gfp-PH was again represented by the least intense band of all investigated constructs. To further investigate the activity and functionality of HRP- α Gfp, ELISA assays against Gfp as antigen and BSA as antigen control were conducted (Fig. 2.5 B, C). Defined amounts of cell extracts from AB33, AB33P5 Δ HRP- α Gfp-NB-Cts1 and AB33kex2 Δ α Gfp-NB-Cts1 were used either in ELISA assays based on α -HA primary antibody detection (Fig. 2.5 B) or in ELISA assays using only a chemifluorescent substrate (Fig. 2.5 C). With detection via the HA-tag antigen binding could be observed for AB33P5 Δ HRP- α Gfp-NB-Cts1 and AB33kex2 Δ α Gfp-NB-Cts1 cell extracts. As the activity measured for AB33kex2 Δ α Gfp-NB-Cts1 cell extracts does not increase with increasing amounts of protein, it can be assumed that the ligand capacity limit is already reached with 25 μ g. In contrast for AB33P5 Δ HRP- α Gfp-NB-Cts1 cell extracts, a volumetric activity that reaches higher levels than the AB33kex2 Δ α Gfp-NB-Cts1 cell extracts can be observed (Fig. 2.5 B). This is likely due to an additive effect of the HRP- α Gfp activity and the HRP activity of the used secondary α -Mouse-HRP conjugate. Importantly, using only the chemifluorescent substrate for ELISA, the AB33kex2 Δ α Gfp-NB-Cts1 cell extracts show no activity whereas AB33P5 Δ HRP- α Gfp-NB-Cts1 cell extracts again display volumetric HRP activity (Fig. 2.5 C). Antigen control and the wildtype strain showed no or only minimal background activity in both assays.

Antigen binding activity could not be detected in ELISA assays with culture supernatants, suggesting that either the secretion of the fusion protein is too low or that the addition of the HRP enzyme hampers the antigen binding activity for example by sterical interferences. Since peroxidase activity of unconventionally secreted HRP- α Gfp could be shown in ECL microtiter plate assays using AB33P5 Δ HRP- α Gfp-NB-Cts1 supernatants the latter case is probably more likely (Reindl, 2016; Dennis Bleidorn, unpublished).

In summary, the results show that in principle active HRP- α Gfp-NB could be generated, enabling one-step detection and showing an example for nanobody functionalization and valorization. However, the use of this functionalization after Cts1-mediated secretion seems to be limited, because the fusion hampers both the secretion and the antigen binding activity of the fusion protein.

2.2 Expression, unconventional secretion and biochemical characterization of an α BoNTA nanobody

To extend the portfolio of proteins expressed in *U. maydis* towards real biopharmaceuticals, strains for the expression of nanobodies directed against Botulinum neurotoxin A (α BoNTA)

from *Clostridium botulinum* were generated. These nanobodies were reported to bind and clear Botulinum neurotoxin A in a mouse model *in vivo* (Mukherjee et al., 2012). The published sequence was dicodon optimized for optimal translation in *U. maydis* and integrated into the pRabX2 expression vector backbone (Sarkari et al., 2014; Terfrüchte, 2013; Zarnack et al., 2006). The construct was integrated into the AB33kex2Δ strain background using the *ip* integration method (Brachmann, 2001; Broomfield and Hargreaves, 1992) and resulting single insertion strains were verified by Southern blot analysis. To investigate expression and secretion of the fusion protein αBoNTA-NB-Cts1, cell extracts and supernatants of strain AB33kex2Δ αBoNTA-NB-Cts1 were subjected to SDS-PAGE and Western blot analysis (Fig. 2.6 A). Full length αBoNTA-NB-Cts1 (αBoNTA = 74 kDa) could be detected in comparable amounts like αGfp-NB-Cts1 (αGfp = 76 kDa) in cell extracts (Fig. 2.6 A, left panel). By contrast,

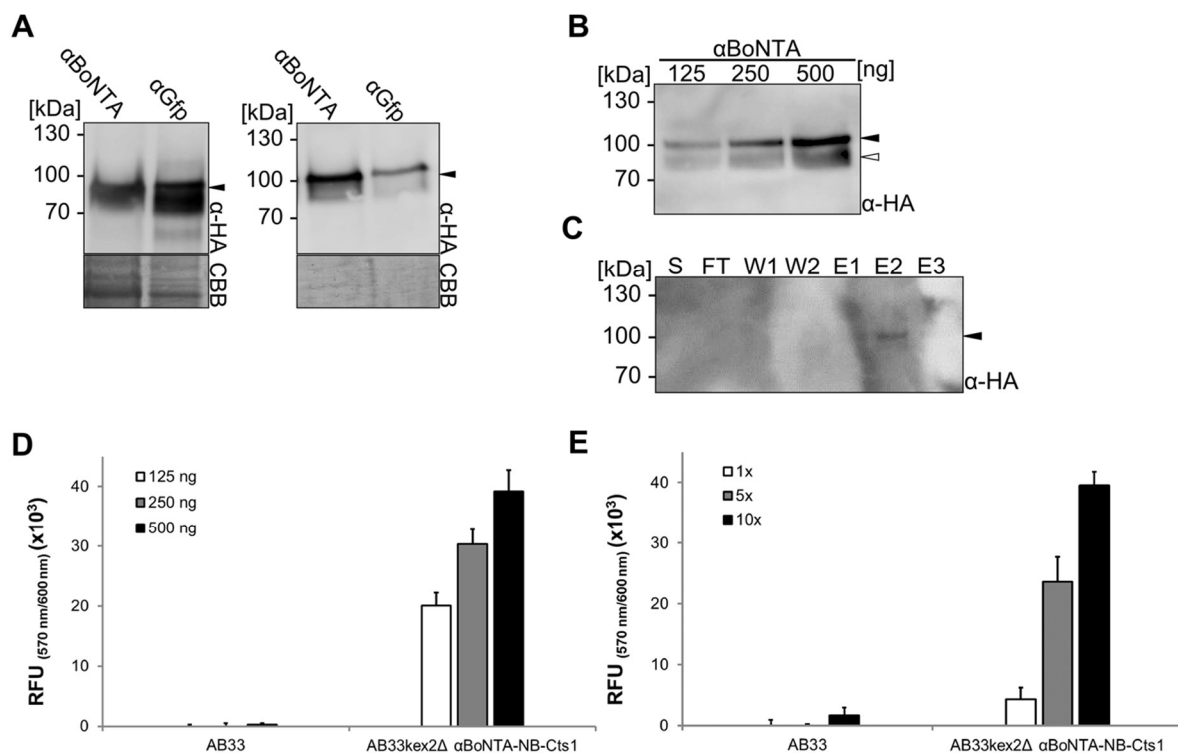


Fig. 2.6: Expression, purification and characterization of camelid V_{HH} derived αBoNTA-NB proteins

A. Western blot analysis of whole cell extracts and precipitated supernatants of αBoNTA-NB-Cts1 (αBoNTA) and αGfp-NB-Cts1 (αGfp) expressing *U. maydis* strains (AB33kex2Δ αBoNTA-NB-Cts1 and AB33kex2Δ αGfp-NB-Cts1). 10 μg of whole cell extracts (left panel) or 1 mL of precipitated supernatant (right panel) were subjected to SDS-PAGE and Western blot analysis. Fusion proteins were detected using α-HA primary antibodies and the membrane was stained with Coomassie brilliant blue after detection (CBB). **B.** Western blot analysis of different amounts of αBoNTA-NB-Cts1 whole cell extract expressed by strain AB33kex2Δ αBoNTA-NB-Cts1. Heterologous protein was detected using α-HA primary antibodies. The full length protein band migrates slightly higher than the calculated 74 kDa (filled arrowhead) and a degradation band can be observed (open arrowhead). The depicted protein amounts were used in ELISA (s. Fig. 2.6 D). **C.** Western blot analysis of IMAC purified αBoNTA-NB-Cts1 from supernatant of AB33kex2Δ αBoNTA-NB-Cts1. 14 μL of the supernatant (S), flow through (FT), wash fraction 1 and 2 (W1, W2) and elution fraction 1, 2 and 3 (E1, E2, E3) were analyzed. Detection was performed using α-HA primary antibodies. The full length protein migrates slightly higher than the calculated 74 kDa (filled arrowhead). Enrichment of αGfp-NB-Cts1 can be observed in E2 and E3, thus these fractions were used for ELISA (s. Fig. 2.6 E). **D.** Varying amounts of AB33 and AB33kex2Δ αBoNTA-NB-Cts1 whole cell extracts (also see Fig. 2.6 B) were analyzed in triplicates by ELISA against Botulinum neurotoxin A as antigen. **E.** Elution fractions from IMAC purifications of AB33 and AB33kex2Δ αBoNTA-NB-Cts1 supernatant (also see Fig. 2.6 C) were analyzed in different concentrations by ELISA against Botulinum neurotoxin A. ELISA was performed in triplicates.

unconventional secretion of α BoNTA-NB-Cts1 seemed to be more efficient (Fig. 2.6 A, right panel). In addition to the full length fusion protein band marked by filled arrowheads, the previously mentioned major degradation band, migrating slightly below the full length band, could be detected in low amounts. To investigate the antigen binding activity and specificity of α BoNTA-NB, ELISA assays were conducted. To this end, microtiter plates coated with Botulinum neurotoxin A (Metabio Inc.) were used. First, defined amounts of cell extracts from AB33 and AB33kex2 Δ α BoNTA-NB-Cts1 were applied. Volumetric activity could be detected for α BoNTA-NB whereas the wildtype samples did show hardly any background (Fig. 2.6 B, D). The same could be observed when ascending concentrations of purified supernatant were applied to ELISA (Fig. 2.6 C, E). These experiments indicate that indeed the nanobody is functional. As the secretion efficiency of α BoNTA-NB-Cts1 was very high, additional experiments in which supernatant was directly applied without concentration were performed. Using only 300 μ L of supernatant, volumetric activity with similar intensities could be detected in ELISA (Fig. 2.19 B). Hence, the produced nanobody seems to be very stable in the culture supernatant. These results show that functional α BoNTA-NB could be produced by Cts1-mediated unconventional secretion, suggesting that the application of the previously established conditions can be easily transferred to other pharmaceutically relevant nanobodies.

2.3 Application of unconventional secretion for expression of the potential malaria antigen PfRH5

The *P. falciparum* reticulocyte binding protein homologue 5 (PfRH5) was selected as an additional interesting pharmaceutical target for Cts1-mediated unconventional secretion. This protein has been found to be a potential antigen for vaccine development against malaria (Ord et al., 2014). First studies on PfRH5 revealed that binding to its receptor, Basigin, on mammalian reticulocytes, requires the protein to be unglycosylated in order to exhibit proper functionality (Sony Reddy et al., 2014). To prevent glycosylation during expression of the protein in mammalian and insect cells, a version in which the four potential N-glycosylation sites were mutagenized is usually used nowadays (Fig. 6.1). However, expression of this version still leads to only low yields of active full length protein (Bustamante et al., 2013; Crosnier et al., 2011). This may be due to the general structure of PfRH5. Besides a series of α -helices, β -sheets and three disulfide bridges, the protein consists of long disordered regions that might hinder proper folding (Wright et al., 2014). To avoid the flexible N-terminus, expression of an N-terminally truncated version, lacking most of the 140 amino acid long N-terminal region, was described. This variant has been reported to still be capable of receptor binding (Wright et al., 2014). Due to all these problems, it is essential to test alternate

expression systems for P α RH5. Unconventional secretion in *U. maydis* would be perfectly suited for this purpose and was thus tested for its abilities to express functional P α RH5.

2.3.1 Expression and purification of UmRH5

To investigate the applicability of Cts1-mediated unconventional secretion for production of P α RH5, the gene for a P α RH5 variant lacking N-glycosylation sites (obtained from the Wellcome Trust Sanger Institute, Cambridge) was dicodon optimized for *U. maydis* (UmRH5) and the sequence for the native signal peptide was deleted to avoid entry into the conventional secretory pathway. Additionally, three intrinsic *Bsa*I endonuclease recognition sites were mutated for cloning purposes. Of note, amino acid substitutions accidentally introduced during mutagenesis in some of the constructs did not display divergent characteristics compared to a correct version as investigated in comparative assays with non-mutated versions (Fig. 6.1; data not shown). Besides the full length UmRH5 protein, a strain expressing a version of UmRH5 lacking the flexible N-terminal region was generated (Wright et al., 2014). 134 amino acids were removed from the N-terminus, leading to the truncated protein Δ N-UmRH5 (Fig. 6.1). Both variants were fused to Cts1 to mediate unconventional secretion.

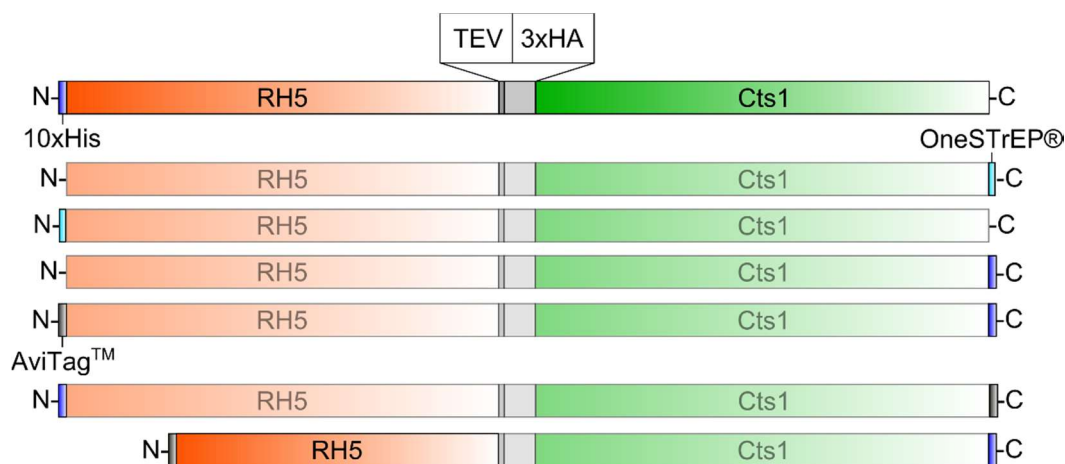


Fig. 2.7: Schematic overview of expressed UmRH5 variants

The basic fusion protein consisted of the UmRH5 protein (orange), followed by a TEV protease cleavage site (dark grey), a 3xHA-tag (light grey) and the Cts1 protein (green). Purification tags were either added to the N- (N) or C-terminus (C) and included a 10xHis-tag (dark blue), a OneSTrEP®-tag (light blue) and an AviTag™ (black).

To identify the optimal protein variant that allows not only expression and unconventional secretion of UmRH5 but also its purification and activity detection, again several combinations of purification tags and protease cleavage sites were tested. These included N- and C-terminal 10xHis-tags, OneSTrEP®-tags, TEV protease cleavage sites and the AviTag™ for biotinylation. An overview of the tested constructs is provided in Fig. 2.7. All constructs were introduced into the genome of *U. maydis* strains in single insertion via the *ip* integration method (Brachmann, 2001; Broomfield and Hargreaves, 1992).

In order to identify the optimal expression strength, a selected construct was expressed under the control of the two promoters P_{otef} and P_{oma}. Previous results indicated an increased

expression for scFvs using the strong synthetic P_{oma} promoter compared to the weaker P_{otef} promoter (Sarkari et al., 2014). To additionally test the effect of proteases, the construct was expressed not only in the AB33 wildtype strain but also in the two protease deficient strains AB33kex2 Δ and AB33P5 Δ (Fig. 2.8). Western blot analysis of cell extracts from the corresponding strains AB33 P_{otef} S-UmRH5*-Cts1 (P_{otef}), AB33kex2 Δ P_{otef} S-UmRH5*-Cts1 (kex2 Δ P_{otef}), AB33 P_{oma} S-UmRH5*-Cts1 (P_{oma}) and AB33kex2 Δ P_{oma} S-UmRH5*-Cts1 (kex2 Δ P_{oma}) showed that the UmRH5-Cts1 fusion protein was produced. Reduced proteolytic degradation clearly increased the amount of heterologous protein whereas in this case the promoter exchange did not influence the protein levels (Fig. 2.8 A). This observation was unexpected but could be verified by observing the same phenomenon with other UmRH5 constructs (data not shown). As the full length protein was repeatedly reported to be hard to express, strong overexpression might induce stress reactions like UPR or ERAD and thus does not yield elevated protein levels (Heimel, 2014; Mattanovich et al., 2004; Wright et al., 2014). Western blot analyses of cell extracts (Fig. 2.8 B, left panel) and supernatants (Fig. 2.8 B, right panel) of AB33 P_{otef} S-UmRH5*-Cts1, AB33kex2 Δ P_{otef} S-UmRH5*-Cts1 and AB33P5 Δ P_{otef} S-UmRH5*-Cts1 revealed that the increased protein yield in both protease deficient strain backgrounds compared to the wildtype strain was on an equal level in cell extracts. Nevertheless, in supernatants of the AB33P5 Δ P_{otef} S-UmRH5*-Cts1 expression strain, a prominent degradation band of full length S-UmRH5-Cts1 could be observed. This indicates additional proteolysis of the major degradation product in *kex2* deficient strains. Other tested

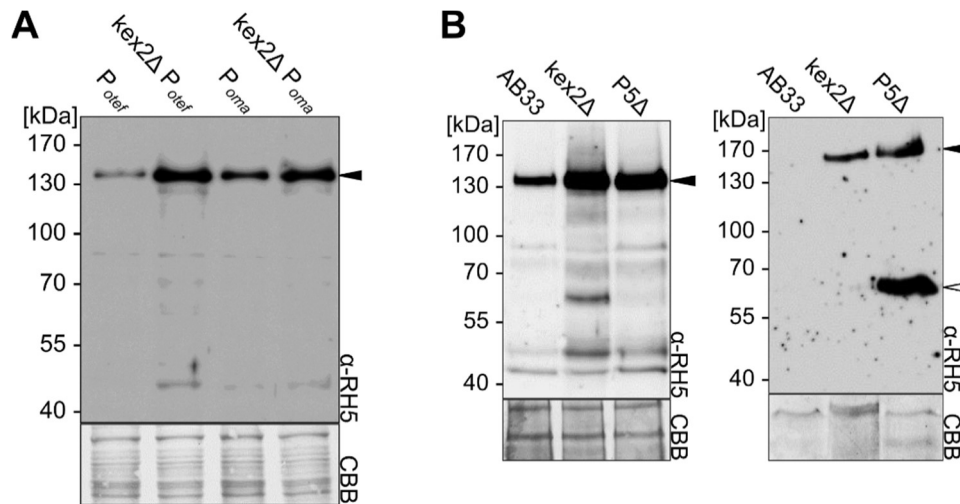


Fig. 2.8: Expression and unconventional secretion of *U. maydis* RH5-Cts1 fusion proteins

A. Western blot analysis of One-STREP®-UmRH5*-TEV-HA-Cts1 fusion protein (S-UmRH5 = 122 kDa) expression in strains AB33 P_{otef} S-UmRH5*-Cts1 (P_{otef}), AB33kex2 Δ P_{otef} S-UmRH5*-Cts1 (kex2 Δ P_{otef}), AB33 P_{oma} S-UmRH5*-Cts1 (P_{oma}) and AB33kex2 Δ P_{oma} S-UmRH5*-Cts1 (kex2 Δ P_{oma}). 10 μ g of whole cell extracts were subjected to SDS-PAGE and subsequent Western blotting. Protein was detected using antibodies directed against UmRH5. Full length S-UmRH5 is depicted with a filled arrowhead. The membrane was stained with Coomassie brilliant blue (CBB) after development. **B.** Western blot analysis of cell extracts and supernatants of AB33 P_{otef} S-UmRH5*-Cts1 (AB33), AB33kex2 Δ P_{otef} S-UmRH5*-Cts1 (kex2 Δ) and AB33P5 Δ P_{otef} S-UmRH5*-Cts1 (P5 Δ). 10 μ g of whole cell extracts (left panel) or 1 mL of TCA precipitated culture supernatants (right panel) were subjected to SDS-PAGE and subsequent Western blotting. Protein was detected using antibodies directed against UmRH5. Full length S-UmRH5 is depicted with a filled arrowhead, whereas a prominent degradation band is depicted with an open arrowhead. The membrane was stained with Coomassie brilliant blue (CBB) after development.

construct variants showed a very similar behavior (data not shown). The results show that UmRH5 can be produced and secreted as a Cts1 fusion protein if protease deficient strains are exploited as expression hosts.

Next, to allow functional characterization of UmRH5 produced in *U. maydis*, several strategies were tested to purify the protein using a variety of purification tags (Fig. 2.9). However, even purification from cell extracts via C- or N-terminal 10xHis-tags resulted in very low amounts of purified full length UmRH5 in the elution fractions (Fig. 2.9, left and central panel). The same results were obtained for purifications via N- and C-terminal OneSTrEP®-tags (Fig. 2.9, right panel). The main reason for the low amounts was a poor binding of the UmRH5 protein to the respective purification resin, indicated by high amounts of UmRH5 in flow through fractions. Neither variations in the lysis buffer- or equilibration buffer composition nor prolonged incubation time of the cell extract on the resin did improve the binding (data not shown). Thus, an alternate purification strategy exploiting the ability of Cts1 to bind to chitin (Jankowski, 2013) was tested (Fig. 2.9 C). As no substrate competition based elution of proteins bound to chitin is available, a method to elute the protein of interest from the chitin resin had to be established. To this end, it was intended to use the internal TEV protease cleavage site for elution of the heterologous target protein from the chitin resin. To test if proteolytic cleavage works efficiently, first native cell extracts of AB33P5Δ *P_{oter}*S-UmRH5*-Cts1 were hydrolyzed using the ProTEV Plus protease (Promega) (Fig. 2.9 B). Western blot results confirmed the specific hydrolysis of the full length S-UmRH5 protein into the OneSTrEP®-UmRH5 containing fragment (filled arrowhead) and the 3xHA-Cts1 containing fragment (open arrowhead) without unspecific proteolysis or degradation. This showed that in principle the proteolytic cleavage is possible. Next, native cell extracts of AB33P5Δ *P_{oter}*S-UmRH5*-Cts1 were subjected to a chitin resin and on-column cleavage of the full length protein was conducted with ProTEV Plus protease (Promega). Western blot analysis of the resulting purification fractions clearly showed that a large portion of the protein did again not stick to the column, as protein amounts in the flow through fraction were very high (Fig. 2.9 C). Furthermore, on-column cleavage of the bound full length protein (filled arrowhead) was very inefficient. Here it might be necessary to switch to another protease with higher on-column cleavage potential (Waugh, 2011). Nevertheless, a small amount of pure OneSTrEP®-UmRH5 (open arrowhead) could be eluted from the column. Additional elution steps with harsher conditions did not result in further elution. Therefore, this approach could also not be used for efficient purification. Boiling of the resin in denaturing Laemmli buffer eluted large amounts of full length and cleaved protein, indicating that it was still sticking to the chitin resin after initial elution under native conditions. It also shows that the cleaved fragments themselves bind unspecifically to chitin and confirms again that on-column cleavage is highly inefficient using the TEV protease. Using other tag removal strategies and cleavage conditions might however improve chitin based purification (Kimple et al., 2015).

In summary, multiple attempts to purify the RH5-Cts1 fusion protein turned out to be very inefficient, suggesting structural interferences with purification tags.

2.3.2 Biochemical characterization of UmRH5

Purification resulted in very poor amounts of the UmRH5-Cts1 fusion protein. These were thus not well suited for biochemical characterization. However, as previous studies described a very sensitive assay based on biotinylation (Kerr and Wright, 2012), UmRH5 and Δ N-UmRH5 were alternatively equipped with an AviTag™ (Fig. 2.7). The AviTag™ peptide sequence originates

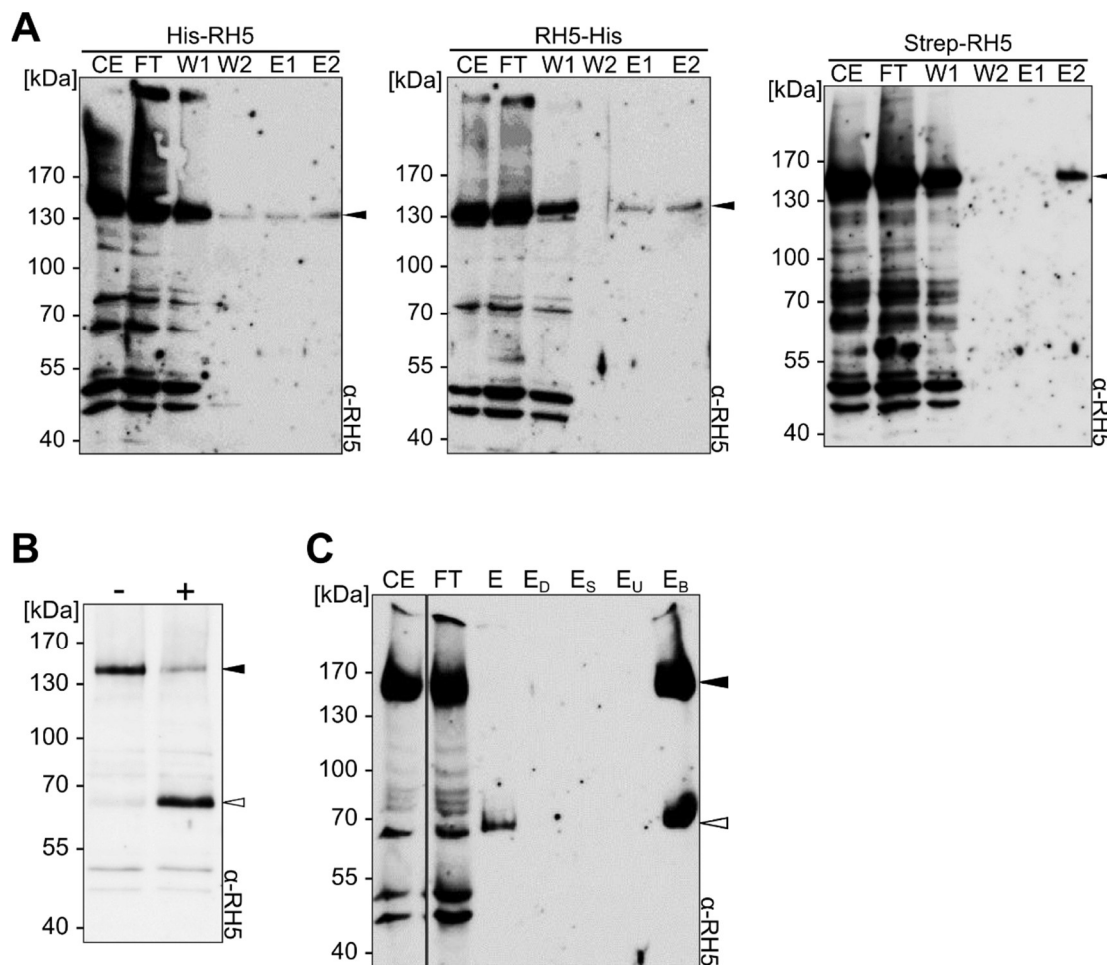


Fig. 2.9: Purification of *U. maydis* UmRH5

A. IMAC purification of native AB33P5 Δ 10xHis-UmRH5*-TEV-HA-Cts1 cell extracts (His-RH5 = 123 kDa, left panel), AB33P5 Δ UmRH5*-TEV-HA-Cts1-10xHis cell extracts (UmRH5-His = 123 kDa, center panel) and Streptavidin® purification of native AB33kex2 Δ One-STrEP®-UmRH5*-TEV-HA-Cts1 cell extracts (Strep-UmRH5 = 122 kDa, right panel). Cell extract (CE), flow through (FT), wash fractions (W1, W2) and elution fractions (E1, E2), were subjected to SDS-PAGE and Western blotting. Protein was detected using antibodies directed against UmRH5. Full length His-UmRH5, UmRH5-His and Strep-UmRH5 protein is depicted with a filled arrowhead. **B.** TEV protease hydrolysis of One-STrEP®-UmRH5*-TEV-HA-Cts1 fusion protein (S-UmRH5). Cell extracts of AB33kex2 Δ P_{otef} S-UmRH5* were prepared in native TEV lysis buffer and incubated overnight on 4°C with 1 U ProTEV Plus (Promega) (+) or water as a negative control (-). Samples were then analyzed by Western blotting, using antibodies directed against UmRH5. Full length S-UmRH5 (122 kDa) is marked with a filled arrowhead, while the One-STrEP®-UmRH5 containing part (60 kDa) is depicted by an open arrowhead. **C.** Chitin Resin purification of One-STrEP®-UmRH5*-TEV-HA-Cts1 fusion protein (S-UmRH5) from native AB33P5 Δ P_{otef} S-UmRH5* cell extracts. Cell extract (CE), flow through (FT) and elution fractions (also see 4.2.3: E; E_D; E_S; E_U; E_B (supernatant of boiled resin) were subjected to SDS-PAGE and Western blotting. Protein was detected using antibodies against UmRH5. Full length S-UmRH5 (122 kDa) is marked with a filled arrowhead while the One-STrEP®-UmRH5 containing part (60 kDa) is depicted by an open arrowhead.

from *E. coli* and is recognized by *E. coli* biotin ligase A (BirA), resulting in the addition of a single biotin molecule (Beckett et al., 2008; Elia, 2010). This enables the purification and immobilization of the biotinylated protein on Streptavidin® coated materials (Elia, 2010; Kerr and Wright, 2012). Biotinylated P₇RH5 has been successfully used in a prey-bait based interaction screening termed AVEXIS (Avidity based Extracellular Interaction Screening (Kerr and Wright, 2012)). In order to analyze the binding affinity of UmRH5 to Basigin, biotinylation approaches with full length and N-terminally truncated AviTag™-tagged proteins from *U. maydis* cell extracts and supernatants were performed. However, most attempts were unsuccessful and modified ELISA protocols, aiming on the detection of interaction between UmRH5 and Basigin did also not show reliable results (data not shown). As purification turned out to be a problem, sufficient amounts of purified UmRH5 for interaction screens, like surface plasmon resonance or microscale thermophoresis, could not be obtained. Using the truncated version did also not improve the purification (data not shown). Hence, these limitations did not yet allow a detailed biochemical characterization.

Nevertheless, the results show that *U. maydis* is potentially suited for the production of unglycosylated RH5 protein as the Cts1-mediated export into the culture supernatant could be demonstrated. Further studies should concentrate on the expression of modified RH5 variants probably containing linkers as well as a native variant without mutagenized *N*-glycosylation sites. Additionally it might be beneficial to perform chromatographic size exclusion purifications, as the structure of RH5 might hinder proper binding to standard purification resins via terminal tags.

2.4 Optimization of cultivation conditions for heterologous protein expression in *U. maydis*

Until now, establishment of *U. maydis* as an expression platform for heterologous proteins has largely focused on standard techniques adopted from basic research. Here, methods are mainly based on working with low cell densities and not focused on cost efficiency or high protein yields. Thus, in this part the cultivation conditions were optimized for efficient protein expression and subsequent unconventional secretion. Of note, in this framework effects occurring during prolonged cultivation to high optical densities were studied for the first time.

2.4.1 Online monitoring of standard *U. maydis* cultivations using RAMOS

Getting insights into the metabolic state of a culture during growth is a difficult task as usually elaborate sampling has to be conducted. This can only cover selected time points, disturbs the growth and does not sufficiently reflect the cells condition during cultivation. To overcome this problem the Respiration Activity Monitoring System (RAMOS) device was used. The device is built up of an orbital shaker equipped with eight standard shaking flasks, each capped with an

oxygen partial pressure probe. Inlet and outlet valves guarantee controlled aeration and measuring conditions (Anderlei et al., 2004). Typically measurements in closed systems are performed in bioreactors, being very laborious and costly. In contrast, the RAMOS device gives the opportunity to directly transfer knowledge from standard laboratory shaking flask experiments and besides enables the parallel investigation of up to eight different conditions. To gain further information on pH, metabolite concentrations, product concentrations and cell density, the setup is combined with additional shake flasks on a separate shaker, containing the same inocula that can be sacrificed for additional analytics during cultivation. The combination of online and offline sampling thus gives a broad overview about physiological state, nutrient availability and product yield during cultivation.

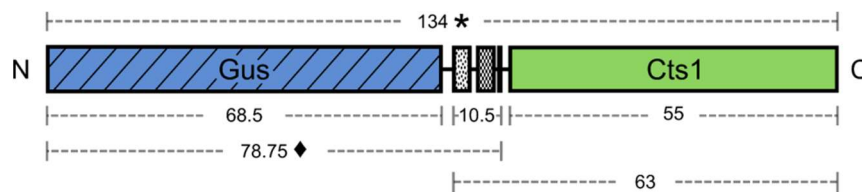


Fig. 2.10: Graphical representation of Gus-SHH-Cts1 fusion protein

The fusion protein consists of the N-terminal Gus protein (blue, hatched), followed by the SHH linker (OneSTrEP®-tag, sprinkles; 3xHA-tag, checkers; 10xHis-tag, black) and the Cts1 protein (green). Numbers between grey dashed lines indicate the calculated sizes (in kDa) of the full length protein (*), the Gus-SHH fragment (♦) and other possible degradation products.

To investigate the cultivation conditions for *U. maydis* during expression and unconventional secretion of heterologous proteins, the established β -glucuronidase (Gus) reporter system was used (Stock et al., 2012; Stock et al., 2016). The system is based on the property of Gus to lose its activity if the protein is modified by *N*-glycosylation. As the previously described Cts1-mediated unconventional secretion pathway avoids ER passage and thereby *N*-glycosylation, the enzyme is secreted in its active state. The used Gus-Cts1 construct containing an internal SHH linker is schematically shown in Fig. 2.10. To first get insights on the general behavior of *U. maydis* during cultivation, the wildtype strain AB33 was cultivated under standard laboratory conditions in a RAMOS device (Fig. 2.11). The oxygen transfer rate (OTR) monitored for *U. maydis* AB33 batch cultivation resembled a diphasic growth, starting with an exponential increase of the OTR until around 15.8 mmol/L/h were reached. Here most likely the preferred nitrogen source became limiting, as glucose was still available and the OTR decreased slightly below 10 mmol/L/h. The cells then started to feed on a secondary nitrogen source, depicted by an increasing OTR, which again drastically decreased as soon as glucose became limiting (Fig. 2.11 A). In direct negative correlation with the initial increase of the OTR and the optical density of the cells, the culture supernatant acidified down to a pH level of ≤ 4.5 until the end of the cultivation (Fig. 2.11 B). This showed on the one hand that the OTR is directly correlating with cell growth and on the other hand that increasing biomass leads to a strong decrease of the pH level. To investigate the effect of acidification on unconventionally secreted Gus-Cts1, AB33 Gus-Cts1 was cultivated in CM medium supplemented with 10 g/L glucose in a RAMOS

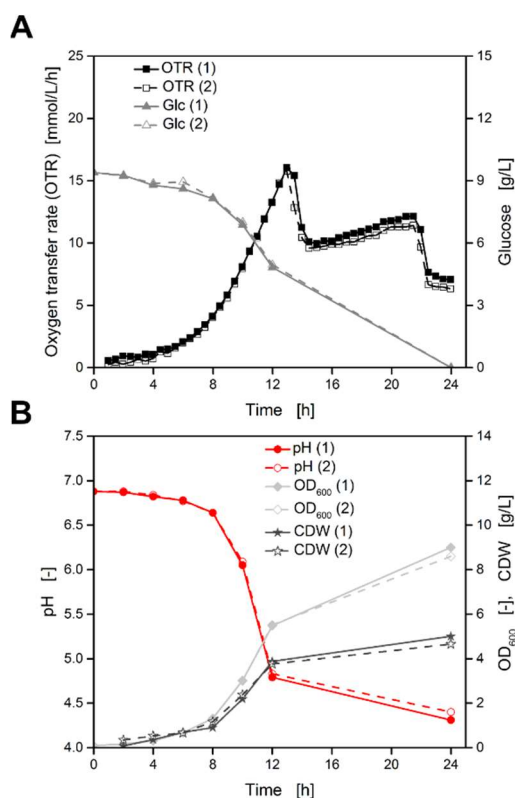


Fig. 2.11: RAMOS cultivation and offline analysis of *U. maydis* AB33

U. maydis AB33 was inoculated to an OD₆₀₀ of 0.08 in 20 mL CM medium, supplemented with 10 g/L glucose. Cultivation was performed in technical duplicate on a RAMOS orbital shaker (5 cm shaking diameter), on 28°C at 300 rpm. **A.** The oxygen transfer rate (OTR) resembles a diauxic growth, while HPLC determined glucose concentration decreases exponentially with increasing OTR. **B.** Offline parameters determined from additional shaking flasks. OD₆₀₀ and CDW can be directly correlated. pH decreases exponentially in direct negative correlation to the increasing cell density.

device. To get information about pH, glucose levels, OD₆₀₀ and unconventional secretion of Gus-Cts1, additional offline sampling from equally treated shaking flasks was performed (Fig. 2.12 A-C). The OTR again resembled a diphasic growth behavior as detected for AB33 (Fig. 2.12 A-C). The progression of the optical density increase, glucose consumption and pH decrease over time was also directly comparable. To get a semi quantitative view on the unconventionally secreted Gus-Cts1 protein, Gus assays were performed and precipitated supernatants were analyzed by Western blotting (Fig. 2.12 B, C). Interestingly, Gus activity initially increased with increasing OD₆₀₀ but then decreased at 10 hours post inoculation (hpi) and was then not detectable anymore. This finding was also mirrored by the results of the Western blot in which antibodies directed against Gus were used for detection (Fig. 2.12 C). In early stages of the cultivation, only a major degradation product of the Gus-Cts1 fusion protein could be detected (Fig. 2.12 C, marked by ♦). This fragment most likely resembled the 79 kDa Gus-SHH containing part. The amount of this fragment was constantly increasing over time until 10 hpi when it started to be further degraded. This further degradation intensified from 10 hpi on (Fig. 2.12, marked by straight line). Both events correlated with a steep drop in pH from ≥ 6.5 to 5, between 8 hpi and 12 hpi. Thus the decreased pH could be the crucial factor influencing activity and stability of the Gus-Cts1 fusion protein.

2.4.2 Determination of optimal buffer conditions for Gus-Cts1 expression in *U. maydis*

To further investigate the effect of acidification on unconventionally secreted Gus-Cts1, 0.1 M MOPS buffered cultivations covering a sampling range from 0 - 12 hpi (Fig. 2.12 D - F) and a sampling range from 12 - 28 hpi (Fig. 2.12 G - I) were conducted. Indeed, the buffering stabilized the pH leading to a constant pH of ≥ 6.5 during the whole cultivation. In contrast to unbuffered cultures the Gus activity measured in culture supernatants was steadily increasing until it reached a static plateau after around 18 hpi (Fig. 2.12 E, H). Having a closer look on the stability of the protein by Western blot analysis revealed that the amount of protein increased until the end of the cultivation and most of the additional degradation fragments

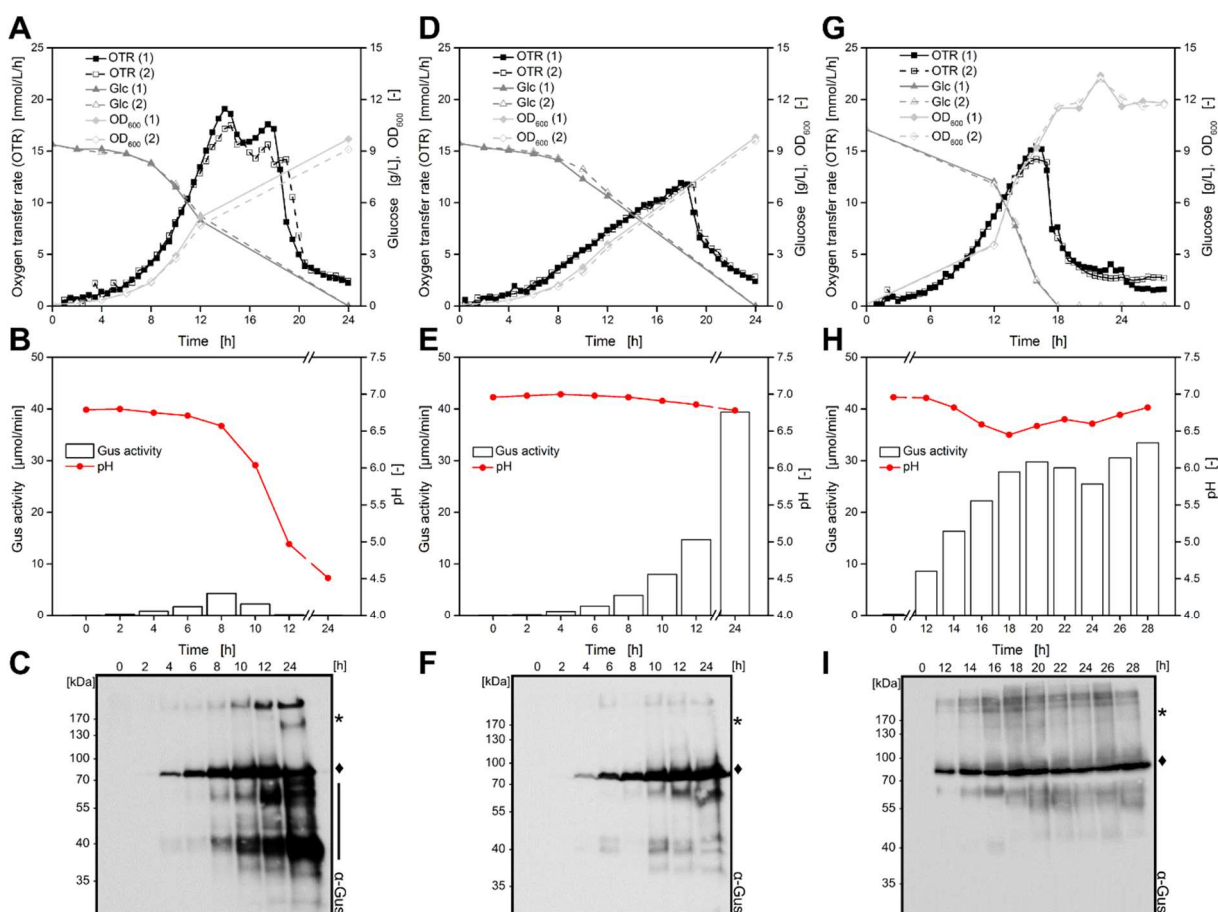


Fig. 2.12: Offline and online cultivation parameters of unbuffered and buffered AB33 Gus-Cts1 cultivations

U. maydis AB33 Gus-Cts1 was inoculated to an OD₆₀₀ of 0.08 in 20 mL CM medium, supplemented with 10 g/L glucose (A-C) and additionally with 0.1 M MOPS (D-I). Cultivation was performed in technical duplicates on a RAMOS orbital shaker (5 cm shaking diameter), on 28°C at 300 rpm. Sampling of the offline parameters pH, OD₆₀₀, HPLC samples and supernatants was focused either on 0 - 12 hpi (A-F) or on 12 - 28 hpi (G-I). A, D, G. The OTR was determined by online RAMOS measurements, while OD₆₀₀ and HPLC samples for glucose concentration determination were taken from additional, equally treated shaking flasks. B, E, H. pH progression is depicted in red, while bars resemble the unconventional secretion, on the basis of Gus activity measured in supernatant samples. C, F, I. Western blot analysis of 1 mL precipitated supernatant samples, exemplifying the stability status of the unconventionally secreted Gus-Cts1 fusion protein. Protein was detected using antibodies directed against Gus. The full length protein on 134 kDa is marked by an asterisk (*), while a major degradation product on 79 kDa is marked by a rhombus (◆). Additional undefined degradation products are marked with a straight line. For C, F, I, results for one technical replicate are shown.

could not be detected anymore (Fig. 2.12 F, I). This finding strongly supports the hypothesis of pH dependent activity and stability of unconventionally secreted Gus-Cts1.

Interestingly, the OTR progression of the unbuffered and buffered cultures were quite different. The OTR in the buffered culture increased less steep and had only one maximum, indicating that the two peaks in unbuffered cultures could be due to a stress response of the cells towards changing pH levels thus resulting in slower metabolism. However, growth was not affected by buffering the culture (Fig. 2.12 A, D, G). Additionally to MOPS, HEPES was also tested as a

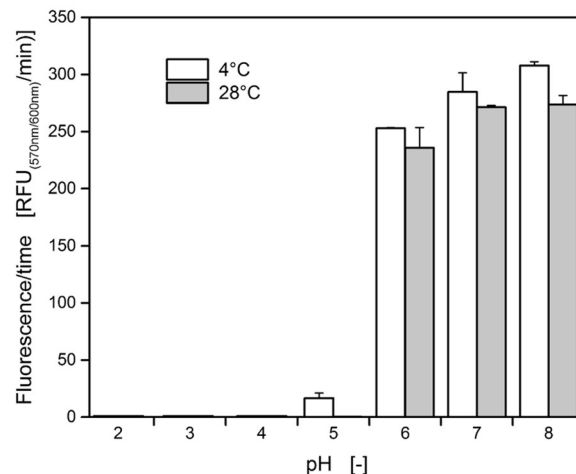


Fig. 2.13: Influence of different pH levels on Gus activity

Equal amounts of Gus-SHH purified from *E. coli* were incubated in CM medium (supplemented with 10 g/L glucose) with varying pH levels. Incubation was performed for 22 h at 4°C and 28°C. Gus activity is displayed as a function of substrate conversion over time, showing almost no effect at pH 6 - 7 while activity drastically drops at pH levels ≤ 5 .

buffer substance showing similar results but causing problems in processing of the samples due to precipitation of the buffer substance (data not shown). Further investigation on the pH effect on Gus activity was conducted using purified Gus-SHH protein from *E. coli* (Fig. 2.13). To this end, defined amounts of purified protein were incubated for 22 h, at either 4°C or 28°C, in CM-glucose medium adjusted to different pH levels (ranging from pH 2 to 8). Gus activity remained stable when incubated in pH ≥ 6 while almost all activity was lost when incubated at pH levels below 6. This finding is in line with previous reports (Zenser et al., 1999). As loss in activity and degradation of Gus-Cts1 could already be observed at pH levels above 6 (Fig. 2.12 B), acidic pH might trigger processes responsible for degradation but can't be the only reason for decreasing activity and degradation of the protein.

2.4.3 Combining protease deficient *U. maydis* strains with optimized buffering

Previous studies on unconventional secretion of Cts1 revealed a strong influence of secreted proteases on the stability of the protein (Sarkari et al., 2014). Thus, an *in vitro* assay to investigate the influence of pH decrease and protease deficiency was conducted. To this end, AB33 and the protease deficient strains AB33kex2Δ and AB33P5Δ were grown in CM-glucose

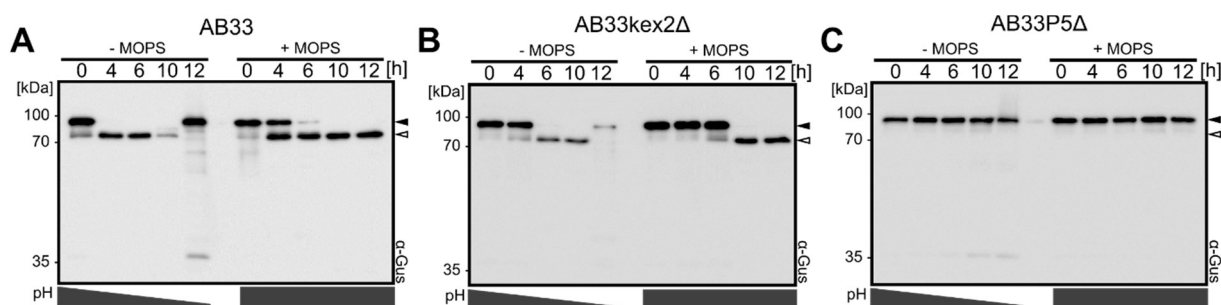


Fig. 2.14: Stability of Gus-SHH in culture supernatant from buffered and unbuffered *U. maydis* cultivations

Equal amounts of Gus-SHH purified from *E. coli* were incubated for 2 h with culture supernatants obtained from *U. maydis* wildtype (A) and protease deficient strains AB33kex2Δ and AB33P5Δ (B, C). Cell free supernatant samples were collected at different time points during cultivation in 20 mL CM medium (supplemented with 10 g/L glucose), with or without 0.1 MOPS buffering. Dark grey bars below the graphs indicate steady or decreasing pH (corresponding pH values are listed in Tab. 2.1). After incubation samples were subjected to SDS-PAGE and Western blot analysis, using antibodies directed against Gus for detection. Full length Gus-SHH protein (79 kDa) is indicated by filled arrowheads, while open arrowheads mark the major degradation product, most probably referring to Gus without the SHH linker.

medium under 0.1 M MOPS buffered and unbuffered conditions for 12 hours. Samples were collected over time and defined amounts of Gus-SHH purified from *E. coli* were incubated for 2 h with the cleared supernatants. After incubation the samples were subjected to SDS-PAGE and analyzed by Western blotting, using antibodies directed against Gus (Fig. 2.14). As observed in earlier cultivations, pH of the buffered cultures remained constant at a level of around 7, while pH decreased to a level of almost 4 without proper buffering (see also Tab. 2.1).

Supernatants of AB33 rapidly lead to a degradation of the full length protein (Fig. 2.14 A, filled arrowhead) and after 10 hpi even the degradation band, most likely referring to Gus without the SHH-linker (open arrowhead), vanished. At 12 hpi again full length protein was detectable, indicating that at such low pH levels no more active degradation of the protein occurs. For buffered AB33 samples, the stability of the full length protein was prolonged but after 6 to 10

Tab. 2.1: Approximate pH values of supernatants for *in vitro* Gus stability assay (Fig. 2.14)

		CM-glc					CM ^M -glc				
strain	Time [h]	0	4	6	10	12	0	4	6	10	12
AB33		7.00	6.75	6.50	5.00	4.00	7.00	7.00	7.00	7.00	7.00
AB33kex2Δ Gus-Cts1		7.00	6.75	6.50	6.00	4.00	7.00	7.00	7.00	7.00	7.00
AB33P5Δ Gus-Cts1		7.00	6.75	6.50	5.00	4.00	7.00	7.00	7.00	7.00	7.00

hpi no more full length protein was detectable, whilst the major degradation product was stable even at 12 hpi. The same effects could be observed for samples treated with AB33kex2Δ supernatants (Fig. 2.14 B), whereas the degradation of the full length protein was delayed compared to AB33 supernatant treated samples (Fig. 2.14 A, B). For AB33P5Δ supernatant treated samples (Fig. 2.14 C) the results gave a completely different picture as no degradation

of the full length protein could be detected at all. This finding strongly supports the combinational influence of pH decrease and proteolytic degradation of *U. maydis* supernatants on the stability of Gus. The effect of protease deficient strain backgrounds on the stability of unconventionally secreted Gus-Cts1 was thus further investigated. AB33kex2Δ Gus-Cts1 was already available while the Gus-Cts1 expression construct still had to be introduced into AB33P5Δ using the *ip* insertion method (Brachmann, 2001; Broomfield and Hargreaves, 1992). The resulting AB33P5Δ Gus-Cts1 strain as well as AB33 Gus-Cts1 and AB33kex2Δ Gus-Cts1 were investigated in MOPS buffered RAMOS cultivations, focusing on a sampling time between 12 and 28 h (Fig. 2.15). Interestingly, the OTR progression and growth behavior of AB33 and AB33P5Δ were almost identical whereas OTR progression and growth of the AB33kex2Δ strain was reduced. This is in line with previous results and observations showing

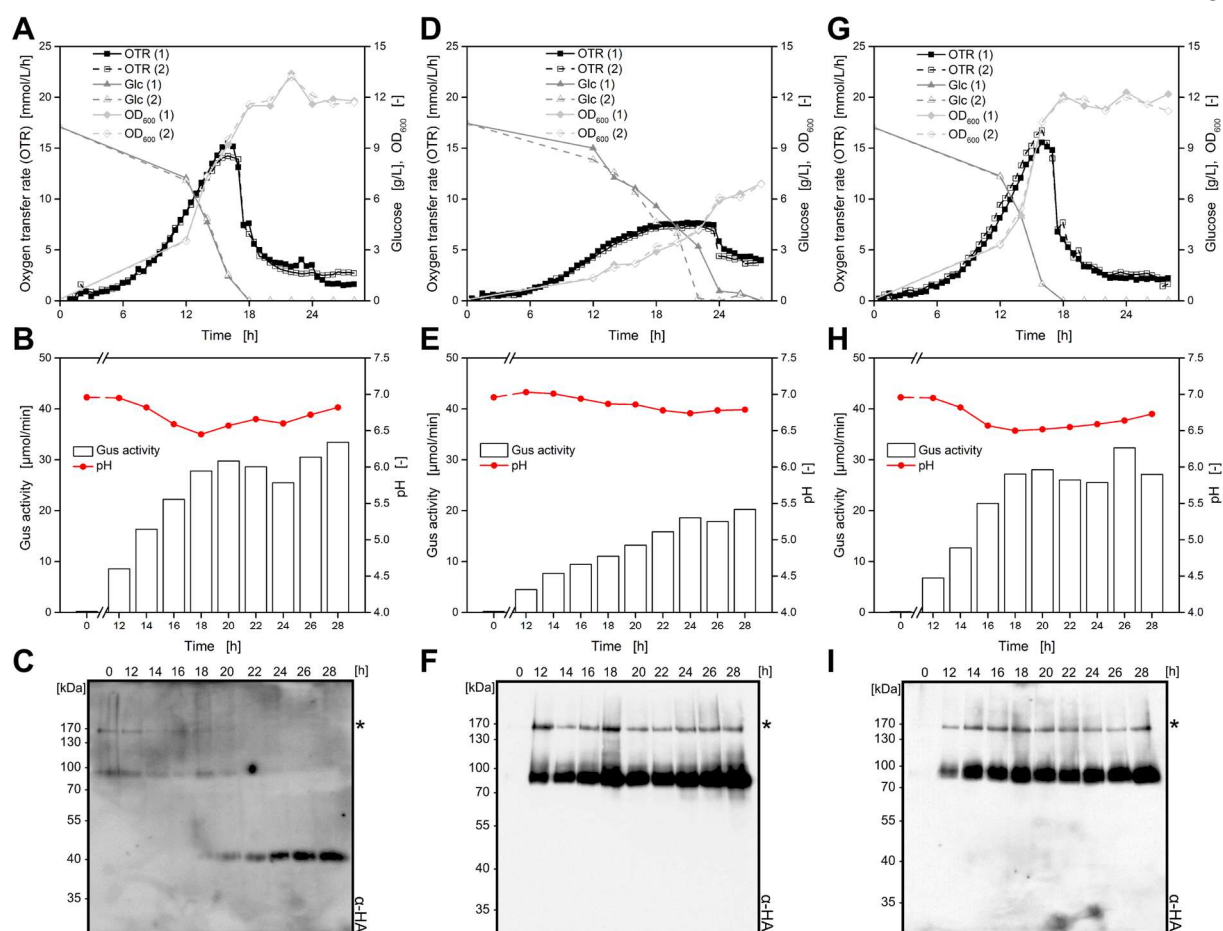


Fig. 2.15: Offline and online parameters of buffered cultivations of wildtype and protease deficient *U. maydis* Gus-Cts1 expression strains

U. maydis AB33 Gus-Cts1 (A-C), AB33kex2Δ Gus-Cts1 (D-F) and AB33P5Δ Gus-Cts1 (G-I) were inoculated to an OD₆₀₀ of 0.08 in 20 mL CM medium, supplemented with 10 g/L glucose and 0.1 M MOPS. Cultivation was performed in technical duplicates on a RAMOS orbital shaker (5 cm shaking diameter), on 28°C at 300 rpm. Sampling of the offline parameters pH, OD₆₀₀, HPLC samples and supernatants was focused on 12 - 28 hpi. A, D, G. The OTR was determined by online RAMOS measurements, while OD₆₀₀ and HPLC samples for glucose concentration determination were taken from additional, equally treated shaking flasks. B, E, H. pH progression is depicted in red while bars resemble the unconventional secretion on the basis of Gus activity, measured in supernatant samples. C, F, I. Western blot analysis of 1 mL precipitated supernatant samples, exemplifying the stability status of the unconventionally secreted Gus-Cts1 fusion protein. Protein was detected using antibodies directed against the internal 3xHA-tag. The full length protein on 134 kDa is marked by an asterisk (*). For C, F, I, results for one technical replicate are shown.

the drawbacks of the *kex2* deletion phenotype leading to aggregation of cells (Fig. 2.15 A, D, G). As Gus activity and thus protein yield is in strong dependency of the biomass, the slower growth also resulted in lowered Gus activity (Fig. 2.15 B, E, H). As before, Gus activity in AB33 Cts1-Gus and AB33*kex2*Δ Gus-Cts1 samples showed a constant increase until reaching a plateau at 18 hpi (Fig. 2.15 B, H). Though pH was constant during all cultivations, a difference in Gus-Cts1 stability could again be observed in Western blots of precipitated supernatants (Fig. 2.15 C, F, I). Whilst in the two protease deletion strain backgrounds, besides a major degradation product, stable full length protein (marked with an asterisk, *) could be observed, severe fragmentation of the full length protein and major degradation product took place in AB33 samples (Fig. 2.15 C). This again proves the strong influence of proteolytic degradation on unconventionally secreted Gus-Cts1.

2.4.4 Studying the effects of carbon and nitrogen concentration on growth and unconventional secretion

As expected for batch cultures, the OTR curves indicated nutrient limitations. To further elaborate on this the next experiments focused on the most important nutritional parameters, carbon and nitrogen. Thus, different RAMOS batch cultivations were performed using AB33 Gus-Cts1. A control experiment with standard concentrations of glucose (10 g/L) and ammonium nitrate (1.5 g/L) was performed with a sampling time from 12 to 46 h. The results were as expected and comparable to previous findings (Fig. 2.12 A – C, Fig. 2.16 A – C). Next, one culture with doubled amount of glucose (Fig. 2.16 D - F, 20 g/L) and one culture with doubled amounts of glucose and ammonium nitrate (Fig. 2.16 G - H, 20 g/L, 3 g/L) were investigated. The increased amount of glucose led to a prolonged progression of the OTR and an increased final OD₆₀₀. Nevertheless, a little peak in the OTR at 20 hpi again indicated a limiting component. As glucose was still available at this point, most probably nitrogen became limiting. Likely cells could recover from this and started feeding on another less preferred nitrogen source, for instance from components of the yeast extract (Fig. 2.16 D). The little peak was not visible anymore with an additionally increased amount of ammonium nitrate and only a slight shoulder at 20 hpi indicated a change in metabolic activity of the cells (Fig. 2.16 G). As this was directly correlating with a decrease of the culture pH, indicating the buffer capacity limit, the short lack in OTR progression is most likely due to a metabolic adaption process (see also Fig. 2.12 A). The OTR further increased to around 19 mmol/L/h and then collapsed to basal level. Since at this point almost all glucose was fed up, this might be a combinational effect of another unknown limiting nutrient and carbon source depletion (Fig. 2.16 G). Due to the increased biomass and prolonged growth phase, the buffer reached its capacity limit and pH dropped below 6 (Fig. 2.16 E) or even below 5.5, mirrored by the brake down of Gus activity at this point (Fig. 2.16 H). Later, recovery of the pH started with the cells entry into stationary

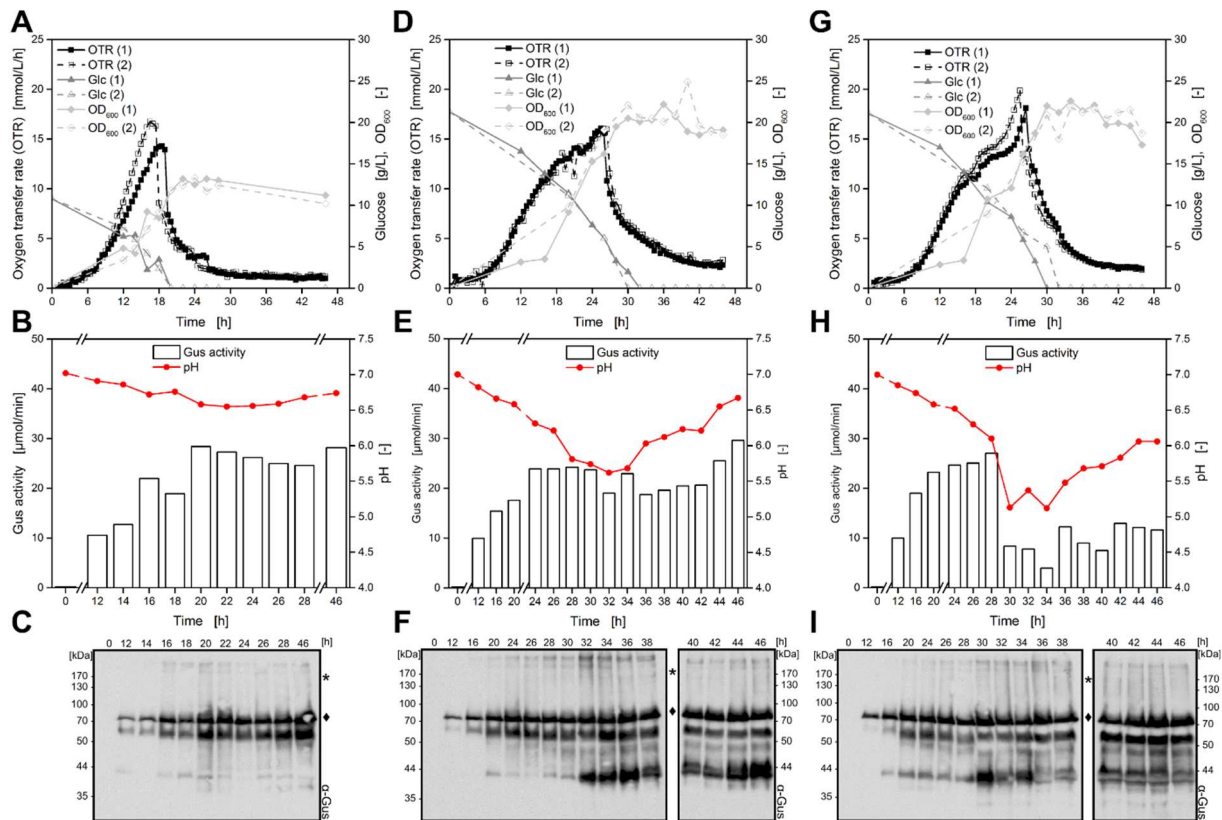


Fig. 2.16: Effects of elevated carbon and nitrogen supply on offline and online parameters of buffered cultivations of AB33 Gus-Cts1 expression strain

AB33 Gus-Cts1 was inoculated to an OD₆₀₀ of 0.08 in 20 mL CM medium buffered with 0.1 M MOPS, and either supplemented with 10 g/L glucose (**A-C**) or with 20 g/L glucose (**D-I**) and 1.5 g/L NH₄NO₃ (**A-F**) or 3 g/L NH₄NO₃ (**G-I**). Cultivation was performed in technical duplicates on a RAMOS orbital shaker (5 cm shaking diameter), on 28°C at 300 rpm. Sampling of the offline parameters pH, OD₆₀₀, HPLC samples and supernatants was focused on 12 - 46 hpi. **A, D, G.** The OTR was determined by online RAMOS measurements, while OD₆₀₀ and HPLC samples for glucose concentration determination were taken from additional, equally treated shaking flasks. **B, E, H.** pH progression is depicted in red, while bars resemble the unconventional secretion on the basis of Gus activity, measured in supernatant samples. **C, F, I.** Western blot analysis of 1 mL precipitated supernatant samples, exemplifying the stability status of the unconventionally secreted Gus-Cts1 fusion protein. Protein was detected using antibodies directed against Gus. The full length protein on 134 kDa is marked by an asterisk (*), while a major degradation product on 79 kDa is marked by a rhombus (♦). For **C, F, I**, results for one technical replicate are shown.

phase, most likely due to a stop of ammonium consumption and reduced metabolic activity. During the whole cultivation the major Gus-Cts1 degradation product could be detected in culture supernatants (Fig. 2.16 C, F, I, marked by rhombus (♦)) and increased amounts of undefined degradation fragments could be observed with prolonged incubation time. In general the results show that increased carbon and nitrogen source concentrations are needed for prolonged cultivation, leading to prolonged metabolic activity and thus unconventional secretion of Gus-Cts1. Nevertheless, buffer concentrations would need to be adjusted to maintain strict pH control in these cultures.

Previous experiments on the influence of different carbon sources on the unconventional secretion in *U. maydis* revealed a beneficial effect of fructose (Terfrüchte, 2013). Thus studies on the use of fructose instead of glucose in buffered and unbuffered cultivations were performed (Fig. 2.17). Unbuffered cultivation with glucose as carbon source led to a constant increase of the major Gus-Cts1 degradation product (marked by rhombus) and further

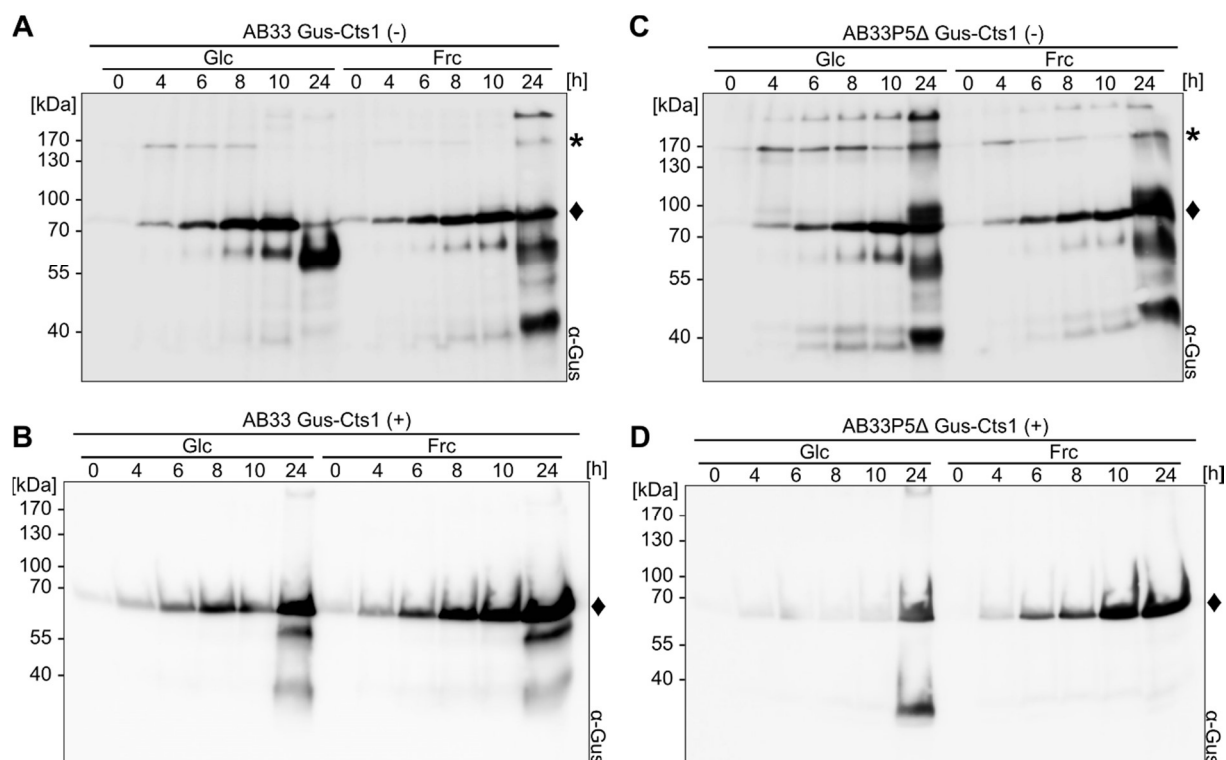


Fig. 2.17: Effect of different carbon sources on stability of unconventionally secreted Gus-Cts1

AB33 Gus-Cts1 (**A**, **B**) and AB33P5Δ Gus-Cts1 (**C**, **D**) were inoculated to an OD₆₀₀ of 0.08 in 20 mL CM medium, supplemented with either 10 g/L glucose or 10 g/L fructose (**A**, **C**). The experiment was additionally conducted with buffered glucose or fructose containing media (**B**, **D**). Cultivation was performed on 28°C at 300 rpm. Supernatant samples for Gus activity determination and Western blot analysis were taken at the designated time points. While pH dropped to a final level of 5 in unbuffered glucose supplemented cultivations and to a final level of 3 in fructose supplemented cultivations (**A**, **C**), pH remained constant at 7 in buffered cultivations (**B**, **D**). Unconventionally secreted Gus-Cts1 fusion protein, was detected using antibodies directed against Gus. The full length protein on 134 kDa is marked by an asterisk (*), while a major degradation product on 79 kDa is marked by a rhombus (♦).

degradation at 24 hpi, when pH levels dropped below 5.5 (Fig. 2.17 A, left panel). This is in line with previous findings (see also Fig. 2.12 C). Using fructose as a carbon source again led to a constant increase of Gus-Cts1 protein over time, lacking the further degradation of the major degradation product although pH dropped even below 4 at 24 hpi (Fig. 2.17 A, right panel). This was also supported by Gus activity measurements of the samples showing an increased activity in fructose supplemented cultures (data not shown). Repeating the same cultivations under buffered conditions (Fig. 2.17 B) showed no differences to the fructose based cultivation but less degradation at 24 hpi in glucose based cultivations. The experiment was then repeated using AB33P5Δ Gus-Cts1 (Fig. 2.17 C, D). As expected, the terminal degradation of the major Gus-Cts1 degradation product (♦) could be avoided in both cultivations while the full length protein (*) could now be detected in almost all samples. Thus, combining the buffered cultivation of AB33P5Δ Gus-Cts1 with fructose as carbon source (Fig. 2.17 D, right panel) could not further improve the stability but in fact the amount of unconventionally secreted Gus-Cts1. This indicates a direct influence of carbon source utilization and differential expression or activity of proteases as it had been shown for other organisms (Gusek et al., 1988).

2.4.5 Studying unconventional secretion in minimal media

In order to elucidate the exact limitations and optimal medium combinations occurring in batch cultivations, it will be necessary to repeat some of the experiments using minimal media. In contrast to complex media, minimal media do not contain any unknown compound concentration and can thus be precisely adjusted. Another advantage of minimal media can be that due to a non-excessive use of nutrients, organisms usually have slower growth rates and thus spend more time in the growth phase before entering the non-productive stationary phase. This had for example been shown to enhance proper protein folding (Siller et al., 2010). To briefly investigate the use of the established AM-glc minimal medium (Holliday, 1974) for unconventional secretion of Gus-Cts1, AB33 Gus-Cts1 was cultivated in unbuffered and 0.1 M MOPS buffered AM for 48 h. During cultivation offline sampling was performed in order to get information about pH, OD₆₀₀ and Gus activity (Fig. 2.18). As a control experiment, AB33 Gus-Cts1 was cultivated in CM-glc (Fig. 2.18 A) showing the expected increase of Gus activity over time and the loss of activity with decreasing pH. In this experiment Gus activity partially recovered at 48 hpi, most likely due to a stop of acidification due to cell death after prolonged incubation time. The growth rate of AB33 Gus-Cts1 in unbuffered AM-glc medium was reduced by about 50 % as for CM-glc cultivations (data not shown). Nevertheless, Gus activity reached higher levels and increased over a longer cultivation period (Fig. 2.18 B). This can probably be explained with a slower acidification of the medium, due to slower increase of the biomass. Between 12 and 24 hpi, Gus activity decreases in correlation with the decreasing culture pH. Using buffered AM medium (Fig. 2.18 C), the pH was constantly neutral over the whole cultivation period, leading to a steady increase of Gus activity even at late sampling points. As the final OD₆₀₀ of around 5 (data not shown) did not at all reach the maximum levels obtained in optimized CM cultivations (also see Fig. 2.16 A, D, G), yields are though not comparable. In general it can be said that AM-glc seems to be a suitable minimal medium for further optimizations and step-by step elimination of limitations, showing a better performance than CM in unbuffered cultivations.

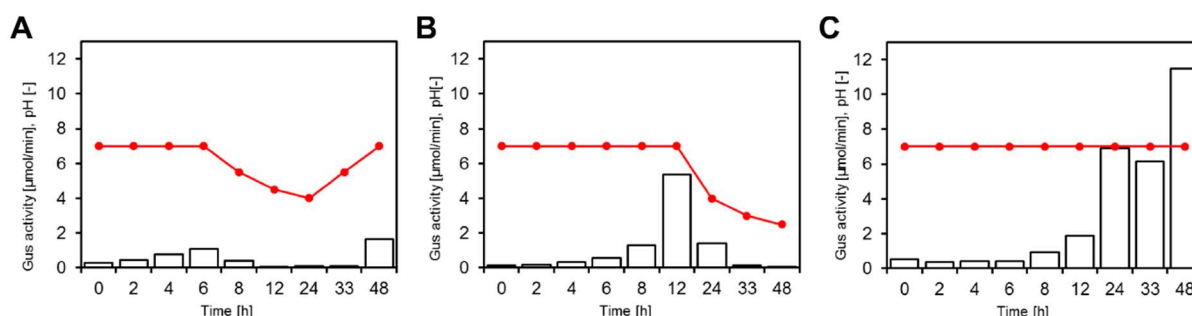


Fig. 2.18: Effect of minimal medium cultivation on unconventional Gus-Cts1 secretion

AB33 Gus-Cts1 was inoculated to an OD₆₀₀ of 0.08 in 20 mL CM medium (A), AM medium (B) or AM medium with 0.1 M MOPS (C), supplemented with 10 g/L glucose. Cultivation was performed on 28°C at 300 rpm. Supernatant samples for Gus activity and pH determination were taken at the designated time points. pH progression is depicted in red, while bars resemble the unconventional secretion determined on the basis of Gus activity measured in supernatant samples. Investigations had been performed as single experiments.

2.5 Application and upscaling of optimized cultivation conditions

A crucial step in the development of a microbial expression platform is the establishment of large scale processes to enable the cost efficient production of large product quantities. However, the transfer of knowledge gained in small scale processes to large scale processes and vice versa is often not trivial (Wewetzer et al., 2015). First optimization steps mostly require high throughput platforms, enabling the parallel investigation of multiple parameters. As this limits the size of the cultivation device, subsequent verification of the elaborated conditions in laboratory scale fermentations needs to be performed. Thus, after elaborating cultivation conditions using the RAMOS device, this section deals with the application and upscaling of gained knowledge.

2.5.1 Expression, unconventional secretion and biochemical analysis of α BoNTA from buffered cultivation

To apply the finding that buffered cultures result in enhanced stability and activity of unconventionally secreted Gus-Cts1, identical parameters were used to cultivate AB33kex2 Δ α BoNTA-NB-Cts1 for production of a biopharmaceutically relevant target. Therefore, AB33 (control) and AB33kex2 Δ α BoNTA-NB-Cts1 were cultivated in unbuffered or 0.1 M MOPS buffered CM medium, supplemented with 10 g/L glucose. Sampling was performed over 9 hpi, including pH and OD₆₀₀ determination as well as supernatant collection for Western blot and ELISA analysis. While growth rate and final OD₆₀₀ did not differ significantly between AB33 and AB33kex2 Δ α BoNTA-NB-Cts1, the final OD₆₀₀ in buffered cultivations was 1.5 fold higher compared to unbuffered cultivations (data not shown). This had been observed previously and might indicate a prolonged growth phase due to reduced acid stress at high cell densities. pH could be kept constantly neutral in buffered cultivations but dropped to a final level of 5.5 at 9 hpi in unbuffered cultivations (data not shown). Western blot analysis of precipitated supernatants showed the expression and unconventional secretion of full length α BoNTA-NB in all samples (Fig. 2.19 A). Interestingly, the amount of secreted protein increased steadily during cultivation in unbuffered medium (-), whereas the amount was constantly high during buffered cultivations (+). The elevated amount of secreted protein at the first sample point is most likely an artefact originating from the pre-culture conditions. As the overnight pre-cultures were also buffered or unbuffered, depending on the main culture, buffering prevented α BoNTA-NB degradation and intact protein was likely transferred from the pre-culture into the main culture. This again shows the huge impact of constant pH to overall protein stability. As the amount of secreted α BoNTA-NB in buffered cultivations was very high, aliquots of cell-free supernatants were directly subjected to ELISA without prior IMAC purification as described in 2.2 (Fig. 2.19 B). For both cultivation conditions volumetric activity with high specificity could be detected and only very little background activity was detected for AB33 control samples.

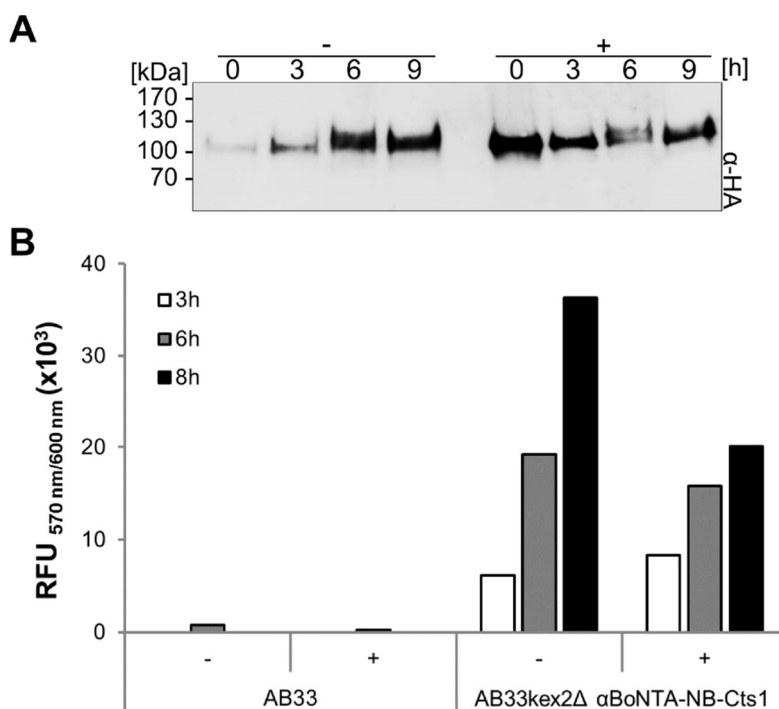


Fig. 2.19: Unbuffered and buffered cultivation of AB33kex2Δ αBoNTA-NB-Cts1

A. Western blot analysis of TCA precipitated supernatants of αBoNTA-NB-Cts1 expressing *U. maydis* strain AB33kex2Δ αBoNTA-NB-Cts1. Cultivations were performed in CM, supplemented with 10 g/L glucose (-), or 10 g/L glucose with additional 0.1 M MOPS buffering (+), at 28°C and 300 rpm. The cultures were inoculated to an OD₆₀₀ of 0.8 and sampling was performed at the designated time points. Protein was detected using antibodies directed against the internal 3xHA-tag. The full length protein band (74 kDa) can be detected in all samples, migrating higher than the calculated molecular weight. **B.** 250 μL of cell free supernatant samples from unbuffered (-) and buffered (+) cultivations of AB33 and AB33kex2Δ αBoNTA-NB-Cts1 were subjected to ELISA. Botulinum neurotoxin A was used as antigen and AB33 served as control. Volumetric activity can be observed for unbuffered and buffered AB33kex2Δ αBoNTA-NB-Cts1 samples whilst no or only minimal background activity is detectable in AB33 control samples. Experiments had been performed in duplicates and one representative result is shown.

Unexpectedly, the overall activity was higher in samples from unbuffered cultures (Fig. 2.19 B). The results show again that optimized conditions increase the amount and stability of the heterologous protein but will need to be reevaluated and adjusted for each new target.

2.5.2 Upscaling unconventional secretion of Gus-Cts1 and αGfp-NB-Cts1 in batch fermentations

As strain AB33P5Δ Gus-Cts1 was the most promising after optimization of the cultivation parameters for expression and subsequent unconventional secretion of Gus-Cts1, it was used for a batch cultivation in a laboratory scale fermenter. RAMOS experiments revealed that the use of protease deficient strains in combination with a constantly neutral pH is crucial for efficient production of stable fusion protein (see 2.4). Thus, the cultivation setup included tight automated pH control using a pH probe and acid-base titration. To obtain higher cell densities, the initial sugar concentration was set to 20 g/L glucose in 3 L of CM medium and constant aeration was applied. Using this setup, AB33P5Δ Gus-Cts1 was inoculated to an OD₆₀₀ of 0.8 and cultivated for 24 hours (Fig. 2.20 A). The first 14 h involved tight offline sampling every 2 h, including pH verification, OD₆₀₀ determination and supernatant sampling for Gus activity

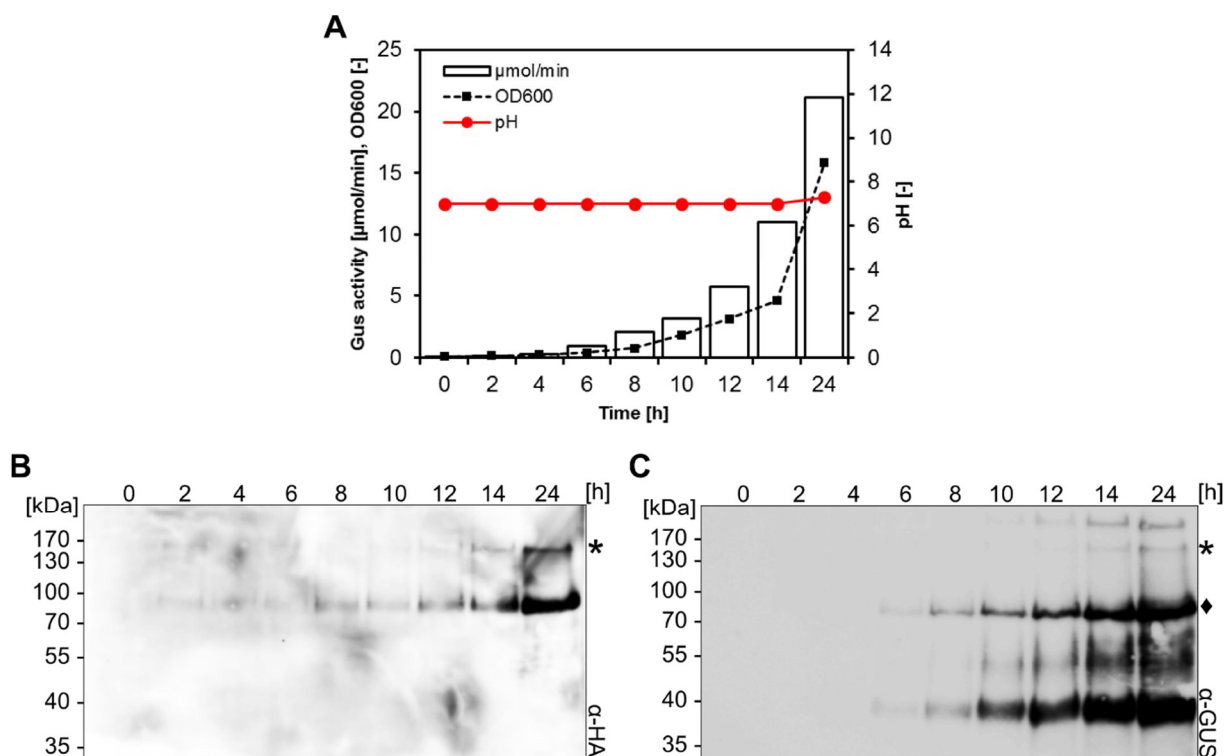


Fig. 2.20: AB33P5Δ Gus-Cts1 small scale fermentation

AB33P5Δ Gus-Cts1 was inoculated from an exponential overnight culture to an OD₆₀₀ of 0.08 in 3 L CM medium, supplemented with 20 g/L glucose. Cultivation was performed in a Minifors benchtop bioreactor (Infors HT) on 28°C at 500 - 750 rpm. A pH of 7 was maintained over the whole cultivation using automated titration of 2.5 M NaOH and 1 M H₂SO₄. Supernatant samples for Gus activity, pH comparison and Western blotting were taken at the designated time points. pH progression is depicted in red, OD₆₀₀ progression with a dashed black line, while bars resemble the unconventional secretion, on the basis of Gus activity measured in supernatant samples (A). B, C. TCA precipitated supernatant samples were subjected to SDS-PAGE and Western blot analysis. Protein was detected using antibodies directed against the internal 3xHA-tag (B) or against Gus (C). Full length Gus-Cts1 protein at 134 kDa is marked with an asterisk (*), while the major degradation product at 79 kDa is marked with a rhombus (♦). All fragments migrate higher than the calculated size.

measurements as well as for Western blot analysis. In this setup pH could be kept neutral during the whole cultivation and hence, Gus activity increased with increasing biomass (Fig. 2.20 A). In line with that, Western blotting revealed constant increase of protein over time (Fig. 2.20 B, C). Full length Gus-Cts1 protein could be detected in samples from 12 hpi on (marked with asterisk (*)) whereas the previously described major Gus-Cts1 degradation band was already detectable from 4 hpi (♦). Further undefined degradation products detected with antibodies directed against Gus (Fig. 2.20 C) indicated decreased stability of the full length protein at high cell densities. Of note, different from shaking flask cultivations, Gus-Cts1 could now also be detected in Western blots where only little amounts of supernatant was subjected to SDS-PAGE without the need of concentrating it by precipitation (data not shown).

Next, the same fermenter setup was used for cultivation of AB33kex2Δ αGfp-NB-Cts1 in order to produce αGfp-NB. Fermentation was followed for 25 h and sampling was performed at the designated time points (Fig. 2.21 A). Sampling involved the verification of online measured pH, OD₆₀₀ determination and supernatant fractions for Western blot analyses. Additionally, a final sampling of 500 mL cell free supernatants at 25 hpi was conducted and subjected to IMAC

purification (Fig. 2.21 C). The pH could be kept constant until 24 hpi, dropping slightly below 7 only at 25 hpi. This correlated directly with decreased oxygen consumption and OD₆₀₀, indicating that the culture started to decrease at that time. Taking the previously gained results into account this is most likely due to depletion of glucose (Fig. 2.21 A; see also Fig. 2.16 A, D, G). Again only small amounts of non-precipitated supernatant were sufficient to detect increasing amounts of full length α Gfp-NB in Western blot analysis, with a maximal yield at 24 hpi (Fig. 2.21 B, filled arrowheads). Nevertheless, a major α Gfp-NB degradation band (open arrowhead) could be detected in all samples. Strikingly, the amount of detectable protein drastically dropped from 24 hpi to 25 hpi. Only slight amounts of full length α Gfp-NB could be detected in precipitated supernatant samples at 25 hpi (data not shown). Still, Western blot analysis of the 500 mL supernatant IMAC purification showed enrichment of full length α Gfp-NB in the elution fractions (filled arrowhead) with only minor amounts of detectable degradation.

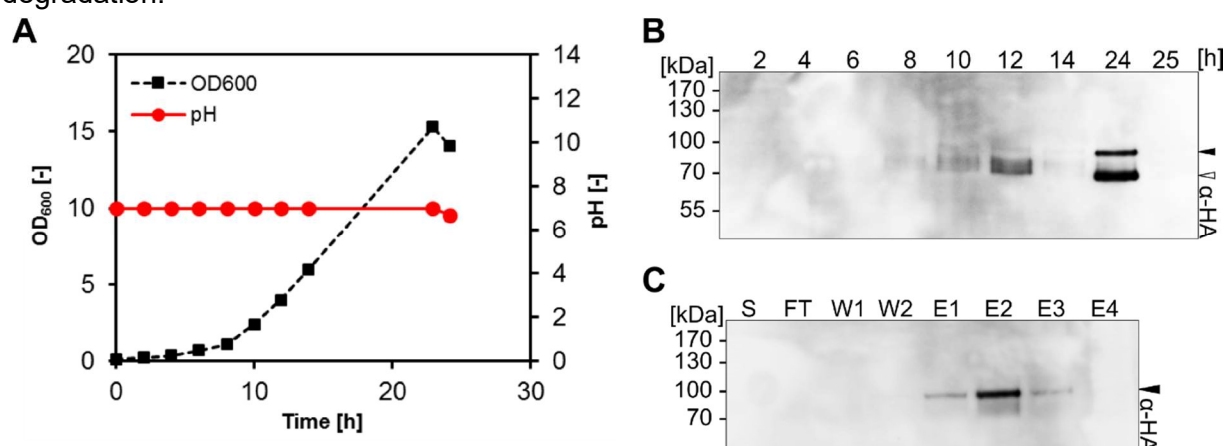


Fig. 2.21: AB33kex2 Δ α Gfp-NB-Cts1 small scale fermentation

U. maydis AB33kex2 Δ α Gfp-NB-Cts1 was inoculated from an exponential overnight culture to an OD₆₀₀ of 0.08 in 3 L CM medium, supplemented with 20 g/L glucose. Cultivation was performed in a Minifors benchtop bioreactor (Infors HT) on 28°C at 500 - 750 rpm. A pH of 7 was maintained over the whole cultivation using automated titration of 2.5 M NaOH and 1 M H₂SO₄. Supernatant samples for pH comparison, purification and Western blotting were taken at the designated time points. pH progression is depicted in red and OD₆₀₀ progression with a dashed black line (**A**). **B**. Supernatant samples were subjected to SDS-PAGE and Western blot analysis. Protein was detected using antibodies directed against the internal 3xHA-tag full length α Gfp-NB-Cts1 protein at 76 kDa is marked with a filled arrowhead, while the major degradation product is marked with an open arrowhead. **C**. 500 mL of cell free supernatant was harvested at 25 hpi and subjected to IMAC purification. Supernatant (S), flow through (FT), wash fractions (W1, W2) and elution fractions (E1-E4) were then subjected to SDS-PAGE and Western blotting, using antibodies directed against the internal 3xHA-tag. Full length α Gfp-NB-Cts1 can be found enriched in the elution fractions (filled arrowhead). All fragments migrate higher than the calculated size.

The results confirm that *U. maydis* can easily be cultivated in small scale fermentations, including strong agitation and high cell densities. It could be shown that with respect to unconventional secretion the possibility of pH control in the bioreactor offers strong advantages compared to shake flasks. Western blot analyses and purifications additionally suggest that increased protein yields can be obtained with optimized large scale conditions. Nevertheless, as uptake of nutrients is increased due to high cell densities and oxygen excess, media composition will need to be adjusted for further upscaling.

3 Discussion

In previous studies, differential proteomic analyses revealed a link between the chitinase Cts1 and the microtubule-associated long-distance mRNA transport in filaments of *U. maydis*. Furthermore, Cts1 activity could be measured on the cell surface indicating that it is secreted (Koepke et al., 2011). As no N-terminal signal peptide could be predicted, the idea of an unconventional secretion mechanism arose (Langner et al., 2015; Stock et al., 2012). After verifying that Cts1 is unconventionally secreted, initial studies on the use of Cts1 as a carrier for unconventional secretion of various heterologous target proteins were conducted (Stock et al., 2012; Terfrüchte, 2013). Easy and safe handling as well as good genetic amenability supported the development as an expression system. Since the yield of secreted target proteins was very low, first optimization approaches including promoter screens and the reduction of proteolytic potential were conducted and improved the system substantially (Reindl, 2013; Sarkari et al., 2014). Nevertheless, the yields of about 30 µg/L were still not satisfying and competitive. Thus the main objective of this project was the further optimization of the *U. maydis* expression system at different levels. As it is not sufficient for developing an efficient expression system to only focus on the organism and the basic underlying mechanism but also on the cultivation conditions and the construct design, these parameters were specifically taken into account.

3.1 Towards improved nanobody expression in *U. maydis*

In order to establish and optimize a protein expression platform it is necessary to increase the target portfolio steadily and thus expand the applicability. In initial studies the bacterial reporter enzyme Gus had been unconventionally secreted in *U. maydis* as a proof-of-principle and to furthermore verify the hypothesis of unconventional secretion (Stock, 2013; Stock et al., 2012). The study revealed that no *N*-glycosylation is added to the secreted proteins and that secretion of large proteins up to at least 173 kDa is possible (Stock et al., 2012). This displays one of the key advantages of using unconventional secretion as no size limitation could be observed so far. Further studies showed the successful expression of cofactor dependent enzymes and proteins that are in need of disulfide bridge formation (Reindl, 2016; Sarkari et al., 2014). The expression of unglycosylated proteins using eukaryotic organisms is of big interest for the biopharmaceutical industry. This is mainly due to the fact that on the one hand non-human glycosylation patterns can cause severe immunogenic reactions (De Groot and Scott, 2007) and that on the other hand often other post translational modifications like disulfide bond formation are needed for proper functionality. The production of therapeutic proteins for medical application in humans is to date mainly performed using mammalian cell lines, as products from these have the highest chance to be accepted by the host-immune system (Berlec and Štrukelj, 2013; De Groot and Scott, 2007; Walsh and Jefferis, 2006). One of the

major drawbacks in biotechnological antibody production is the high cost factor. Development and cultivation of mammalian cell lines is very laborious and the risk of virus contaminations is high (Khan, 2013). Thus, alternative expression platforms are requested. Production of antibody fragments has also successfully been performed in *E. coli* whereas expression often leads to inclusion bodies (Huang et al., 2012; Muyldermans, 2001). The downstream processing and especially purification can be very elaborate and therefore represents a high cost factor in biopharma (Pina et al., 2014; Roque et al., 2004). Most yeasts and fungi can be used to overcome this problem as they are in possession of efficient secretion machineries, facilitating the purification process (Berlec and Štrukelj, 2013; Puxbaum et al., 2015). Nevertheless, yeasts and fungi are known to often glycosylate secreted proteins using patterns quite different from the human glycosylation, making it necessary to deglycosylate certain proteins after expression (Gerngross, 2004; Ward, 2012). In contrast, using the Cts1 mediated unconventional protein secretion in *U. maydis*, unglycosylated proteins can directly be exported into the culture supernatant (Sarkari et al., 2014; Stock et al., 2012).

One of the driving factors of biopharmaceutical industry is the development and production of therapeutic antibodies (Berlec and Štrukelj, 2013; Sha et al., 2016). Antibodies and antibody fragments are widely used as precautionary or curative therapeutics as well as for analytics, mainly due to their high specificity (Fridy et al., 2014; Joosten et al., 2003). Thus, the expression of antibody fragments using Cts1-mediated unconventional secretion in *U. maydis* was conducted. The system could so far be applied for the expression of an scFv-fragment directed against the human c-myc epitope. Additionally a Llama (*Lama glama*) derived V_{HH} nanobody (NB) directed against Gfp could be expressed in initial studies (Rothbauer et al., 2007; Sarkari, 2014). To expand the target portfolio and improve stability as well as applicability of the *U. maydis* expression system, the so far gained improvements were now combined and comparatively investigated in the present study.

To this end a set of modified constructs containing the NB directed against Gfp (Sarkari, 2014) was used. Using Gfp as an antigen facilitates the biochemical analysis in the laboratory as it is an easily accessible and safe target (Liu et al., 1999; Richards et al., 2003). First the influence of the two previously described protease deficient strains AB33kex2 Δ and AB33P5 Δ on the expression, secretion and stability of the standard α Gfp-NB-Cts1 construct was investigated (Sarkari, 2014). It could be shown that different from cell extracts secretion rates varied between the strains. Protein amounts detected in supernatants of AB33kex2 Δ α Gfp-NB-Cts1 were comparatively increased whereas stability of α Gfp-NB in AB33P5 Δ α Gfp-Cts1 supernatants was higher. This might be due to the pleiotropic phenotype of AB33kex2 Δ , including the cell separation defect induced formation of cell-clusters. This possibly leads to increased cell lysis at high cell densities and thus exposition of intracellular proteases to the secreted protein (Sarkari et al., 2014). Nevertheless, higher secretion rates were also mirrored

by ELISA activity assays showing higher activity for AB33kex2Δ αGfp-NB-Cts1 supernatants. Despite the negative effects of the AB33kex2Δ growth phenotype it enables higher secretion rates and thus higher yields. For the scFv-Cts1 fusion protein the opposite observation had been made (Sarkari et al., 2014). Hence, depending on the nature and stability of the expression target it might be necessary to choose one or the other protease deficient strain. Moreover, as the application of nanobodies and other antibody based products for analytical purposes requires the possibility of specific detection and readout, the simplification of the detection process was targeted. Thus, Protein A fusion proteins were generated and corresponding constructs integrated into *U. maydis* AB33, AB33kex2Δ and AB33P5Δ. The Protein A epitope from *Staphylococcus aureus* has the characteristic to bind the immunoglobulin domain (Ig) of IgG antibodies. This domain is present in all mammalian antibodies making it possible to use almost any kind of commercially available antibodies for detection of the epitope (Page and Thorpe, 2009; Rigaut et al., 1999). As HRP conjugated secondary antibodies can thus directly bind to the Protein A epitope an incubation step with a primary antibody, as it is done in standard detection, becomes needless. Using HRP based conversion of chemifluorescent or chemiluminescent substrates the presence of the epitope tagged protein can be detected.

All Protein A containing fusion proteins could be detected in cell extracts whereas secretion seemed to be significantly impaired. This was also shown by ELISA assays, displaying almost no activity in purified supernatant samples. This might be due to the overall architecture of the constructs. The finally investigated αGfp-PC-Cts1 and αGfp-PH-Cts1 constructs consist of 8 and 9 linked elements respectively. All elements are connected by flexible linker regions. Secretion of very flexible multi domain proteins might be problematic due to sterical hindrance and instability. This could also pinpoint a drawback of the unconventional secretion system: ER passage involves multiple quality control steps that ensure proper folding prior to secretion (Ellgaard and Helenius, 2003). As this is bypassed during unconventional secretion in *U. maydis*, overexpression might lead to accumulation of misfolded product before or after secretion. It had been shown for *S. cerevisiae* for example that upregulation of the ER chaperone BiP and the disulfide isomerase Pdi1p lead to a significantly improved secretion of correctly folded protein (Tang et al., 2015). For future applications the constructs would thus need to be again simplified and reduced to the essential elements. This could ease the folding process and thus increase the overall stability. The nevertheless conducted detailed characterization of the different fusion proteins using cell extracts included comparison of activity and purification. Detection of all Protein A containing proteins in cell extracts was possible using only secondary α-Mouse-HRP or α-Goat-HRP antibodies, whilst the latter worked best. Binding affinity to Gfp was analyzed using ELISA either by classical primary- and secondary antibody detection or by only using α-Goat-HRP secondary antibodies. Classical

detection revealed volumetric activity of both constructs whereas α Gfp-PC-Cts1 showed overall higher activity. This can be explained with the tag architecture as α Gfp-PC-Cts1 harbors a very good accessible C-terminal HA-tag, while α Gfp-PH-Cts1 harbors an additional 10xHis-tag, potentially blocking the HA epitope. This finding is supported with equally high activity in α -Goat-HRP based ELISA assays where no differential tag localization is given.

In order to further simplify the detection process, HRP- α Gfp-NB fusion constructs were generated and integrated into AB33P5 Δ . By directly fusing the HRP to the nanobody no further antibody is needed for detection, thus even enabling one-step analytics. Commercially, antibodies are chemically conjugated to purified HRP, while in-fusion expression does not require an additional preparation step (Wisdom, 2005). A disadvantage of chemical HRP-conjugates is that HRP is typically isolated from horseradish roots (*Amoracia rusticana*) as a mixture of HRP isoenzymes with different biochemical properties (Krainer et al., 2016). As this can lead to preparations with partially inactive HRP, efficient microbial expression should be preferred (Krainer et al., 2016). The *A. rusticana* HRP, catalyzing the hydrolysis of various chemifluorescent and chemiluminescent substrates in the presence of H₂O₂, has previously been shown to be actively expressed and secreted in *U. maydis* (Reindl, 2016; Veitch, 2004). Expression and secretion could be confirmed in this study by Western blot analyses and volumetric activity could be detected in cell extracts. Very specific readout could furthermore be observed by using only HRP chemifluorescent substrate in a one-step detection. Albeit secretion rates were comparatively high and secreted protein was very stable in supernatants, almost no activity could be detected in ELISA. Nevertheless, previous studies could confirm extracellular activity of HRP fused to Cts1 via the TEV-3xHA linker (Reindl, 2016). A reason for that might be an inefficient heme cofactor availability in the supernatant or incorporation during unconventional secretion as this is crucial for HRP activity (Krainer et al., 2015; Spadiut and Herwig, 2013; Veitch, 2004). It is also possible that unconventional secretion in combination with a very strong promoter leads to high rates of misfolded HRP as folding involves the formation of disulfide bridges. A similar approach was conducted using conventional secretion in *Aspergillus awamori*, where the ARP peroxidase from *Arthromyces ramosus* was fused to a NB. It was observed that considerable amounts of the fusion protein resided in the cytoplasm, indicating that it is difficult to secrete. Additionally the binding affinity of the NB was found to be reduced (Joosten et al., 2005a). Studies performed in *P. pastoris* showed improved secretion of active HRP by supplementation of the growth medium with hemin, the ferric-chloride species of heme (Krainer et al., 2015). Yet, hemin supplementation did not result in increased HRP activities or yields for *U. maydis* (Reindl, 2016). Other studies in *A. niger* (Franken et al., 2013), *E. coli* (Li et al., 2014) and *S. cerevisiae* (Hoffman et al., 2003) dealt with the upregulation of heme biosynthesis in order to improve cofactor availability

and obtained promising results. Thus this could also be an option to improve active HRP secretion in *U. maydis* in future.

The Protein A tagged constructs were additionally equipped with C- and N-terminal purification tags as well as TEV- or HRV 3C protease cleavage sites in order to improve the purification process (Bonnerjea, 2004; Graslund, 2008; Waugh, 2011). The TEV protease hydrolyses the peptide sequence ENLYFQ/G highly specific between the glutamine and the glycine (Kapust et al., 2002), whereas the HRV 3C hydrolyses between the glutamine and glycine residues of a LEVLFQ/GP peptide (Dian et al., 2002; Wang and Johnson, 2001). This is especially important when it comes to the expression of therapeutic proteins. While being essential for secretion and purification, using a set of tags, linkers and Cts1 as carrier molecule, adds several non-desired elements to the target protein that need to be cleared off the final product (Waugh, 2011). Thus, for successful application, cleavage of the non-desired elements and recovery of the target needs to be performed. The constructs were also compared with regard to their performance in purification processes. Using the OneSTrEP®-tag and 10xHis-tag in a tandem affinity purification, combined with proteolytic cleavage, revealed no significant difference in the performance of TEV- and HRV 3C protease. In order to see differences low amounts of protease had been used, showing faster turnover rates for HRV 3C. This is mainly due to the reaction characteristics of HRV 3C. To stabilize the fusion protein reactions were performed on 4°C where HRV 3C has a higher activity than TEV protease. Moreover, HRV 3C has a reportedly superior on-column cleavage behavior compared to other commercial proteases (Asano et al., 2010; Dian et al., 2002; Wang and Johnson, 2001). In the end it was possible to purify small amounts of cleaved α Gfp-NB with both fusion proteins, showing an overall good performance of the constructs. The use of tandem affinity purifications hence enables production of the target protein with high purity and thus adds value to the product.

Nevertheless, some constructs showed unsatisfying results in secretion rates and extracellular activity, mainly due to remediable reasons. Initial studies on the use of the Cts1-mediated unconventional secretion pathway for heterologous protein expression demonstrated that proteins up to 173 kDa can be efficiently secreted (Stock et al., 2012). Hence, size was not comprised as limiting factor in the construct design. Thus, the addition of multiple linker and tag sequences to the fusion protein was conducted. The thereby increased complexity though seems to have detrimental effects on unconventional secretion. As a next step all unnecessary components should be excluded from the expression construct in order to fine-tune construct applicability and secretion rates. This also includes the careful selection of linker peptides as these highly influence expression levels and fusion protein stability (Chen et al., 2013). Hence, there is still need and room for improvement and adjustment of the expression constructs.

In order to transfer the knowledge gained for the expression of α Gfp-NB onto the expression of a biopharmaceutical relevant target an Alpaca (*Vicugna pacos*) derived nanobody directed

against Botulinum neurotoxin A from *Clostridium botulinum* was chosen. *C. botulinum* is rated as Category A priority pathogen as its toxins can cause a potentially lethal flaccid paralysis (botulism) (Mukherjee et al., 2012). Especially in animal healthcare and feed industry Botulinum neurotoxin contamination is still a severe problem. Botulinum neurotoxin A is one of the strongest known toxins with a very low LD₅₀ (lethal dose, 50 %) of 0.001 µg/kg bodyweight and is thus also listed as potential bioweapon (Froude et al., 2011). Intoxication often leads to death and besides intentional use of Botulinum neurotoxin A as a bioweapon, feed from spoiled silos can eliminate whole cattle herds. As toxins are very diverse and widespread the development of cheap and effective antitoxins is an important branch in biopharmaceutical industry, even supported by military investigations (Froude et al., 2011; Moayeri et al., 2015; Mukherjee et al., 2012). In contrast to antibodies or antibody fragments, antitoxins are not only binding but also neutralizing their toxin target. This can either be due to inhibition of enzymatic activity or prevention of toxin binding to cellular targets (Mukherjee et al., 2012). After terroristic attacks with *Bacillus anthracis* in the US in 2001, research and development of anthrax antitoxins was expanded (Froude et al., 2011). Recently nanobody based anthrax antitoxins have been successfully tested in animal models (Moayeri et al., 2015). Here, the published sequence of a Botulinum neurotoxin A binding and neutralizing nanobody (Mukherjee et al., 2012) was dicodon optimized for translation in *U. maydis* and integrated into the expression vector backbone pRabX2 (αBoNTA-NB). After integration of the construct into AB33kex2Δ, Western blot experiments confirmed expression and secretion of the αBoNTA-NB at high rates compared to other targets. Purification of the nanobodies also yielded in high amounts of pure αBoNTA-NB-Cts1 fusion protein. ELISA analyses against Botulinum neurotoxin A as antigen revealed high binding affinity and specificity, confirming the high flexibility and transferability of the expression system. Additional experiments using only small amounts of whole AB33kex2Δ αBoNTA-NB supernatant in ELISA supported the observations of high protein titers. Here it was possible for the first time to detect volumetric activity of the nanobody without prior purification or concentration. As this was never possible for earlier investigated targets it shows the suitability of this particular target for unconventional secretion. While binding activity was confirmed, antitoxin activity would need to be separately confirmed in animal models (Mukherjee et al., 2012). Nevertheless, αBoNTA-NB binding to Botulinum neurotoxin A could independently find interesting application in industry. The αBoNTA-NB could be for instance combined with the HRP, in order to generate a one-step ELISA system for feed- and food safety testing. Further application of NB could for example be the use as ‘magic-bullets’. This term describes a fusion construct between a specific nanobody or other antibody fragment and an effector molecule of any kind, directing the effector straight to the target site (Muyldermans, 2001). Due to the elongated hypervariable regions of NB compared to classical antibodies they can penetrate deeper into the pockets of active sites in enzymes and thus also display potent

inhibitory functions (Joosten et al., 2003; Lauwereys et al., 1998). NB thus are of great potential for future applications and NB based fusion proteins could be shown to be a well suited target for unconventional protein secretion in *U. maydis*, especially if combined with protease deficient strains. Nevertheless, the study revealed that expression construct design is crucial for product stability and should thus be kept as simple as possible. A higher grade of complexity might interfere with correct folding as the unconventional secretion machinery could be overburdened with high protein traffic, resulting from constitutive overexpression. It could also be shown that functionalization of NB is possible but not trivial and needs further investigation.

3.2 Expression of a potential malaria antigen in *U. maydis*

Several studies have been conducted in order to elucidate the glycosylation pattern of *Plasmodium* proteins (Cova et al., 2015; de Macedo et al., 2010). Especially *N*-glycosylation remains a controversial topic as many *Plasmodium* proteins contain potential *N*-glycosylation sites, but typical glycosylation patterns cannot be detected (de Macedo et al., 2010). The *P. falciparum* life cycle contains more than six morphological stages in two different hosts and thus hampers general conclusions (Cova et al., 2015). It could so far be shown that GPI anchored proteins are essential for *P. falciparum* infectivity, proving the general ability to produce glycoproteins. Nevertheless, only very few proteins could be shown to be partially *N*-glycosylated and most probably play a role in protein targeting (de Macedo et al., 2010). This is mainly due to the lack of a complete *N*-glycosylation machinery in *P. falciparum* that only enables very limited *N*-glycan biosynthesis (de Macedo et al., 2010). The heterologous expression of plasmodial proteins without *N*-glycosylation is thus very important, making it an attractive and interesting target for unconventional protein secretion in *U. maydis* (de Macedo et al., 2010; Sony Reddy et al., 2014).

The prevention and treatment of widespread infectious diseases is one of the biggest challenges of the medical industry. Most often, such diseases are transmitted by insects and thus exhibit high pandemic potential. One of these diseases is the Malaria tropica, a febrile infection caused by the protozoan parasite *Plasmodium falciparum* (Miller et al., 2013). Symptoms of the disease are due to the blood-stage of the infection where the parasite invades mature erythrocytes and proliferates until the cells burst. As this can lead to anemic conditions infection often leads to neuronal disorders or even death (Miller et al., 2013; Ord et al., 2014). About half of the world's population lives in areas that are at risk of malaria, leading to 214 million reported infections and more than 400000 deaths in 2015 (WHO fact sheet, 2016). As the majority of the affected people is very poor and not well educated, prevention and medication must be inexpensive and administration of the therapeutic must be coordinated. In order to facilitate wide spread treatments and contain new infection the therapeutic must as well be long lasting. Vaccination has turned out to be a very effective and safe way to prevent

numerous infectious diseases like smallpox, polio or measles (Nabel, 2013). Thus, numerous attempts on finding a suitable Malaria vaccine have been conducted (Draper et al., 2015; Ewer et al., 2015; Kaiser, 2013). The best studied candidate to date is the 'RTS,S/AS01' vaccine that is based on a *P. falciparum* protein, leading to a precautionary adaption of the host-immune system to the parasite. Nevertheless, clinical studies could show that only around 50 % of the immunized patients developed full immunity (RTS S Clinical Trials Partnership, 2012). Therefore several other potential antigens were identified and investigated (Draper et al., 2015). The *P. falciparum* reticulocyte binding protein homologue 5 (PfRH5) has been found to be essential for erythrocyte invasion by *Plasmodium* blood stage merozoites (Volz et al., 2016; Wright and Rayner, 2014) and is thus another promising vaccine target candidate. Studies on *Aotus nancymae* animal models revealed that PfRH5 administration leads to efficient immunization against *P. falciparum* merozoites (Douglas et al., 2015). As the protein structure of PfRH5 contains several long disordered regions and unglycosylated expression is crucial for proper folding, the cost efficient large scale production of PfRH5 remains a bottleneck (Crosnier et al., 2011; de Macedo et al., 2010). Attempts to express full length PfRH5 protein were of limited success so far and could be shown in mammalian cells, insect cells, virus based and cell free expression systems (Bustamante et al., 2013; Hjerrild et al., 2016; Wanaguru et al., 2013). As these systems are very laborious and expensive they are not suitable for large scale production (Demain and Vaishnav, 2009). Expression of PfRH5 in *E. coli* was successful though leading to inclusion bodies and thus laborious downstream processing (Sony Reddy et al., 2014). For expression in *U. maydis*, a PfRH5 sequence was dicodon optimized for efficient translation and the native signal peptide encoding sequence was deleted. As it had been reported that a very instable N-terminal 140 aa long disordered region is of no importance for proper functionality, a version lacking this region was also investigated (Wright et al., 2014). All constructs were expressed in fusion with chitinase Cts1 to enforce export via the unconventional secretion pathway in *U. maydis*.

Expression and secretion of diverse constructs could be confirmed by Western blot analyses. However, other than for most heterologously expressed proteins in *U. maydis*, a promoter exchange with the very strong synthetic P_{oma} promoter did not lead to increased amounts of full length protein. As the fusion protein is very large and folding might be complex, a too strong expression level can lead to misfolded protein that is thus degraded, in order to reduce stress for the cell (Mattanovich et al., 2004). In addition, intermediate-strength promoters for use in *U. maydis* could be identified in recent promoter screens. It would thus be worth trying the ribosomal P_{rpl40} promoter for UmRH5 expression for example (Hußnätter, 2015). Strikingly, using different constructs for purification including OneSTrEP®, 10xHis-tags or AviTag™ disclosed very poor binding affinity of the protein to the matrices. This again indicates that the fusion protein structure might hinder proper accessibility. *In vitro* biotinylation of all AviTag™

fused proteins was also unsuccessful. The co-expression of *E. coli* biotin ligase BirA in UmRH5 expression strains may solve this problem and has been conducted before, but could again contribute to an increased cell stress and thus to reduced expression (Heimel, 2014; Kim et al., 2009; Mattanovich et al., 2004). Analysis on the functionality of Cts1 as a chitinase could show strong binding affinity of the C-terminal GH18 region to chitin matrices (Jankowski, 2013; Stock et al., 2012). Chitin based purification kits are commercially available for example with the intein self-cleavage system (Bell et al., 2013) suggesting that this could be a successful approach. Thus, purification attempts with UmRh5-Cts1 fusion proteins on various chitin matrices were performed. These however also showed poor binding to the material as well as unspecific chitin binding of most elements of the fusion protein. Chitin binding has been reported to be a characteristic of a big variety of proteins, being a clear drawback of the system (Raikhel et al., 1993). It must also be considered that the used chitin matrices have low capacity, thus one reason for high protein amounts in flow through fractions might be the amount of matrix used. A possible application of the chitin binding potential of Cts1 could nevertheless be the coating of chitin tissues or fibers with therapeutic or marker proteins. These are more and more used in industrial or medical industry as they are light-weight, very stable and flexible materials (Fernandez and Ingber, 2013; Nakajima et al., 1986). Using matrix binding independent purification methods like size exclusion- or ion exchange chromatography, might improve purification for UmRH5 (Bonnerjea, 2004; Graslund, 2008). However, using various constructs, promoters, labelling and purification attempts did not lead to sufficient amounts of secreted UmRH5 protein for biochemical analysis. Receptor binding could thus not be unambiguously clarified. As in this study a provided P ρ RH5 sequence with mutated *N*-glycosylation sites was used that was needed for unglycosylated expression in mammalian cells (Crosnier et al., 2011), it might additionally be worth trying the expression and secretion of an unmodified variant in *U. maydis*. This could result in improved stability and downstream processing (Crosnier et al., 2011; Sony Reddy et al., 2014). In case of a successful secretion and purification, this would have been also the next step in order to come as close as possible to the native protein, allowing efficient immunization. Furthermore it could be interesting to analyze other plasmodial proteins for expression and unconventional secretion in *U. maydis*. This might reveal whether expression of plasmodial proteins in general is difficult using the *U. maydis* expression system as this had been reported for other organisms (Crosnier et al., 2013). Multiple proteins from the RBL (reticulocyte-binding protein homologues) and EBL (erythrocyte-binding proteins/ligands) superfamilies could be shown to be used as potential vaccine targets (Iyer et al., 2007) and thus display interesting proteins to be tested in *U. maydis*.

3.3 Increasing the yield by cultivation optimization

Establishment of a protein expression platform requires interplay of multiple parameters. These include modifications on the transcriptional, translational and posttranslational level. By individually looking at these parameters, one very important aspect is not addressed: the general performance and physiology of the expressing cell during cultivation. Cultivation parameters such as temperature, nutrient availability, pH or aeration significantly contribute to cell fitness, expression rates and product stability (Battistoni et al., 1992; Khoo and Suntrarachun, 2012). Previous studies on *U. maydis* have so far, if at all, focused on media and cultivation conditions for low cell density applications. Thus, in this part of the project the general optimization of *U. maydis* cultivation conditions up to high cell densities with regard to heterologous protein expression was addressed.

To get detailed insights on the physiology of a cell during cultivation it is necessary to combine a set of analytical means. To this end the Respiration Activity Monitoring System (RAMOS) was used in combination with offline analytics (cooperation with Sandra Wewetzer, RWTH Aachen). The RAMOS system is based on a standard shaking flasks setup, equipped with probes to monitor oxygen transfer rates (OTR) during cultivation (Anderlei and Büchs, 2001; Anderlei et al., 2004). The OTR is a display of the cells respiration and, as most metabolic and expression related reactions of aerobic organisms are oxygen dependent, it indirectly pictures the production status of the cells (Baez and Shiloach, 2014; Klement et al., 2012; Knoll et al., 2005). To additionally perform sampling and offline analytics, shaking flasks with identical inocula were cultivated and sacrificed for each sampling point. Thus, the setup provided information about respiration, pH, cell density, carbon source concentration and protein yield. To have a readout for the protein yield over time the established Gus-Cts1 fusion protein connected via an internal SHH-linker was expressed and activity was measured in cell free supernatants (Mead et al., 1967; Stock et al., 2012; Stock et al., 2016). Quantification of unconventionally secreted protein yields is in general a difficult task as they are still too low for densitometric analysis in SDS-PAGE or photometric quantification. Thus the combination of activity based assays, defined protein standards and qualitative Western blot results were employed for yield determination. In future the application of fluorescence protein fusions could alternatively be used for quantification until yields are high enough for direct measurements. First cultivations revealed a strong pH decrease with increasing biomass. In direct correlation with the drop of pH in the culture, Gus activity diminished. Western blot analyses of supernatant samples supported this finding by revealing degradation of the Gus-Cts1 protein at low pH values. To analyze the direct effect on Gus activity, incubation of recombinant protein with media set to different pH values showed an inhibitory pH effect at pH levels ≤ 6 . In line with this, previous studies on the activity of Gus purified from *E. coli* revealed an optimal enzyme activity at neutral pH whereas a drastic decrease in activity was observed at acidic pH. At pH

5.5 less than 50 % Gus activity was detected using 4-methylumbelliferyl β -D-glucuronide hydrate (MUG) as a substrate (Zenser et al., 1999). Interestingly, a decrease of Gus activity was already visible at pH levels of 6.5 in RAMOS experiments. Indeed, buffering of the medium lead to a significantly increased stability of the fusion protein and a constant increase of Gus activity until the cells entered stationary phase. This, together with the observations of the Western blot analyses, lead to the hypothesis that acidic activated proteases could play a role in degradation of heterologous proteins in *U. maydis*.

The activity and expression of proteases is indeed known to be pH dependent in many cases (Denison, 2000; Pringle, 1975) and acidic activation has been shown for *S. cerevisiae* protease-A for example where an optimum of pH 2 to 4 was determined (Hata et al., 1967). The proteolytic effect of acidic pH on protein expression had also been shown in *A. niger*. Here a 10-fold increased yield of recombinant Gfp could be obtained by keeping a constant pH of 6, compared to unbuffered cultivations at a pH of 3 to 4 (O'Donnell et al., 2001). Nevertheless, proteolysis could not be totally abolished by keeping a constant pH. Another approach to target unwanted proteolysis could be the addition of BSA to the medium, as an alternative protease substrate. This has been reported to decrease the yield loss due to proteolysis of NB in *Aspergillus awamori* 5-fold (Joosten et al., 2005b). Protease inhibitors are widely used in order to minimize proteolytic degradation. Unfortunately, personal experience revealed that the use of potent protease inhibitors during cultivation of *U. maydis* leads to severe growth defects and is besides very expensive. Thus, an approach to investigate the impact of the two earlier described protease deficient strain backgrounds AB33kex2 Δ and AB33P5 Δ was conducted (Sarkari, 2014; Sarkari et al., 2014). The results of the *in vitro* and *in vivo* studies clearly supported the hypothesis of increased proteolysis with decreasing pH. Importantly, the combination of buffering and reduced proteolytic potential led to drastic increase in stability of the heterologous protein. Nevertheless, RAMOS cultivations of AB33kex2 Δ again disclosed the drawbacks of this strain. Reduced OTR and correlating reduced growth rates were reflected by lower Gus activity in the supernatant. The combined results of OTR measurements and offline sampling in RAMOS cultivations allowed to correlate entrance of the cells into stationary phase to glucose depletion. Studies on the localization of Cts1 during the cell cycle indicate a correlation of cell separation and unconventional Cts1 secretion (Langner, 2015; Langner et al., 2015), suggesting that efficient unconventional secretion takes place during cell growth. Thus, additional comparative RAMOS cultivations with increased amounts of glucose were conducted in order to prolong the growth phase. Control cultivations with standard media composition and nutrient concentration indicated an additional nitrogen limitation. Interestingly, nitrogen limitation could already be linked to increased proteolysis, for example in algae (Berges and Falkowski, 1998) or soil microorganisms (Sims and Wander, 2002). Following this, cultivations with increased amounts of NH_4NO_3 were also investigated. The results

confirmed that increased carbon source concentrations could prolong the growth and thus production phase. The supplementation with additional NH_4NO_3 resulted in an increased maximal OTR, indicating increased metabolic activity. As the increased biomass led to an increased ammonium consumption, the acidification of the medium overran the 0.1 M MOPS buffer capacity (Scheidle et al., 2011). This could be observed in pH progression and was reflected by Gus activity. Thus an increased concentration of buffer substance is crucial for proper pH maintenance at high cell densities. Studies on the tolerance of *U. maydis* towards high MOPS concentrations (not shown) showed no significant influence on the growth rates up to a concentration of 0.25 M MOPS. Nevertheless, buffer substances are in general very expensive making such an approach unfeasible. It could also be beneficial to further increase the initial glucose concentration as it had been reported that high glucose concentrations repress extracellular proteases in *A. nidulans* (van den Hombergh et al., 1997; Wang et al., 2005). Another approach could be buffering with CaO_3 which is very inexpensive and has previously been shown to work for *U. maydis* cultivations (Geiser et al., 2016b; Klement et al., 2012). Nevertheless, CaO_3 is highly insoluble in neutral aqueous solutions and might cause problems in downstream applications and analytics.

Overall, using optimized buffered conditions in combination with reduced proteolysis, yields could be increased to at least 420 $\mu\text{g/L}$ unconventionally secreted Gus-Cts1 in the supernatant of shaking flask batch cultivations. Compared to quantifications prior to this study this represents a 14-fold increase (Sarkari et al., 2014). Still, it is obvious that even under these conditions heterologously expressed proteins in the supernatant are prone to degradation. In fact at least 26 secreted proteases have been predicted for *U. maydis* (Sarkari, 2014) of which only five were deleted in AB33P5 Δ . Current projects are dealing with the sequential deletion of more of these candidates, contributing to even more reduced degradation in future (Stollewerk, 2015; unpublished).

The obtained data clearly demonstrate that in future cultivations should be conducted in bioreactors, offering continuous and tight pH control, for instance via acid-base titration. Initial studies on Gus-Cts1 production in batch fermentations already resulted in higher yields of stable full-length protein. Here the application of ammonia as buffer substance could be beneficial as this would enable continuous replenishment of ammonia and in consequence pH control coupled to nitrogen supplementation (Knabben et al., 2010).

Investigations on the use of different carbon sources for heterologous protein expression in *U. maydis* revealed fructose to have a positive effect on unconventional Gus secretion rates. Comparative cultivation in sucrose, glucose and fructose supplemented media did not depict changes in growth rate but extracellular Gus activity reached values twice as high using fructose as carbon source (Terfrüchte, 2013). To further analyze the influence of fructose on expression and stability of the protein, AB33 Gus-Cts1 was here cultivated with glucose and

fructose as carbon source. Growth rates under both conditions were again very similar. Interestingly, Western blot and Gus activity analyses showed a reduction in proteolytic degradation of Gus-Cts1 in unbuffered fructose supplemented supernatants, although pH decreased to levels below 4. This could on the one hand indicate that fructose consumption leads to different metabolic intermediates and end products that have adverse effects on acidic activated proteases. On the other hand it might hint on differential gene expression with fructose as carbon source. Comparative RNA-seq experiments, using different carbon sources in the growth medium, could in future be performed in order to get more insights on the underlying processes. The influence of carbon sources on proteolytic potential of microorganisms had for example previously been shown for the ascomycete *Thermomonospora fusca* YX. Investigations on the expression of a thermostable protease using cellulose, glucose and xylose among others, revealed significantly higher proteolytic potential when the fungus was grown on cellulose (Gusek et al., 1988). This is very likely due to the nature of the fungus as it feeds on cellulosic biomass. However, the results are very promising and further investigations on the use of waste-stream carbon sources will be conducted in future studies. The use of molasses as a waste-stream from sugar refineries is for example very interesting as it still contains roughly 35 % sucrose as well as 10 % glucose and fructose each (www.deutsche-melasse.de; Rajakylä and Paloposki, 1983). Many fungi harbor a broad set of CAZymes as they naturally feed on biomass. The basidiomycete *Laetisaria arvalis* has for example a very efficient set of cellulose degrading enzymes, enabling a fast breakdown of cellulosic biomass in industry (Navarro et al., 2014). It is thus to mention that *U. maydis* also has a limited but potent set of carbohydrate active enzymes (CAZymes), potentially enabling the direct use of biomass waste-streams as carbon source (Couturier et al., 2012). In initial studies intrinsic CAZymes could be activated in *U. maydis* strains, resulting in enhanced growth on cellobiose and xylan as sole carbon sources (Geiser et al., 2016b). Current investigations focus on the degradation of pectin for use as waste-stream carbon source, being one of the most abundant polysaccharides on earth (Xiao and Anderson, 2013). Here the unconventional secretion pathway will also be exploited to additionally secrete heterologous pectinolytic enzymes that *U. maydis* does not naturally produce. However, the efficient and economic use of carbon sources from organic waste-streams still requires a lot of work in strain- and process development. Thus it can only be a long-term goal. Especially with regard to the expression of biopharmaceuticals, concentration on refined carbon sources will be needed in order to meet the strict safety demands for medical products (Berlec and Štrukelj, 2013).

Besides buffer conditions and carbon source, there is still need for further optimization of the media composition in order to eliminate nutrient limitations at low concentrations. Thus, initial analysis of secretion behavior in minimal medium cultivations was conducted. As expected,

growth rates were drastically reduced in AM minimal medium compared to standard CM cultivations. The slow growth led to a delayed acidification of the medium and thus a higher Gus activity in the supernatant. However, using buffered AM medium, maximum Gus activity was reduced compared to buffered CM medium. Although it would be expected that more protein is produced with fast biomass increase, the results show that slow growing cultures might be beneficial for protein production, due to longer growth and thus prolonged production phases. Additionally slower metabolism could support proper folding of heterologous proteins. It could for instance been shown that slowing down the translation speed in *E. coli*, drastically improved folding of heterologously expressed eukaryotic proteins (Siller et al., 2010).

The next step after elucidation of suited cultivation conditions was the transfer of gathered information to cultivations in higher volumes. Batch fermenter cultivations of AB33P5Δ Gus-Cts1 showed similar results on protein yield and stability as observed in optimized RAMOS cultivations, suggesting that upscaling is easily achievable. Hence, batch fermentation with αGfp-NB expressing strain AB33kex2Δ αGfp-NB-Cts1 was conducted (Sarkari, 2014). Cultivation was performed for 25 h under strict pH control, using acid-base titration and an initial glucose concentration of 20 g/L. Sampling revealed that increased protein amounts could be secreted so that no concentration of the samples was necessary for distinct detection. Interestingly, it could be observed that after cells entered dying phase, pH and protein stability rapidly decreased. Although sampling for purification of the protein was performed during this stage, stable protein could be enriched. This shows the problems that a transfer from shaking flask to bioreactor can cause. As the bioreactor enables a very high rate of aeration, oxygen does not become limiting and metabolic activity of the cells is increased until depletion of the carbon source. This leads to higher cell densities and thus, when cells are confronted with limitations, to an increased stress level. Increased stress levels as well as cell lysis could then again be responsible for increased acidification and proteolysis. This effect is well known for long term cultivations of yeast species (Sinha et al., 2005). As previously mentioned a solution to that could be ammonia buffering. Nitrogen limitation and acidification would thus be prevented with only one comparably cheap substitute. Due to the higher cell titer it would also be necessary to increase the initial carbon source concentration or switch to fed-batch fermentation with continuous medium or carbon source replenishment (Cos et al., 2006; Knabben et al., 2010; Zhang et al., 2000). This could prevent stress conditions due to nutrient limitations and prolong the productive growth phase. Alternatively, continuous cultivations in a chemostat or the CosBios could be conducted (Sieben et al., 2016). These make it possible to keep the cells steadily at a certain density and can thus drastically prolong the productive phase (Akgün et al., 2004; De Gooijer et al., 1996; Velur Selvamani et al., 2014; Weinhhammer and Blass, 1994). The gathered results could demonstrate that the cell density correlates with the secreted protein yield. It would thus be beneficial to increase cell density as far as possible

under non-stress conditions. Carbon source or nutrient availability in general can be regulated by continuous replenishment. However, oxygen becomes limiting very fast at high cell titers due to increased viscosity and in turn decreased oxygen intake. In order to solve this problem, pressurized bioreactors can be used to decrease viscosity under high pressure conditions (Knabben et al., 2010; Knoll et al., 2005; Knoll et al., 2007). A first attempt has already been conducted in collaboration with the Aachener Verfahrenstechnik (RWTH Aachen), using Gus-Cts1 expressing strain AB33P5Δ Gus-Cts1 in a pressurized fermentation with up to 1 bar overpressure (Knoll et al., 2007). Due to media composition restrictions the cultivation needed to be operated at pH 6.5 using ammonia buffering. Although this pH level had previously been shown to impair stability of Gus-Cts1, at least 5-fold higher Gus activity, compared to standard fermentation, could be obtained (preliminary data, not shown).

3.4 Outlook and future perspectives

The constant establishment and improvement of protein expression platforms is a prerequisite to meet all the requirements of modern biotechnological industry (Demain and Vaishnav, 2009; Feldbrügge et al., 2013; Kirk et al., 2002; Schmidt, 2004; Spadiut et al., 2014). Product safety, low cost production and correct posttranslational modifications are essential factors that need to be ensured, especially for biopharmaceutical protein production (Berlec and Štrukelj, 2013; Gerngross, 2004). The *U. maydis* protein expression platform is contributing to this with an unconventional protein secretion mechanism that enables *N*-glycosylation free secretion of large target proteins on cheap media (Feldbrügge et al., 2013; Sarkari et al., 2014; Stock et al., 2012). By optimizing the construct design, purification, product stability and applicability could be increased in this study. However, it also became obvious that the construct design needs to be carefully adjusted for each target protein, which can turn out to be very time consuming and elaborate. One of the key challenges could hereby be the unconventional secretion itself as some modifications led to significantly impaired secretion or to the secretion of inactive target protein. Results on purification approaches of RH5 fusion proteins furthermore revealed inefficient binding and thus another possible limitation of the expression system. Adjustment of media compositions and pH maintenance, in combination with previously established protease deficient strain backgrounds, finally lead to a more than 14-fold increased yield of stable protein. This demonstrates the power of process optimization and indicates that further studies on process optimization should be performed to fully exploit its potential.

Despite the major improvements of this study there still is a lot of room for optimization. In parallel to this study, the serial deletion of secreted proteases was continued in order to further decrease the proteolytic potential (Stollewerk, 2015). Besides the deletion of secreted proteases it can also be useful to target proteases that are typically found in vacuoles or other

compartments associated with the endomembrane system as these might also act on secreted proteins (van den Hombergh et al., 1997).

Hypothesizing that construct size is not limiting to the system (Stock et al., 2012) many features were added to the fusion proteins tested in this study. However, results demonstrated that this is probably overburdening the secretion machinery. As the constructs were designed to investigate the functionality of various purification and detection tags they harbor multiple unnecessary fragments. Thus, reduction to the essential parts will likely lead to further stabilization of the product.

So far the expression medium of choice is still based on complex medium (Holliday, 1974). To further analyze nutrient limitations and optimal media compositions in detail, the use of minimal medium and automated parallel screening processes should be conducted. Here the RAMOS derived BioLector system will be the method of choice, enabling online monitored high throughput screening in microtiter plate format. The benefit of the combined use of those two systems could already be proven in recent studies, investigating the cultivation and production behavior of bacterial and yeast organisms (Wewetzer et al., 2015). Recent studies also focused on the valorization of organic waste streams (Geiser et al., 2016; Peter Stoffels, unpublished).

One major bottleneck of the unconventional protein secretion in *U. maydis* is the secretion efficiency. Despite good yields in supernatants huge parts of the expressed protein still resides in the cytoplasm. Engineering of the secretion pathway will be essential to overcome this problem. Several studies on the molecular engineering of conventional secretion machinery components have been conducted in various species, leading to improved secretion of heterologous target proteins. These included the deletion of lectin-like cargo receptors in *A. oryzae* (Hoang et al., 2015), the overexpression of involved chaperones in *S. cerevisiae* (Ma et al., 1990) or modification of the SRP- and translocase complex in *B. subtilis* (Diao et al., 2012; Kakeshtia et al., 2010). Similar approaches could be conducted on unconventional secretion in *U. maydis* after elucidation of the involved components. In this context it would also be very beneficial to get more information on the folding state of the fusion protein during unconventional secretion. Using a dihydrofolate hydrolase (DHFR) - aminopterin based assay, it could be shown for example that FGF2 unconventional secretion happens in a fully folded state (Backhaus et al., 2004). If this would also be the case for Cts1, intracellular chaperones could play a role in quality control during unconventional secretion and thus be a target for improvements. To date, one additional protein, Jps1, could be identified as part of Cts1 based unconventional secretion using a genetic screen. This protein is of unknown function but has been shown to be unconventionally secreted itself and to co-localize with Cts1 in *U. maydis* sporidia (Janpeter Stock, Michéle Reindl, unpublished). Interaction screens will be conducted in future and hopefully reveal more involved components. Additionally, a glucanase had been

identified in bioinformatic analysis that is related to Exg1 α -1,3-glucanase from *S. cerevisiae*. Albeit this enzyme is predicted to locate on the cell exterior and to be involved in cell-wall remodeling, it does not contain a predictable secretion signal (Lesage and Bussey, 2006). Unconventional secretion of the putative glucanase could recently be proven by constitutive overexpression of the glucanase fused to Gus (Joern Aschenbroich, Philipp Rink unpublished). By investigating other unconventionally secreted proteins, elucidation of the involved mechanisms and components will be accelerated.

In summary, the overall improved *U. maydis* expression platform offers a variety of applications with promising potential. Looking into the future, conventional secretion as well as unconventional secretion may enable glycosylated or unglycosylated protein secretion tailored to the desired application. Flexible construct design, variable purification strategies and easy handling as well as the ability to valorize multiple carbon sources and even waste streams are positive attributes of the system. Thus, *U. maydis* has high prospects for future use as a protein expression host in biotechnological industry.

4 Material and Methods

4.1 Materials

4.1.1 Chemicals, enzymes, kits

4.1.1.1 Chemicals

The chemicals used in this study were all purchased from the following companies unless specified otherwise: Roche, Fluka, Difco, Merck, Sigma-Aldrich, Thermo Fisher Scientific, BioRad, GE Healthcare, Pharmacia, BioWorld, Invitrogen, Serva, Carl Roth, Caelo, Applichem, Acros Organics and VWR Chemicals. All used chemicals were of *p.a.* quality.

4.1.1.2 Enzymes and kits

The following tables list the enzymes, protease inhibitors and various kits used in this study.

Tab. 4.1: Enzymes used in this study

Name	Application	Company
HRV 3C Protease	Hydrolysis of fusion proteins, protein purification	Thermo Fisher Scientific
Lysozyme (muraminidase)	Plasmid isolation	Merck
Novozyme 234	Protoplasting of <i>U. maydis</i> sporidia	Novozymes
Phusion-HF DNA-Polymerase	Amplification of DNA molecules	Finnzymes (or own preparation)
ProTEV Protease	Hydrolysis of fusion proteins, protein purification	Promega (or own preparation)
Restriction enzymes	Restriction of DNA molecules	New England Biolabs
RNAse A	Plasmid isolation, genomic DNA isolation	Boehringer Ingelheim
T4 DNA-Ligase	Ligation of DNA molecules	Roche
Taq DNA-Polymerase	Amplification of DNA molecules	Own preparation

Tab. 4.2: Protease inhibitors used in this study

Name	Application	Company
Benzamidine	Preparation of cell extracts	Sigma-Aldrich
cOmplete™ EDTA-free Protease Inhibitor Cocktail	Preparation of cell extracts and supernatant samples	Roche

Phenylmethylsulfonylfluorid (PMSF)	Preparation of cell extracts	Serva
Pepstatin A	Preparation of cell extracts	Sigma-Aldrich

Tab. 4.3: Kits used in this study

Name	Application	Company
AceGlow™ Chemiluminescence substrate	Chemiluminescent substrate for horseradish peroxidase in Western blot analysis	PeqLab
BirA-500: BirA biotin-ligase standard reaction kit	Mono-biotinylation of AviTag®-labeled proteins	Avidity
CDP-Star®	Chemiluminescent substrate for alkaline phosphatase in Southern blot analysis	Roche
JETQUICK DNA CleanUp Spin Kit	Purification of plasmids from boiling plasmid preparations	Genomed
JETQUICK Gel Extraction Spin Kit	Elution and purification of DNA fragments from agarose gels	Genomed
JETSORB Gel Extraction Kit	Elution and purification of DNA fragments from agarose gels	Genomed
PCR DIG Labeling Mix	Digoxigenin labeling of PCR products (generation of Southern blot probes)	Roche
Plasmid Midi Kit	Large scale plasmid preparations	Qiagen
QuantaRed™ Enhanced Chemifluorescent HRP substrate Kit	Chemifluorescent substrate for horseradish peroxidase in ELISA assays	Thermo Fisher Scientific
QuikChange Site-Directed Mutagenesis Kit	Site-directed mutagenesis	Agilent Technologies
SureClean	Purification of DNA fragments and PCR products	Bioline

Tab. 4.4: Protein- and DNA size standards used in this study

Name	Application	Company
PageRuler™ Prestained Protein Ladder (10 – 180 kDa)	SDS-PAGE	Thermo Fisher Scientific
PageRuler™ Plus Prestained Protein Ladder (10 – 250 kDa)	SDS PAGE	Thermo Fisher Scientific
GeneRuler 1 kb DNA Ladder	DNA Gel electrophoresis	Thermo Fisher Scientific
λ PstI (PstI digested Enterophage λ DNA)	DNA Gel electrophoresis	own preparation

4.1.2 Solutions and media

Standard buffer and media were prepared using protocols published in Ausubel et al., 1987 and Sambrook et al., 1989. Special buffers and media are specified in detail below the respective method.

4.1.2.1 Cultivation of *E. coli*

Media for the cultivation of *E. coli* were prepared according to Sambrook et al., 1989.

YT-medium (solid)	dYT-medium (liquid)
8 g tryptone	16 g tryptone
5 g yeast extract	10 g yeast extract
5 g NaCl	5 g NaCl
15 g agar	ad 1 L H ₂ O _{bid.} , autoclaved
ad 1 L H ₂ O _{bid.} , autoclaved	

Tab. 4.5: Antibiotics used in *E. coli* cultivations

Antibiotic	Final concentration [µg/mL]
Ampicillin	100
Kanamycin	50
Chloramphenicol	34
Gentamycin	40

4.1.2.2 Cultivation of *U. maydis*

Media for the cultivation of *U. maydis* were prepared according to Banuett and Herskowitz, 1989 and Holliday, 1974. For sterilization media were either autoclaved for 5 min at 121°C or filter sterilized with a 0.22 µm Filtropur BT50 bottle top filter (Sarstedt).

CM (complete medium)	CM variations
2.5 g casaminoacids	CM-glc (CM; 10 g/L glucose)
1.5 g NH ₄ NO ₃	CM ^{M0.1} -glc (CM; 10 g/L glucose and 0.1 M MOPS)
0.5 g DNA degr. free acid	CM ^{M0.5} -glc (CM; 10 g/L glucose and 0.5 M MOPS)
1 g yeast extract	CM ^{M0.25} -glc (CM; 10 g/L glucose and 0.25 M MOPS)
10 mL vitamin solution	CM ^{M0.05} -glc (CM; 10 g/L glucose and 0.05 M MOPS)
62.5 mL salt solution	CM ^{H0.1} -glc (CM; 10 g/L glucose and 0.1 M HEPES)
ad 1 L H ₂ O _{bid.} , pH 7.0, autoclaved	CM ^{M0.1} -frc (CM; 10 g/L fructose and 0.1 M MOPS)
The medium was then supplemented with 10 g/L (f.c.) glucose.	CM ^{M0.1} -glc ^{2x} (CM; 20 g/L glucose and 0.1 M MOPS)
(for solid medium 20 g agar was added prior to autoclaving)	CM ^{M0.1} -glc ^{2x} -N ^{2x} (CM; 20 g/L glucose, 3 g/L NH ₄ NO ₃ and 0.1 M MOPS)

Vitamin solution	NSY-glycerol	Regeneration agar light (RegLight)
200 mg thiamine hydrochloride	3 g beef extract	10 g yeast extract
100 mg riboflavin	5 g peptone	4 g peptone
100 mg pyridoxine monohydrochlorate	1 g yeast extract	4 g sucrose
400 mg Ca-panthotenate	5 g sucrose	182.2 g sorbitol
100 mg aminobenzoic acid	800 mL glycerol (87%)	15 g agar
400 mg nicotinic acid	ad 1 L H ₂ O _{bid.} , autoclaved	ad 1 L H ₂ O _{bid.} , autoclaved
400 mg cholinchloride		For selection of <i>U. maydis</i> transformants RegLight was supplemented with 2 µg/mL Carboxin
2000 mg myo-inositol		
ad 1 L H ₂ O _{bid.}		

YEPS_{light}	Trace element solution	Salt solution
10 g yeast extract	60 mg H ₃ BO ₃	16 g KH ₂ PO ₄
4 g peptone	140 mg MnCl ₂ *4H ₂ O	4 g Na ₂ SO ₄
4 g sucrose	400 mg ZnCl ₂	8 g KCl
ad 1 L H ₂ O _{bid.} , autoclaved	40 mg Na ₂ MoO ₄ *2H ₂ O	1.32 g CaCl ₂ * 2H ₂ O
	100 mg FeCl ₃ *6H ₂ O	8 mL trace element solution
	40 mg CuSO ₄ *5H ₂ O	2 g MgSO ₄
	ad 1 L H ₂ O _{bid.} , autoclaved	ad 1 L H ₂ O _{bid.} , filter sterilized

AM (ammonium minimal medium)

3 g (NH₄)₂SO₄
 50 mL salt solution
 ad 1 L H₂O_{bid.}, pH 7.0, autoclaved

4.1.3 Oligonucleotides

The oligonucleotides used in this study were synthesized by Metabion GmbH (Martinsried) or Integrated DNA Technologies Inc. (Coralville).

Tab. 4.6: Cloning oligonucleotides used in this study

Name	Nucleotide sequence 5' – 3'
DD135	CACACTAGTCTCGAGGTCCTCTTCCAGGGTCCCCTCCAGGCCAACGCGGCCTACC CC
DD183	CACACTAGTCTCGAGGTGTTGTTTCAGGGTCCTCTCCAGGCCAACGCGGCCTACCC C
DD478	TCCATGGGTAATGCAGCTTGGTCGCACCCGCAGTTCGAGAAGGCTATGGCCGACG TCCAGCTCGTCG
DD479	ATGGGTCTCTGCAGTAACCGACGAGACGGTGACCTGGGTGC
DD480	CACGGTCTCGCGGTATGTTTGGACGTAAGTACTCCAG
DD481	TGGGCCCTAGGCGGCACCGGCATAGTCGGGCACGTCGTATGGATAGGCCGCGTTC TTGAGGCCGTTCTTGACATT

DD482	TACGGTCTCTTCCTAAGGCCGGTAGGGCCGTCGTAGTCG
DD483	CACGGTCTCTAGGACCATGTTTGGACGTAAGTACTCCAG
DD484	TACGGGCCCTAATGGTGGTGATGGTGGTGATGGTGGTGATGGGCCGCTACGGCAT AGTCGGGCACGTCGTATGG
DD486	TACGGCCGGTAGGGCCGTCGTAGTCAGGACCCTGAAACAACACCTCGAGGGCCTC GTCGTGCTGGGCGAGAGCG
MB38	GTGGGGCCCCCTCGTGCCACTCGATCTTCTGCGCCTCGAAGATGTCGTTGAGACCG TGCTTGAGGCCGTTCTTGACATTG
MB273	CACCCCGGGCTGCAGGAATTCGATCCCATGGGCGGTCTGAACGACATCTTCGAGG CGCAGAAGATCGAGTGGCACGAGGGTGCTGGATTCGAGAACGCCATCAAG
MB274	CACCCCGGGCTGCAGGAATTCGATCCCATGGGCGGTCTGAACGACATCTTCGAGG CGCAGAAGATCGAGTGGCACGAGGGTGCTGGATCGATCGACATCCTCCAG
MB293	GTGCCCCGGGAGAACCACTAGTCGAGTTCGAGTTGACG
MB294	CACCCCGGGGGTTCAATGGCCGACGTCCAGCTCGTCG
MF502	ACGACGTTGTAAAACGACGGCCAG
MF503	TTCACACAGGAAACAGCTATGACC
RL882	AAGCCATGGGTCACGATTTCAACCACC
RL963	CACACTAGTGAAAACCTCTACTTCCAGGGCCTCGAGGCCAACGCGGCCTACCCC
RL964	GTGGGCGCGCCTATAGTCGGGCACGTCGTAGGGGTAACC
RL982	GTGGGGCCCATGGTGGTGATGGTGGTGATGGTGGTGATGACCGGTGGCCGCCTT GAGGCCGTTCTTGACATTGTCC
RL983	GTGGGGCCCCCTTCTCGAACTGCGGGTGCGACCAGGCCGCGTTACCGGTGGCCGC CTTGAGGCCGTTCTTGACATTGTCC
RL984	CACCCATGGGTAACGCGGCCTGGTCGCACCCGCAGTTCGAGAAGCATATGGGCTT CGAGAACGCCATCAAGAAGACC
RL1089	CGTCAACGACGGTGTCAAGTACCTCTTCATCC
RL1090	GGATGAAGAGGTACTTGACACCGTCGTTGACG
RL1091	CGGAAGACACCGACGACGACACCGAGGAGG
RL1092	CCTCCTCGGTGTCGTGTCGGTGTCTTCCG
RL1347	CATCACTGAGACGGTACCG
RL1386	GTGGGATCCTTAACCTCAGCTCCCAGAACATGGC
RL1431	CACCCATGGGCCATCACCACCATCACCACCATCACCACCATCATATGGGCTTCGAG AACGCCATCAAGAAGACC
RL1573	TTTGGTCTCGGTGCGCCCAATACGCAAACC
SL937	CTGTGCTTCTTGCAATGG

Tab. 4.7: Sequencing oligonucleotides used in this study

Name	Nucleotide sequence 5' – 3'
DD134	GGGCTGGCTTAACTATGC
DD136	GAAAACCTCTACTTCCAGGGC
DD141	CGAGGTCCTCTTCCAGGG
DD187	GAGGTGTTGTTTCAGGGTC
DD455	CTAGTTTAGTGGTGATGGTGGTGATGATAGTCGGGCACGTCGTAGGGGTAGG
MB39	CCTCGAAGATGTCGTTTCAGACC
MF748	TTCGCTCTACCGATGCCTT
RL19	GGCCGCGTTGGCCGCACCAGCAGCAGAGGCTGTTGC
RL152	AATATTGTGCCGCCACCAGAC
RL182	CACCCGCAGTTCGAGAAG
RL393	TCTGCGCGGCAGAGACG
RL405	AAGCTAGAGAGAACGACGGGTTGGATGG
RL553	GGTCTCCGAAACCAACCCGTACCTACTG
RL884	CAGATAGGCGCGCCGCGCAATGCTTGTACTGTGCC
RL945	GTGCCATGGCGGGGATCCTGATAGAGTAAGG
RL1120	CGATGAATTCTCATGTTTGAC
RL1214	ATGTCGCTATTCAACGTCAG
RL1215	CGACGAAGCCATGATAGGGCG
RL1578	GACTAGTCGACGAGACGGTGA
RL1823	GCGAAGTCCATCTTCTGC
SL71	AGGAGAAGTGCTGCTGGG
SL226	ATGGTCAGGTCCACAGGG
SL466	ATAGCGGCCGCACGCGTTACGACTGCACAGGCACG
SL549	ATTGTCGTTAGAACGCGGC
SL554	GTACTIONGAGTCTAGACGGCACAACCAAGAATAAC
SL929	GTGGTGTGCGATGTGTTG
SL939	ACCAGCAGCAGAGGCTGTTG
SL941	CCTTGCGAGTCGATGTTG
SL943	GGCGAAAGCGTAGAGAAC
SL955	GGCGATGAGACTCCTTTC

4.1.4 Plasmids

Plasmid generation was performed by standard molecular cloning techniques as described in Sambrook et al., 1989 or by Golden Gate cloning as described in Terfrüchte et al., 2014. Oligonucleotides used for cloning purposes are listed in Tab. 4.6. Plasmids containing synthetic genes were synthesized by Integrated DNA Technologies (Coralville) or GeneART® (Thermo Fisher Scientific, Waltham). Sequencing of all constructs was performed at the Sequencing Service of the Genomics Service Unit at Ludwig-Maximilians-University München or at Eurofins Genomics (Ebersberg).

4.1.4.1 *E. coli* expression plasmids

pET-TEV (pUMa1316)

Expression plasmid carrying the sequence for Tobacco etch virus protease (TEV) fused to a N-terminal 6xHis-tag for purification. The plasmid encodes the β -lactamase enzyme for selection on ampicillin containing media (Amp^R).

pET15b-Gus-SHH (pUMa1671)

pET-15b (Novagen) derived expression plasmid carrying the sequence for the reporter enzyme β -Glucuronidase (Gus), N-terminally fused to a One-STrEP-tag® (IBA Lifesciences), followed by a 3xHA-Tag and a 10xHis-tag for purification (Stock et al., 2012). The plasmid encodes the β -lactamase enzyme for selection on ampicillin containing media (Amp^R). (Stock et al., 2012)

pET15b-6xHis-Gfp (pUMa2156)

pET-15b (Novagen) derived expression plasmid carrying the sequence for the green fluorescence protein (Gfp), C-terminally fused to a 6xHis-tag for purification. The plasmid encodes the β -lactamase enzyme for selection on ampicillin containing media (Amp^R). (Sarkari, 2014)

4.1.4.2 Plasmids for use in *U. maydis*

All plasmids for gene expression in *U. maydis* are integrative vectors, derived from p123 (Aichinger et al., 2003). The plasmids carry a sequence for homologous recombination at the *ip*^R-locus enabling stable genomic integration and selection on carboxin containing media (Cbx^R) (Brachmann, 2001).

UmRH5 proteins labeled with an asterisk (UmRH5*, Δ N UmRH5*) are referring to a mutated version of UmRH5 (L95V; E286D; T299A). The mutations have accidentally been introduced by site-directed mutagenesis with the original purpose of removing of *Bsa*I restriction sites. Exchange of the mutated with a non-mutated version in selected constructs (pUMa2995 - 3000) did not reveal any effect of the mutations in any performed control experiment suggesting that the mutations are not harmful to the protein.

Cts1 proteins labeled with an asterisk (Cts1*) are referring to a mutated version of Cts1 (P747H or P719H depending on the construct) that occurred during PCR amplification. Exchange of the mutated with a non-mutated version (pUMa2657 - 2658) did not reveal any effect of the mutations.

pTC-Cbx(+) (pUMa260)

Plasmid encoding for the *ip^R*-locus (mediating Cbx resistance) and the β -lactamase enzyme, for selection on ampicillin containing media (Amp^R). It served as a template to generate the *ip* Southern blot probe by PCR. (Brachmann, 2001; Loubradou et al., 2001)

pMF5-9c pHA3_Cbx(+) (pUMa791)

This vector contains the sequence for a 3xHA-tag followed by the *ip^R*-locus, enabling homologous recombination (*ip^R*). Additionally, the plasmid encodes the β -lactamase enzyme for selection on ampicillin containing media (Amp^R). (Brachmann, 2001)

pDest (pUMa1467)

pUC57 derivative used in Golden Gate cloning approaches. It serves as a destination vector for the final ligation construct. It contains the sequence for a multiple cloning site, including *Bsa*I recognition sites and the β -lactamase enzyme for selection on ampicillin containing media (Amp^R). (Terfrüchte et al., 2014)

pRabX1 P_{otef}Gus-SHH-Cts1 (pUMa1521)

Vector for the constitutive expression of a Gus-SHH-Cts1 fusion protein. The construct is under the control of the constitutive P_{otef} promoter. Translation termination is mediated by a 3'-*T_{nos}* terminator. For integration via homologous recombination into the *ip*-locus, the plasmid also codes for a carboxin resistance (*ip^R*). The plasmid encodes the β -lactamase enzyme for selection on ampicillin containing media (Amp^R). (Stock et al., 2012)

DF-cdc3 (pUMa1696)

The vector contains the 961 bp long downstream flanking region of *umag10503* (*cdc3*). Additionally the plasmid encodes a gentamycin resistance for selection on gentamycin containing media (Gent^R). The vector was used for Golden Gate Cloning approaches. (this study)

pRabX1 P_{otef}Gus-SHH-Cts1 (pUMa1711)

This vector contains the sequence for a Gus-SHH-Cts1 fusion protein and is designed to serve as a storage vector for Golden Gate cloning. The plasmid encodes a gentamycin resistance for selection on gentamycin containing media (Gent^R). (Stock, 2013)

pRabX1 P_{otef}UmRH5-SHH-Cts1 (pUMa1738)

Vector for the constitutive expression of a UmRH5-SHH-Cts1 fusion protein in *U. maydis*. For pUMa1738 the *U. maydis* codon optimized RH5 coding sequence (1514 bp) from pUMa1781 was cloned into the pUMa1521 expression vector backbone, using the restriction endonucleases *Nco*I and *Spe*I. The plasmid contains the DNA sequence for UmRH5 N-terminally fused to a One-STrEP-tag® (IBA Lifesciences), followed by a 3xHA-tag, a 10xHis-tag for purification and the Cts1 protein. The construct is under the control of the constitutive P_{otef} promoter. Translation termination is mediated by a 3'-*T_{nos}* terminator. For integration via homologous recombination into the *ip*-locus, the plasmid also codes for a carboxin resistance (*ip^R*). The plasmid encodes the β -lactamase enzyme for selection on ampicillin containing media (Amp^R). (this study)

UmRH5_pMK-RQ (pUMa1781)

Cloning vector containing a chemically synthesized, codon optimized UmRH5 sequence. The plasmid encodes the kanMX marker for selection on kanamycin containing media (Kan^R). (this study)

pRabX1 P_{otef}UmRH5-SHH-Cts1 (pUMa1902)

Vector for the constitutive expression of a UmRH5-SHH-Cts1-His fusion protein in *U. maydis*. For pUMa1902 a 1514 bp fragment, containing the sequence for the UmRH5 protein from pUMa1738 was cloned into the pUMa1711

expression vector backbone, using the restriction endonucleases *NcoI* and *SpeI*. The plasmid contains the DNA sequence for UmRH5 N-terminally fused to a One-STrEP-tag® (IBA Lifesciences), followed by a 3xHA-tag, a 10xHis-tag for purification and the Cts1 protein. The construct is under the control of the constitutive *P_{otef}* promoter. Translation termination is mediated by a 3'-*T_{nos}* terminator. The plasmid encodes a gentamycin resistance for selection on gentamycin containing media (Gent^R). (this study)

pRabX2 *P_{otef}*UmRH5-TH-Cts1 (pUMa1912)

Vector for the constitutive expression of a UmRH5-TEV-HA-Cts1 fusion protein in *U. maydis*. For pUMa1912 a 156 bp fragment, containing the sequence for a 3xHA-tag was generated by PCR using the oligonucleotides RL963 and RL964 on pUMa791 as template. A 143 bp fragment was cloned into the pUMa1902 expression vector backbone, using the endonucleases *Ascl* and *SpeI*. The plasmid contains the DNA sequence for UmRH5 N-terminally fused to a TEV protease cleavage site, followed by a 3xHA-tag and the Cts1 protein. The construct is under the control of the constitutive *P_{otef}* promoter. Translation termination is mediated by a 3'-*T_{nos}* terminator. The plasmid encodes a gentamycin resistance for selection on gentamycin containing media (Gent^R). (this study)

pRabX2 *P_{otef}*Strep-UmRH5-TH-Cts1 (pUMa1921)

Vector for the constitutive expression of a Strep-UmRH5-TEV-HA-Cts1 fusion protein in *U. maydis*. For pUMa1921 a 1712 bp fragment, containing the sequence for a Strep-UmRH5-TEV-HA fusion protein was generated by PCR using the oligonucleotides RL984 and RL964 on pUMa1912 as template. A 1699 bp fragment was cloned into the pUMa1912 expression vector backbone, using the endonucleases *Ascl* and *NcoI*. The plasmid contains the DNA sequence for a One-STrEP-tag® (IBA Lifesciences) for purification, N-terminally fused to UmRH5, followed by a TEV protease cleavage site, a 3xHA-tag and the Cts1 protein. The construct is under the control of the constitutive *P_{otef}* promoter. Translation termination is mediated by a 3'-*T_{nos}* terminator. The plasmid encodes a gentamycin resistance for selection on gentamycin containing media (Gent^R). (this study)

UF-cdc3C-HygR (pUMa1924)

The vector contains the 907 bp long upstream flanking region of umag10503 (*cdc3*), followed by the *cdc3* 3'UTR and a hygromycin resistance cassette (Hyg^R). Additionally the plasmid encodes a gentamycin resistance for selection on gentamycin containing media (Gent^R). The vector was used for Golden Gate Cloning approaches. (this study)

pRabX2 *P_{otef}*UmRH5*-TH-Cts1-His (pUMa1986)

Vector for the constitutive expression of a UmRH5*-TEV-HA-Cts1-His fusion protein in *U. maydis*. For pUMa1986 a 1796 bp fragment, containing the sequence for a Cts1-His fusion protein was generated by PCR using the oligonucleotides RL963 and RL982 on pUMa1912 as template. A 1645 bp fragment was cloned into the pUMa2048 expression vector backbone, using the endonucleases *Ascl* and *Apal*. The plasmid contains the DNA sequence for UmRH5* N-terminally fused to a TEV protease cleavage site, a 3xHA-tag, the Cts1 protein and a 10xHis-tag for purification. The construct is under the control of the constitutive *P_{otef}* promoter. Translation termination is mediated by a 3'-*T_{nos}* terminator. The plasmid encodes a gentamycin resistance for selection on gentamycin containing media (Gent^R). (this study)

pRabX2 *P_{otef}*Strep-UmRH5*-TEV-HA-Cts1 (pUMa1988)

Vector for the constitutive expression of a Strep-UmRH5*-TEV-HA-Cts1 fusion protein in *U. maydis*. For pUMa1988 a 1712 bp fragment, containing the sequence for a Strep-UmRH5*-TEV-HA fusion protein was generated by PCR using the oligonucleotides RL984 and RL964 on pUMa1912 as template. A 1699 bp fragment was cloned into the pUMa2048 expression vector backbone, using the endonucleases *Ascl* and *NcoI*. The plasmid contains the DNA sequence for a One-STrEP-tag® (IBA Lifesciences) for purification N-terminally fused to UmRH5*, followed by a

TEV protease cleavage site, a 3xHA-tag and the Cts1 protein. The construct is under the control of the constitutive *P_{otef}* promoter. Translation termination is mediated by a 3'-*T_{nos}* terminator. For integration via homologous recombination into the *ip*-locus, the plasmid also codes for a carboxin resistance (*ip^R*). The plasmid encodes the β -lactamase enzyme for selection on ampicillin containing media (*Amp^R*). (this study)

pRabX2 *P_{otef}*UmRH5*-TH-Cts1-His (pUMa2024)

Vector for the constitutive expression of a UmRH5*-TEV-HA-Cts1-His fusion protein. The vector was cloned using the Golden Gate Cloning method, based on (Terfrüchte et al., 2014). *Bsa*I fragments from pUMa1986 (UmRH5*-TEV-HA-Cts1-His), pUMa1696 (*cdc3* downstream flanking region) and pUMa1924 (*cdc3* upstream flanking region-*Hyg^R*) were cloned into the destination vector pUMa1467. The final construct contains the DNA sequence for UmRH5* N-terminally fused to a TEV protease cleavage site, a 3xHA-tag, the Cts1 protein and a 10xHis-tag for purification. The construct is under the control of the constitutive *P_{otef}* promoter. For integration via homologous recombination into the *cdc3* locus (umag10503), the plasmid also codes for the *cdc3* upstream and downstream flanking regions as well as a hygromycin resistance (*Hyg^R*). The plasmid encodes the β -lactamase enzyme for selection on ampicillin containing media (*Amp^R*). (this study)

pRabX2 *P_{otef}*UmRH5*-TH-Cts1 (pUMa2048)

Vector for the constitutive expression of a UmRH5*-TH-Cts1 fusion protein in *U. maydis*. For pUMa2048 a 1556 bp fragment, containing the sequence for UmRH5* was cloned into the pUMa1912 expression vector backbone, using the endonucleases *Nco*I and *Spe*I. The plasmid contains the DNA sequence for UmRH5* N-terminally fused to a TEV protease cleavage site, followed by a 3xHA-tag and the Cts1 protein. The construct is under the control of the constitutive *P_{otef}* promoter. Translation termination is mediated by a 3'-*T_{nos}* terminator. The plasmid encodes a gentamycin resistance for selection on gentamycin containing media (*Gent^R*). (this study)

pRabX2 *P_{otef}*UmRH5*-TH-Cts1-His (pUMa2105)

Vector for the constitutive expression of a UmRH5*-TEV-HA-Cts1-His fusion protein in *U. maydis*. For pUMa2105 a 4206 bp fragment, containing the sequence for a UmRH5*-TEV-HA-Cts1-His fusion protein from pUMa2024 was cloned into the pUMa1521 expression vector backbone, using the restriction endonucleases *Kpn*I and *Sac*II. The plasmid contains the DNA sequence for UmRH5* N-terminally fused to a TEV protease cleavage site, followed by a 3xHA-tag, the Cts1 protein and a 10xHis-tag for purification. The construct is under the control of the constitutive *P_{otef}* promoter. Translation termination is mediated by a 3'-*T_{nos}* terminator. For integration via homologous recombination into the *ip*-locus, the plasmid also codes for a carboxin resistance (*ip^R*). The plasmid encodes the β -lactamase enzyme for selection on ampicillin containing media (*Amp^R*). (this study)

pRabX2 *P_{otef}*UmRH5*-TH-Cts1-Strep (pUMa2106)

Vector for the constitutive expression of a UmRH5*-TEV-HA-Cts1-Strep fusion protein in *U. maydis*. For pUMa2106 a 4209 bp fragment, containing the sequence for a UmRH5*-TEV-HA-Cts1-Strep fusion protein from pUMa2025 was cloned into the pUMa1521 expression vector backbone, using the restriction endonucleases *Kpn*I and *Sac*II. The plasmid contains the DNA sequence for UmRH5* N-terminally fused to a TEV protease cleavage site, followed by a 3xHA-tag, the Cts1 protein and a One-STrEP-tag® (IBA Lifesciences) for purification. The construct is under the control of the constitutive *P_{otef}* promoter. Translation termination is mediated by a 3'-*T_{nos}* terminator. For integration via homologous recombination into the *ip*-locus, the plasmid also codes for a carboxin resistance (*ip^R*). The plasmid encodes the β -lactamase enzyme for selection on ampicillin containing media (*Amp^R*). (this study)

pRabX1 *P_{oma}*Gus-SHH-Cts1 (pUMa2113)

Vector for the constitutive expression of a Gus-SHH-Cts1 fusion protein in *U. maydis*. The plasmid contains the DNA sequence for β -Glucuronidase N-terminally fused to a One-STrEP-tag® (IBA Lifesciences), followed by a

3xHA-tag, a 10xHis-tag for purification and the Cts1 protein. The construct is under the control of the constitutive *P_{oma}* promoter. Translation termination is mediated by a 3'-*T_{nos}* terminator. For integration via homologous recombination into the *ip*-locus, the plasmid also codes for a carboxin resistance (*ip^R*). The plasmid encodes the β -lactamase enzyme for selection on ampicillin containing media (Amp^R). (Reindl, 2013)

pRabX2 *P_{oter}*Strep-UmRH5*-TH-Cts1 (pUMa2148)

Vector for the constitutive expression of a Strep-UmRH5*-TEV-HA-Cts1 fusion protein in *U. maydis*. For pUMa2148 a 896 bp fragment, containing the sequence for the constitutive *P_{oter}* promoter from pUMa1988 was cloned into the pUMa2124 expression vector backbone, using the restriction endonucleases *KpnI* and *NcoI*. The plasmid contains the DNA sequence for a One-STrEP-tag® (IBA Lifesciences) for purification N-terminally fused to UmRH5*, followed by a TEV protease cleavage site, a 3xHA-tag and the Cts1 protein. The promoter was exchanged due to a strange sequencing pattern. Translation termination is mediated by a 3'-*T_{nos}* terminator. For integration via homologous recombination into the *ip*-locus, the plasmid also codes for a carboxin resistance (*ip^R*). The plasmid encodes the β -lactamase enzyme for selection on ampicillin containing media (Amp^R). (this study)

pRabX2 *P_{oma}*Strep-UmRH5*-TH-Cts1 (pUMa2150)

Vector for the constitutive expression of a Strep-UmRH5*-TEV-HA-Cts1 fusion protein in *U. maydis*. For pUMa2150 a 2797 bp fragment, containing the sequence for the constitutive *P_{oma}* promoter from pUMa2113 was cloned into the pUMa2124 expression vector backbone, using the restriction endonucleases *AgeI* and *NcoI*. The plasmid contains the DNA sequence for a One-STrEP-tag® (IBA Lifesciences) for purification N-terminally fused to UmRH5*, followed by a TEV protease cleavage site, a 3xHA-tag and the Cts1 protein. Translation termination is mediated by a 3'-*T_{nos}* terminator. For integration via homologous recombination into the *ip*-locus, the plasmid also codes for a carboxin resistance (*ip^R*). The plasmid encodes the β -lactamase enzyme for selection on ampicillin containing media (Amp^R). (this study)

pRabX2 *P_{oma}*Strep-UmRH5*-TH-Cts1-His (pUMa2151)

Vector for the constitutive expression of a Strep-UmRH5*-TEV-HA-Cts1 fusion protein in *U. maydis*. For pUMa2150 a 2797 bp fragment, containing the sequence for the constitutive *P_{oma}* promoter from pUMa2113 was cloned into the pUMa2124 expression vector backbone, using the restriction endonucleases *AgeI* and *NcoI*. The plasmid contains the DNA sequence for a One-STrEP-tag® (IBA Lifesciences) for purification N-terminally fused to UmRH5*, followed by a TEV protease cleavage site, a 3xHA-tag, the Cts1 protein and a 10xHis-tag. Translation termination is mediated by a 3'-*T_{nos}* terminator. For integration via homologous recombination into the *ip*-locus, the plasmid also codes for a carboxin resistance (*ip^R*). The plasmid encodes the β -lactamase enzyme for selection on ampicillin containing media (Amp^R). (this study)

pRabX2 *P_{oma}*His- α Gfp-NB-TH-Cts1 (pUMa2240)

Plasmid encoding for a llama derived, *U. maydis* codon optimized, anti Gfp nanobody under the control of the constitutive *P_{oma}* promoter. The nanobody sequence is C-terminally fused to a 10xHis-tag for purification, a TEV protease cleavage site, followed by a 3xHA-tag and the Cts1 encoding sequence. The plasmid encodes the β -lactamase enzyme for selection on ampicillin containing media (Amp^R). (Sarkari, 2014)

pRabX2 *P_{oter}*His-UmRH5*-TH-Cts1 (pUMa2310)

Vector for the constitutive expression of a His-UmRH5*-TEV-HA-Cts1 fusion protein in *U. maydis*. For pUMa2310 a 3308 bp fragment, containing the sequence for a His-UmRH5*-TEV-HA-Cts1-Strep fusion protein from pUMa2176 was cloned into the pUMa1738 expression vector backbone, using the restriction endonucleases *ApaI* and *NcoI*. The plasmid contains the DNA sequence for a 10xHis-tag for purification N-terminally fused to UmRH5*, followed by a TEV protease cleavage site, a 3xHA-tag and the Cts1 protein. The construct is under the control of the

constitutive P_{otef} promoter. Translation termination is mediated by a 3'- T_{nos} terminator. For integration via homologous recombination into the *ip*-locus, the plasmid also codes for a carboxin resistance (*ip^R*). The plasmid encodes the β -lactamase enzyme for selection on ampicillin containing media (Amp^R). (this study)

pRabX2 P_{otef} UmRH5*-PH-Cts1-His (pUMa2441)

Vector for the constitutive expression of a UmRH5*-HRV 3C-HA-Cts1-His fusion protein in *U. maydis*. For pUMa2441 a 1619 bp fragment, containing the sequence for a HRV 3C-HA fusion protein was generated by PCR using the oligonucleotides DD183 and RL1386 on pUMa2310 as template. A 1350 bp fragment was cloned into the pUMa2105 expression vector backbone, using the restriction endonucleases *Spe*II and *Bst*BI. The plasmid contains the DNA sequence for UmRH5* N-terminally fused to a HRV 3C protease cleavage site, followed by a 3xHA-tag, the Cts1 protein and a 10xHis-tag for purification. The construct is under the control of the constitutive P_{otef} promoter. Translation termination is mediated by a 3'- T_{nos} terminator. For integration via homologous recombination into the *ip*-locus, the plasmid also codes for a carboxin resistance (*ip^R*). The plasmid encodes the β -lactamase enzyme for selection on ampicillin containing media (Amp^R). (this study)

pRabX2 P_{otef} His-UmRH5*-PH-Cts1 (pUMa2442)

Vector for the constitutive expression of a His-UmRH5*-HRV 3C-HA-Cts1 fusion protein in *U. maydis*. For pUMa2442 a 1350 bp fragment, containing the sequence for a HRV 3C-HA-Cts1 fusion protein from pUMa2441 was cloned into the pUMa2310 expression vector backbone, using the restriction endonucleases *Bst*BI and *Spe*I. The plasmid contains the DNA sequence for a 10xHis-tag for purification N-terminally fused to UmRH5*, followed by a HRV 3C protease cleavage site, a 3xHA-tag and the Cts1 protein. The construct is under the control of the constitutive P_{otef} promoter. Translation termination is mediated by a 3'- T_{nos} terminator. For integration via homologous recombination into the *ip*-locus, the plasmid also codes for a carboxin resistance (*ip^R*). The plasmid encodes the β -lactamase enzyme for selection on ampicillin containing media (Amp^R). (this study)

pRabX2 P_{oma} His- α Gfp-NB-PH-Cts1 (pUMa2480)

Vector for the constitutive expression of a His- α Gfp-NB-HRV 3C-HA-Cts1 fusion protein in *U. maydis*. For pUMa2480 a 1350 bp fragment, containing the sequence for a HRV 3C-HA-Cts1 fusion protein from pUMa2441 was cloned into the pUMa2240 expression vector backbone, using the restriction endonucleases *Bst*BI and *Spe*I. The plasmid contains the DNA sequence for a 10xHis-tag for purification N-terminally fused to α Gfp-NB, followed by a HRV 3C protease cleavage site, a 3xHA-tag and the Cts1 protein. The construct is under the control of the constitutive P_{oma} promoter. Translation termination is mediated by a 3'- T_{nos} terminator. For integration via homologous recombination into the *ip*-locus, the plasmid also codes for a carboxin resistance (*ip^R*). The plasmid encodes the β -lactamase enzyme for selection on ampicillin containing media (Amp^R). (this study)

pRabX2 P_{oma} UmHRP-Cts1 (pUMa2553)

Vector for the constitutive expression of a HRP-HRV 3C-HA-Cts1 fusion protein in *U. maydis*. The construct is under the control of the constitutive P_{oma} promoter. Translation termination is mediated by a 3'- T_{nos} terminator. For integration via homologous recombination into the *ip*-locus, the plasmid also codes for a carboxin resistance (*ip^R*). The plasmid encodes the β -lactamase enzyme for selection on ampicillin containing media (Amp^R). (Reindl, 2016)

pRabX2 P_{oma} Strep- α Gfp-NB-ProtA-T-CBP-Cts1*-H (pUMa2624)

Vector for the constitutive expression of a Strep- α Gfp-NB-ProtA-TEV-CBP-Cts1*-HA fusion protein in *U. maydis*. For pUMa2624 a 414 bp fragment, containing the sequence for a Strep- α Gfp-NB fusion protein was generated by PCR using the oligonucleotides DD478 and DD479 on pUMa2240 as template. A 400 bp fragment (*Bsa*I cut) was used for cloning. A 1654 bp fragment, containing the sequence for a Cts1-HA fusion protein was generated by PCR using the oligonucleotides DD480 and DD481 on pUMa2240 as template. A 1644 bp fragment (*Bsa*I cut) was used

for cloning. Both fragments were ligated together with a 547 bp *Bsa*I cut fragment from pUMa2628. The resulting molecule was cloned into the pUMa2240 expression vector backbone, using the endonucleases *Apal* and *Nco*I. The plasmid contains the DNA sequence for an One-STrEP-tag® (IBA Lifesciences) for purification N-terminally fused to the anti Gfp nanobody, followed by Protein A, a TEV protease cleavage site, a Calmodulin Binding Peptide, the Cts1* protein and a 3xHA-tag. The construct is under the control of the constitutive *P_{oma}* promoter. Translation termination is mediated by a 3'-*T_{nos}* terminator. For integration via homologous recombination into the *ip*-locus, the plasmid also codes for a carboxin resistance (*ip^R*). The plasmid encodes the β -lactamase enzyme for selection on ampicillin containing media (Amp^R). (Beier, 2015)

pRabX2 *P_{oma}*Strep- α Gfp-NB-ProtA-T-Cts1*-H-His (pUMa2625)

Vector for the constitutive expression of a Strep- α Gfp-NB-ProtA-TEV-CBP-Cts1*-HA-His fusion protein in *U. maydis*. For pUMa2625 a 875 bp fragment, containing the sequence for a Strep- α Gfp-NB-Protein A-TEV fusion protein was generated by PCR using the oligonucleotides DD478 and DD482 on pUMa2624 as template. A 1688 bp fragment, containing the sequence for a Cts1-HA-His fusion protein was generated by PCR using the oligonucleotides DD483 and DD484 on pUMa2624 as template. Both fragments were ligated together using the endonuclease *Bsa*I. The resulting molecule was cloned into the pUMa2240 expression vector backbone, using the endonucleases *Apal* and *Nco*I. The plasmid contains the DNA sequence for an One-STrEP-tag® (IBA Lifesciences) for purification N-terminally fused to the anti Gfp nanobody, followed by Protein A, a TEV protease cleavage site, the Cts1* protein, a 3xHA-tag and a 10xHis-tag for purification. The construct is under the control of the constitutive *P_{oma}* promoter. Translation termination is mediated by a 3'-*T_{nos}* terminator. For integration via homologous recombination into the *ip*-locus, the plasmid also codes for a carboxin resistance (*ip^R*). The plasmid encodes the β -lactamase enzyme for selection on ampicillin containing media (Amp^R). (Beier, 2015)

pRabX2 *P_{oma}*Strep- α Gfp-NB-ProtA-P-CBP-Cts1-H (pUMa2626)

Vector for the constitutive expression of a Strep- α Gfp-NB-ProtA-HRV 3C-CBP-Cts1-HA fusion protein in *U. maydis*. For pUMa2626 a 865 bp fragment, containing the sequence for a Strep- α Gfp-NB-Protein A-HRV 3C fusion protein was generated by PCR using the oligonucleotides DD478 and DD486 on pUMa2657 as template. A 855 bp fragment, was cloned into the pUMa2624 expression vector backbone, using the endonucleases *Sfi*I and *Nco*I. The plasmid contains the DNA sequence for a One-STrEP-tag® (IBA Lifesciences) for purification N-terminally fused to the anti Gfp nanobody, followed by Protein A, a HRV 3C protease cleavage site, a Calmodulin Binding peptide, the Cts1 protein and a 3xHA-tag. The construct is under the control of the constitutive *P_{oma}* promoter. Translation termination is mediated by a 3'-*T_{nos}* terminator. For integration via homologous recombination into the *ip*-locus, the plasmid also codes for a carboxin resistance (*ip^R*). The plasmid encodes the β -lactamase enzyme for selection on ampicillin containing media (Amp^R). (Beier, 2015)

pRabX2 *P_{oma}*Strep- α Gfp-NB-ProtA-P-Cts1-H-His (pUMa2627)

Vector for the constitutive expression of a Strep- α Gfp-NB-ProtA-HRV 3C-CBP-Cts1-HA-His fusion protein in *U. maydis*. For pUMa2627 a 865 bp fragment, containing the sequence for a Strep- α Gfp-NB-Protein A-HRV 3C fusion protein was generated by PCR using the oligonucleotides DD478 and DD486 on pUMa2658 as template. A 855 bp fragment, was cloned into the pUMa2625 expression vector backbone, using the endonucleases *Sfi*I and *Nco*I. The plasmid contains the DNA sequence for a One-STrEP-tag® (IBA Lifesciences) for purification N-terminally fused to the anti Gfp nanobody, followed by Protein A, a HRV 3C protease cleavage site, the Cts1 protein, a 3xHA-tag and a 10xHis-tag for purification. The construct is under the control of the constitutive *P_{oma}* promoter. Translation termination is mediated by a 3'-*T_{nos}* terminator. For integration via homologous recombination into the *ip*-locus, the plasmid also codes for a carboxin resistance (*ip^R*). The plasmid encodes the β -lactamase enzyme for selection on ampicillin containing media (Amp^R). (Beier, 2015)

pIDTSMART-AMP : inverseTT_idtopt (pUMa2628)

Cloning vector containing the sequence for a chemically synthesized, codon optimized Protein A-TEV-Calmodulin Binding Peptide fusion construct. The plasmid encodes the β -lactamase enzyme for selection on ampicillin containing media (Amp^R). (Beier, 2015)

pRabX2 P_{oma}Strep- α Gfp-NB-ProtA-T-CBP-Cts1-H (pUMa2657)

Vector for the constitutive expression of a Strep- α Gfp-NB-ProtA-TEV-CBP-Cts1-HA fusion protein in *U. maydis*. For pUMa2657 a 1790 bp fragment, containing the sequence for a Cts1-HA fusion protein was generated by PCR using the oligonucleotides DD136 and DD481 on pUMa2240 as template. A 446 bp fragment was cloned into the pUMa2624 expression vector backbone, using the endonucleases *Apal* and *BstBI*. The plasmid contains the DNA sequence for an One-STrEP-tag® (IBA Lifesciences) for purification N-terminally fused to the anti Gfp nanobody, followed by Protein A, a TEV protease cleavage site, a Calmodulin Binding Peptide, the Cts1 protein and a 3xHA-tag. The construct is under the control of the constitutive P_{oma} promoter. Translation termination is mediated by a 3'-T_{nos} terminator. For integration via homologous recombination into the *ip*-locus, the plasmid also codes for a carboxin resistance (*ip*^R). The plasmid encodes the β -lactamase enzyme for selection on ampicillin containing media (Amp^R). (Beier, 2015)

pRabX2 P_{oma}Strep- α Gfp-NB-ProtA-T-Cts1-H-His (pUMa2658)

Vector for the constitutive expression of a Strep- α Gfp-NB-ProtA-TEV-CBP-Cts1-HA-His fusion protein in *U. maydis*. For pUMa2658 a 1807 bp fragment, containing the sequence for a Cts1-HA fusion protein was generated by PCR using the oligonucleotides DD136 and DD484 on pUMa2657 as template. A 476 bp fragment was cloned into the pUMa2625 expression vector backbone, using the endonucleases *Apal* and *BstBI*. The plasmid contains the DNA sequence for a One-STrEP-tag® (IBA Lifesciences) for purification N-terminally fused to the anti Gfp nanobody, followed by Protein A, a TEV protease cleavage site, the Cts1 protein, a 3xHA-tag and a 10xHis-tag for purification. The construct is under the control of the constitutive P_{oma} promoter. Translation termination is mediated by a 3'-T_{nos} terminator. For integration via homologous recombination into the *ip*-locus, the plasmid also codes for a carboxin resistance (*ip*^R). The plasmid encodes the β -lactamase enzyme for selection on ampicillin containing media (Amp^R). (Beier, 2015)

pUCIDT_UmciA-H7 (pUMa2858)

Cloning vector containing a chemically synthesized, codon optimized ciA-H7 nanobody (α BoNTA; directed against botulinum toxin A) sequence. The plasmid encodes the β -lactamase enzyme for selection on ampicillin containing media (Amp^R). (this study)

pRabX2 P_{otef}His-UmRH5*-PH-Cts1-UmAviTag (pUMa2859)

Vector for the constitutive expression of a His-UmRH5*-HRV 3C-HA-Cts1-UmAviTag fusion protein in *U. maydis*. For pUMa2859 a 1265 bp fragment, containing the sequence for an AviTag™ (Avidity) protein was generated by PCR using the oligonucleotides RL882 and MB38 on pUMa2442 as template. A 447 bp fragment was cloned into the pUMa2442 expression vector backbone, using the restriction endonucleases *Apal* and *BstBI*. The plasmid contains the DNA sequence for a 10xHis-tag for purification N-terminally fused to UmRH5*, followed by a HRV 3C protease cleavage site, a 3xHA-tag, the Cts1 protein and a AviTag™ (Avidity) for biotinylation. The construct is under the control of the constitutive P_{otef} promoter. Translation termination is mediated by a 3'-T_{nos} terminator. For integration via homologous recombination into the *ip*-locus, the plasmid also codes for a carboxin resistance (*ip*^R). The plasmid encodes the β -lactamase enzyme for selection on ampicillin containing media (Amp^R). (this study)

pRabX2 P_{oma}His-αBoNTA-NB-TH-Cts1 (pUMa2863)

Vector for the constitutive expression of a His-αBoNTA-NB-TEV-HA-Cts1 fusion protein in *U. maydis*. For pUMa2863 a 371 bp fragment, containing the sequence for a His-UmciA-H7 NB (αBoNTA) fusion protein from pUMa2858 was cloned into the pUMa2240 expression vector backbone, using the restriction endonucleases *NcoI* and *SpeI*. The plasmid contains the DNA sequence for a 10xHis-tag for purification N-terminally fused to αBoNTA-NB, followed by a TEV protease cleavage site, a 3xHA-tag and the Cts1 protein. The construct is under the control of the constitutive P_{oma} promoter. Translation termination is mediated by a 3'-*T_{nos}* terminator. For integration via homologous recombination into the *ip*-locus, the plasmid also codes for a carboxin resistance (*ip^R*). The plasmid encodes the β-lactamase enzyme for selection on ampicillin containing media (Amp^R). (this study)

pRabX2 P_{otef}UmAviTag-UmRH5*-PH-Cts1-His (pUMa2967)

Vector for the constitutive expression of a UmAviTag-UmRH5*-HRV 3C-HA-Cts1-His fusion protein in *U. maydis*. For pUMa2967 a 1749 bp fragment, containing the sequence for an AviTag™-UmRH5* fusion protein was generated by PCR using the oligonucleotides MB273 and RL964 on pUMa2441 as template. A 1590 bp fragment was cloned into the pUMa2441 expression vector backbone, using the restriction endonucleases *SpeI* and *XmaI*. The plasmid contains the DNA sequence for a AviTag™ (Avidity) for biotinylation N-terminally fused to UmRH5*, followed by a HRV 3C protease cleavage site, a 3xHA-tag, the Cts1 protein and a 10x tag for purification. The construct is under the control of the constitutive P_{otef} promoter. Translation termination is mediated by a 3'-*T_{nos}* terminator. For integration via homologous recombination into the *ip*-locus, the plasmid also codes for a carboxin resistance (*ip^R*). The plasmid encodes the β-lactamase enzyme for selection on ampicillin containing media (Amp^R). (this study)

pRabX2 P_{otef}Um-ΔN UmRH5*-PH-Cts1-His (pUMa2968)

Vector for the constitutive expression of a AviTag™-ΔN UmRH5*-HRV 3C-HA-Cts1-His fusion protein in *U. maydis*. For pUMa2968 a 1344 bp fragment, containing the sequence for an AviTag™-ΔN UmRH5* fusion protein was generated by PCR using the oligonucleotides MB274 and RL964 on pUMa2441 as template. A 1185 bp fragment was cloned into the pUMa2441 expression vector backbone, using the restriction endonucleases *SpeI* and *XmaI*. The plasmid contains the DNA sequence for a AviTag™ (Avidity) for biotinylation N-terminally fused to a N-terminally truncated UmRH5*, followed by a HRV 3C protease cleavage site, a 3xHA-tag, the Cts1 protein and a 10xHis-tag for purification. The construct is under the control of the constitutive P_{otef} promoter. Translation termination is mediated by a 3'-*T_{nos}* terminator. For integration via homologous recombination into the *ip*-locus, the plasmid also codes for a carboxin resistance (*ip^R*). The plasmid encodes the β-lactamase enzyme for selection on ampicillin containing media (Amp^R). (this study)

pRabX2 P_{oma}His-HRP-αGfp-NB-PH-Cts1 (pUMa2976)

Vector for the constitutive expression of a His-HRP-αGfp-NB-HRV 3C-HA-Cts1 fusion protein in *U. maydis*. For pUMa2976 a 1153 bp fragment, containing the sequence for a His-UmHRP fusion protein was generated by PCR using the oligonucleotides RL1347 and MB293 on pUMa2553 as template. A 983 bp fragment (*NcoI* and *XmaI* cut) was used for cloning. A 3058 bp fragment, containing the sequence for a αGfp-NB-HRV 3C-HA-Cts1 fusion protein was generated by PCR using the oligonucleotides RL1573 and MB294 on pUMa2480 as template. A 2916 bp fragment (*EcoRI* and *XmaI* cut) was used for cloning. Both PCR generated fragments were cloned into the pUMa2480 expression vector backbone, using the restriction endonucleases *EcoRI* and *NcoI*. The plasmid contains the DNA sequence for a 10xHis-tag for purification N-terminally fused to UmHRP, followed by αGfp-NB, a HRV 3C protease cleavage site, a 3xHA-tag and the Cts1 protein. The construct is under the control of the constitutive P_{otef} promoter. Translation termination is mediated by a 3'-*T_{nos}* terminator. For integration via homologous recombination into the *ip*-locus, the plasmid also codes for a carboxin resistance (*ip^R*). The plasmid encodes the β-lactamase enzyme for selection on ampicillin containing media (Amp^R). (this study)

pRabX2 *P_{otef}*UmRH5-TH-Cts1-His (pUMa2995)

Vector for the constitutive expression of a UmRH5-TEV-HA-Cts1-His fusion protein in *U. maydis*. For pUMa2995 a 1536 bp fragment, containing the sequence for a UmRH5 protein from pUMa1738 was cloned into the pUMa2105 expression vector backbone, using the restriction endonucleases *SpeI* and *XmaI*. The plasmid contains the DNA sequence for UmRH5 N-terminally fused to a TEV protease cleavage site, followed by a 3xHA-tag, the Cts1 protein and a 10xHis-tag for purification. The construct is under the control of the constitutive *P_{otef}* promoter. Translation termination is mediated by a 3'-*T_{nos}* terminator. For integration via homologous recombination into the *ip*-locus, the plasmid also codes for a carboxin resistance (*ip^R*). The plasmid encodes the β -lactamase enzyme for selection on ampicillin containing media (Amp^R). (this study)

pRabX2 *P_{otef}*UmRH5-TH-Cts1-Strep (pUMa2996)

Vector for the constitutive expression of a UmRH5-TEV-HA-Cts1-Strep fusion protein in *U. maydis*. For pUMa2996 a 1536 bp fragment, containing the sequence for a UmRH5 protein from pUMa1738 was cloned into the pUMa2106 expression vector backbone, using the restriction endonucleases *SpeI* and *XmaI*. The plasmid contains the DNA sequence for UmRH5 N-terminally fused to a TEV protease cleavage site, followed by a 3xHA-tag, the Cts1 protein and a One-STREP-tag® (IBA Lifesciences) for purification. The construct is under the control of the constitutive *P_{otef}* promoter. Translation termination is mediated by a 3'-*T_{nos}* terminator. For integration via homologous recombination into the *ip*-locus, the plasmid also codes for a carboxin resistance (*ip^R*). The plasmid encodes the β -lactamase enzyme for selection on ampicillin containing media (Amp^R). (this study)

pRabX2 *P_{otef}*His-UmRH5-TH-Cts1(pUMa2997)

Vector for the constitutive expression of a His-UmRH5-TEV-HA-Cts1 fusion protein in *U. maydis*. For pUMa2997 a 1883 bp fragment, containing the sequence for an His-UmRH5 fusion protein was generated by PCR using the oligonucleotides RL1431 and SL937 on pUMa1738 as template. A 1553 bp fragment was cloned into the pUMa2310 expression vector backbone, using the restriction endonucleases *SpeI* and *NcoI*. The plasmid contains the DNA sequence for a 10xHis-tag for purification N-terminally fused to UmRH5, followed by a TEV protease cleavage site, a 3xHA-tag and the Cts1 protein. The construct is under the control of the constitutive *P_{otef}* promoter. Translation termination is mediated by a 3'-*T_{nos}* terminator. For integration via homologous recombination into the *ip*-locus, the plasmid also codes for a carboxin resistance (*ip^R*). The plasmid encodes the β -lactamase enzyme for selection on ampicillin containing media (Amp^R). (this study)

pRabX2 *P_{otef}*UmAviTag-UmRH5-PH-Cts1-His (pUMa2998)

Vector for the constitutive expression of a UmAviTag-UmRH5-HRV 3C-HA-Cts1-His fusion protein in *U. maydis*. For pUMa2998 a 1920 bp fragment, containing the sequence for an AviTag™-UmRH5 fusion protein was generated by PCR using the oligonucleotides MB273 and SL937 on pUMa1738 as template. A 1590 bp fragment was cloned into the pUMa2967 expression vector backbone, using the restriction endonucleases *SpeI* and *XmaI*. The plasmid contains the DNA sequence for a AviTag™ (Avidity) for biotinylation N-terminally fused to UmRH5, followed by a HRV 3C protease cleavage site, a 3xHA-tag, the Cts1 protein and a 10xHis-tag for purification. The construct is under the control of the constitutive *P_{otef}* promoter. Translation termination is mediated by a 3'-*T_{nos}* terminator. For integration via homologous recombination into the *ip*-locus, the plasmid also codes for a carboxin resistance (*ip^R*). The plasmid encodes the β -lactamase enzyme for selection on ampicillin containing media (Amp^R). (this study)

pRabX2 *P_{otef}*UmAviTag-ΔN UmRH5-PH-Cts1-His (pUMa2999)

Vector for the constitutive expression of a UmAviTag-ΔN UmRH5-HRV 3C-HA-Cts1-His fusion protein in *U. maydis*. For pUMa2999 a 1515 bp fragment, containing the sequence for an AviTag™-ΔN UmRH5 fusion protein was generated by PCR using the oligonucleotides MB274 and SL937 on pUMa1738 as template. A 1185 bp fragment was cloned into the pUMa2968 expression vector backbone, using the restriction endonucleases *SpeI* and *XmaI*.

The plasmid contains the DNA sequence for a AviTag™ (Avidity) for biotinylation N-terminally fused to a N-terminally truncated UmRH5, followed by a HRV 3C protease cleavage site, a 3xHA-tag, the Cts1 protein and a 10xHis-tag for purification. The construct is under the control of the constitutive P_{otef} promoter. Translation termination is mediated by a 3'- T_{nos} terminator. For integration via homologous recombination into the *ip*-locus, the plasmid also codes for a carboxin resistance (*ip^R*). The plasmid encodes the β -lactamase enzyme for selection on ampicillin containing media (Amp^R). (this study)

pRabX2 P_{otef} His-UmRH5-PH-Cts1-UmAviTag (pUMa3000)

Vector for the constitutive expression of a His-UmRH5-HRV 3C-HA-Cts1-UmAviTag fusion protein in *U. maydis*. For pUMa3000 a 1883 bp fragment, containing the sequence for an UmRH5 protein was generated by PCR using the oligonucleotides RL1431 and SL937 on pUMa1738 as template. A 1553 bp fragment was cloned into the pUMa2859 expression vector backbone, using the restriction endonucleases *NcoI* and *SpeI*. The plasmid contains the DNA sequence for a 10xHis-tag for purification N-terminally fused to UmRH5, followed by a HRV 3C protease cleavage site, a 3xHA-tag, the Cts1 protein and a AviTag™ (Avidity) tag for biotinylation. The construct is under the control of the constitutive P_{otef} promoter. Translation termination is mediated by a 3'- T_{nos} terminator. For integration via homologous recombination into the *ip*-locus, the plasmid also codes for a carboxin resistance (*ip^R*). The plasmid encodes the β -lactamase enzyme for selection on ampicillin containing media (Amp^R). (this study)

4.1.5 Strains

Tab. 4.8: Strains used in this study

Strain name	UMa	Reference	Relevant genotype	Resistance	Integrated plasmid (pUMa)	Locus	Progenitor
<i>Escherichia coli</i>							
Top10	1027	Invitrogen	<i>F- mcrA Δ(mrr-hsdRMS-mcrBC) φ80lacZΔM15 ΔlacX74 nupG recA1 araD139 Δ(ara-leu)7697 galE15 galK16 rpsL(StrR) endA1 λ-</i>	Streptomycin		-	K-12
Rosetta2 (DE3) pLysS:His-TEV	-	This study	<i>F- ompT hsdSB (rB-mB-) gal dcm pLysSRARE2 (CamR) pHis-TEV (AmpR)</i>	Amp, Cam	1316	-	Rosetta2 (DE3) pLysS
Rosetta2 (DE3) pLysS:Gus-SHH	-	(Stock et al., 2012)	<i>F- ompT hsdSB (rB-mB-) gal dcm pLysSRARE2 (CamR) pGus-SHH (AmpR)</i>	Amp, Cam	1671	-	Rosetta2 (DE3) pLysS
Rosetta2 (DE3) pLysS:10xHis-Gfp	-	(Sarkari, 2014)	<i>F- ompT hsdSB (rB-mB-) gal dcm pLysSRARE2 (CamR) pHis-Gfp (AmpR)</i>	Amp, Cam	2156	-	Rosetta2 (DE3) pLysS
<i>Ustilago maydis</i>							
SG200	67	(Kämper et al., 2006)	<i>a1:mfa2, bE1, bW2</i>	Phleo	-	<i>a</i>	FB1
AB33	133	(Brachmann, 2001)	<i>a2, P_{nar}bE1, P_{nar}bW2</i>	Phleo	-	<i>b</i>	FB2
SG200_ P_{otef} -3xe Gfp	587	(Kämper et al., 2006)	<i>ip^r [P_{otef}egfp:egfp:egfp] ip^s</i>	Cbx		<i>ip</i>	SG200
AB33_ P_{oma} -Gus-Cts1	1289	(Stock et al., 2012)	<i>ip^r [P_{omagus}:strep:ha:his:c ts1:ubi1 3'UTR] ip^s</i>	Phleo	2113	<i>ip</i>	AB33

AB33kex2Δ_P _{otef} _UmRH5*-TEV-HA-Cts1-His	1297	(Terfrüchte, 2013)	<i>FRTwt[um02843Δ::hyg]FRTwt ip^r [P_{otef}rh5*:tev:ha:cts1:his:ubi1 3'UTR] ip^s</i>	Phleo, Cbx, Hyg	2105	<i>ip</i>	UMa803
AB33kex2Δ_P _{otef} _UmRH5*-TEV-HA-Cts1-Strep	1298	(Terfrüchte, 2013)	<i>FRTwt[um02843Δ::hyg]FRTwt ip^r [P_{otef}rh5*:tev:ha:cts1:strep:ubi1 3'UTR] ip^s</i>	Phleo, Cbx, Hyg	2106	<i>ip</i>	UMa803
AB33kex2Δ_P _{otef} _Strep-UmRH5*-TEV-HA-Cts1	1299	(Terfrüchte, 2013)	<i>FRTwt[um02843Δ::hyg]FRTwt ip^r [P_{otef}strep:rh5*:tev:ha:cts1:ubi1 3'UTR] ip^s</i>	Phleo, Cbx, Hyg	2124	<i>ip</i>	UMa803
AB33kex2Δ_P _{oma} _Gus-Cts1	1339	(Reindl, 2013)	<i>FRTwt[um02843Δ::hyg]FRTwt ip^r [P_{oma}gus:strep:ha:his:cts1:ubi1 3'UTR] ip^s</i>	Phleo, Cbx, Hyg	2113	<i>ip</i>	UMa803
AB33_P _{oma} _αGfp-NB-Cts1	1396	(Sarkari, 2014)	<i>ip^r [P_{oma}his:agpf:tev:ha:cts1:ubi1 3'UTR] ip^s</i>	Phleo, Cbx	2240	<i>ip</i>	AB33
AB33kex2Δ_P _{oma} _αGfp-NB-Cts1	1397	(Sarkari, 2014)	<i>FRTwt[um02843Δ::hyg]FRTwt ip^r [P_{oma}his:agpf:tev:ha:cts1:ubi1 3'UTR] ip^s</i>	Phleo, Cbx, Hyg	2240	<i>ip</i>	UMa803
AB33kex2Δ_P _{oma} _αGfp-NB-Prot A-TEV-CBP-Cts1*-HA	1662	(Beier, 2015)	<i>FRTwt[um02843Δ::hyg]FRTwt ip^r [P_{oma}strep:agpf:protein a:tev:cbp:cts1*:ha:ubi1 3'UTR] ip^s</i>	Phleo, Cbx, Hyg	2624	<i>ip</i>	UMa803
AB33kex2Δ_P _{oma} _αGfp-NB-Prot A-TEV-CBP-Cts1*-HA-His	1664	(Beier, 2015)	<i>FRTwt[um02843Δ::hyg]FRTwt ip^r [P_{oma}strep:agpf:protein a:tev:cts1*:ha:his:ubi1 3'UTR] ip^s</i>	Phleo, Cbx, Hyg	2625	<i>ip</i>	UMa803
AB33kex2Δ_P _{oma} _αGfp-NB-Prot A-HRV 3C-CBP-Cts1-HA	1713	(Beier, 2015)	<i>FRTwt[um02843Δ::hyg]FRTwt ip^r [P_{oma}strep:agpf:protein a:hrv3c:cbp:cts1:ha:ubi1 3'UTR] ip^s</i>	Phleo, Cbx, Hyg	2626	<i>ip</i>	UMa803
AB33kex2Δ_P _{oma} _αGfp-NB-Prot A-HRV 3C-CBP-Cts1-HA-His	1715	(Beier, 2015)	<i>FRTwt[um02843Δ::hyg]FRTwt ip^r [P_{oma}strep:agpf:protein a:hrv3c:cts1:ha:his:ubi1 3'UTR] ip^s</i>	Phleo, Cbx, Hyg	2627	<i>ip</i>	UMa803

Tab. 4.9: Strains generated in this study

Strain name	UMA	Reference	Relevant genotype	Resistance	Integrated plasmid (pUMA)	Locus	Progenitor
<i>Ustilago maydis</i>							
AB33P5Δ_P _{oma} _Gus-Cts1	1261	This study	<i>FRT5[um04400 Δ::hyg]FRT5 FRT3[um11908Δ] FRT2[um00064 Δ] FRTwt[um02178Δ] FRT1[um04926Δ] ip^r [P_{oma}gus:strep:ha:his:cts1:ubi1 3'UTR] ip^s</i>	Phleo, Cbx	2113	<i>ip</i>	UMa1391
AB33_P _{otef} _Strep-UmRH5*-TEV-HA-Cts1	1322	This study	<i>ip^r [P_{otef}strep:rh5*:tev:ha:cts1:ubi1 3'UTR] ip^s</i>	Phleo	2148	<i>ip</i>	AB33

AB33kex2Δ_P _{oma} __Strep- UmRH5*-TEV- HA-Cts1	1337	This study	<i>FRTwt[um02843Δ::hyg] FRTwt ip^r [P_{oma}strep:rh5*:tev:ha:ct s1:ubi1 3'UTR] ip^s</i>	Phleo, Cbx, Hyg	2150	<i>ip</i>	UMa803
AB33P5Δ_P _{otef} _H is-UmRH5*-TEV- HA-Cts1	1460	This study	<i>FRT5[um04400 Δ::hyg]FRT5 FRT3[um11908Δ] FRT2[um00064 Δ] FRTwt[um02178Δ] FRT1[um04926Δ] ip^r [P_{otef}his:rh5*:tev:ha:cts1: ubi1 3'UTR] ip^s</i>	Phleo, Cbx	2310	<i>ip</i>	UMa1391
AB33P5Δ_P _{otef} _S trep-UmRH5*- TEV-HA-Cts1	1461	This study	<i>FRT5[um04400 Δ::hyg]FRT5 FRT3[um11908Δ] FRT2[um00064 Δ] FRTwt[um02178Δ] FRT1[um04926Δ] ip^r [P_{otef}strep:rh5*:tev:ha:cts 1:ubi1 3'UTR] ip^s</i>	Phleo, Cbx	2148	<i>ip</i>	UMa1391
AB33P5Δ_P _{oma} _α Gfp-NB-Cts1	1465	This study	<i>FRT5[um04400 Δ::hyg]FRT5 FRT3[um11908Δ] FRT2[um00064 Δ] FRTwt[um02178Δ] FRT1[um04926Δ] ip^r [P_{oma}his:agpf:tev:ha:cts1 :ubi1 3'UTR] ip^s</i>	Phleo, Cbx	2240	<i>ip</i>	UMa1391
AB33P5Δ_P _{otef} _U mRH5*-TEV-HA- Cts1-His	1466	This study	<i>FRT5[um04400 Δ::hyg]FRT5 FRT3[um11908Δ] FRT2[um00064 Δ] FRTwt[um02178Δ] FRT1[um04926Δ] ip^r [P_{otef}rh5*:tev:ha:cts1:his: ubi1 3'UTR] ip^s</i>	Phleo, Cbx	2105	<i>ip</i>	UMa1391
AB33kex2Δ_P _{otef} _His- UmRH5*-HRV 3C-HA- Cts1-Avi	1868	This study	<i>FRTwt[um02843Δ::hyg] FRTwt ip^r [P_{oma}his:rh5*:hrv3c:ha:ct s1:avi:ubi1 3'UTR] ip^s</i>	Phleo, Cbx, Hyg	2859	<i>ip</i>	UMa803
AB33P5Δ- _P _{otef} _His- UmRH5*-HRV 3C-HA-Cts1-Avi	1869	This study	<i>FRT5[um04400Δ]FRT5 FRT3[um11908Δ] FRT2[um00064Δ] FRTwt[um02178Δ] FRT1[um04926Δ] [P_{otef}his:rh5*:hrv3c:ha:ct s1:avi:ubi1 3'UTR] ip^s</i>	Phleo, Cbx	2859	<i>ip</i>	UMa1391
AB33kex2Δ_P _{oma} _αBoNTA-NB- Cts1	1870	This study	<i>FRTwt[um02843Δ::hyg] FRTwt ip^r [P_{oma}his:abonta:tev:ha:ct s1:ubi1 3'UTR] ip^s</i>	Phleo, Cbx, Hyg	2863	<i>ip</i>	UMa803
AB33P5Δ_P _{oma} _α BoNTA-NB-Cts1	1871	This study	<i>FRT5[um04400 Δ::hyg]FRT5 FRT3[um11908Δ] FRT2[um00064 Δ] FRTwt[um02178Δ] FRT1[um04926Δ] ip^r [P_{oma}his:abonta:tev:ha:ct s1:ubi1 3'UTR] ip^s</i>	Phleo, Cbx	2863	<i>ip</i>	UMa1391

AB33P5Δ _{P_{otef}} _A vi-RH5*-HRV 3C- HA-Cts1-His	1973	This study	<i>FRT5[um04400Δ]FRT5 FRT3[um11908Δ] FRT2[um00064Δ] FRTwt[um02178Δ] FRT1[um04926Δ] [P_{otef}avi:rh5*:hrv3c:ha:ct s1:his:ubi1 3'UTR] ip^s</i>	Phleo, Cbx	2967	<i>ip</i>	UMa1391
AB33P5Δ _{P_{otef}} _A vi-ΔN UmRH5*- HRV 3C-HA- Cts1-His	1975	This study	<i>FRT5[um04400Δ]FRT5 FRT3[um11908Δ] FRT2[um00064Δ] FRTwt[um02178Δ] FRT1[um04926Δ] [P_{otef}avi:Δnrh5*:hrv3c:ha: cts1:his:ubi1 3'UTR] ip^s</i>	Phleo, Cbx	2968	<i>ip</i>	UMa1391
AB33kex2Δ _{P_{otef}} _A UmRH5-TEV-HA- Cts1-His	1995	This study	<i>FRT5[um04400 Δ::hyg]FRT5 FRT3[um11908Δ] FRT2[um00064 Δ] FRTwt[um02178Δ] FRT1[um04926Δ] ip^r [P_{otef}rh5:tev:ha:cts1:his:u bi1 3'UTR] ip^s</i>	Phleo, Cbx, Hyg	2995	<i>ip</i>	UMa803
AB33kex2Δ _{P_{otef}} _A UmRH5-TEV-HA- Cts1-Strep	1996	This study	<i>FRTwt[um02843Δ::hyg] FRTwt ip^r [P_{otef}rh5:tev:ha:cts1:stre p:ubi1 3'UTR] ip^s</i>	Phleo, Cbx, Hyg	2996	<i>ip</i>	UMa803
AB33P5Δ _{P_{otef}} _H is-UmRH5-TEV- HA-Cts1	1997	This study	<i>FRT5[um04400 Δ::hyg]FRT5 FRT3[um11908Δ] FRT2[um00064 Δ] FRTwt[um02178Δ] FRT1[um04926Δ] ip^r [P_{otef}his:rh5:tev:ha:cts1:u bi1 3'UTR] ip^s</i>	Phleo, Cbx	2997	<i>ip</i>	UMa1391
AB33P5Δ _{P_{otef}} _A vi-UmRH5-HRV 3C-HA-Cts1-His	1998	This study	<i>FRT5[um04400Δ]FRT5 FRT3[um11908Δ] FRT2[um00064Δ] FRTwt[um02178Δ] FRT1[um04926Δ] [P_{otef}avi:rh5:hrv3c:ha:cts 1:his:ubi1 3'UTR] ip^s</i>	Phleo, Cbx	2998	<i>ip</i>	UMa1391
AB33P5Δ _{P_{otef}} _A vi-ΔN UmRH5- HRV 3C-HA- Cts1-His	1999	This study	<i>FRT5[um04400Δ]FRT5 FRT3[um11908Δ] FRT2[um00064Δ] FRTwt[um02178Δ] FRT1[um04926Δ] [P_{otef}avi:Δnrh5:hrv3c:ha: cts1:his:ubi1 3'UTR] ip^s</i>	Phleo, Cbx	2999	<i>ip</i>	UMa1391
AB33P5Δ _{P_{otef}} _H is-UmRH5-HRV 3C-HA-Cts1-Avi	2000	This study	<i>FRT5[um04400Δ]FRT5 FRT3[um11908Δ] FRT2[um00064Δ] FRTwt[um02178Δ] FRT1[um04926Δ] [P_{otef}his:rh5:hrv3c:ha:cts 1:avi:ubi1 3'UTR] ip^s</i>	Phleo, Cbx	3000	<i>ip</i>	UMa1391
AB33P5Δ _{P_{oma}} _H RP-αGfp-NB-Cts1	2023	This study	<i>FRT5[um04400 Δ::hyg]FRT5 FRT3[um11908Δ] FRT2[um00064 Δ] FRTwt[um02178Δ] FRT1[um04926Δ] ip^r [P_{oma}his:hrp:agfp:tev:ha: cts1:ubi1 3'UTR] ip^s</i>	Phleo, Cbx	2976	<i>ip</i>	UMa1391

4.2 Methods

4.2.1 Molecular biology methods

Standard techniques including purification, precipitation, restriction and electrophoretic separation of nucleic acids were performed according to protocols published in Ausubel et al., 1987 and Sambrook et al., 1989. Kits were used as stated in the enclosed manuals.

4.2.1.1 Determination of nucleic acid concentration

Nucleic acid concentrations were measured photometrical with the NanoDrop 2000c spectral photometer (Thermo Fisher Scientific). An $OD_{260} = 1$ refers to a concentration of 50 $\mu\text{g/ml}$ double stranded DNA at 1 cm layer thickness. Purity was determined by calculating the A_{260}/A_{280} quotient with an optimum of 1.8.

4.2.1.2 Isolation and purification of nucleic acids

Isolation of plasmid DNA from *E. coli*

Isolation of plasmid DNA from *E. coli* cells was performed using the boiling lysis according to Sambrook et al., 1989. 2 mL of an overnight *E. coli* culture was pelleted (13000 rpm, 2 min), the pellet was resuspended in 200 μL STET and 20 μL Lysozyme. After boiling the solution for 1 min on 95°C, denatured proteins and genomic DNA were pelleted (13000 rpm, 10 min) and the resulting pellet was discarded. Plasmid DNA was then precipitated by adding 20 μL 3 M Na^{2+} -acetate (pH 4.8) and 500 μL isopropanol. After 10 min centrifugation (13000 rpm) the pelleted plasmid DNA was washed with 200 μL 70% ethanol, dried and resuspended in 100 μL TE/RNase.

STET:

10 mM Tris-HCl (pH 8.0)
1 mM $\text{Na}_2\text{-EDTA}$
100 mM NaCl
5% (v/v) Triton X-100
in $\text{H}_2\text{O}_{\text{bid}}$.

Lysozyme:

10 mg/ml Lysozyme
in 1xTE-buffer

TE/RNase:

20 $\mu\text{g/ml}$ RNase A
in 1x TE-buffer

Isolation of genomic DNA from *U. maydis*

Genomic DNA was isolated from *U. maydis* cultures according to modified protocols published in Bösch et al., 2016 and Hoffman and Winston, 1987. 2 mL of a dense 24 h *U. maydis* culture, grown in CM-glc medium, were pelleted (13000 rpm, 2 min). Approximately 200 μL glass beads, 500 μL *Ustilago* lysis-buffer and 500 μL phenol/chloroform were added before shaking on 1000 rpm for 8 min on a Vibrax® shaker (Ika). Phase separation was ensured by centrifugation (13000 rpm, 15 min). 400 μL of the aqueous supernatant was supplemented with 1 mL ethanol, resulting in precipitation of the genomic DNA. After pelleting the DNA

(13000, 5 min) and washing with 200 µL 70% ethanol (13000 rpm, 2 min), it was resuspended in 50 µL TE-RNase.

***Ustilago* lysis-buffer:**

50 mM Tris-HCl (pH 7.5)
50 mM Na₂-EDTA
1% (w/v) SDS
in H₂O_{bid.}

phenol/chloroform:

50% (v/v) Roti®-phenol (TE- buffer equilibrated)
50% (v/v) chloroform

4.2.1.3 Amplification of DNA (PCR)

Polymerase chain reaction (PCR) was used to amplify DNA-fragments (Saiki et al., 1985). Depending on size and application, polymerases and PCR programs were modified. Reactions were performed in a PTC-200 Peltier Thermal Cycler (MJ Research) or a SensoQuest Labcycler (SensoQuest). A standard PCR reaction is depicted below.

Standard Phusion-HF PCR reaction:

50 ng DNA (template)
200 µM dNTPs
1 µM oligonucleotide 1 (forward)
1 µM oligonucleotide 2 (reverse)
5x Phusion-HF buffer (Finnzymes)
1 U Phusion-HF DNA polymerase

4.2.1.4 PCR mutagenesis

In order to exchange single bases in DNA-fragments, PCR mutagenesis was performed according to the protocol of the QuikChange II Site-Directed Mutagenesis Kit (Agilent Technologies).

4.2.1.5 Sequencing of plasmid DNA

For sequencing the DNA was purified using a JETQUICK DNA Purification Kit (Genomed).

Sequencing at Genomics Service Unit (Ludwig-Maximilians-University Munich)

250 ng purified plasmid DNA and 2 pmol of the respective sequencing oligonucleotide were mixed and sent to the sequencing facility. There the automated sequencing reaction was performed with a BigDye® Terminator v3.1 Cycle Sequencing Kit (Thermo Fisher Scientific). The subsequent analysis of the raw data was performed using Clone Manager 9 software.

Overnight sequencing at Eurofins Genomics (Ebersberg)

1 µg purified plasmid DNA and 20 pmol of the respective sequencing oligonucleotide were mixed and sent to the sequencing facility. The subsequent analysis of the raw data was performed using Clone Manager 9 software.

4.2.1.6 Southern blot

Transfer of DNA

The transfer of DNA fragments from agarose gels onto nylon membranes was performed according to modified protocols published in Southern, 1975.

After hydrolysis of isolated gDNA from *U. maydis* with a respective endonuclease, the fragmented gDNA was separated via gel electrophoreses on a 0.8% (w/v) agarose gel. The gel was then washed for 20 min in 0.25 M HCl, DENAT-solution and RENAT-solution. Separated DNA was then transferred to a nylon membrane (Hybond-N⁺-Nylon-Membrane, GE Healthcare) using capillary force. Here the transfer is mediated by the transfer buffer (20x SSPE) running through a Whatman filter paper salt-bridge. On top of the salt-bridge the agarose gel, nylon membrane and Whatman filter paper is stacked. The flowing transfer buffer pulls the DNA from the agarose gel onto the nylon membrane and the DNA is crosslinked after blotting using 120 mJ UV-irradiation. The blot was performed for 4 h or overnight.

0.25 M HCl:

3.26 % (v/v) HCl (25%)
in H₂O_{bid.}

DENAT:

87.6 g NaCl
16 g NaOH
in 1L H₂O_{bid.}

RENAT:

87.6 g NaCl
44.4 g Tris-HCl
26.5 g Tris
in 1L H₂O_{bid.}

20x SSPE:

175.3 g NaCl
31.2 g NaH₂PO₄*H₂O
7.4 g Na₂-EDTA*2H₂O
in 1L H₂O_{bid.}, pH 7.4

Detection of immobilized DNA (DIG labeling method)

Fixed DNA on nylon membranes was detected using probes generated with the PCR DIG Labeling Mix (Roche). The probes were denatured in hybridization buffer for 10 min on 98°C. The membrane was pre-hybridized in hybridization buffer for 30 min on 65°C in a hybridization oven and subsequently incubated over night with the denatured probe. After hybridization the membrane was washed for each 15 min in Southern-wash I, Southern-wash II and Southern-wash III at 65°C. All following steps were performed on room temperature in a hybridization tube. First the membrane was washed for 5 min in DIG-wash and then blocked with DIG-2 solution for 30 min. Then the membrane was incubated with anti-DIG antibody solution and

afterwards washed twice in DIG-wash for 15 min. The membrane was then equilibrated in DIG-3 solution for 5 min and subsequently incubated with 8 mL CDP-Star solution (Roche) solution in a sealed waste-bag. Chemiluminescence was detected using a LAS4000 (Fujifilm).

Hybridization buffer:

260 mL 20x SSPE
50 mL Denhardt solution
50 mL SDS (10% stock solution)
in 1L H₂O_{bid.}

Southern-wash I:

100 mL 20x SSPE
10 mL SDS (10% stock solution)
in 1L H₂O_{bid.}

Southern-wash II:

50 mL 20x SSPE
10 mL SDS (10% stock solution)
in 1L H₂O_{bid.}

Southern-wash III:

5 mL 20x SSPE
10 mL SDS (10% stock solution)
in 1L H₂O_{bid.}

DIG-1:

11.6 g maleic acid
8.77 g NaCl
in 1L H₂O_{bid.}, pH 7.5

DIG-2:

10 g skimmed milk powder
ad 1L DIG-1

DIG-3:

12.1 g Tris-HCl
5.84 g NaCl
in 1L H₂O_{bid.}, pH 9.5

DIG-wash:

997 mL DIG-1
3 mL Tween-20

CDP-Star solution:

8 mL DIG-3
80 µL CDP-Star (Roche)

Denhardt solution:

20 g bovine serum albumin
20 g ficoll
20 g polyvinyl pyrrolidone (PVP-360)
in 1L H₂O_{bid.}

4.2.2 Microbiological methods

4.2.2.1 Microbiological work with *E. coli*

Standard cultivation conditions for *E. coli*

E. coli cells were grown in dYT medium supplemented with the respective antibiotics on 37°C either on a rotary wheel in glass tubes or in shaking flasks with 110 rpm shaking. All cultures were inoculated with single colonies from selective agar plates.

Determination of cell density in *E. coli* cultures

The cell density in liquid cultures was determined photometrical using a Novospec II photometer (Pharmacia Biotech). The OD₆₀₀ (optical density at $\lambda = 600$ nm) was measured using dilutions of the cultures to maintain linearity and the respective culture medium was used as a reference. Linearity is given between OD₆₀₀ = 0.3 and 0.8. An OD₆₀₀ = 1 resembles 1.0 x 10⁹ cells/mL for *E. coli*.

Transformation of *E. coli*

Chemically competent *E. coli* Top10 cells were available in aliquots stored at -80°C. The competence was mediated by a modified treatment with RbCl₂ and CaCl₂ as described in Cohen et al., 1972. 50 µL competent cells were thawed 10 min on 4°C and 1-10 µL plasmid solution was added. The suspension was incubated for 30 min on 4°C, treated with a heat shock (42°C, 45 s) and again incubated on 4°C for 2 min. Supplementation with 200 µL dYT medium and incubation on 37°C (1100 rpm, Vibrax®) for 30 to 60 min ensured regeneration of the cells and expression of the transformed antibiotic resistance marker. Transformed cells were plated on antibiotic containing agar plates and incubated overnight on 37°C.

4.2.2.2 Microbiological work with *U. maydis*

Standard cultivation conditions for *U. maydis*

U. maydis strains were mostly grown on solid or liquid CM-medium, supplemented with a carbon source and in some cases buffer substances (s. 4.1.2.2). Cultivation was performed in glass tubes on a rotary wheel or in baffled as well as non-baffled shaking flasks. Cultivation conditions in baffled flasks were always 28°C and 200 rpm, whereas the shaking speed for cultivation in non-baffled flasks was increased to 300 rpm. If necessary, solid CM-medium was supplemented with 2 µg/mL carboxin for selection. Permanent storage of *U. maydis* strains was ensured by generating cryogenic glycerol stocks. To this end an exponential culture was mixed 1:1 with NSY-glycerol and stored at -80°C. Inoculation was always conducted from fresh strains grown on solid medium without antibiotics.

RAMOS (Respiration Activity Monitoring System) cultivations for *U. maydis*

For cultivations in RAMOS devices (Adolf Kühner AG), various CM-medium compositions were used (s. 4.1.2.2). In parallel to the 250 mL non-baffled shaking flasks used in the RAMOS, a set of additional 250 mL non-baffled shaking flasks was cultivated for offline sampling on an external shaker. To maintain the same starting conditions and OD₆₀₀ in all flasks belonging to a RAMOS flask, a master mix was inoculated from a pre-culture to a starting OD₆₀₀ of 0.08 in the respective medium and 20 mL of the master mix was distributed to the RAMOS and external sampling flasks. One of the external sampling flasks was sacrificed per sampling point and spent for the required analyses. Cultivation was performed at 28°C, 300 rpm and 5 cm shaking diameter. Standardized sampling included 1 mL supernatant samples for TCA precipitations, supernatant samples for HPLC analyses, OD₆₀₀ determination (Genesys 20 photometer, Thermo Fisher Scientific), cell dry weight determination (CDW) in 2 mL tubes and pH measurements directly in the fermentation broth (CyberScan pH 510 pH-meter, Eutech). All cultivations and offline analyses were conducted in technical duplicates.

***U. maydis* fermentation**

Fermentation of *U. maydis* strains was performed in an Infors™ Minifors Benchtop Bioreactor (Infors AG). Technical data of the device are listed in Tab. 4.10.

Tab. 4.10: Technical data Infors™ Minifors Benchtop Bioreactor

Total volume	5.0 L
Working volume	1.4 – 3.5 L
Baffles	3 stainless steel baffles
Impeller	2x Rushton-Impeller (6 blades each)
Rotor	80 W external motor (50 – 1250 rpm)
O ₂ -probe	Hamilton™ Oxyferm FDA (10 ppb – 40 ppm)
pH-probe	Mettler Toledo™ 405-DPAS-SC-K8S/325 (pH 2 – pH 12)
Peristaltic pumps	3.2 cm diameter, 0.14 – 12.5 mL/min
Temperature regulation	PT-100 sensor (5°C – 60°C), active water cooling/heating
Gassing	Air gassing through internal sparger (8 x 0.8 mm holes, 16 - 166 ccm/min)
Antifoam probe	Circuit completion

Fermentation was performed with 3 L CM-medium supplemented with 20 g/L glucose. 2.88 L CM-medium were autoclaved in the fully equipped fermenter and 120 mL sterile filtered 50% (w/v) glucose solution was added under sterile conditions. To maintain a stable pH of 7.0, 2.5 M NaOH and 1 N H₂SO₄ was used. To reduce foaming approximately 100 µL of Antifoam 204 (Sigma-Aldrich) was added to the medium after autoclaving.

Determination of cell density in *U. maydis* cultures

The cell density in liquid cultures was determined photometrically using a Novospec II photometer (Pharmacia Biotech). The OD₆₀₀ (optical density at $\lambda = 600$ nm) was measured using dilutions of the cultures to maintain linearity and the respective culture medium was used as a reference. Linearity is given between OD₆₀₀ 0.3 and 0.8. An OD₆₀₀ of 1 resembles 1.5×10^7 cells/mL for *U. maydis*.

Protoplasting of *U. maydis* cells

To generate competent *U. maydis* cells a modified protocol from Gillissen et al., 1992 and Schulz et al., 1990 was used. A 50 mL YEPS_{light} main culture was inoculated and grown to an OD₆₀₀ of 0.7 to 0.9. The cells were then pelleted (3000 rpm, 5 min) and resuspended in 25 mL SCS. After another centrifugation step (3000 rpm, 5 min) the pellet was resuspended in 2 mL Novozyme 234 solution and incubated until 50% of the cells were round or had a pinhead like appearance. The incubation was then stopped immediately by diluting with 10 mL ice cold SCS and centrifuged for 5 min at 2400 rpm on 4°C. After washing the pellet twice with 10 mL ice cold SCS and once with 10 mL ice cold STC, it was taken up in 1 mL ice cold STC and frozen at -80°C in 100 µL aliquots.

SCS:

Solution 1:
 5.9 g tri-Na-citrate*2H₂O
 182.2 g sorbitol in 1L H₂O_{bid.}
 Solution 2:
 4.2 g citrate*H₂O
 182.2 g sorbitol in 1L H₂O_{bid.}
 Titrate solution 2 to solution 1 until
 pH5.8 is reached
 autoclaved

STC:

500 mL sorbitol solution (1M)
 10 mL Tris-HCl pH7.5 (1M)
 100 mL CaCl₂ solution (1M)
 in 1L H₂O_{bid.}

Novozyme 234 solution:

7 mg Novozyme 234
 2 mL SCS
 sterile filtered

Transformation of *U. maydis* protoplasts

For *U. maydis* transformation 100 µL protoplasted cells were thawed on ice for 10 min and subsequently incubated with 5 µg of linear DNA as well as 1 µL heparin solution (10 mg/mL). After 10 min incubation on ice, the suspension was supplemented with 500 µL STC/PEG and again incubated on ice for 15 min. The transformation reaction was then plated on a top-agar overlaid (Bösch et al., 2016), antibiotic containing RegLight-Agar plate and incubated for 5 - 10 days on 28°C. Single colonies were singled out on solid CM-medium supplemented with the respective antibiotic and tested for correct transformation in Southern blot analysis.

STC/PEG:

600 mL STC
 400 g polyethyleneglycol (PEG, MW 3350)
 50 mL SDS (10% stock solution)
 in 1L H₂O_{bid.}

4.2.3 Protein biochemical methods**Protein extraction from *U. maydis***

To extract proteins from *U. maydis* cells, a main culture was inoculated from a pre-culture in 40 mL CM-glc which was grown to an OD₆₀₀ of approximately 0.75. Cells were then collected (5000 rpm, 5 min, 4°C) and resuspended in 2 mL lysis buffer (either native, denaturing or for protease cleavage (TEV-lysis buffer or HRV 3C-lysis buffer)). The suspension was transferred into liquid nitrogen pre-chilled metal containers, two metal balls were added and the closed metal containers were again incubated for 1 min in liquid nitrogen. Cell disruption was performed with a pebble mill (MM 400, Retsch GmbH) at 30 Hz for 10 min on 4°C. After thawing the container on 4°C for 1 h, the extract was transferred into a 2 mL reaction tube and centrifuged for 30 min on 4°C. The cleared cell extract was then transferred into fresh reaction tubes and either stored on -20°C (denaturing conditions) or on 4°C (native conditions). In general, cell extracts used only for analytics in SDS-PAGE and Western blotting were prepared

under denaturing conditions, whereas cell extracts used for activity assays (e.g. ELISA, AVEXIS, modified Western blot ELISA) were prepared under native conditions.

Lysis-buffer (denaturing, pH 8):	Lysis-buffer (native):	Lysis-buffer biotinylation (native):
93.2 mL Na ₂ HPO ₄ solution (1M)	50 mL 1xPBS	50 mL Tris-HCl (pH 8.0)
6.8 mL NaH ₂ PO ₄ solution (1M)	2.5 mM benzamidine	2.5 mM benzamidine
1 mM PMSF	1 mM PMSF	1 mM PMSF
1 cOmplete EDTA-free (Roche) tablet	1 cOmplete EDTA-free (Roche) tablet	1 cOmplete EDTA-free (Roche) tablet
1 mM DTT		
9.6 g urea		
200 µL Tris-HCl pH 8.0		
TEV-lysis buffer (native):	HRV 3C-lysis buffer (native):	
100 mM Tris-HCl (pH 8.0)	100 mM Tris-HCl (pH 8.0)	
0.5 mM EDTA	500 mM NaCl	
1 mM DTT	in H ₂ O _{bid.}	
in H ₂ O _{bid.}		

Trichloric acid (TCA) precipitations of *U. maydis* supernatants

To enrich secreted proteins from *U. maydis* supernatants, a main culture was inoculated from a pre-culture in 40 mL CM-glc which was grown to an OD₆₀₀ of approximately 0.75. 2 mL of the culture was then transferred into a reaction tube and centrifuged for (13000 rpm, 2 min, 4°C). 1 mL of the supernatant was then mixed with 250 µL TCA and incubated for at least 2 hours on ice. The precipitate was pelleted at 13000 rpm for 30 min on 4°C and subsequently washed twice in -20°C cold acetone (20 min, 4°C, 13000 rpm). After drying the protein pellet for 15 min on RT it was resuspended in 15 µL 3x-Laemmli-buffer and 2 µL NaOH (1M) and afterwards boiled on 98°C for 10 min. After centrifugation on 13000 rpm for 5 min the samples were directly used or stored on -20°C until further use.

Trichloric acid (TCA):	3x Laemmli buffer (Laemmli, 1970):
500 g trichloric-acid	300 mL Tris-HCl (0.5 M stock, pH 6.8)
in 1L H ₂ O _{bid.}	60 g SDS
	300 mg glycerol
	150 mL β-mercapto-ethanol
	300 mg bromophenol blue
	in 1L H ₂ O _{bid.}

Concentration of *U. maydis* supernatants

To concentrate supernatant samples and elutes from purifications, Amicon® centrifugal filter units (Merck Millipore) were used following company provided protocols. The filter units were

chosen according to the molecular weight cut off and the initial volume that had to be concentrated. Different used filter units are listed in Tab. 4.11.

Tab. 4.11: Amicon® centrifugation filter units used in this study.

Amicon® type	MW cut off [kDa]	Used centrifugal force [x g]
Ultra-4, PLBC Ultracel-PL membrane	3	7500
Ultra-15, PLGC Ultracel-PL membrane	10	5000
Ultra-15, PLTK Ultracel-PL membrane	30	5000

Protein expression and extraction from *E. coli*

For expression of heterologous proteins from *E. coli* cells, the expression strain Rosetta (DE3) pLysS was transformed with the respective expression plasmid (s. 4.1.4.1). A single colony from a fresh transformation plate was used to inoculate an overnight pre-culture in dYT-medium. The pre-culture was used to inoculate a main culture to an OD₆₀₀ of 0.1 and was grown to an OD₆₀₀ of 0.5. When optimal cell density was reached, the expression was induced using 0.5 to 1 mM IPTG (isopropyl- β -D-thiogalactopyranosid). Samples for SDS-PAGE analysis were taken at 0, 1, 2 and 3 hours post induction. At 3 h the cells from the complete culture were pelleted (8000 rpm, 5 min, 4°C) and frozen at -20°C until further use.

For protein extraction from the gained pellets, the cells were resuspended in 10 mL cold lysis buffer and incubated on ice for 20 min. Cell disruption was performed using an ultrasonic sonotrode (5 mm microtip (Heinemann)) used with the Cell Disruptor B15 (Branson; stage 4, 30 s pulse, 30 s rest on ice, 5 repetitions). Protein containing supernatant was subsequently separated from cell debris by centrifugation (8500 rpm, 15 min, 4°C). The proteins were then purified using IMAC.

IPTG:

0.5 - 1 mM IPTG (isopropyl- β -D-galactopyranosid)
in H₂O_{bid.}

***E. coli* lysis buffer (native):**

50 mM NaH₂PO₄
300 mM NaCl
10 mM Imidazole
in 1L H₂O_{bid.}, pH 8.0

Determination of protein concentration by Bradford assay

To determine the protein concentration of cell extracts, concentrated supernatants and purified protein samples, the Bradford method was applied (Bradford, 1976). To ensure linearity, 10 μ L of an appropriately diluted sample was incubated with 200 μ L 1:5 diluted Bradford solution (Protein Assay Dye, BioRad) for 5 min and readout was performed at 595 nm using an Infinite M200 plate reader (Tecan). As a reference a BSA standard was measured ranging from 0 μ g/mL to 200 μ g/mL BSA in H₂O_{bid.}.

SDS-Polyacrylamide-gel-electrophoretic separation of proteins

To separate proteins according to their molecular weight, standard SDS-PAGE (denaturing SDS-polyacrylamide-gel-electrophoreses) was used (Laemmli, 1970). 1 mm 10 % separation gels were casted using utensils from the Mini-Protean series (BioRad). Samples were supplemented with 3x concentrated Laemmli-buffer and boiled for 10 min on 98°C. After centrifugation (5 min, 13000 rpm), the samples were loaded and SDS-PAGE was performed at 30 mA per gel until an appropriate separation was achieved.

Separation gel:

6.75 mL Tris-HCl (1 M stock solution, pH 8.8)
6 mL 30% acrylamide, 0.8 % bisacrylamide
90 µL SDS (20% stock solution)
450 µL glycerol (50% stock solution)
5.8 mL H₂O_{bid.}
90 µL APS (10% ammonium peroxydisulfate stock)
18 µL TEMED (N,N,N',N'-Tetramethylethylenediamin)

Stacking gel:

1.2 mL Tris-HCl (0.5 M stock solution, pH 6.8)
0.8 mL 30% acrylamide, 0.8 % bisacrylamide
24 µL SDS (20% stock solution)
2.8 mL H₂O_{bid.}
24 µL APS (10% ammonium peroxydisulfate stock)
4.8 µL TEMED (N,N,N',N'-Tetramethylethylenediamin)

1x SDS running buffer:

25 mM Tris (pH 8.4)
192 mM glycine
0.1 % (w/v) SDS (sodium dodecyl sulfate)
in H₂O_{bid.}

Transfer of denatured proteins – Western blot

After electrophoretic size separation of proteins by SDS-PAGE, proteins were transferred onto PVDF membranes (Amersham Hybond-P, GE Healthcare), using a semi-dry Western blot chamber (846-015-200, Biometra). To this end, the membrane was activated for 1 min in methanol and subsequently washed in Anode buffer 2. Two Whatman filter-papers were soaked in Anode buffer 1 and placed on the anode. On top of these, one Whatman filter-paper soaked in Anode buffer 2 was placed, followed by the activated PVDF membrane, the stacking gel from SDS-PAGE and 3 Whatman filter-paper soaked in Cathode buffer. The stack was covered with the cathode and transfer was performed at 1 mA per cm² membrane for 1 h.

Anode buffer 1:

300 mM Tris-HCl (pH10.4)
15 % (v/v) methanol
in 1L H₂O_{bid.}

Anode buffer 2:

30 mM Tris-HCl (pH 10.4)
15% (v/v) methanol
in 1L H₂O_{bid.}

Cathode buffer:

25 mM Tris-HCl (pH 9.4)
15 % (v/v) methanol
40 mM 6-aminohexanoic acid
in 1L H₂O_{bid.}

Detection of immobilized proteins

To specifically detect immobilized proteins on PVDF membranes, an antibody labeling was performed. After the protein was transferred to the membrane, it was incubated for at least 1 h

in blocking solution, to block areas with no bound protein. Depending on the used antibodies, BSA or skimmed milk powder was used for blocking. Afterwards the membrane was incubated with a primary antibody in blocking solution (s. Tab. 4.12) for 1 h at RT or overnight on 4°C. After washing 3x for 5 min in TBST or PBST, the membrane was incubated with a HRP conjugated secondary antibody in blocking solution (s. Tab. 4.13) for 1 h at RT. The membrane was then washed 3x for 5 min in TBST or PBST and 1x for 5 min in TBS or PBS. After incubating the membrane for 1 min in HRP-substrate solution (AceGlow™, Peqlab), chemiluminescence was detected using the LAS4000 (GE Healthcare).

Tab. 4.12: Primary antibodies used in this study

Antibody	Origin	Dilution	Buffer used	Blocking reagent used
α-HA (monoclonal, Roche)	mouse	1:4000	TBST	Skimmed milk 3 % (w/v)
α-Gfp (monoclonal, Roche)	mouse	1:1000	TBST	Skimmed milk 3 % (w/v)
α-Gus (polyclonal, Sigma-Aldrich)	rabbit	1:5000	TBST	Skimmed milk 3 % (w/v)
α-RH5 (polyclonal, Gavin Wright)	rabbit	1:50000	PBST	BSA 2 % (w/v)

Tab. 4.13: Secondary antibodies used in this study

Antibody	Origin	Dilution	Buffer used	Blocking reagent used
α-Mouse-HRP (Promega)	horse	1:10000	TBST	Skimmed milk 3 % (w/v)
α-Rabbit-HRP (NEB Cell Signaling)	goose	1:10000	TBST/PBST	Skimmed milk 3 % (w/v) or BSA 2 % (w/v)
α-Goat-HRP (Sigma-Aldrich)	mouse	1:10000	TBST	Skimmed milk 3 % (w/v)
α-Biotin-HRP (NEB Cell Signaling)	rabbit	1:10000	PBST	BSA 5 % (w/v)

TBS (/TBST):

20 mM Tris-HCl

136 mM NaCl

in H₂O_{bid.}, pH 7.6

For TBST 0.05 % (v/v) Tween-20 was added

PBS (/PBST):

137 mM NaCl

2.7 mM KCl

10 mM Na₂HPO₄

1.8 mM KH₂PO₄

in H₂O_{bid.}, pH 7.4

For PBST 0.05 % (v/v) Tween-20 was added

Stripping of PVDF-membranes after Western blotting

In order to remove bound antibodies from a protein covered PVDF-membrane after Western blotting and detection, mild stripping was conducted. To this end, the membrane was washed in H₂O_{bid.} for 5 min and transferred into 0.2 M NaOH. After incubation on an orbital shaker for 5 min, the membrane was again washed in H₂O_{bid.}, blocked in the respective blocking solution for 1 h at RT and the Western blot detection protocol was followed as described earlier.

Coomassie staining of PVDF membranes and SDS-polyacrylamide gels

Coomassie brilliant blue staining was used to stain polyacrylamide gels and PVDF membranes. Gels were incubated in Coomassie staining solution for 1 h on an orbital shaker and then washed with H₂O. After incubation for at least 4 h in destaining solution, the gel was washed for 1 h in H₂O and analyzed afterwards. Membranes were incubated for 20 min in Coomassie staining solution and 20 min in destaining solution with a subsequent 10 min H₂O washing step. The membranes were then dried at RT before documentation to reduce background staining.

Coomassie staining solution:

0.05 % Coomassie Brilliant Blue R250
15 % (v/v) acetic acid
15 % (v/v) methanol
in H₂O_{bid.}

Destaining solution:

15 % (v/v) acetic acid
15 % (v/v) methanol
in H₂O_{bid.}

Modified Western blot for analyzing αGfp-NB activity

To analyze the binding affinity and activity of αGfp nanobodies isolated from *U. maydis* cell extracts, a modified Western blot protocol was applied. First 10 µg of native *U. maydis* cell extracts from a 3xGfp expressing strain (UMa587) and of a wildtype negative control (Uma67) were run on an SDS-PAGE und subsequently blotted on a PVDF membrane. The membrane was then blocked as described earlier. To specifically detect the Gfp on the PVDF membrane, IMAC purified αGfp-NB from UMa1397 or Uma1465 cell extracts or supernatants were used as primary antibodies. The membrane was therefore incubated overnight on 4°C with the purified nanobodies mixed with blocking buffer (PBST with 3 % (v/v) skimmed milk). After 3x washing with PBST the standard Western blot detection protocol was followed using α-HA as primary and α-Mouse-HRP as secondary antibody.

Indirect enzyme linked immunosorbent assay (ELISA)

ELISA was used to analyze the binding affinity and specificity of αGfp-, αGfp-Protein A-, HRP-αGfp- and αBoNTA nanobodies (NB).

For all αGfp nanobodies, protein adsorbing 96 well microtiter plates (MaxiSorp®, Nunc/ Thermo Fisher Scientific) were coated with 2 µg Gfp or 2 µg BSA per well. The used Gfp protein was expressed in *E. coli* and Ni²⁺-NTA purified. Coating was performed on 4°C overnight in 100 mM bicarbonate coating buffer. The coated wells were then blocked for at least 4 h on RT with 4 % (w/v) skimmed milk in PBS and subsequently washed 3x with PBST. αGfp-NB containing cell extracts, supernatants, purified αGfp-NB from cell extract or supernatant were applied to the washed wells either in defined volumes or in defined amounts. Previously all samples were supplemented with 20 % (w/v) skimmed milk in PBS to a final

concentration of 4 % (w/v) skimmed milk. The plate was incubated with the samples and appropriate controls overnight at 4°C. After 3x PBST washing, α -HA primary antibodies were added (detection of α Gfp-NB) and incubated for 2 h at RT. 3x PBST washing followed with subsequent addition of α -Mouse-HRP secondary antibodies and incubation for 1 h RT (detection of α Gfp-NB and α Gfp-Prot A-NB). Another 3x PBST washing step was followed by 3x washing with PBS and addition of 100 μ L QuantaRed™ Enhanced Chemifluorescent HRP substrate (Thermo Fisher Scientific) per well (detection of α Gfp-NB, α Gfp-Prot A-NB and HRP- α Gfp-NB). After incubation on RT for 1 h, the reaction was stopped with 10 μ L of provided stop solution and the reactions were transferred into black microtiter plates (chimney well, Sarstedt). Fluorescence readout was performed using the Infinite M200 plate reader (Tecan) at 570 nm/ 600 nm.

For α BoNTA-NB, a Botulinum neurotoxin A coated 96 well microtiter plate (Metabio Inc.) was used. The wells were blocked with 4% skimmed milk in PBS for at least 4 h at RT and after 3x PBST washing, α BoNTA-NB containing cell extracts, supernatants or purified α BoNTA-NB from cell extracts or supernatants were applied to the blocked wells either in defined volumes or defined concentrations. After that the protocol for the ELISA was followed as described in the upper section. For detection a primary α -HA antibody and a secondary α -Mouse-HRP antibody was used.

Bicarbonate coating solution:

100 mM HCO₃⁻

in H₂O_{bid.}

Determination of β -Glucuronidase (Gus) activity

Gus activity in culture supernatants of *U. maydis* was determined using a modified, previously described protocol (Stock et al., 2012; Stock et al., 2016). The principle behind this method is the ability of Gus to hydrolyze the fluorogenic substrate 4-methylumbelliferyl β -D-glucuronide hydrate (MUG, bioWORLD) (Mead et al., 1967). Culture samples of Gus-SHH-Cts1 expressing *U. maydis* strains were pelleted (13000 rpm, 2 min, 4°C) and supernatants were transferred into fresh reaction tubes. In dependency of the OD₆₀₀ of the culture, the samples were diluted to ensure linearity (s. Tab. 4.14). For activity measurements, 10 μ L of the diluted or undiluted samples were mixed with 90 μ L of H₂O_{bid.} and 100 μ L of 2x Gus assay-buffer (final concentration 1x). Fluorescence was determined in a kinetic measurement for 90 min using a Tecan Infinite M200 plate reader (Tecan) at 365 nm/ 465 nm. For calculations, a fluorescence standard was prepared using different concentrations (ranging from 0.1 to 1000 μ M) of the product 4-methylumbelliferone (MU).

For quantitation of Gus activity a standard Gus activity curve with defined amounts (1 pg to 10 ng) of Gus-SHH protein, IMAC purified from *E. coli* was used.

To analyze the influence of different pH conditions on the activity of Gus, 4.75 µg of IMAC purified Gus-SHH from *E. coli* was incubated with 45 µL CM-glc medium with varying pH (ranging from 2 to 8). After incubation on 4°C and on 28°C for 22 h the samples were diluted 1/100 in H₂O_{bid.} and 10 µL were used for Gus activity determination as described above.

Tab. 4.14: Dilution factors in dependency of OD₆₀₀ values for Gus activity measurements

OD ₆₀₀	Dilution in H ₂ O
0 - 0.8	-
0.8 - 2.5	1/2
2.5 - 25	1/3

2x Gus extraction-buffer:

28 µM β-mercapto ethanol

0.8 mM EDTA (1 M stock, pH 8.0)

10 mM NaPO₄ buffer (1 M stock, pH 7.0)

0.004 % (v/v) lauroyl-sarcosin

0.004 % (v/v) triton-X-100

in H₂O_{bid.}

2x Gus assay-buffer:

1x Gus extraction-buffer

0.2 mg/mL BSA

2 mM MUG

High performance liquid chromatography (HPLC)

To measure the abundance of various soluble compounds in supernatant samples of RAMOS cultivations, HPLC analysis was performed (in collaboration with Sandra Wewetzer, RWTH Aachen). To remove insoluble compounds, samples were centrifuged (13000 rpm, 2 min, 4°C) and the corresponding supernatants were filtered with 0.2 µm PVDF filters (Rotilabo® PVDF, non-sterile 15 mm, 0.2 µm (Roth)). Filtered samples were analyzed on a 250 mm organic acid column (CS chromatography) and HPLC measurements were performed at 60°C with 50 mM sulfuric acid as mobile phase (0.8 L/min flow rate).

Ni²⁺-NTA purification of poly-histidine-tagged proteins (IMAC)

For purification of poly-histidine-tagged proteins from *U. maydis* cell extracts and supernatants, Ni²⁺-NTA agarose (Protino®, Macherey Nagel) was used. 1 mL of the matrix was equilibrated with 10 mL His-lysis buffer and either 1.5 mL of native cell extracts or 200 - 500 mL of filtered supernatant was incubated with the equilibrated matrix (1 h, 4°C). For supernatant purifications, a *U. maydis* 200 to 500 mL main culture was grown to an OD₆₀₀ of 0.75, centrifuged (7000 rpm, 10 min, 4°C) and subsequently filtered. After addition of 1 cComplete™

EDTA-free Protease Inhibitor Cocktail tablet (Roche) per 200 mL supernatant, it was incubated with the equilibrated Ni²⁺-NTA matrix. Native cell extracts were prepared as described earlier.

After incubation, the matrix was transferred into empty purification columns and washed with 2 mL of different concentrations of imidazole (20 mM, 50 mM and 100 mM). For elution, the matrix was first washed with 1 mL of 250 mM imidazole and finally 2 mL of 500 mM imidazole. Samples of all fractions (cell extract or supernatant, flow through, wash 1 - 3, elute 1 - 2) were collected and analyzed in SDS-PAGE. The whole purification procedure was performed at 4°C.

His-lysis buffer:	His-wash buffer:	His-elution buffer:
50 mM NaH ₂ PO ₄	50 mM NaH ₂ PO ₄	50 mM NaH ₂ PO ₄
300 mM NaCl	300 mM NaCl	300 mM NaCl
10 mM imidazole	20 mM, 50 mM and 100 mM imidazole	250 mM and 500 mM imidazole
in H ₂ O _{bid.} , pH 8.0	in H ₂ O _{bid.} , pH 8.0	in H ₂ O _{bid.} , pH 8.0

Purification of OneSTrEP®-tagged proteins

For purification of OneSTrEP®-tagged proteins from *U. maydis* cell extracts, native cell extracts were generated as described earlier. 1 mL of Strep-Tactin® Sepharose matrix (IBA GmbH) was equilibrated with 10 mL wash buffer and subsequently incubated for 1 h on 4°C with 1.5 mL native cell extract. After incubation, the matrix was transferred to an empty purification column and washed thrice with 2 mL wash buffer. Elution was performed using 1 mL elution buffer and in a second step 2 mL elution buffer. Samples of all fractions (cell extract, flow through, wash 1 - 3, elute 1 - 2) were collected and analyzed in SDS-PAGE. The whole purification procedure was performed at 4°C.

Strep-wash buffer	Strep-elution buffer:
100 mM Tris-HCl (1 M stock, pH 8.0)	100 mM Tris-HCl (1 M stock, pH 8.0)
150 mM NaCl	150 mM NaCl
1 mM EDTA	1 mM EDTA
in H ₂ O _{bid.}	2.5 mM desthiobiotin
	in H ₂ O _{bid.}

Biotinylation of AviTag™ labeled proteins in *U. maydis* cell extracts

To biotinylate proteins expressed in *U. maydis in vitro*, the Avidity AviTag™ system was used. The AviTag™ is a 15 aa long peptide which is recognized and processed by *E. coli* biotin ligase BirA, resulting in a covalent monobiotinylation of the peptide (Terpe, 2003; Tropea et al., 2009). In this study N- and C-terminal tagged proteins were analyzed. Native cell extracts with Tris-HCl lysis-buffer were prepared as described earlier. 1.5 mL cell extract was concentrated 10x to 150 µL using Amicon centrifugal units and subsequently split into two aliquots of 75 µL. 0.5 µL (0.5 µg) BirA enzyme was then added to one of the aliquots and 0.5 µL H₂O_{bid.} to the

negative control. 10 μ L BioMixA solution and 10 μ L BioMixB solution were added and the reaction was incubated on RT overnight. Biotinylated samples were then either analyzed on SDS-PAGE and Western blot or used in AVEXIS assays. In some cases a buffer exchange using Amicon centrifugal units was performed after biotinylation to reduce background due to free biotin in BioMixB.

Avidity-based Extracellular Interaction Screening (AVEXIS)

To analyze the binding affinity and specificity of UmRH5 proteins in *U. maydis* cell extracts, the AVEXIS assay was applied (Kerr and Wright, 2012). Native cell extracts were prepared as described earlier. Either complete cell extracts, purified cell extracts or biotinylated proteins were used in the assay. Depending on the tag (OneSTrEP®-tag, AviTag™, His-tag), the 96 well plate was chosen and the protocol was modified (s. Tab. 4.15). Bradford assay was used for protein concentration determination prior to sample addition.

The wells were washed once with PBS in case of the MaxiSorp™ plates. They were either coated with UmRH5 protein or a Basigin-Cd4d3+4-COMP- β -lactamase fusion protein (representing the RH5-receptor coupled to a pentamerizing COMP domain, followed by a β -lactamase reporter enzyme) in 100 mM bicarbonate coating buffer. Coating was performed overnight. After washing thrice with PBST and blocking with PBST/2% (w/v) BSA for 1 h RT, UmRH5 samples or Basigin-Cd4d3+4-COMP- β -lactamase protein were added respectively.

In case of the biotin- and the streptavidin-coated plates, UmRH5 samples were added directly. All wells were subsequently incubated for 1 h at RT or overnight on 4°C. After washing thrice with PBST, the wells were incubated for 1 h at RT with blocking solution (1x PBST with 2% (w/v) BSA) and then 100 μ L 1:10 diluted Basigin-Cd4d3+4-COMP- β -lactamase protein was applied for 1 h on RT.

For detection, all wells were washed thrice in PBST and once in PBS prior to the addition of 60 μ L of 242 μ M Nitrocefin solution. After incubation on RT for 2h, readout was performed using an Infinite M200 plate reader (Tecan) at 485 nm. To also detect very weak interactions, the incubation was continued for 16 h on 4°C and a second readout was performed.

Tab. 4.15: Protein-tag and 96 well-plate combinations for AVEXIS assays

Protein-tag	96 well-plate type
OneSTrEP®	Biotin Coated Plate (Pierce/ Thermo Fisher Scientific)
AviTag™	Immobilizer™ Streptavidin Plate (Nunc/ Thermo Fisher Scientific)
His-tag	MaxiSorp® (Nunc/ Thermo Fisher Scientific)

0.5 mg/mL Nitrocefin stock solution:

1 mg Nitrocefin
100 μ L DMSO
1.9 mL NaPO₄ buffer (0.1 M stock, pH 8)

242 μ M Nitrocefin solution:

1 mL 0.5 mg/mL Nitrocefin stock solution
3 mL PBS

Directed proteolytic cleavage of protease cleavage sites in fusion proteins

For TAP (Tandem affinity purification) and directed hydrolysis of fusion proteins, *U. maydis* cell extracts were prepared in either TEV-lysis buffer or HRV 3C-lysis buffer as described earlier. 1.5 mL of the cell extracts were then supplemented with 1 U of ProTEV Plus-protease (Promega or own preparation) or 1 U of HRV 3C-protease (HRV 3C protease, Thermo Fisher Scientific). Hydrolysis was performed overnight on 4°C (rotary wheel). Samples taken before, after 2 h incubation and after overnight hydrolysis were analyzed in SDS-PAGE and Western blot as described earlier.

TEV reaction buffer

50 mM Tris-HCl
0.5 mM EDTA
1 mM DTT

HRV 3C reaction buffer

(provided by Pierce/Thermo Fisher Scientific)

Purification of Cts1 fusion proteins with chitin coated matrices

For purification of Cts1 fusion proteins from *U. maydis* cell extracts, whole cell extracts were prepared as described earlier. For the purification chitin coated magnetic beads (Chitin Magnetic Beads, New England BioLabs) or chitin coated sepharose (Chitin Resin, New England BioLabs) was used.

Purification with magnetic beads was performed by adding 50 μ L of the slurry into a reaction tube and washing twice with 500 μ L CBD-buffer. Cell extract was added to the washed beads and incubated on a rotary wheel for 1 h or overnight (4°C). After washing thrice with 500 μ L CBD-buffer the binding was either analyzed by boiling the magnetic beads in 3x Laemmli buffer or hydrolysis by TEV-protease or HRV 3C-protease was performed as described earlier to release the non-bound fusion protein part.

Purification with chitin coated Sepharose was performed similar to the protocol for chitin magnetic bead purification. 500 μ L of chitin resin was transferred into an empty purification column and equilibrated with 10 mL of CBD-buffer. 1.5 mL of native cell extracts were added and incubated with the matrix for 1 h on 4°C. The matrix was then washed once with CBD buffer and equilibrated with TEV reaction buffer. Incubation with 1 U of ProTEV Plus protease (Promega) or TEV from own preparation was performed overnight on 4°C. Elution was performed using 500 μ L E buffer (TEV reaction buffer), 1 mL E_D buffer (E buffer + 0.1 % (w/v)

Tween20), 1 mL E_S buffer (E buffer + 0.5 M NaCl) and 1 mL E_U buffer (E buffer + 0.5 M urea). All fractions were sampled and analyzed in SDS-PAGE and Western blot.

CBD-buffer:

500 mM NaCl

20 mM Tris-HCl

1 mM EDTA

0.1 % Tween-20

in H₂O_{bid.}, pH 8.0

4.2.4 Computer programs and bioinformatics

Nucleic and amino acid analysis

Clone Manager 9 (Sci Ed Central Software)

PEDANT (<http://pedant.helmholtz-muenchen.de/>)

BLAST2 (<http://blast.ncbi.nlm.nih.gov/Blast.cgi>)

Clustal-Ω (<http://www.clustal.org/omega/>)

SignalP V4.1 (<http://www.cbs.dtu.dk/services/SignalP/>)

ESPrict 3.0 (<http://esprict.ibcp.fr/>) (Robert and Gouet, 2014)

Literature research and sequence information

NCBI - National Centre for Biotechnology Information (<http://www.ncbi.nlm.nih.gov/>)

Operation of special devices and data analysis

Iris V5.3 Bioreactor operation software (Infors AG)

i-control™ Microplate Reader Software (Tecan Trading AG)

ImageQuant LAS4000 Control Software (GE Healthcare)

Data analysis, writing and graphics

Microsoft Office 2010 (Microsoft Corporation)

Inkscape 0.91 (Software Freedom Conservancy)

Canvas 12 (ACDSee Systems)

(websites last accessed on 11/08/2016)

5 References

- Adrio, J. L. and Demain, A. L.** (2010). Recombinant organisms for production of industrial products. *Bioeng. Bugs* **1**, 116–131.
- Ahmad, M., Hirz, M., Pichler, H. and Schwab, H.** (2014). Protein expression in *Pichia pastoris*: Recent achievements and perspectives for heterologous protein production. *Appl. Microbiol. Biotechnol.* **98**, 5301–5317.
- Aichinger, C., Hansson, K., Eichhorn, H., Lessing, F., Mannhaupt, G., Mewes, W. and Kahmann, R.** (2003). Identification of plant-regulated genes in *Ustilago maydis* by enhancer-trapping mutagenesis. *Mol. Genet. Genomics* **270**, 303–314.
- Akgün, A., Maier, B., Preis, D., Roth, B., Klingelhöfer, R. and Büchs, J.** (2004). A novel parallel shaken bioreactor system for continuous operation. *Biotechnol. Prog.* **20**, 1718–1724.
- Anderlei, T. and Büchs, J.** (2001). Device for sterile online measurement of the oxygen transfer rate in shaking flasks. *Biochem. Eng. J.* **7**, 157–162.
- Anderlei, T., Zang, W., Papaspyrou, M. and Büchs, J.** (2004). Online respiration activity measurement (OTR, CTR, RQ) in shake flasks. *Biochem. Eng. J.* **17**, 187–194.
- Asano, R., Ikoma, K., Kawaguchi, H., Ishiyama, Y., Nakanishi, T., Umetsu, M., Hayashi, H., Katayose, Y., Unno, M., Kudo, T., et al.** (2010). Application of the Fc fusion format to generate tag-free bi-specific diabodies. *FEBS J.* **277**, 477–487.
- Ausubel, F. M., Brent, R., Kingston, R. E., Moore, D. D., Seidman, J. G., Smith, J. A. and Struhl, K.** (1987). *Current Protocols in Molecular Biology*. New York, NY: John Wiley & Sons, Inc.
- Backhaus, R., Zehe, C., Wegehangel, S., Kehlenbach, A., Schwappach, B. and Nickel, W.** (2004). Unconventional protein secretion: membrane translocation of FGF-2 does not require protein unfolding. *J. Cell Sci.* **117**, 1727–36.
- Baez, A. and Shiloach, J.** (2014). Effect of elevated oxygen concentration on bacteria, yeasts, and cells propagated for production of biological compounds. *Microb. Cell Fact.* **13**, 181.
- Banuett, F.** (1992). *Ustilago maydis*, the delightful blight. *Trends Genet.* **8**, 8252–8256.
- Banuett, F. and Herskowitz, I.** (1989). Different alleles of *Ustilago maydis* are necessary for maintenance of filamentous growth but not for meiosis. *Proc. Natl. Acad. Sci. U. S. A.* **86**, 5878–5882.
- Battistoni, A., Card, M. T., Mazzetti, A. P. and Rotilio, G.** (1992). Temperature-Dependent Protein Folding *in vivo* - Lower Growth Temperature Increases Yield of Two Genetic Variants of *Xenopus laevis* Cu,Zn Superoxide Dismutase in *Escherichia coli*. *Biochem. Biophys. Res. Commun.* **186**, 1339–1344.
- Becht, P., Vollmeister, E. and Feldbrügge, M.** (2005). Role for RNA-Binding Proteins Implicated in Pathogenic Development of *Ustilago maydis*. *Eukaryot. Cell* **4**, 121–133.
- Becht, P., König, J. and Feldbrügge, M.** (2006). The RNA-binding protein Rrm4 is essential for polarity in *Ustilago maydis* and shuttles along microtubules. *J. Cell Sci.* **119**, 4964–4973.
- Beckett, D., Kovaleva, E. and Schatz, P. J.** (2008). A minimal peptide substrate in biotin holoenzyme synthetase-catalyzed biotinylation. *Protein Sci.* **8**, 921–929.

- Beier, S.** (2015). Optimierung der Expression und Aufreinigung von synthetischen anti-Gfp Nanobodies in *Ustilago maydis*. *Bachelor's thesis*. Heinrich Heine University Düsseldorf.
- Bell, M. R., Engleka, M. J., Malik, A. and Strickler, J. E.** (2013). To fuse or not to fuse: What is your purpose? *Protein Sci.* **22**, 1466–1477.
- Berges, J. A. and Falkowski, P. G.** (1998). Physiological stress and cell death in marine phytoplankton: induction of proteases in response to nitrogen or light limitation. *Limnol. Oceanogr.* **43**, 129–135.
- Berlec, A. and Štrukelj, B.** (2013). Current state and recent advances in biopharmaceutical production in *Escherichia coli*, yeasts and mammalian cells. *J. Ind. Microbiol. Biotechnol.* **40**, 257–274.
- Bhat, M. K.** (2000). Cellulases and related enzymes in biotechnology. *Biotechnol. Adv.* **18**, 355–383.
- Blount, Z. D.** (2015). The unexhausted potential of *E. coli*. *Elife* **4**, e05826.
- Bölker, M., Böhnert, H. U., Braun, K. H., Görl, J. and Kahmann, R.** (1995). Tagging pathogenicity genes in *Ustilago maydis* by restriction enzyme-mediated integration (REMI). *MGG Mol. Gen. Genet.* **248**, 547–552.
- Bölker, M., Basse, C. W. and Schirawski, J.** (2008). *Ustilago maydis* secondary metabolism - From genomics to biochemistry. *Fungal Genet. Biol.* **45**, 88–93.
- Bonnerjea, J.** (2004). Purification of Therapeutic Proteins. In *Protein Purification Protocols* (ed. Cutler, P.), pp. 455–462. Totowa, NJ: Humana Press.
- Bösch, K., Frantzeskakis, L., Vraneš, M., Kämper, J., Schipper, K. and Göhre, V.** (2016). Genetic Manipulation of the Plant Pathogen *Ustilago maydis* to Study Fungal Biology and Plant Microbe Interactions. *J. Vis. Exp.* **115**, e54522, doi:10.3791/54522.
- Brachmann, A.** (2001). Die frühe Infektionsphase von *Ustilago maydis*: Genregulation durch das bW/bE-Heterodimer. *Dissertation*. Ludwig-Maximilians-University Munich.
- Brachmann, A., König, J., Julius, C. and Feldbrügge, M.** (2004). A reverse genetic approach for generating gene replacement mutants in *Ustilago maydis*. *Mol. Genet. Genomics* **272**, 216–226.
- Bradford, M. M.** (1976). A rapid and sensitive method for the quantitation of microgram quantities of protein utilizing the principle of protein-dye binding. *Anal. Biochem.* **72**, 248–254.
- Brefort, T., Doehlemann, G., Mendoza-Mendoza, A., Reissmann, S., Djamei, A. and Kahmann, R.** (2009). *Ustilago maydis* as a Pathogen. *Annu. Rev. Phytopathol.* **47**, 423–445.
- Brenner, C. and Fuller, R. S.** (1992). Structural and enzymatic characterization of a purified prohormone-processing enzyme: secreted, soluble Kex2 protease. *Proc. Natl. Acad. Sci. U. S. A.* **89**, 922–926.
- Broomfield, P. L. E. and Hargreaves, J. A.** (1992). A single amino-acid change in the iron-sulphur protein subunit of succinate dehydrogenase confers resistance to carboxin in *Ustilago maydis*. *Curr. Genet.* **22**, 117–121.

- Buerth, C., Kovacic, F., Stock, J., Terfrüchte, M., Wilhelm, S., Jaeger, K.-E., Feldbrügge, M., Schipper, K., Ernst, J. F. and Tielker, D. (2014). Uml2 is a novel CalB-type lipase of *Ustilago maydis* with phospholipase A activity. *Appl. Microbiol. Biotechnol.* **98**, 4963–4973.
- Bustamante, L. Y., Bartholdson, S. J., Crosnier, C., Campos, M. G., Wanaguru, M., Nguon, C., Kwiatkowski, D. P., Wright, G. J. and Rayner, J. C. (2013). A full-length recombinant *Plasmodium falciparum* PfRH5 protein induces inhibitory antibodies that are effective across common PfRH5 genetic variants. *Vaccine* **31**, 373–379.
- Carter, P. J. (2011). Introduction to current and future protein therapeutics: A protein engineering perspective. *Exp. Cell Res.* **317**, 1261–1269.
- Chen, X., Zaro, J. L. and Shen, W. C. (2013). Fusion protein linkers: Property, design and functionality. *Adv. Drug Deliv. Rev.* **65**, 1357–1369.
- Christensen, J. J. (1963). Corn smut caused by *Ustilago maydis*. Minnesota, USA: American Phytopathological Society.
- Cohen, S. N., Chang, A. C. and Hsu, L. (1972). Nonchromosomal antibiotic resistance in bacteria: genetic transformation of *Escherichia coli* by R-factor DNA. *Pnas* **69**, 2110–2114.
- Cos, O., Ramón, R., Montesinos, J. L. and Valero, F. (2006). Operational strategies, monitoring and control of heterologous protein production in the methylotrophic yeast *Pichia pastoris* under different promoters: a review. *Microb. Cell Fact.* **5**, 17.
- Costa, S., Almeida, A., Castro, A. and Domingues, L. (2014). Fusion tags for protein solubility, purification, and immunogenicity in *Escherichia coli*: The novel Fh8 system. *Front. Microbiol.* **5**, 63.
- Costa, T. R. D., Felisberto-Rodrigues, C., Meir, A., Prevost, M. S., Redzej, A., Trokter, M. and Waksman, G. (2015). Secretion systems in Gram-negative bacteria: structural and mechanistic insights. *Nat. Rev. Microbiol.* **13**, 343–359.
- Couturier, M., Navarro, D., Olivé, C., Chevret, D., Haon, M., Favel, A., Lesage-Meessen, L., Henrissat, B., Coutinho, P. M. and Berrin, J.-G. (2012). Post-genomic analyses of fungal lignocellulosic biomass degradation reveal the unexpected potential of the plant pathogen *Ustilago maydis*. *BMC Genomics* **13**, 57.
- Cova, M., Rodrigues, J. A., Smith, T. K. and Izquierdo, L. (2015). Sugar activation and glycosylation in *Plasmodium*. *Malar. J.* **14**, 427.
- Crosnier, C., Bustamante, L. Y., Bartholdson, S. J., Bei, A. K., Theron, M., Uchikawa, M., Mboup, S., Ndir, O., Kwiatkowski, D. P., Duraisingh, M. T., et al. (2011). Basigin is a receptor essential for erythrocyte invasion by *Plasmodium falciparum*. *Nature* **480**, 534–538.
- Crosnier, C., Wanaguru, M., McDade, B., Osier, F. H., Marsh, K., Rayner, J. C. and Wright, G. J. (2013). A library of functional recombinant cell surface and secreted *Plasmodium falciparum* merozoite proteins. *Mol. Cell. Proteomics* **12**, 3976–86.
- Curwin, A. J., Brouwers, N., Adell, M. A. Y., Teis, D., Turacchio, G., Parashuraman, S., Ronchi, P. and Malhotra, V. (2016). ESCRT-III drives the final stages of CUPS maturation for unconventional protein secretion. *Elife* **5**, e16299.
- De Gooijer, C. D., Bakker, W. A. M., Beeftink, H. H. and Tramper, J. (1996). Bioreactors in series. An overview of design procedures and practical applications. *Enzyme Microb. Technol.* **18**, 202–219.

- De Groot, A. S. and Scott, D. W.** (2007). Immunogenicity of protein therapeutics. *Trends Immunol.* **28**, 482–490.
- de Macedo, C. S., Schwarz, R. T., Todeschini, A. R., Previato, J. O. and Mendonça-Previato, L.** (2010). Overlooked post-translational modifications of proteins in *Plasmodium falciparum*: N- and O-glycosylation - A review. *Mem. Inst. Oswaldo Cruz* **105**, 949–956.
- De Meyer, T., Muyldermans, S. and Depicker, A.** (2014). Nanobody-based products as research and diagnostic tools. *Trends Biotechnol.* **32**, 263–270.
- Dean, R., Van Kan, J. A. L., Pretorius, Z. A., Hammond-Kosack, K. E., Di Pietro, A., Spanu, P. D., Rudd, J. J., Dickman, M., Kahmann, R., Ellis, J., et al.** (2012). The Top 10 fungal pathogens in molecular plant pathology. *Mol. Plant Pathol.* **13**, 414–430.
- de Souza, P. M., Lisa, M., Bittencourt, D. A., Caprara, C. C., de Freitas, M., Paula, R., de Almeida, C., Silveira, D., Fonseca, Y. M., Ximenes, E., et al.** (2015). A biotechnology perspective of fungal proteases. *Brazilian J. Microbiol.* **46**, 337–346.
- Degering, C., Eggert, T., Puls, M., Bongaerts, J., Evers, S., Maurer, K.-H. and Jaeger, K.-E.** (2010). Optimization of protease secretion in *Bacillus subtilis* and *Bacillus licheniformis* by screening of homologous and heterologous signal peptides. *Appl. Environ. Microbiol.* **76**, 6370–6376.
- Demain, A. L. and Vaishnav, P.** (2009). Production of recombinant proteins by microbes and higher organisms. *Biotechnol. Adv.* **27**, 297–306.
- Denison, S. H.** (2000). pH regulation of gene expression in fungi. *Fungal Genet. Biol.* **29**, 61–71.
- Dian, C., Baráth, P., Knaust, R., Mcsweeney, S., Moss, E., Hristova, M., Ambros, V. and Birse, D.** (2002). Overcoming protein instability problems during fusion protein cleavage. *Sci. News* 1–5.
- Diao, L., Dong, Q., Xu, Z., Yang, S., Zhou, J. and Freudl, R.** (2012). Functional implementation of the posttranslational SecB-SecA protein-targeting pathway in *Bacillus subtilis*. *Appl. Environ. Microbiol.* **78**, 651–659.
- Djamei, A. and Kahmann, R.** (2012). *Ustilago maydis*: Dissecting the Molecular Interface between Pathogen and Plant. *PLoS Pathog.* **8**, 11–14.
- Djamei, A., Schipper, K., Rabe, F., Ghosh, A., Vincon, V., Kahnt, J., Osorio, S., Tohge, T., Fernie, A. R., Feussner, I., et al.** (2011). Metabolic priming by a secreted fungal effector. *Nature* **478**, 395–398.
- Douglas, A. D., Williams, A. R., Illingworth, J. J., Kamuyu, G., Biswas, S., Goodman, A. L., Wyllie, D. H., Crosnier, C., Miura, K., Wright, G. J., et al.** (2011). The blood-stage malaria antigen PfRH5 is susceptible to vaccine-inducible cross-strain neutralizing antibody. *Nat. Commun.* **2**, doi:10.1038/ncomms1615.
- Douglas, A. D., Baldeviano, G. C., Lucas, C. M., Lugo-Roman, L. A., Crosnier, C., Bartholdson, S. J., Diouf, A., Miura, K., Lambert, L. E., Ventocilla, J. A., et al.** (2015). A PfRH5-based vaccine is efficacious against heterologous strain blood-stage *Plasmodium falciparum* infection in Aotus monkeys. *Cell Host Microbe* **17**, 130–139.
- Draper, S. J., Angov, E., Horii, T., Miller, L. H., Srinivasan, P., Theisen, M. and Biswas, S.** (2015). Recent advances in recombinant protein-based malaria vaccines. *Vaccine* **33**, 7433–7443.

- Ecker, D. M., Jones, S. D. and Levine, H. L.** (2015). The therapeutic monoclonal antibody market. *MAbs* **7**, 9–14.
- Economou, A., Christie, P. J., Fernandez, R. C., Palmer, T., Plano, G. V. and Pugsley, A. P.** (2006). Secretion by numbers: Protein traffic in prokaryotes. *Mol. Microbiol.* **62**, 308–319.
- Elia, G.** (2010). Protein biotinylation. In *Current protocols in Protein Science* (ed. Coligan, J. E.), p. 3.6.1–3.6.21. New York, NY: John Wiley & Sons, Inc.
- Ellgaard, L. and Helenius, A.** (2003). Quality control in the endoplasmic reticulum. *Nat. Rev. cell Biol.* **4**, 181–191.
- Ellgaard, L., McCaul, N., Chatsisvili, A. and Braakman, I.** (2016). Co- and Post-Translational Protein Folding in the ER. *Traffic* **17**, 615–638.
- Ewer, K. J., Sierra-Davidson, K., Salman, A. M., Illingworth, J. J., Draper, S. J., Biswas, S. and Hill, A. V. S.** (2015). Progress with viral vectored malaria vaccines: A multi-stage approach involving “unnatural immunity.” *Vaccine* **33**, 7444–7451.
- Feldbrügge, M., Kämper, J., Steinberg, G. and Kahmann, R.** (2004). Regulation of mating and pathogenic development in *Ustilago maydis*. *Curr. Opin. Microbiol.* **7**, 666–672.
- Feldbrügge, M., Kellner, R. and Schipper, K.** (2013). The biotechnological use and potential of plant pathogenic smut fungi. *Appl. Microbiol. Biotechnol.* **97**, 3253–3265.
- Fernandez, J. G. and Ingber, D. E.** (2013). Bioinspired Chitinous Material Solutions for Environmental Sustainability and Medicine. *Adv. Funct. Mater.* **23**, 4454–4466.
- Fernández-Álvarez, A., Elías-Villalobos, A. and Ibeas, J. I.** (2010). Protein glycosylation in the phytopathogen *Ustilago maydis*: From core oligosaccharide synthesis to the ER glycoprotein quality control system, a genomic analysis. *Fungal Genet. Biol.* **47**, 727–735.
- Fewell, S. W. and Brodsky, J. L.** (2009). Entry into the Endoplasmic Reticulum: Protein Translocation, Folding and Quality Control. In *Trafficking Inside Cells: Pathways, Mechanisms and Regulation* (ed. Segev, N.), pp. 119–142. New York, NY: Springer New York.
- Franken, A. C. W., Werner, E. R., Haas, H., Lokman, B. C., Van Den Hondel, C. A. M. J. J., Ram, A. F. J., De Weert, S. and Punt, P. J.** (2013). The role of coproporphyrinogen III oxidase and ferrochelatase genes in heme biosynthesis and regulation in *Aspergillus niger*. *Appl. Microbiol. Biotechnol.* **97**, 9773–9785.
- Fridy, P. C., Li, Y., Keegan, S., Thompson, M. K., Nudelman, I., Scheid, J. F., Oeffinger, M., Nussenzweig, M. C., Fenyö, D., Chait, B. T., et al.** (2014). A robust pipeline for rapid production of versatile nanobody repertoires. *Nat. Methods* **11**, 1253–60.
- Froude, J. W., Stiles, B., Pelat, T. and Thullier, P.** (2011). Antibodies for biodefense. *MAbs* **3**, 517–527.
- Gee, H. Y., Noh, S. H., Tang, B. L., Kim, K. H. and Lee, M. G.** (2011). Rescue of $\Delta f508$ -CFTR trafficking via a GRASP-dependent unconventional secretion pathway. *Cell* **146**, 746–760.
- Geiser, E., Przybilla, S. K., Friedrich, A., Buckel, W., Wierckx, N., Blank, L. M. and Bölker, M.** (2016a). *Ustilago maydis* produces itaconic acid via the unusual intermediate trans-aconitate. *Microb. Biotechnol.* **9**, 116–126.

- Geiser, E., Reindl, M. S., Blank, L. M., Feldbrügge, M., Wierckx, N. and Schipper, K.** (2016b). Activating intrinsic CAZymes of the smut fungus *Ustilago maydis* for the degradation of plant cell wall components. *Appl. Environ. Microbiol.* **49**, 5174–5185.
- Gellissen, G.** (2000). Heterologous protein production in methylotrophic yeasts. *Appl. Microbiol. Biotechnol.* **54**, 741–750.
- Gerngross, T. U.** (2004). Advances in the production of human therapeutic proteins in yeasts and filamentous fungi. *Nat. Biotechnol.* **22**, 1409–1414.
- Ghorai, S., Banik, S. P., Verma, D., Chowdhury, S., Mukherjee, S. and Khowala, S.** (2009). Fungal biotechnology in food and feed processing. *Food Res. Int.* **42**, 577–587.
- Gillissen, B., Bergemann, J., Sandmann, C., Schroeer, B., Bölker, M. and Kahmann, R.** (1992). A two-component regulatory system for self/non-self recognition in *Ustilago maydis*. *Cell* **68**, 647–657.
- Göhre, V., Vollmeister, E., Bölker, M. and Feldbrügge, M.** (2012). Microtubule-dependent membrane dynamics in *Ustilago maydis*: Trafficking and function of Rab5a-positive endosomes. *Commun. Integr. Biol.* **5**, 485–490.
- Graslund** (2008). Protein production and purification. *Nat. Methods* **5**, 135–146.
- Gusek, T. W., Wilson, D. B. and Kinsella, J. E.** (1988). Influence of carbon source on production of a heat stable protease from *Thermomonospora fusca* YX. *Appl. Microbiol. Biotechnol.* **28**, 80–84.
- Hamers-Casterman, C., Atarhouch, T., Muyldermans, S., Robinson, G., Hamers, C., Songa, E. B., Bendahman, N. and Hamers, R.** (1993). Naturally occurring antibodies devoid of light chains. *Nature* **363**, 446–448.
- Harmsen, M. M. and De Haard, H. J.** (2007). Properties, production, and applications of camelid single-domain antibody fragments. *Appl. Microbiol. Biotechnol.* **77**, 13–22.
- Hartmann, H. A., Krüger, J., Lottspeich, F. and Kahmann, R.** (1999). Environmental Signals Controlling Sexual Development of the Corn Smut Fungus *Ustilago maydis* through the Transcriptional Regulator Prf1. *Plant Cell* **11**, 1293–1306.
- Hata, T., Hayashi, R. and Doi, E.** (1967). Purification of Yeast Proteinases. *Agric. Biol. Chem.* **31**, 150–169.
- Heimel, K.** (2014). Unfolded protein response in filamentous fungi - implications in biotechnology. *Appl. Microbiol. Biotechnol.* **99**, 121–132.
- Hewald, S., Josephs, K. and Bölker, M.** (2005). Genetic Analysis of Biosurfactant Production in *Ustilago maydis*. *Appl. Environ. Microbiol.* **71**, 3033–3040.
- Hewald, S., Linne, U., Scherer, M., Marahiel, M. A., Kämper, J. and Bölker, M.** (2006). Identification of a gene cluster for biosynthesis of mannosylerythritol lipids in the basidiomycetous fungus *Ustilago maydis*. *Appl. Environ. Microbiol.* **72**, 5469–5477.
- Hjelm, H., Hjelm, K. and Sjöquist, J.** (1972). Protein a from *Staphylococcus aureus*. Its isolation by affinity chromatography and its use as an immunosorbent for isolation of immunoglobulins. *FEBS Lett.* **28**, 73–76.
- Hjerrild, K. A., Jin, J., Wright, K. E., Brown, R. E., Marshall, J. M., Labbé, G. M., Silk, S. E., Cherry, C. J., Clemmensen, S. B., Jørgensen, T., et al.** (2016). Production of full-length soluble *Plasmodium falciparum* RH5 protein vaccine using a *Drosophila melanogaster* Schneider 2 stable cell line system. *Sci. Rep.* **6**, DOI: 10.1038/srep30357.

- Hoang, H. D., Maruyama, J. I. and Kitamoto, K.** (2015). Modulating endoplasmic reticulum-Golgi cargo receptors for improving secretion of carrier-fused heterologous proteins in the filamentous fungus *Aspergillus oryzae*. *Appl. Environ. Microbiol.* **81**, 533–543.
- Hoffman, C. S. and Winston, F.** (1987). A ten-minute DNA preparation from yeast efficiently releases autonomous plasmids for transformation of *Escherichia coli*. *Gene* **57**, 267–272.
- Hoffman, M., Góra, M. and Rytka, J.** (2003). Identification of rate-limiting steps in yeast heme biosynthesis. *Biochem. Biophys. Res. Commun.* **310**, 1247–1253.
- Holliday, R.** (1964). The Induction of Mitotic Recombination By Mitomycin C in *Ustilago* and *Saccharomyces*. *Genetics* **50**, 323–335.
- Holliday, R.** (1974). Molecular aspects of genetic exchange and gene conversion. *Genetics* **78**, 273–287.
- Huang, C. J., Lin, H. and Yang, X. M.** (2012). Industrial production of recombinant therapeutics in *Escherichia coli* and its recent advancements. *J. Ind. Microbiol. Biotechnol.* **39**, 383–399.
- Hußnätter, K. P.** (2015). Establishing new regulatory elements for protein expression in *Ustilago maydis*. *Bachelor's thesis*. Heinrich Heine University Düsseldorf.
- Idiris, A., Tohda, H., Bi, K., Isoai, A., Kumagai, H. and Giga-Hama, Y.** (2006). Enhanced productivity of protease-sensitive heterologous proteins by disruption of multiple protease genes in the fission yeast *Schizosaccharomyces pombe*. *Appl. Microbiol. Biotechnol.* **73**, 404–420.
- Iyer, J., Grüner, A. C., Rénia, L., Snounou, G. and Preiser, P. R.** (2007). Invasion of host cells by malaria parasites: A tale of two protein families. *Mol. Microbiol.* **65**, 231–249.
- Jackson, D. A., Symons, R. H. and Berg, P.** (1972). Biochemical method for inserting new genetic information into DNA of Simian Virus 40: circular SV40 DNA molecules containing lambda phage genes and the galactose operon of *Escherichia coli*. *Proc. Natl. Acad. Sci. U. S. A.* **69**, 2904–2909.
- Jankowski, S.** (2013). Charakterisierung der unkonventionell sekretierten Endochitinase Cts1 in *Ustilago maydis*. *Master's thesis*. Heinrich Heine University Düsseldorf.
- Johnson, N., Powis, K. and High, S.** (2013). Post-translational translocation into the endoplasmic reticulum. *Biochim. Biophys. Acta - Mol. Cell Res.* **1833**, 2403–2409.
- Joosten, V., Lokman, C., van den Hondel, C. A. and Punt, P. J.** (2003). The production of antibody fragments and antibody fusion proteins by yeasts and filamentous fungi. *Microb. Cell Fact.* **2**, 1.
- Joosten, V., Roelofs, M. S., Van Den Dries, N., Goosen, T., Verrips, C. T., Van Den Hondel, C. A. M. J. J. and Lokman, B. C.** (2005a). Production of bifunctional proteins by *Aspergillus awamori*: Llama variable heavy chain antibody fragment (VHH) R9 coupled to *Arthomyces ramosus* peroxidase (ARP). *J. Biotechnol.* **120**, 347–359.
- Joosten, V., Gouka, R. J., Van Den Hondel, C. A. M. J. J., Verrips, C. T. and Lokman, B. C.** (2005b). Expression and production of llama variable heavy-chain antibody fragments (VHHs) by *Aspergillus awamori*. *Appl. Microbiol. Biotechnol.* **66**, 384–392.
- Kaiser, J.** (2013). Unconventional Vaccine Shows Promise Against Malaria. *Science* **341**, 605.

- Kakeshtia, H., Kageyama, Y., Ara, K., Ozaki, K. and Nakamura, K.** (2010). Enhanced Extracellular Production of Heterologous Proteins in *Bacillus subtilis* by Deleting the C-terminal Region of the SecA Secretory Machinery. *Mol. Biotechnol.* **46**, 250–257.
- Kämper, J.** (2004). A PCR-based system for highly efficient generation of gene replacement mutants in *Ustilago maydis*. *Mol. Genet. Genomics* **271**, 103–110.
- Kämper, J., Kahmann, R., Bölker, M., Ma, L.-J., Brefort, T., Saville, B. J., Banuett, F., Kronstad, J. W., Gold, S. E., Müller, O., et al.** (2006). Insights from the genome of the biotrophic fungal plant pathogen *Ustilago maydis*. *Nature* **444**, 97–101.
- Kapust, R. B., Tözsér, J., Copeland, T. D. and Waugh, D. S.** (2002). The P1' specificity of tobacco etch virus protease. *Biochem. Biophys. Res. Commun.* **294**, 949–955.
- Kavšček, M., Stražar, M., Curk, T., Natter, K. and Petrovič, U.** (2015). Yeast as a cell factory: current state and perspectives. *Microb. Cell Fact.* **14**, 94.
- Keen, H., Pickup, J. C., Bilous, R. W., Glynne, A., Viberti, G. C., Jarrett, R. J. and Marsden, R.** (1980). Human Insulin Produced By Recombinant DNA Technology: Safety and Hypoglycæmic Potency in Healthy Men. *Lancet* **316**, 398–401.
- Kensy, F., Zang, E., Faulhammer, C., Tan, R.-K. and Büchs, J.** (2009). Validation of a high-throughput fermentation system based on online monitoring of biomass and fluorescence in continuously shaken microtiter plates. *Microb. Cell Fact.* **8**, 31.
- Kerr, J. S. and Wright, G. J.** (2012). Avidity-based Extracellular Interaction Screening (AVEXIS) for the Scalable Detection of Low-affinity Extracellular Receptor-Ligand Interactions. *J. Vis. Exp.* **61**, e3881.
- Khan, K. H.** (2013). Gene expression in mammalian cells and its applications. *Adv. Pharm. Bull.* **3**, 257–263.
- Khow, O. and Suntrarachun, S.** (2012). Strategies for production of active eukaryotic proteins in bacterial expression system. *Asian Pac. J. Trop. Biomed.* **2**, 159–162.
- Khrunyk, Y., Münch, K., Schipper, K., Lupas, A. N. and Kahmann, R.** (2010). The use of FLP-mediated recombination for the functional analysis of an effector gene family in the biotrophic smut fungus *Ustilago maydis*. *New Phytol.* **187**, 957–968.
- Kim, J., Cantor, A. B., Orkin, S. H. and Wang, J.** (2009). Use of *in vivo* biotinylation to study protein-protein and protein-DNA interactions in mouse embryonic stem cells. *Nat Protoc* **4**, 506–517.
- Kimple, M. E., Brill, A. L. and Pasker, R. L.** (2015). Overview of Affinity Tags for Protein Purification. *Curr. Protoc. protein Sci.* **73**, 608–616.
- Kirk, O., Borchert, T. V. and Fuglsang, C. C.** (2002). Industrial enzyme applications. *Curr. Opin. Biotechnol.* **13**, 345–351.
- Kleizen, B. and Braakman, I.** (2004). Protein folding and quality control in the endoplasmic reticulum. *Curr. Opin. Cell Biol.* **16**, 343–349.
- Klement, T., Milker, S., Jager, G., Grande, P. M., Dominguez de Maria, P. and Büchs, J.** (2012). Biomass pretreatment affects *Ustilago maydis* in producing itaconic acid. *Microb. Cell Fact.* **11**, 43.
- Knabben, I., Regestein, L., Grumbach, C., Steinbusch, S., Kunze, G. and Büchs, J.** (2010). Online determination of viable biomass up to very high cell densities in *Arxula adenivorans* fermentations using an impedance signal. *J. Biotechnol.* **149**, 60–66.

- Knoll, A., Maier, B., Tscherrig, H. and Büchs, J.** (2005). The oxygen mass transfer, carbon dioxide inhibition, heat removal, and the energy and cost efficiencies of high pressure fermentation. *Adv. Biochem. Eng. Biotechnol.* **92**, 77–99.
- Knoll, A., Bartsch, S., Husemann, B., Engel, P., Schroer, K., Ribeiro, B., Stöckmann, C., Seletzky, J. and Büchs, J.** (2007). High cell density cultivation of recombinant yeasts and bacteria under non-pressurized and pressurized conditions in stirred tank bioreactors. *J. Biotechnol.* **132**, 167–179.
- Koepke, J., Kaffarnik, F., Haag, C., Zarnack, K., Luscombe, N. M., König, J., Ule, J., Kellner, R., Begerow, D. and Feldbrügge, M.** (2011). The RNA-binding protein Rrm4 is essential for efficient secretion of endochitinase Cts1. *Mol. Cell. Proteomics* **10**, doi:10.1074/mcp.M111.011213–1.
- Krainer, F. W., Capone, S., Jäger, M., Vogl, T., Gerstmann, M., Glieder, A., Herwig, C. and Spadiut, O.** (2015). Optimizing cofactor availability for the production of recombinant heme peroxidase in *Pichia pastoris*. *Microb. Cell Fact.* **14**, 4.
- Krainer, F. W., Darnhofer, B., Birner-Gruenberger, R. and Glieder, A.** (2016). Recombinant production of a peroxidase-protein G fusion protein in *Pichia pastoris*. *J. Biotechnol.* **219**, 24–27.
- La Venuta, G., Zeitler, M., Steringer, J. P., Müller, H. M. and Nickel, W.** (2015). The startling properties of fibroblast growth factor 2: How to exit mammalian cells without a signal peptide at hand. *J. Biol. Chem.* **290**, 27015–27020.
- Laemmli, U. K.** (1970). Cleavage of Structural Proteins during Assembly of Head of Bacteriophage-T4. *Nature* **227**, 680–685.
- Langner, T.** (2015). Charakterisierung der chitinolytischen Maschinerie aus *Ustilago maydis*. *Dissertation*. Heinrich Heine University Düsseldorf.
- Langner, T., Öztürk, M., Hartmann, S., Cord-Landwehr, S., Moerschbacher, B., Walton, J. D. and Göhre, V.** (2015). Chitinases are essential for cell separation in *Ustilago maydis*. *Eukaryot. Cell* **14**, 846–857.
- Lauwereys, M., Ghahroudi, M. A., Desmyter, A., Kinne, J., Hölzer, W., De Genst, E., Wyns, L. and Muyldermans, S.** (1998). Potent enzyme inhibitors derived from dromedary heavy-chain antibodies. *EMBO J.* **17**, 3512–3520.
- Lee, M. C. S., Miller, E. A., Goldberg, J., Orci, L. and Schekman, R.** (2004). Bi-Directional Protein Transport Between the ER and Golgi. *Annu. Rev. Cell Dev. Biol.* **20**, 87–123.
- Leenaars, M. and Hendriksen, C. F. M.** (2005). Critical Steps in the Production of Polyclonal and Monoclonal Antibodies: Evaluation and Recommendations. *Ilar J.* **46**, 269–279.
- Lesage, G. and Bussey, H.** (2006). Cell wall assembly in *Saccharomyces cerevisiae*. *Microbiol. Mol. Biol. Rev.* **70**, 317–43.
- Li, F., Wang, Y., Gong, K., Wang, Q., Liang, Q. and Qi, Q.** (2014). Constitutive expression of RyhB regulates the heme biosynthesis pathway and increases the 5-aminolevulinic acid accumulation in *Escherichia coli*. *FEMS Microbiol. Lett.* **350**, 209–215.
- Liu, J. K. H.** (2014). The history of monoclonal antibody development - Progress, remaining challenges and future innovations. *Ann. Med. Surg.* **3**, 113–116.
- Liu, H. S., Jan, M. S., Chou, C. K., Chen, P. H. and Ke, N. J.** (1999). Is green fluorescent protein toxic to the living cells? *Biochem. Biophys. Res. Commun.* **260**, 712–717.

- Loubradou, G., Brachmann, A., Feldbrügge, M. and Kahmann, R.** (2001). A homologue of the transcriptional repressor Ssn6p antagonizes cAMP signalling in *Ustilago maydis*. *Mol. Microbiol.* **40**, 719–730.
- Ma, J., Kearney, J. F. and Hendershot, L. M.** (1990). Association of transport-defective light chains with immunoglobulin heavy chain binding protein. *Mol. Immunol.* **27**, 623–630.
- Maksimenko, O. G., Deykin, A. V., Khodarovich, Y. M. and Georgiev, P. G.** (2013). Use of Transgenic Animals in Biotechnology: Prospects and Problems. *Acta Naturae* **5**, 33–46.
- Mamat, U., Wilke, K., Bramhill, D., Schromm, A. B., Lindner, B., Kohl, T. A., Corchero, J. L., Villaverde, A., Schaffer, L., Head, S. R., et al.** (2015). Detoxifying *Escherichia coli* for endotoxin-free production of recombinant proteins. *Microb. Cell Fact.* **14**, 57.
- Matei, A. and Doehlemann, G.** (2016). Cell biology of corn smut disease: *Ustilago maydis* as a model for biotrophic interactions. *Curr. Opin. Microbiol.* **34**, 60–66.
- Mattanovich, D., Gasser, B., Hohenblum, H. and Sauer, M.** (2004). Stress in recombinant protein producing yeasts. *J. Biotechnol.* **113**, 121–135.
- Mattanovich, D., Branduardi, P., Dato, L., Gasser, B., Sauer, M. and Porro, D.** (2012). Recombinant Protein Production in Yeasts. In *Recombinant Gene Expression* (ed. Lorence, A.), pp. 329–358. Totowa, NJ: Humana Press.
- McCotter, S. W., Horianopoulos, L. C. and Kronstad, J. W.** (2016). Regulation of the fungal secretome. *Curr. Genet.* **62**, 533–545.
- Mead, J. A. R., Smith, J. N. and Williams, R. T.** (1967). Fluorimetric determination of β -Glucuronidase. *Proc. Biochem. Soc.* **104**, 35.
- Messens, J. and Collet, J.-F.** (2006). Pathways of disulfide bond formation in *Escherichia coli*. *Ijbc* **38**, 1050–1062.
- Michaelis, S.** (1993). STE6, the yeast α -factor transporter. *Semin Cell Biol* **4**, 17–27.
- Miller, L. H., Ackerman, H. C., Su, X. and Wellems, T. E.** (2013). Malaria biology and disease pathogenesis: insights for new treatments. *Nat. Med.* **19**, 156–167.
- Moayeri, M., Leysath, C. E., Tremblay, J. M., Vrentas, C., Crown, D., Leppla, S. H. and Shoemaker, C. B.** (2015). A heterodimer of a VHH (variable domains of camelid heavy chain-only) antibody that inhibits anthrax toxin cell binding linked to a VHH antibody that blocks oligomer formation is highly protective in an anthrax spore challenge model. *J. Biol. Chem.* **290**, 6584–6595.
- Mukherjee, J., Tremblay, J. M., Leysath, C. E., Ofori, K., Baldwin, K., Feng, X., Bedenice, D., Webb, R. P., Wright, P. M., Smith, L. A., et al.** (2012). A novel strategy for development of recombinant antitoxin therapeutics tested in a mouse botulism model. *PLoS One* **7**, e29941.
- Muyldermans, S.** (2001). Single domain camel antibodies: Current status. *Rev. Mol. Biotechnol.* **74**, 277–302.
- Muyldermans, S., Atarhouch, T., Saldanha, J., Barbosa, J. A. R. G. and Hamers, R.** (1994). Sequence and structure of VH domain from naturally occurring camel heavy chain immunoglobulins lacking light chains. *Protein Eng.* **7**, 1129–1135.
- Nabel, G. J.** (2013). Designing tomorrow's vaccines. *N. Engl. J. Med.* **368**, 551–560.

- Najafpour, G., Younesi, H. and Ku Ismail, K. S.** (2004). Ethanol fermentation in an immobilized cell reactor using *Saccharomyces cerevisiae*. *Bioresour. Technol.* **92**, 251–260.
- Nakajima, M., Atsumi, K., Kifune, K., Miura, K. and Kanamaru, H.** (1986). Chitin is an effective material for sutures. *Jpn. J. Surg.* **16**, 418–424.
- Narciso, J. E. T., Uy, I. D. C., Cabang, A. B., Chavez, J. F. C., Pablo, J. L. B., Padilla-concepcion, G. P. and Padlan, E. A.** (2012). Anatomy of the antibody molecule: a continuing analysis based on high- resolution crystallographic structures. *Philipp. Sci. Lett.* **5**, 63–89.
- Natale, P., Brüser, T. and Driessen, A. J. M.** (2008). Sec- and Tat-mediated protein secretion across the bacterial cytoplasmic membrane - Distinct translocases and mechanisms. *Biochim. Biophys. Acta - Biomembr.* **1778**, 1735–1756.
- Navarro, D., Rosso, M.-N., Haon, M., Olivé, C., Bonnin, E., Lesage-Meessen, L., Chevret, D., Coutinho, P. M., Henrissat, B. and Berrin, J.-G.** (2014). Fast solubilization of recalcitrant cellulosic biomass by the basidiomycete fungus *Laetisaria arvalis* involves successive secretion of oxidative and hydrolytic enzymes. *Biotechnol. Biofuels* **7**, 143.
- Nickel, W.** (2003). The mystery of nonclassical protein secretion: A current view on cargo proteins and potential export routes. *Eur. J. Biochem.* **270**, 2109–2119.
- Nickel, W.** (2005). Unconventional secretory routes: Direct protein export across the plasma membrane of mammalian cells. *Traffic* **6**, 607–614.
- Nickel, W.** (2007). Unconventional secretion: an extracellular trap for export of fibroblast growth factor 2. *J. Cell Sci.* **120**, 2295–2299.
- Nickel, W. and Rabouille, C.** (2008). Mechanisms of regulated unconventional protein secretion. *Nat. Rev. Mol. Cell Biol.* **10**, 148–155.
- Novy, R., Drott, D., Yaeger, K. and Mierendorf, R.** (2001). Overcoming the codon bias of *E. coli* for enhanced protein expression. *Innovations* **12**, 4–6.
- O'Donnell, D., Wang, L., Xu, J., Ridgway, D., Gu, T. and Moo-Young, M.** (2001). Enhanced heterologous protein production in *Aspergillus niger* through pH control of extracellular protease activity. *Biochem. Eng. J.* **8**, 187–193.
- Ord, R. L., Rodriguez, M., Yamasaki, T., Takeo, S., Tsuboi, T. and Lobo, C. A.** (2012). Targeting sialic acid dependent and independent pathways of invasion in *Plasmodium falciparum*. *PLoS One* **7**, e30251.
- Ord, R. L., Caldeira, J. C., Rodriguez, M., Noe, A., Chackerian, B., Peabody, D. S., Gutierrez, G. and Lobo, C. A.** (2014). A malaria vaccine candidate based on an epitope of the *Plasmodium falciparum* RH5 protein. *Malar. J.* **13**, 326.
- Page, M. and Thorpe, R.** (2009). Purification of IgG Using Protein A or Protein G. In *The Protein Protocols Handbook* (ed. Walker, J. M.), pp. 733–734. Totowa, NJ: Humana Press.
- Pina, A. S., Lowe, C. R. and Roque, A. C. A.** (2014). Challenges and opportunities in the purification of recombinant tagged proteins. *Biotechnol. Adv.* **32**, 366–381.
- Pohlmann, T., Baumann, S., Haag, C., Albrecht, M. and Feldbrügge, M.** (2015). A FYVE zinc finger domain protein specifically links mRNA transport to endosome trafficking. *Elife* **4**, e06041.

- Pringle, J. R.** (1975). Methods for Avoiding Proteolytic Artefacts in Studies of Enzymes and Other Proteins from Yeasts. *Methods Cell Biol.* **12**, 149–184.
- Puigbò, P., Guzmán, E., Romeu, A. and Garcia-Vallvé, S.** (2007). OPTIMIZER: A web server for optimizing the codon usage of DNA sequences. *Nucleic Acids Res.* **35**, 126–131.
- Punt, P. J., van Biezen, N., Conesa, A., Albers, A., Mangnus, J. and van den Hondel, C.** (2002). Filamentous fungi as cell factories for heterologous protein production. *Trends Biotechnol.* **20**, 200–206.
- Puxbaum, V., Mattanovich, D. and Gasser, B.** (2015). Quo vadis? The challenges of recombinant protein folding and secretion in *Pichia pastoris*. *Appl. Microbiol. Biotechnol.* **99**, 2925–2938.
- Rabouille, C., Malhotra, V. and Nickel, W.** (2012). Diversity in unconventional protein secretion. *J. Cell Sci.* **125**, 5251–5255.
- Raikhel, N. V., Lee, H. I. and Broekaert, W. F.** (1993). Structure and Function of Chitin-Binding Proteins. *Annu. Rev. Plant Physiol. Plant Mol. Biol.* **44**, 591–615.
- Rajakylä, E. and Paloposki, M.** (1983). Determination of sugars (and betaine) in molasses by high-performance liquid chromatography. *J. Chromatogr. A* **282**, 595–602.
- Reddy, K. S., Amlabu, E., Pandey, A. K., Mitra, P., Chauhan, V. S. and Gaur, D.** (2015). Multiprotein complex between the GPI-anchored CyRPA with PfRH5 and PfRipr is crucial for *Plasmodium falciparum* erythrocyte invasion. *Proc. Natl. Acad. Sci.* **112**, 1179–1184.
- Reindl, M. S.** (2013). Steigerung des Expressionslevels der Endochitinase Cts1 zur Optimierung der unkonventionellen Proteinsekretion in *Ustilago maydis*. *Bachelor's thesis*. Heinrich Heine University Düsseldorf.
- Reindl, M. S.** (2016). Using unconventional secretion for the export of heterologous, cofactor-dependent enzymes in *Ustilago maydis*. *Master's thesis*. Heinrich Heine University Düsseldorf.
- Richards, H. A., Han, C.-T., Hopkins, R. G., Failla, M. L., Ward, W. W. and Stewart, C. N.** (2003). Safety assessment of recombinant green fluorescent protein orally administered to weaned rats. *J. Nutr.* **133**, 1909–1912.
- Richman, D. D., Cleveland, P. H., Oxman, M. N., Johnson, K. M., Cleveland, P. H., Michael, N. and Johnson, K. M.** (1982). The binding of staphylococcal protein A by the sera of different animal species. *J. Immunol.* **182**, 2300–2305.
- Rigaut, G., Shevchenko, A., Rutz, B., Wilm, M., Mann, M. and Séraphin, B.** (1999). A generic protein purification method for protein complex characterization and proteome exploration. *Nat. Biotechnol.* **17**, 1030–1032.
- Robert, X. and Gouet, P.** (2014). Deciphering key features in protein structures with the new ENDscript server. *Nucleic Acids Res.* **42**, 320–324.
- Rodolfi, L., Zittelli, G. C., Barsanti, L., Rosati, G. and Tredici, M. R.** (2003). Growth medium recycling in *Nannochloropsis* sp. mass cultivation. *Biomol. Eng.* **20**, 243–248.
- Rodriguez, M., Lustigman, S., Montero, E., Oksov, Y. and Lobo, C. A.** (2008). PfRH5: A novel reticulocyte-binding family homolog of *Plasmodium falciparum* that binds to the erythrocyte, and an investigation of its receptor. *PLoS One* **3**, e3300.
- Rodríguez Estévez, M.** (2016). Establishing novel glycolipid variants in *Ustilago maydis*. *Master's thesis*. Heinrich Heine University Düsseldorf.

- Roque, A. C. A., Lowe, C. R. and Taipa, M. Â.** (2004). Antibodies and genetically engineered related molecules: Production and purification. *Biotechnol. Prog.* **20**, 639–654.
- Rothbauer, U., Zolghadr, K., Muyldermans, S., Schepers, A., Cardoso, M. C. and Leonhardt, H.** (2007). A Versatile Nanotrap for Biochemical and Functional Studies with Fluorescent Fusion Proteins. *Mol. Cell. Proteomics* **7**, 282–289.
- RTS S Clinical Trials Partnership, T.** (2012). The Phase 3 Trial of RTS,S/AS01 Malaria Vaccine in African Infants. *N. Engl. J. Med.* **367**, 2284–2295.
- Rubartelli, A., Cozzolino, F., Talio, M. and Sitia, R.** (1990). A novel secretory pathway for interleukin-1 β , a protein lacking a signal sequence. *EMBO J.* **9**, 1503–1510.
- Saiki, R. K., Scharf, S. J., Faloona, F., Mullis, K. B., Horn, G. T., Erlich, H. A. and Arnheim, N.** (1985). Enzymatic amplification of β -Globin genomic sequences and restriction site analysis for diagnosis of sickle cell anemia. *Science*. **230**, 1350–1354.
- Sambrook, J., Fritsch, E. F. and Maniatis, T.** (1989). Molecular Cloning: A Laboratory Manual. New York, NY: Cold Spring Harbor Laboratory Press.
- Sánchez-Sampedro, L., Perdiguero, B., Mejías-Pérez, E., García-Arriaza, J., Di Pilato, M. and Esteban, M.** (2015). The evolution of poxvirus vaccines. *Viruses* **7**, 1726–1803.
- Sarkari, P.** (2014). Optimizing the expression of antibody formats in protease-deficient *Ustilago maydis* strains. *Dissertation*. Heinrich Heine University Düsseldorf.
- Sarkari, P., Reindl, M., Stock, J., Müller, O., Kahmann, R., Feldbrügge, M. and Schipper, K.** (2014). Improved expression of single-chain antibodies in *Ustilago maydis*. *J. Biotechnol.* **191**, 165–175.
- Scheidle, M., Dittrich, B., Klinger, J., Ikeda, H., Klee, D. and Büchs, J.** (2011). Controlling pH in shake flasks using polymer-based controlled-release discs with pre-determined release kinetics. *BMC Biotechnol.* **11**, 25.
- Schmidt, F. R.** (2004). Recombinant expression systems in the pharmaceutical industry. *Appl. Microbiol. Biotechnol.* **65**, 363–372.
- Schmidt, T. G. M., Koepke, J., Frank, R. and Skerra, A.** (1996). Molecular Interaction Between the Strep-tag Affinity Peptide and its Cognate Target, Streptavidin. *J. Mol. Biol.* **255**, 753–766.
- Schotman, H., Karhinen, L. and Rabouille, C.** (2008). dGRASP-Mediated Noncanonical Integrin Secretion Is Required for *Drosophila* Epithelial Remodeling. *Dev. Cell* **14**, 171–182.
- Schulz, B., Banuett, F., Dahl, M., Schlesinger, R., Schäfer, W., Martin, T., Herskowitz, I. and Kahmann, R.** (1990). The b alleles of *U. maydis*, whose combinations program pathogenic development, code for polypeptides containing a homeodomain-related motif. *Cell* **60**, 295–306.
- Schwarz, F. and Aebi, M.** (2011). Mechanisms and principles of N-linked protein glycosylation. *Curr. Opin. Struct. Biol.* **21**, 576–582.
- Sha, S., Agarabi, C., Brorson, K., Lee, D. and Yoon, S.** (2016). N-Glycosylation Design and Control of Therapeutic Monoclonal Antibodies. *Trends Biotechnol.* **34**, 835–846.
- Sieben, M., Steinhorn, G., Müller, C., Fuchs, S., Chin, L. A., Regestein, L. and Büchs, J.** (2016). Testing plasmid stability of *Escherichia coli* using the Continuously Operated Shaken BIOreactor System. *Biotechnol. Prog.* doi:10.1002/btpr.2341.

- Siller, E., DeZwaan, D. C., Anderson, J. F., Freeman, B. C. and Barral, J. M.** (2010). Slowing Bacterial Translation Speed Enhances Eukaryotic Protein Folding Efficiency. *J. Mol. Biol.* **396**, 1310–1318.
- Sims, G. K. and Wander, M. M.** (2002). Proteolytic activity under nitrogen or sulfur limitation. *Appl. Soil Ecol.* **19**, 217–221.
- Sinha, J., Plantz, B. A., Inan, M. and Meagher, M. M.** (2005). Causes of proteolytic degradation of secreted recombinant proteins produced in methylotrophic yeast *Pichia pastoris*: Case study with recombinant ovine interferon- τ . *Biotechnol. Bioeng.* **89**, 102–112.
- Skelly, J. P.** (2010). A history of biopharmaceutics in the Food and Drug Administration 1968–1993. *AAPS J.* **12**, 44–50.
- Sony Reddy, K., Pandey, A. K., Singh, H., Sahar, T., Emmanuel, A., Chitnis, C. E., Chauhan, V. S. and Gaur, D.** (2014). Bacterially expressed full-length recombinant *Plasmodium falciparum* RH5 protein binds erythrocytes and elicits potent strain-transcending parasite-neutralizing antibodies. *Infect. Immun.* **82**, 152–164.
- Southern, E. M.** (1975). Detection of specific sequences among DNA fragments separated by gel electrophoresis. *J. Mol. Biol.* **98**, 503–517.
- Spadiut, O. and Herwig, C.** (2013). Production and purification of the multifunctional enzyme horseradish peroxidase. *Pharm Bioprocess* **1**, 283–295.
- Spadiut, O., Capone, S., Krainer, F., Glieder, A. and Herwig, C.** (2014). Microbials for the production of monoclonal antibodies and antibody fragments. *Trends Biotechnol.* **32**, 54–60.
- Spellig, T., Bottin, A. and Kahmann, R.** (1996). Green fluorescent protein (GFP) as a new vital marker in the phytopathogenic fungus *Ustilago maydis*. *Mol. Gen. Genet.* **252**, 503–509.
- Steinberg, G. and Schuster, M.** (2011). The dynamic fungal cell. *Fungal Biol. Rev.* **25**, 14–37.
- Steringer, J. P., Müller, H. M. and Nickel, W.** (2014). Unconventional Secretion of Fibroblast Growth Factor 2-A Novel Type of Protein Translocation across Membranes? *J. Mol. Biol.* **427**, 1202–1210.
- Stock, J.** (2013). Etablierung eines neuartigen Protein-Expressionssystems in *Ustilago maydis*. *Dissertation*. Heinrich Heine University Düsseldorf.
- Stock, J., Sarkari, P., Kreibich, S., Brefort, T., Feldbrügge, M. and Schipper, K.** (2012). Applying unconventional secretion of the endochitinase Cts1 to export heterologous proteins in *Ustilago maydis*. *J. Biotechnol.* **161**, 80–91.
- Stock, J., Terfrüchte, M. and Schipper, K.** (2016). A Reporter System to Study Unconventional Secretion of Proteins Avoiding N-Glycosylation in *Ustilago maydis*. In *Unconventional Protein Secretion: Methods and Protocols* (ed. Pompa, A. and Marchis, F. De), pp. 149–160. New York, NY: Springer New York.
- Stöckmann, C., Palmen, T. G., Schroer, K., Kunze, G., Gellissen, G. and Büchs, J.** (2014). Definition of culture conditions for *Arxula adenivorans*, a rational basis for studying heterologous gene expression in this dimorphic yeast. *J. Ind. Microbiol. Biotechnol.* **41**, 965–976.

- Stollewerk, D.** (2015). The role of carboxypeptidases in extracellular protein degradation in *Ustilago maydis*. *Master's thesis*. Heinrich Heine University Düsseldorf.
- Streltsov, V. and Nuttall, S.** (2005). Do sharks have a new antibody lineage? *Immunol. Lett.* **97**, 159–160.
- Tang, H., Bao, X., Shen, Y., Song, M., Wang, S., Wang, C. and Hou, J.** (2015). Engineering protein folding and translocation improves heterologous protein secretion in *Saccharomyces cerevisiae*. *Biotechnol. Bioeng.* **112**, 1872–1882.
- Tattersall, R. B.** (1995). A force of magical activity: the introduction of insulin treatment in Britain 1922–1926. *Diabet. Med.* **12**, 739–755.
- Teichmann, B., Linne, U., Hewald, S., Marahiel, M. A. and Bölker, M.** (2007). A biosynthetic gene cluster for a secreted cellobiose lipid with antifungal activity from *Ustilago maydis*. *Mol. Microbiol.* **66**, 525–533.
- Terfrüchte, M.** (2013). Expression des Malaria-Antigens PfRH5 in *Ustilago maydis*. *Master's thesis*. Heinrich Heine University Düsseldorf.
- Terfrüchte, M., Joehnk, B., Fajardo-Somera, R., Braus, G. H., Riquelme, M., Schipper, K. and Feldbrügge, M.** (2014). Establishing a versatile Golden Gate cloning system for genetic engineering in fungi. *Fungal Genet. Biol.* **62**, 1–10.
- Terpe, K.** (2003). Overview of tag protein fusions. *Appl. Microbiol. Biotechnol.* **60**, 523–533.
- Terpe, K.** (2006). Overview of bacterial expression systems for heterologous protein production: From molecular and biochemical fundamentals to commercial systems. *Appl. Microbiol. Biotechnol.* **72**, 211–222.
- Thomas, D. R., Penney, C. A., Majumder, A. and Walmsley, A. M.** (2011). Evolution of plant-made pharmaceuticals. *Int. J. Mol. Sci.* **12**, 3220–3236.
- Tropea, J. E., Cherry, S. and Waugh, D. S.** (2009). High Throughput Protein Expression and Purification. *Methods Mol. Biol.* **498**, 297–307.
- Valderrama-Rincon, J. D., Fisher, A. C., Merritt, J. H., Fan, Y., Reading, A., Chhiba, K., Heiss, C., Azadi, P., Aebi, M. and Delisa, M. P.** (2012). An engineered eukaryotic protein glycosylation pathway in *Escherichia coli*. *Nat Chem Biol* **8**, 434–436.
- van den Hombergh, J. P., Sollewijn Gelpke, M. D., van de Vondervoort, P. J., Buxton, F. P. and Visser, J.** (1997). Disruption of three acid proteases in *Aspergillus niger* - Effects on protease spectrum, intracellular proteolysis, and degradation of target proteins. *Eur. J. Biochem.* **247**, 605–613.
- van Dijl, J. M. and Hecker, M.** (2013). *Bacillus subtilis*: from soil bacterium to super-secreting cell factory. *Microb. Cell Fact.* **12**, 3.
- Veitch, N. C.** (2004). Horseradish peroxidase: A modern view of a classic enzyme. *Phytochemistry* **65**, 249–259.
- Velur Selvamani, R. S., Friehs, K. and Flaschel, E.** (2014). Extracellular recombinant protein production under continuous culture conditions with *Escherichia coli* using an alternative plasmid selection mechanism. *Bioprocess Biosyst. Eng.* **37**, 401–413.
- Vembar, S. S. and Brodsky, J. L.** (2008). One step at a time: endoplasmic reticulum-associated degradation. *Nat Rev Mol Cell Biol* **9**, 944–957.

- Vollmeister, E., Schipper, K., Baumann, S., Haag, C., Pohlmann, T., Stock, J. and Feldbrügge, M.** (2012a). Fungal development of the plant pathogen *Ustilago maydis*. *FEMS Microbiol. Rev.* **36**, 59–77.
- Vollmeister, E., Schipper, K. and Feldbrügge, M.** (2012b). Microtubule-dependent mRNA transport in the model microorganism *Ustilago maydis*. *RNA Biol.* **9**, 261–268.
- Volz, J. C., Yap, A., Sisquella, X., Thompson, J. K., Lim, N. T. Y., Whitehead, L. W., Chen, L., Lampe, M., Tham, W.-H., Wilson, D., et al.** (2016). Essential Role of the PfRh5/PfRipr/CyRPA Complex during *Plasmodium falciparum*. *Cell Host Microbe* **20**, 60–71.
- Walsh, G. and Jefferis, R.** (2006). Post-translational modifications in the context of therapeutic proteins. *Nat. Biotechnol.* **24**, 1241–1252.
- Walter, P. and Lingappa, V.** (1986). Translocation Across the Endoplasmic Reticulum Membrane. *Annu. Rev. Cell Biol.* **2**, 499–516.
- Walter, P., Gilmore, R., Muller, M., Blobel, G. and Campbell, P. N.** (1982). The Protein Translocation Machinery of the Endoplasmic Reticulum. *Philos. Trans. R. Soc. London. B, Biol. Sci.* **300**, 225–228.
- Wanaguru, M., Crosnier, C., Johnson, S., Rayner, J. C. and Wright, G. J.** (2013). Biochemical analysis of the *Plasmodium falciparum* erythrocyte-binding antigen-175 (EBA175)-glycophorin-A interaction; Implications for vaccine design. *J. Biol. Chem.* **288**, 32106–32117.
- Wang, Q. M. and Johnson, R. B.** (2001). Activation of human rhinovirus-14 3C protease. *Virology* **280**, 80–86.
- Wang, L., Ridgway, D., Gu, T. and Moo-Young, M.** (2005). Bioprocessing strategies to improve heterologous protein production in filamentous fungal fermentations. *Biotechnol. Adv.* **23**, 115–129.
- Ward, O. P.** (2012). Production of recombinant proteins by filamentous fungi. *Biotechnol. Adv.* **30**, 1119–1139.
- Waugh, D. S.** (2011). An overview of enzymatic reagents for the removal of affinity tags. *Protein Expr. Purif.* **80**, 283–293.
- Wedlich-Söldner, R., Straube, A., Friedrich, M. W. and Steinberg, G.** (2002). A balance of KIF1A-like kinesin and dynein organizes early endosomes in the fungus *Ustilago maydis*. *EMBO J.* **21**, 2946–2957.
- Weilhammer, C. and Blass, E.** (1994). Continuous fermentation with product recovery by in-situ extraction. *Chem. Eng. Technol.* **17**, 365–373.
- Wewetzer, S. J., Kunze, M., Ladner, T., Luchterhand, B., Roth, S., Rahmen, N., Klotz, R., Costa e Silva, A., Regestein, L. and Büchs, J.** (2015). Parallel use of shake flask and microtiter plate online measuring devices (RAMOS and BioLector) reduces the number of experiments in laboratory-scale stirred tank bioreactors. *J. Biol. Eng.* **9**, 9.
- Wisdom, G. B.** (2005). Conjugation of Antibodies to Horseradish Peroxidase. In *Immunochemical Protocols* (ed. Burns, R.), pp. 127–130. Totowa, NJ: Humana Press.
- Wright, G. J. and Rayner, J. C.** (2014). *Plasmodium falciparum* Erythrocyte Invasion: Combining Function with Immune Evasion. *PLoS Pathog.* **10**, e1003943.

- Wright, K. E., Hjerrild, K. A., Bartlett, J., Douglas, A. D., Jin, J., Brown, R. E., Illingworth, J. J., Ashfield, R., Clemmensen, S. B., de Jongh, W. A., et al.** (2014). Structure of malaria invasion protein RH5 with erythrocyte basigin and blocking antibodies. *Nature* **7**, 427–430.
- Wurm, F. M.** (2004). Production of recombinant protein therapeutics in cultivated mammalian cells. *Nat Biotechnol* **22**, 1393–1398.
- Xiao, C. and Anderson, C. T.** (2013). Roles of pectin in biomass yield and processing for biofuels. *Front. Plant Sci.* **4**, 67.
- Zander, S., Baumann, S., Weidtkamp-Peters, S. and Feldbrügge, M.** (2016). Endosomal assembly and transport of heteromeric septin complexes promote septin cytoskeleton formation. *J. Cell Sci.* **129**, 2778–2792.
- Zarnack, K., Maurer, S., Kaffarnik, F., Ladendorf, O., Brachmann, A., Kämper, J. and Feldbrügge, M.** (2006). Tetracycline-regulated gene expression in the pathogen *Ustilago maydis*. *Fungal Genet. Biol.* **43**, 727–738.
- Zeitler, M., Steringer, J. P., Möller, H. M., Mayer, M. P. and Nickel, W.** (2015). HIV-Tat protein forms phosphoinositide-dependent membrane pores implicated in unconventional protein secretion. *J. Biol. Chem.* **290**, 21976–21984.
- Zenser, T. V., Lakshmi, V. M. and Davis, B. B.** (1999). Human and *Escherichia coli* β -glucuronidase hydrolysis of glucuronide conjugates of benzidine and 4-aminobiphenyl, and their hydroxy metabolites. *Drug Metab. Dispos.* **27**, 1064–1067.
- Zhang, W., Inan, M. and Meagher, M. M.** (2000). Fermentation strategies for recombinant protein expression in the methylotrophic yeast *Pichia pastoris*. *Biotechnol. Bioprocess Eng.* **5**, 275–287.

6 Appendix

	1	10	20	30	40	50	60	70	80
PfRH5	MIRIKKKLILTIYIHLFILNRLS	FENAIKKTKNQENNL	LLPIKSTEEEEKDDIKNGKDIKKEIDNDKENIKTNNAKDHSTYI						
G_RH5RKAVKAASMG	FENAIKKTKNQENNL	LLPIKSTEEEEKDDIKNGKDIKKEIDNDKENIKTNNAKDHSTYI						
IDT_UmRH5	FENAIKKTKNQENNL	LLPIKSTEEEEKDDIKNGKDIKKEIDNDKENIKTNNAKDHSTYI						
UmRH5	FENAIKKTKNQENNL	LLPIKSTEEEEKDDIKNGKDIKKEIDNDKENIKTNNAKDHSTYI						
ΔN-UmRH5	FENAIKKTKNQENNL	LLPIKSTEEEEKDDIKNGKDIKKEIDNDKENIKTNNAKDHSTYI						
	90	100	110	120	130	140	150	160	
PfRH5	KSYLNTNVNDG	KYLFIPSHNSFIKKYSVFNQINDGMLLNEKNDVKNNEDYKNVDYKNVNFQYHFKELSNYNIANS	SIDILQE						
G_RH5	KSYLNTNVNDG	KYLFIPSHNSFIKKYSVFNQINDGMLLNEKNDVKNNEDYKNVDYKNVNFQYHFKELSNYNIANS	SIDILQE						
IDT_UmRH5	KSYLNTNVNDG	KYLFIPSHNSFIKKYSVFNQINDGMLLNEKNDVKNNEDYKNVDYKNVNFQYHFKELSNYNIANS	SIDILQE						
UmRH5	KSYLNTNVNDG	KYLFIPSHNSFIKKYSVFNQINDGMLLNEKNDVKNNEDYKNVDYKNVNFQYHFKELSNYNIANS	SIDILQE						
ΔN-UmRH5	KSYLNTNVNDG	KYLFIPSHNSFIKKYSVFNQINDGMLLNEKNDVKNNEDYKNVDYKNVNFQYHFKELSNYNIANS	SIDILQE						
	170	180	190	200	210	220	230	240	
PfRH5	KEGHLDFVIIPHYTFLDYKHLSYNSIYHKSSTYGY	CI	IAVDAFIKKINE	YDKVSKSCNDIKNDLIATIKKLEHPYDINNKN					
G_RH5	KEGHLDFVIIPHYTFLDYKHLSYNSIYHKSSTYGY	CI	IAVDAFIKKINE	YDKVSKSCNDIKNDLIATIKKLEHPYDINNKN					
IDT_UmRH5	KEGHLDFVIIPHYTFLDYKHLSYNSIYHKSSTYGY	CI	IAVDAFIKKINE	YDKVSKSCNDIKNDLIATIKKLEHPYDINNKN					
UmRH5	KEGHLDFVIIPHYTFLDYKHLSYNSIYHKSSTYGY	CI	IAVDAFIKKINE	YDKVSKSCNDIKNDLIATIKKLEHPYDINNKN					
ΔN-UmRH5	KEGHLDFVIIPHYTFLDYKHLSYNSIYHKSSTYGY	CI	IAVDAFIKKINE	YDKVSKSCNDIKNDLIATIKKLEHPYDINNKN					
	250	260	270	280	290	300	310	320	330
PfRH5	DSYRYDISEEIDDKSE	TDDE	TEEVEDSIQD	TDSNH	APSNKKKNDLMNR	AFKKMMDEYNTKKKKLIKCIKNHENDFNKICMDM			
G_RH5	DSYRYDISEEIDDKSE	TDDE	TEEVEDSIQD	TDSNH	APSNKKKNDLMNR	AFKKMMDEYNTKKKKLIKCIKNHENDFNKICMDM			
IDT_UmRH5	DSYRYDISEEIDDKSE	TDDE	TEEVEDSIQD	TDSNH	APSNKKKNDLMNR	AFKKMMDEYNTKKKKLIKCIKNHENDFNKICMDM			
UmRH5	DSYRYDISEEIDDKSE	TDDE	TEEVEDSIQD	TDSNH	APSNKKKNDLMNR	AFKKMMDEYNTKKKKLIKCIKNHENDFNKICMDM			
ΔN-UmRH5	DSYRYDISEEIDDKSE	TDDE	TEEVEDSIQD	TDSNH	APSNKKKNDLMNR	AFKKMMDEYNTKKKKLIKCIKNHENDFNKICMDM			
	340	350	360	370	380	390	400	410	
PfRH5	KNYGTNLFEOQLSCYNNNF	CNTNGIRYHYDEYIHKLLSVKSKNLNKLSDMTN	ILQOSELLTNLNKKMGSIYIDTIKFIHK						
G_RH5	KNYGTNLFEOQLSCYNNNF	CNTNGIRYHYDEYIHKLLSVKSKNLNKLSDMTN	ILQOSELLTNLNKKMGSIYIDTIKFIHK						
IDT_UmRH5	KNYGTNLFEOQLSCYNNNF	CNTNGIRYHYDEYIHKLLSVKSKNLNKLSDMTN	ILQOSELLTNLNKKMGSIYIDTIKFIHK						
UmRH5	KNYGTNLFEOQLSCYNNNF	CNTNGIRYHYDEYIHKLLSVKSKNLNKLSDMTN	ILQOSELLTNLNKKMGSIYIDTIKFIHK						
ΔN-UmRH5	KNYGTNLFEOQLSCYNNNF	CNTNGIRYHYDEYIHKLLSVKSKNLNKLSDMTN	ILQOSELLTNLNKKMGSIYIDTIKFIHK						
	420	430	440	450	460	470	480	490	
PfRH5	EMKHIFNRIEYHTKIINDKTKIIQDKIKLNIWRTFQKDELLKRIL	DMSNEYSLFITS	SDHLRQMLYNTFY	SKEKHLNNIFHHLI					
G_RH5	EMKHIFNRIEYHTKIINDKTKIIQDKIKLNIWRTFQKDELLKRIL	DMSNEYSLFITS	SDHLRQMLYNTFY	SKEKHLNNIFHHLI					
IDT_UmRH5	EMKHIFNRIEYHTKIINDKTKIIQDKIKLNIWRTFQKDELLKRIL	DMSNEYSLFITS	SDHLRQMLYNTFY	SKEKHLNNIFHHLI					
UmRH5	EMKHIFNRIEYHTKIINDKTKIIQDKIKLNIWRTFQKDELLKRIL	DMSNEYSLFITS	SDHLRQMLYNTFY	SKEKHLNNIFHHLI					
ΔN-UmRH5	EMKHIFNRIEYHTKIINDKTKIIQDKIKLNIWRTFQKDELLKRIL	DMSNEYSLFITS	SDHLRQMLYNTFY	SKEKHLNNIFHHLI					
	500	510	520						
PfRH5	YVLQMKFNDVPIKMEYFQTYKKNKPLTQ								
G_RH5	YVLQMKFNDVPIKMEYFQTYKKNKPLTQ								
IDT_UmRH5	YVLQMKFNDVPIKMEYFQTYKKNKPLTQ								
UmRH5	YVLQMKFNDVPIKMEYFQTYKKNKPLTQ								
ΔN-UmRH5	YVLQMKFNDVPIKMEYFQTYKKNKPLTQ								

Fig. 6.1: Amino acid sequence alignment of RH5 variants

Amino acid sequence alignment of native *Plasmodium falciparum* reticulocyte binding protein homologue 5 with signal peptide (PfRH5) and modified RH5 variants. These include the sequence of an RH5 variant (G_RH5) that is equipped with a mammalian signal peptide and has 4 mutagenized *N*-glycosylation sites (T40A, T216A, T286A and T299A), a synthesized RH5 variant, representing the *U. maydis* dicodon optimized G_RH5 (IDT_UmRH5), a mutated IDT_UmRH5 version, lacking internal *Bsa*I endonuclease recognition sites (UmRH5), and a UmRH5 version lacking 134 aa of the N-terminus (ΔN-UmRH5). The first 24 aa include the signal peptides that have been deleted in IDT_UmRH5, UmRH5 and ΔN-UmRH5. The 134 aa that ΔN-UmRH5 is lacking, are encircled with a black box. L95V, E266D and E270D aa exchanges in UmRH5 and ΔN-UmRH5 that were introduced by PCR-mutagenesis. Black shaded areas display sequence identity.

Author contributions

Results of Section 2.1.2 were partially achieved in the context of a Bachelor thesis (Beier, 2015). Marius Terfrüchte supervised Sofie Beier in wet lab work, planned all experiments and performed them partially.

Parts of this dissertation were submitted for publication to the Applied and Environmental Microbiology journal (Terfrüchte M., Wewetzer S., Schlepütz T., Feldbrügge M., Büchs J. and Schipper K., Optimizing cultivation conditions for unconventional secretion of heterologous proteins in *Ustilago maydis*.) on the 17th of October, 2016. In this publication, M. Terfrüchte and S. Wewetzer share the first authorship. Experiments were conducted in cooperative work with the Aachener Verfahrenstechnik (AVT) at the RWTH Aachen:

Kerstin Schipper, Tino Schlepütz, Sandra Wewetzer and Marius Terfrüchte planned the experiments and analyzed results. Sandra Wewetzer performed RAMOS cultivations and downstream HPLC analysis. Marius Terfrüchte generated expression strains, performed *in vitro* assays and processed the samples from RAMOS cultivations. Kerstin Schipper, Michael Feldbrügge and Jochen Büchs wrote the manuscript with input of all co-authors.

This declaration is intended to clarify the use of figures and sections from this publication:

Sections 2.4.1 – 2.4.4, including Fig. 2.10, Fig. 2.11, Fig. 2.12, Fig. 2.13, Fig. 2.14, Fig. 2.15, Fig. 2.16 and Tab. 2.1, summarize results that are intended to be published in this submitted manuscript.

Acknowledgements

Zunächst möchte ich mich bei Michael dafür bedanken, dass er mich seit dem Bachelorstudium immer unterstützt, gefördert und gefordert hat. Großartige und größtenwahnsinnige Ideen, Einwände und Diskussionen, sowie stets ein offenes Ohr haben mich während der Zeit begleitet!

Bei Prof. Dr. Karl-Erich Jaeger möchte ich mich ausdrücklich für die Annahme des Zweitgutachtens und die immer konstruktiven Projektbesprechungen bedanken.

Ein ganz besonderer Dank gilt Kerstin! Eine so großartige Förderung und Betreuung, bei jedweder denkbaren wissenschaftlichen Freiheit, kann man sich wirklich nur wünschen! Ich bin wahnsinnig froh, dass ich mich damals entschieden habe Michaels Frage - Möchtest du eher in die Grundlagenforschung oder Biotechnologie? - mit Biotechnologie beantwortet zu haben und bei dir in der Gruppe gelandet zu sein!

Ich möchte mich auch bei allen aktiven und verflossenen Feldi-Jüngern für stetige Hilfsbereitschaft, Freundschaft, Trinklaune, Wutausbrüche und Unterstützung bedanken!!! Ganz besonders bei Janpeter, Parveen, Sabrina, Simone, Carl, Thomas, Lilli, Thorsten, Ben, Jörn, Michéle, Sofie, Evelyn, Ronny, Sebastian, Uli, Elisabeth, Ute und Ute! Vielen Dank auch allen Ernstis, Nowacks und Axmanns für eine großartige Flurnachbarschaft!

Ein weiterer Dank gilt dem gesamten CLIB Graduate Cluster und den Koordinatoren Jessica, Sonja und Jenni! Ben, Pia, Pascal, Jenny, Lars, Andreas, Andreas sowie alle anderen Düsseldorfern, Bielefeldern und Dortmundern: Es war mir ein Fest!

Zuletzt möchte ich mich bei meiner ganzen Familie (Terfrüchte, Rosche, Weber) bedanken, die jedes „ich habe letztes eine Doku gesehen“ und jedes „wusstet ihr“ mit echtem und geheucheltem Interesse ertragen haben! Ihr seid die besten und ich bedanke mich herzlich für Unterstützung, Ermutigung und Ablenkung! Danke Jo, dass du mich noch immer aushältst!!!

Nun aber genug des Danks!

Marius Terfrüchte**Geburtstag: 05.07.1988****Geburtsort: Essen****Ausbildung**

08/2013 – 08/2016	Doktorarbeit am Institut für Mikrobiologie, Heinrich-Heine-Universität Düsseldorf („Expression of Biopharmaceuticals in <i>Ustilago maydis</i> “)
10/2012 – 08/2013	Biologiestudium (Master), Heinrich-Heine-Universität Düsseldorf (Abschluss: Master of Science (1,3), Masterarbeit: „Expression des Malaria-Antigens PfRH5 in <i>Ustilago maydis</i> “)
10/2008 – 07/2011	Biologiestudium (Bachelor), Heinrich-Heine-Universität Düsseldorf (Abschluss: Bachelor of Science (1,75), Bachelorarbeit: „Etablierung der „Golden-Gate“ Methode zur Herstellung von Gendelektionsmutanten in <i>Ustilago maydis</i> “)
06/2007	Abitur (2,5) am Gymnasium Essen-Werden (Leistungskurse: Biologie und Englisch)

Berufserfahrung

09/2012	Studentische Hilfskraft am Institut für Mikrobiologie, Heinrich-Heine-Universität Düsseldorf
09/2011	Studentische Hilfskraft am Institut für Mikrobiologie/ iGRAD-plant, Heinrich-Heine-Universität Düsseldorf
08/2010 – 09/2010	Praktikum bei Emscher Genossenschaft Lippe Verband in Essen (Gewässermanagement und Ökophysiologie)
03/2008	Praktikum bei Biomar GmbH in Oberhausen (jetzt Gladbeck) (chemische Analyse geologischer Proben/ Schadstoffproben)
01/2008	Praktikum bei Diagenics in Düsseldorf (jetzt Essen) (Entwicklung von ELISA Tests zur Früherkennung cardio-vasculärer Erkrankungen)

Stipendien

08/2013 – 08/2016	Promotionsstipendium des CLIB Graduate Cluster an der Heinrich-Heine-Universität Düsseldorf
10/2012 – 10/2013	Stipendium „Chancen Nutzen“ an der Heinrich-Heine-Universität Düsseldorf

Zusatzqualifikationen

- „EBC*L A (European Business Competence Licence Stufe A)“ am HIMS (Hagener Institut für Managementstudien), FernUniversität Hagen (Deutschland)
- „Introduction to Project- and Innovation Management and Patent Law“, erfolgreiche Kursteilnahme
- „Lab Course PolyOmics High Throughput Sequencing“ am CeBiTec, Bielefeld (Deutschland)
- „Good Scientific Practice for Doctoral Researchers“, erfolgreiche Kursteilnahme
- „Fortbildungsveranstaltung zur Vermittlung der Sachkunde nach §15 Abs. 2 S. 1 Nr. 3, Abs. 4 Gentechnik-Sicherheitsverordnung“, erfolgreiche Kursteilnahme mit Erlangung der Sachkunde
- „Schreibworkshop Research Paper“, erfolgreiche Kursteilnahme
- „Interdisciplinary Project Preparation and proposal Writing – From Idea to Proposal“, erfolgreiche Kursteilnahme

Sprachen

- Deutsch (Muttersprache)
- Englisch (Fließend in Wort und Schrift)
- Italienisch (fortgeschritten)
- Französisch (Grundlagen)

Publikationen

- Stock J, **Terfrüchte M**, Schipper K. A reporter system to study unconventional secretion of proteins avoiding *N*-glycosylation in *Ustilago maydis* (2016). *Methods Mol Biol.* 2016; 1459:149-60.
- Buerth C, Kovacic F, Stock J, **Terfrüchte M**, Wilhelm S, Jaeger KE, Feldbrügge M, Schipper K, Ernst J, Tielker D. Uml2 is a novel CalB-type lipase of *Ustilago maydis* with phospholipase A activity (2014). *Appl Microbiol Biotechnol.* Jun; 98(11):4963-73.
- **Terfrüchte M**, Joehnk B, Fajardo-Somera R, Braus GH, Riquelme M, Schipper K, Feldbrügge M. Establishing a versatile Golden Gate Cloning system for genetic engineering in fungi (2014). *Fungal Genet Biol.* Jan; 62:1-10.

Präsentation von Forschungsergebnissen

- Vortrag: „Expression and purification of biopharmaceuticals in *Ustilago maydis*”
Molecular Biology of Fungi (MBF) conference 2015, Berlin (Deutschland)
- Poster: „Expression and purification of biopharmaceuticals in *Ustilago maydis*”
VAAM Meeting 2015, Marburg (Deutschland)
- Poster: „Establishment of an efficient Golden Gate cloning system for the generation of gene-replacement mutants in fungal model organisms”
International Fungal Biology Conference 2013, Karlsruhe (Deutschland)
- Vorträge und Poster Präsentationen im Rahmen des CLIB Graduate Cluster
- Vorträge im Rahmen des Mikrobiologie Seminars der Heinrich-Heine-Universität Düsseldorf

Gremienarbeit

01/2014 – 01/2015 Stipendiatensprecher des CLIB Graduate Cluster Düsseldorf
09/2014 Organisation und Moderation des 5. CLIB Graduate Cluster
Symposiums: „From Gene To Protein and Beyond“, Düsseldorf
(Deutschland)

Lehre

- Vorbereitung und Betreuung von praktischen Versuchen im Rahmen des halbjährlich stattfindenden Bachelor-Moduls „Allgemeine Mikrobiologie“ der Heinrich-Heine-Universität Düsseldorf, sowie Korrektur der Versuchsprotokolle.
- Theoretische und praktische Betreuung einer Bachelorarbeit.